

Technologies towards the
Development of a Lab-on-a-Chip
GCxGC for Environmental Research

A Thesis by
Jaydene Halliday, BSc MRSC

Submitted in Partial Fulfilment of the
Requirements for the Degree of
Doctor of Philosophy

University of York
Department of Chemistry
September 2012

Abstract

This thesis presents the development of a portable lab-on-a-chip two-dimensional gas chromatograph (GCxGC). A planar microfabricated system was designed and fitted within a modular built-for-purpose housing unit. The lab-on-a-chip device used acid etched borosilicate glass as the working substrate. The cost and ease of glass fabrication in this manner is attractive when compared to silicon, allowing for the formation of two capillary columns separated by channels designed to allow modulation of the eluent from the first (primary) column to the secondary. Not only were these channels circular in shape, but they also boasted similar dimensions to modern, commercially available fused silica GC columns. All working components needed to make field volatile organic compound (VOC) measurements, i.e. injector, columns, interfaces and detector, were, thus, encapsulated in a single ultra-portable microfabricated glass unit. The use of a miniaturised photoionization detector (PID) in conjunction with the glass chip is reported. The overall system had an attractive peak capacity and detection limit for VOCs, low power demand and an operating temperature range of 0 to 200 °C without cryogenics.

The miniaturised instrument, which offers a novel and alternative route to enabling microfabricated gas chromatography (GC) systems, is intended to be used in the first instance for atmospheric chemistry and air quality observations in relation to the work of the Atmospheric Chemistry research group at the University of York. It is envisaged that, if produced on a commercial scale, it could be used for a range of analyses where a field-portable but highly sensitive and selective gas chromatograph capable of performing high-speed separations is required.

Contents

Abstract.....	2
List of Tables	8
List of Illustrations.....	9
List of Abbreviations	20
Preface	23
References	26
Acknowledgements.....	26
Author’s Declaration	28
1.0 The Atmosphere.....	29
1.1 The Composition of the Atmosphere.....	29
1.1.1 The Troposphere.....	29
1.1.2 The Stratosphere.....	31
1.1.3 The Mesosphere	32
1.1.4 The Thermosphere.....	32
1.1.5 The Exosphere.....	33
1.2 Atmospheric chemistry.....	34
1.2.1 The History of Atmospheric Chemistry	35
1.2.2 Atmospheric Chemistry Methodology.....	36
1.3 Atmospheric Pollutants of Concern	39
1.3.1 Particulate Matter (PM).....	41
1.3.2 Ammonia (NH ₃)	45
1.3.3 Sulphur Dioxide (SO ₂).....	45
1.3.4 Nitrogen Oxides (NO _x).....	46
1.3.5 Volatile Organic Compounds (VOCs).....	47
1.3.6 Tropospheric Ozone (O ₃).....	50
1.4 A Summary.....	55
1.5 References	56
2.0 Chromatography	62
2.1 The History of Chromatography	62
2.2 Gas Chromatography	63
2.3 Principles of Chromatography	66
2.3.1 The Partition Coefficient (K).....	67

2.3.2	The Retention Factor (k')	70
2.3.3	Phase Ratio (β)	73
2.3.4	The Selectivity Factor (α)	74
2.3.5	The Efficiency Factor (N)	76
2.3.6	Band Broadening.....	78
2.3.7	Chromatographic Resolution	85
2.4	The Gas Chromatograph	88
2.4.1	The Carrier Gas Supply	89
2.4.2	Preconcentration	92
2.4.3	Flow Control.....	94
2.4.4	Sample Injection.....	95
2.4.5	Nuts and Ferrules.....	104
2.4.6	GC Columns.....	105
2.4.7	Stationary Phases.....	109
2.4.8	The Column Oven.....	120
2.5	GC Detectors	120
2.5.1	The Flame Ionization Detector (FID)	121
2.5.2	The Photoionization Detector (PID)	122
2.5.3	The Electron Capture Detector (ECD)	124
2.5.4	The Thermal Conductivity Detector (TCD)	125
2.5.5	The Nitrogen-Phosphorous Detector (NPD)	126
2.6	The Data Acquisition System	129
2.7	Validation and Calibration	129
2.7.1	Specificity (Selectivity)	132
2.7.2	Quantitative Analysis – The Calibration Curve.....	133
2.7.3	Linearity.....	133
2.7.4	Repeatability and Reproducibility.....	134
2.7.5	Precision.....	134
2.7.6	Accuracy.....	135
2.7.7	Limit of Detection (LOD)	136
2.7.8	Limit of Quantitation (LOQ)	137
2.8	References	137
3.0	Two-Dimensional Gas Chromatography	142
3.1	Multidimensional Gas Chromatography (GC-GC)	142

3.2	Comprehensive Two-Dimensional GC (GCxGC)	143
3.2.1	Principles of GCxGC Separation	145
3.2.2	GCxGC Instrumentation	147
3.2.3	GCxGC Data and Plots	154
3.2.4	The Future of GCxGC.....	155
3.3	References	155
4.0	GC Miniaturisation	159
4.1	Miniaturised Capillary GC Instruments.....	159
4.2	Microfabricated GC Instruments	160
4.2.1	Microfabrication Substrates	162
4.2.2	Channel Shape	163
4.2.3	Miniaturised Detectors	165
4.3	Microfabricated GCxGC Systems	165
4.4	The Potential of Microfabrication.....	166
4.5	References	166
5.0	Experimental - Benchtop GC-FID	170
5.1	Commercial Fused Silica Columns.....	170
5.1.1	Peak Shape	172
5.2	Coating of Deactivated Fused Silica Capillaries.....	174
5.2.1	Dynamic Column Coating.....	174
5.2.2	Static Column Coating.....	175
5.2.3	Experimental Column Coating Procedure.....	175
5.2.4	Removal of Stationary Phase Coating.....	179
5.2.5	Performance Testing of Coated Fused Silica Columns.....	180
5.2.6	Stationary Phase – Solvent Solubility Testing	181
5.3	References	184
6.0	Experimental – The Glass Lab-on-a-Chip Devices	186
6.1	Fabrication of the Glass Chips.....	186
6.2	Chip Designs.....	189
6.2.1	LOC 1	190
6.2.2	LOC 2	190
6.2.3	LOC 3	191
6.2.4	LOC 4	192
6.3	Commercial GC-FID with LOC Column	193

6.3.1	Chip Connections	194
6.3.2	LOC 1	195
6.3.3	LOC 2	199
6.4	References	208
7.0	Fabrication of the Lab-on-a-Chip GC Manifold	208
7.1	The Preconcentrator	209
7.1.1	Preconcentrator Performance Testing.....	210
7.2	Temperature Control	213
7.3	The Modulator	215
7.4	The Detector	217
7.4.1	Detector Performance Testing.....	217
7.5	Real-Time Control and Data Acquisition.....	219
7.6	References	220
8.0	Experimental –Stand Alone One-Dimensional GC.....	221
8.1	LOC 1	221
8.2	LOC 2	223
9.0	Experimental –Two-Dimensional GCxGC.....	229
9.1	Initial Attempts at Stand-Alone GCxGC-PID.....	229
9.1.1	Dynamic Coating of Secondary Column.....	229
9.1.2	Two-Dimensional Performance Testing of LOC 2	230
9.1.3	Static Coating of Both Columns	230
9.1.4	Introduction of Make-Up Gas	232
9.1.5	Improving PID Performance.....	233
9.2	Stand-Alone GCxGC-Commercial FID.....	233
9.3	Benchtop GCxGC-FID.....	236
9.3.1	Static Coating of Both Columns	236
9.3.2	Two-Dimensional Performance Testing of LOC 4	236
9.3.3	New FID Interconnect	244
9.4	Benchtop GC-FID.....	249
9.4.1	Validation and Calibration: LOC 4 GCxGC-FID.....	252
9.5	References	263
10.0	Experimental – Stand-Alone LOC GCxGC-PID	264
10.1	Pressure Determinations	265
10.2	Temperature Program Determinations	266

10.3	Commercial FID and Heated Transfer Line	267
10.4	Optimisation of PID	269
10.5	Heating the Inlet	272
10.6	Manifold Deterioration	277
11.0	Conclusion	279
11.1	A Summary	279
11.2	Limitations and Problems Experienced.....	282
11.3	Future Work	284
11.4	Final Words	285
11.5	References	285

List of Tables

Table 1: Composition of pure dry air	30
Table 2: Components of particulate matter	43
Table 3: A classification of chromatographic techniques.....	64
Table 4: Typical GC Applications.....	68
Table 5: Common phase ratios	74
Table 6: Parameters capable of altering selectivity.....	76
Table 7: Typical column efficiency measures for a standard 30 m polydimethylsiloxane column	78
Table 8: Relevant characteristics of carrier gases	90
Table 9: A comparison of split and splitless injection	100
Table 10: A comparison of popular liner types.....	102
Table 11: A comparison of ferrule types	104
Table 12: Comparison of wall-coated capillary, support-coated capillary and packed columns	108
Table 13: Polarity and its relationship with electronegativity	111
Table 14: Interaction Energies	114
Table 15: Polysiloxane phases.....	116
Table 16: "Cyano" Dimethylpolysiloxane phases.....	117
Table 17: Glycol (wax) phases.....	118
Table 18: Stationary phase interaction summary	118
Table 19: FID vs PID	123
Table 20: Detector Summary.....	129
Table 21: Selected applications of GCxGC	144
Table 22: Acceptable and unacceptable peak symmetry values	173
Table 23: The surface tension and viscosity of common solvents and stationary phases used to coat the columns described in this body of work .	177
Table 24: A comparison of the commercially sourced HP-5 column and the coated OV-101 fused silica column	183
Table 25: PID specifications	218
Table 26: Average peak area and height per concentration of 2-butanone in ethylbenzene.....	254

Table 27: Average peak area and height per concentration of pentane in cyclohexanone	254
Table 28: Average peak area and height per concentration of ethyl acetate in ethylbenzene.....	255
Table 29: Calculated % RSD for the varying concentrations of each standard	257
Table 30: Estimated limits of detection for each standard calibration curve	260
Table 31: Estimated limits of quantitation for each standard calibration curve	261
Table 32: Retention time repeatability at different concentrations of 2-butanone	262
Table 33: Retention time repeatability at different concentrations of pentane	262
Table 34: Retention time repeatability at different concentrations of ethyl acetate	262
Table 35: The composition of lavender oil.....	271
Table 36: The composition of tea tree oil.....	272

List of Illustrations

Figure 1: The Earth's atmosphere.....	29
Figure 2: Global average radiative forcing in 2005 for CO ₂ , CH ₄ , N ₂ O and other important agents and mechanisms, together with the typical geographical extent (spatial scale) of the forcing and the assessed level of scientific understanding (LOSU)	35
Figure 3: The Keeling Curve: Atmospheric CO ₂ concentrations as measured at Mauna Loa Observatory.....	37
Figure 4: The size of particle pollution.....	41
Figure 5: Schematic of secondary particulate matter/secondary organic aerosol formation	42
Figure 6: PM ₁₀ emissions in kilotonnes in the UK by source from 1970 to 2001....	44
Figure 7: Ammonia emissions from 1980 to 2009	45
Figure 8: Emissions of SO ₂ from 1970 to 2009	46
Figure 9: Emissions of NO _x from 1970 to 2009	47
Figure 10: Schematic of the reactions involved in an NO-to-NO ₂ conversion and O ₃ formation in an NO-NO ₂ -O ₃ system in the absence of VOCs	52
Figure 11: Schematic of the reactions involved in NO-to-NO ₂ conversion and O ₃ formation in an NO-NO ₂ -O ₃ system in the presence of VOCs	53
Figure 12: A typical VOC degradation scheme.....	55
Figure 13: A typical chromatogram for a two-component mixture where the small peak on the left represents a species that is not retained on the column.....	69
Figure 14: Effect of k' on resolution.....	72
Figure 15: Selectivity factor	75
Figure 16: Resolution as a function of selectivity	75
Figure 17: Resolution as a function of efficiency	78
Figure 18: A van Deemter plot for a packed column illustrating the relationship of A, B, and C with linear velocity, and the corresponding effect on H.....	79
Figure 19: A comparison of Eddy Diffusion occurring within a column with large packing particles, as well as one with small packing materials	80
Figure 20: The effect of the A term on the height equivalent to a theoretical plate at given linear velocities.....	81

Figure 21: A schematic illustration of Longitudinal Diffusion.....	82
Figure 22: Effect of longitudinal diffusion on height equivalent to a theoretical plate at given linear velocities.....	82
Figure 23: An illustration of mass transfer	83
Figure 24: The effect of mass transfer on height equivalent to a theoretical plate for given linear velocities	84
Figure 25: A Golay Plot showing the relationship between C_M , C_S , and B with linear velocity, and the effect these factors have on H , within a capillary column.....	84
Figure 26: Separation at three resolutions.....	86
Figure 27: The main factors effecting resolution.....	88
Figure 28: A typical gas chromatograph.....	89
Figure 29: An illustration of the adsorption process of a preconcentrator.....	93
Figure 30: An illustration of the thermal desorption process of a preconcentrator.....	93
Figure 31: A typical manual split/splitless inlet.....	94
Figure 32: Typical split/splitless inlet.....	99
Figure 33: Typical cross-section of a wall coated open tubular (WCOT) capillary.....	107
Figure 34: Cl_2 - non-polar bond. The electron charge cloud is uniformly spread in this homonuclear diatomic molecule	110
Figure 35: HCl - polar bond. Electrons spend more time drawn towards chlorine	110
Figure 36: Non-polar analyte interacting with a non-polar stationary phase	111
Figure 37: Polar analyte interacting with a polar stationary phase.....	112
Figure 38: Dispersive interactions.....	112
Figure 39: Dipole-dipole interaction between two HCl molecules.....	113
Figure 40: Dipole-induced dipole interaction between permanent dipole and induced dipole	114
Figure 41: a. Hydrogen bonding interaction between methanol and water, and b. between methanol and ammonia.....	114
Figure 42: a) 100%-Dimethylpolysiloxane; b) Phenyl dimethyl-polysiloxane, where the monomer n typically equals 5%, 35% or 50%. A higher percentage of the functional monomer, n , indicates a higher degree of interaction.....	115

Figure 43: Cyanopropylphenyl-dimethylpolysiloxane, where n typically equals 6%, 14% or 50%.....	117
Figure 44: Polyethylene glycol or wax stationary phase.....	118
Figure 45: A typical packed GC column, detailing a solid particle coated in stationary phase	119
Figure 46: The FID sensor.....	122
Figure 47: A typical photoionization detector configuration	123
Figure 48: A schematic of an electron capture detector	124
Figure 49: A schematic of a thermal conductivity detector	125
Figure 50: The Nitrogen Phosphorous Detector.....	127
Figure 51: A schematic of a magnetic sector mass spectrometer	128
Figure 52: Schematic representing a raw GCxGC chromatogram indicating the positions of individual slices and illustrating how a 3D chromatogram is reconstructed from the raw chromatogram	145
Figure 53: Schematic of a gas chromatogram set up for GCxGC analysis	147
Figure 54: Comprehensive and one-dimensional separations of VOCs in urban air. A. benzene; B. heptane, C. toluene; D. xylenes; E. C ₃ -benzenes; F. C ₄ -benzenes; G. C ₅ -benzenes; H. naphthalene. 1. aliphatic band; 2. carbonyl band; 3. aromatic band; 4. bi-aromatics.....	148
Figure 55: Schematic of duel-jet cryogenic modulation. (B1) Right hand side jet traps analytes eluting from first column; (B2) Right hand side jet switched off, cold spot heats up rapidly and analyte pulse is released into second column; simultaneously, left hand side jet switched on to prevent leakage of first-column material; (B3) next modulation cycle is started.....	151
Figure 56: Configuration of Seeley's 6-port modulation valve	153
Figure 57: a) The Agilent 3000 Micro GC; b) The ASI Inc. microFAST GC; c) The SLS Micro Technology GCM 5000.....	160
Figure 58: The μ ChemLab developed by Sandia National Laboratories.....	161
Figure 59: Columns composed of A. Carbon nanotubes; B. Porous silicon; D. Metal; E. Ceramic	162
Figure 60: SEM of a side view of Potkay's μ GC column	164
Figure 61: The separation of the headspace vapour of a cyclohexane, toluene and propyl acetate mixture using an Agilent HP-5 0.32 mm x 0.25 μ m column cut to a length of 7.5 m.....	171

Figure 62: The separation of tridecane, tetradecane, pentadecane and hexadecane using the 7.5 m cut-to-size HP-5 column.....	172
Figure 63: Measurement of peak symmetry	172
Figure 64: Dynamic capillary column coating.....	174
Figure 65: Static capillary coating.....	175
Figure 66: Fused silica column coating setup	178
Figure 67: The lack of separation seen between cyclohexane, propyl acetate and toluene when run on a column which has undergone stationary phase removal	180
Figure 68: Separation of cyclohexane, toluene and propyl acetate using a 7.5 m x 0.32 mm deactivated fused silica column coated with OV-101 (in pentane) to a film thickness of 1 μm	181
Figure 69: Separation using a 7.5 m x 0.32 mm fused silica column coated to a thickness of 1 μm with OV-101 in a) dichloromethane; and b) pentane	182
Figure 70: Separation using a 7.5 m x 0.32 mm fused silica column coated to a thickness of 1 μm with OV-101 in a) dichloromethane; and b) pentane	183
Figure 71: Illustration of the etch profile, with and without stirring, using an isotropic wet chemical etchant	187
Figure 72: The glass microfluidic lab-on-a-chip GCxGC fabrication process..	188
Figure 73: Cross sectional views of a portion of the glass GC chip.....	189
Figure 74: A) Close up image of column turns; B) close up image of injector region coupled to 7.5 m column via a 50 μm restrictor region	189
Figure 75: An image of LOC 1 clearly showing both the size of the glass chip in comparison to a regular 50 p coin, and the lack of interconnecting microfluidic channels between the primary and secondary columns.....	190
Figure 76: LOC 2, which had a preconcentrating trap, modulator, and inter-connecting channels, as well as an edge connector for easy sample introduction	191
Figure 77: The operation of the edge connector.....	191
Figure 78: A photo of the reduced LOC 3 chip	192
Figure 79: LOC 4 showing the 4 m serpentine primary column, the spiral 7.5 m secondary column, and the relocated and resized modulator channels.....	193
Figure 80: Shellac flakes. These were melted and then used to secure transfer lines to the glass chips during evaluations of bonding agents.....	194

Figure 81: Dismantled view of one of many peek edge connectors used and examples of the varying screw lengths that were observed.....	195
Figure 82: On-chip solvent evaporation using 6 pentane pressure buffer vials	197
Figure 83: Response of FID (Varian) to injection of the BTEX standard mixture (blue) and a mixture of 2 ppm nonane, alpha-pinene and 3-carene (red) with a 0.5 ml sample loop	198
Figure 84: The flow path of the coating solution for LOC	199
Figure 85: Glass chip column coating set up	200
Figure 86: GC set-up to allow direct attachment of glass chip.....	201
Figure 87: The lack of separation of cyclohexane, propyl acetate and toluene using two 10 cm lengths of HP-5 commercial column and a short length of peek tubing	201
Figure 88: Experimental set-up to determine the effect of the peek tubing on chromatography	202
Figure 89: Separation of cyclohexane, toluene and propyl acetate using a 7.5 m x 0.32 mm x 0.25 μ m HP-5 column connected to two lengths of peek tubing.....	202
Figure 90: Separation of cyclohexane, propyl acetate and toluene using the 7.5 m x 0.25 mm on-chip primary column coated with a 2% v/v solution of OV-101 in pentane.....	203
Figure 91: Pentane and 2-pentanone. Primary column coated dynamically with a a) 2% v/v solution of OV-101 in pentane; b) 10% v/v OV-101 in pentane; c) 20% v/v OV-101 in pentane; and d) the separation achieved on a column coated statically with a 2% v/v solution of OV-101 in pentane.....	204
Figure 92: Acetone, pentane, hexane, benzene, toluene and o-xylene. Primary column statically coated with a 20% v/v solution of OV-101 in pentane	205
Figure 93: Microscopic evidence of liquid droplets of stationary phase present in microcolumn.....	205
Figure 94: Acetone, pentane, hexane, benzene, toluene, o-xylene and dodecane using the 7.5 m x 0.25 mm on-chip glass column dynamically coated with a 20% v/v solution of OV-101 in pentane.....	206
Figure 95: Separation of the same mixture using a column coated statically with a 2% v/v solution of OV-101 in pentane.....	207
Figure 96: CAD model of the preconcentrator stage (provided by Dr Christopher Rhodes).....	209

Figure 97: Microscopic image of preconcentrator packed with Carbopak B 60/80 mesh.....	209
Figure 98: Microscopic image of preconcentrator packed with micro-glass beads on either end and Carbopak B 60/80 mesh inbetween	210
Figure 99: Set-up for trap section testing.....	210
Figure 100: Desorption of a) pentane drawn through the preconcentrator by a pump at ambient temperature; b) pentane propelled through the preconcentrator with N ₂ carrier at 10 °C before thermal desorption for 30 s; c) isoprene propelled through the preconcentrator with N ₂ carrier at 10 °C before thermal desorption for 30 s.....	211
Figure 101: Views of a) the packing in the trap section; b) the lamp; c) the trap installed for testing; d) condensation of water on the exposed surface of the trap	212
Figure 102: Side view showing the layout of components in the temperature controlled stack used for heating and cooling the glass GC.....	213
Figure 103: Plan view layout of the temperature controlled stacks. Stack 1 is under the primary 7.5 m long column. Stacks 2 and 3 are positioned under the secondary 1.4 m column and the injection region, respectively	214
Figure 104: Measured temperature profile with a) stack 1 (under the 7.5 m column) heated to 100 °C, all other stacks left at ambient; b) stack 1 cooled to 10 °C whilst holding the temperature of stack 2 (the 1.4 m column) at 100 °C. The temperature remained uniform (± 2 °C) over stack 1 and the unheated stack 3 remained at ambient temperature.....	214
Figure 105: CAD model of the thermal control unit (provided by Dr Christopher Rhodes)	215
Figure 106: A schematic illustrating the layout of the on-chip modulator, as well as showing gas flow direction when in a) load; b) inject position	216
Figure 107: The photoionization detector sourced from Alphasense	217
Figure 108: PID response to ambient air and varying concentrations of pentane vapour. FWHM = Full Width at Half Maximum	218
Figure 109: Photo (provided by NPL) of the heating and data acquisition set-up applied for performance testing of the primary column of LOC 1 with the miniaturised PID	221
Figure 110: a) The side view and b) the over-head view of the testing set-up for LOC 1.....	222

Figure 111: Response of PID to injection of the BTEX standard mixture with a 0.2 ml sample loop, run on LOC 1	223
Figure 112: The separation of BTEX on LOC 2 achieved using the method detailed for LOC 1 but in the in-house built GC manifold with photoionization detection	224
Figure 113: The separation of BTEX, achieved using LOC 2 in the in-house built GC manifold with photoionization detection. A 0.25 ml sample loop was used, helium carrier gas, a flow rate of 1.5 ml·min ⁻¹ , and a temperature program of 20-100 °C at 20 °C·min ⁻¹	224
Figure 114: The separation of a 10 ppm BTEX gas mixture on the in-house built GC manifold, achieved using a 0.25 ml sample loop and a temperature program of 30-100 °C ramping at 20 °C·min ⁻¹ , with a flow rate of a) 1.5 ml·min ⁻¹ , b) 10 ml·min ⁻¹ , and c) 15 ml·min ⁻¹	225
Figure 115: The separation of petrol on the stand-alone LOC system with a temperature ramp of 10 °C·min ⁻¹ and a starting temperature of a) 30 °C, b) 10 °C, and c) 3 °C.....	226
Figure 116: The separation of petrol in a) hydrogen carrier gas at 12 psi, with a temperature program starting at 3 °C, ramping at 10 °C·min ⁻¹ and b) air carrier at a pressure of 22 psi, with a starting temperature of 30 °C, ramping at 10 °C·min ⁻¹	227
Figure 117: The separation of a BTEX gas sample in air carrier gas at 22 psi, starting at 10 °C and ramping at 10 °C·min ⁻¹	228
Figure 118: An example of the initial "2D" separation achieved with the fully coated LOC chip in the in-house-built manifold and the PID. Individual peaks have been rescaled to give common peak maxima intensity.....	230
Figure 119: An 8 component 2D separation achieved with the stand-alone LOC GCxGC system	230
Figure 120: The separation of a 10 component oxygenated VOC mix on the stand-alone system using the LOC 2 chip with both columns statically coated	231
Figure 121: The modulated response of pentane using two different PIDs, but otherwise identical conditions	232
Figure 122: A schematic showing the set-up for PID make-up gas testing, and one of the resulting blank chromatograms	232

Figure 123: One of the many methods evaluated of transferring the eluate emerging from the secondary column into the PID.....	233
Figure 124: Separation of an 8 component mixture via the glass chip in the GC manifold with the FID of a commercial Agilent FID	234
Figure 125: The results of the separation of a 10 component mixture via the glass chip in the GC manifold with the FID of a commercial Agilent FID.....	235
Figure 126: The separation of a 12 component mixture run on LOC 4 within a commercial GC with FID detection	237
Figure 127: The separation of lavender oil by LOC 4 in a commercial GC with FID detection	238
Figure 128: The separation of isobutyraldehyde, hexane, 2-pentanone, and nonane with a primary column pressure of 75 psi and a secondary column pressure of 60 psi	239
Figure 129: The separation of isobutyraldehyde, hexane, 2-pentanone, and nonane with a primary column pressure of 25 psi and a secondary column pressure of 35 psi	240
Figure 130: The separation achieved with a 220:1 split ratio.....	242
Figure 131: Separation achieved with a modulation ratio of a) 2.5:2.5; b) 3.0:2.0; c) 4.0:5.0; d) 4.5:4.5; and e) 5.0:1.0	242
Figure 132: a) The separation of a 7 component mixture using the final method developed as described above; and b) Magnification to better show the two-dimensional separation achieved	243
Figure 133: a) The separation of 3-ethyltoluene to 2-methylbuty-raldehyde ; b) the addition of propan-2-ol resulting in two peaks; c) No further peaks seen despite the addition of hexane and 2-methylpentane.....	244
Figure 134: A modulated pentane peak. a) Pressure ratio = 11.0:19.6, Modulation ratio = 3.0:2.0; b) Pressure ratio = 10.5:20.0, Modulation ratio = 3.0:2.0; c) Pressure ratio = 16.4:30.0, Modulation ratio = 3.0:2.0; d) Pressure ratio = 10.5:20.0, Modulation ratio = 4.0:2.0.....	245
Figure 135: The separation of a) diesel; b) kerosene; c) lavender oil.....	247
Figure 136: 1. pentane, 2. 2-methylpentane, 3. isobutyraldehyde, 4. hexane, 5. propan-2-ol, 6. 2-methylbutyraldehyde, 7. 2-pentanone, 8. toluene, 9. ethylbenzene, 10. 3-methyloctane, 11. ethyltoluene, 12. nonane. a) Pressure ratio = 10.5:20 psi, Modulation ratio = 3:2 s; b) Pressure ratio = 10.5:20 psi,	

Modulation ratio = 4:2 s; c) Pressure ratio = 16.4:30, Modulation ratio = 3:2	248
Figure 137: The separation of a 16 component mixture, with a pressure ratio of 16.4:30 psi and a modulation ratio of 3:2 s.....	249
Figure 138: The one dimensional separation of diesel, achieved using only the 4 m x 1.8 mm primary column of the glass chip, with a split ratio of 220:1 and a temperature program of 30 °C to 160 °C at 5 °C·min ⁻¹	250
Figure 139: The separation of pentane, 2-methylpentane, isobutyraldehyde, hexane, propan-2-ol, 2-methylbutyraldehyde, 2-pentanone, toluene, ethylbenzene, 3-methyloctane, ethyltoluene, and nonane	250
Figure 140: The separation of pentane, 2-butanone, isobutyraldehyde, hexane, butanal, ethyl acetate, cyclohexane, propan-2-ol, 2-methylbutyr-aldehyde, propyl acetate, 3-methyl-3-buten-2-one, 2-butenal, 2-pentanone, ethylbenzene, 3-methyloctane, nonane.....	251
Figure 141: The one-dimensional separation of lavender oil using the before mentioned conditions on the primary column of LOC 4	251
Figure 142: Calibration curve generated for 2- butanone in ethylbenzene ...	255
Figure 143: Calibration curve generated for pentane in cyclohexanone.....	256
Figure 144: Calibration curve generated for ethyl acetate in ethylbenzene ..	256
Figure 145: Calibration curve generated for 2-butanone by plotting measured peak height against concentration.....	258
Figure 146: Calibration curve generated for pentane by plotting measured peak height against concentration.....	258
Figure 147: Calibration curve generated for ethyl acetate by plotting measured peak height against concentration.....	259
Figure 148: Images illustrating the chip within its housing. Input and output transfer lines are clearly visible. Connection to the PID was by a small 5 cm length of capillary.....	264
Figure 149: The 2D separation of pentane, hexane and heptane. Carrier gas and modulator gas pressure = 62 psi, temperature difference between primary and secondary column = 10 °C, temperature ramp = 25-60 °C at 10 °C·min ⁻¹ , ramp delay = 20 s. a) Modulation ratio = 3:1 s; b) Modulation ratio = 5:1 s; c) Modulation ratio = 7:1 s; d) Modulation ratio = 9:1 s; e) Modulation ratio = 9:0.5 s. Due to operation parameters injections were not 100% reproducible.....	265

Figure 150: Pentane, hexane and heptane. Modulation ratio = 9:1 s, carrier and modulator gas pressures = 62 psi, temperature difference between columns = 10 °C, temperature program = 25-60 °C at 10 °C·min ⁻¹ , ramp delay = 60 s....	266
Figure 151: Pentane, hexane and heptane. Modulation ratio = 9:1 s, carrier and modulator gas pressures = 62 psi, temperature program = 25-60 °C at 10 °C·min ⁻¹ , ramp delay = 60 s, and temperature difference between columns = 50 °C	266
Figure 152: Pentane, hexane and heptane. Modulation ratio = 9:1 s, carrier and modulator gas pressures = 62 psi, temperature program = 25-60 °C at 10 °C·min ⁻¹ , ramp delay = 60 s, and temperature difference between columns = 80 °C	267
Figure 153: Pentane, hexane and heptane using a commercial FID for detection. Modulation ratio = 9:1 s, carrier and modulator gas pressures = 62 psi, temperature difference between columns = 20 °C, temperature program = 25-60 °C at 10 °C·min ⁻¹ , ramp delay = 60 s.....	267
Figure 154: A schematic of the expected 2-dimensional plot that would result from the GCxGC separation of pentane, hexane, 2-butanone, 2-methylbutanal, toluene and ethylbenzene.....	268
Figure 155: Separation of a 6 component mixture using a commercial FID for detection. Modulation ratio = 9:1 s, carrier and modulator gas pressures = 62 psi, temperature difference between columns = 20 °C, temperature program = 25-120 °C at 5 °C·min ⁻¹ , ramp delay = 120 s	268
Figure 156: Separation of an 8 component mixture using a commercial FID for detection. Modulation ratio = 9:1 s, carrier and modulator gas pressure = 62 psi, temperature difference between columns = 20 °C, temperature program = 25-120 °C at 5 °C·min ⁻¹ , ramp delay = 120 s	269
Figure 157: Separation of an 8 component mixture using the PID for detection. Modulation ratio = 9:1 s, carrier and modulator gas pressure = 62 psi, temperature difference between columns = 20 °C, temperature program = 25-120 °C at 5 °C·min ⁻¹ , ramp delay = 120 s	270
Figure 158: The separation of lavender oil. Modulation ratio = 9:1 s, carrier gas pressure = 65 psi, modulator gas pressure = 64 psi, temperature difference between columns = 10 °C, temperature program = 20-120 °C at 5 °C·min ⁻¹ , ramp delay = 120 s	270

Figure 159: The separation of lavender oil as previously described. However, this time a heated metal fitting was used as inlet.....	272
Figure 160: The commercial inlet coupled to LOC 4 within the in-house built GC manifold.....	273
Figure 161: Pentane, hexane and heptane. Modulation ratio = 9:1 s, carrier and modulator gas pressure = 62 psi, temperature difference between columns = 20 °C, temperature program = 25-100 °C at 10 °C·min ⁻¹ , ramp delay = 60 s, a) without the extra heating applied to the inlet; b) with the extra heating applied	274
Figure 162: The separation of an 8 component mixture. Modulation ratio = 9:1 s, carrier and modulator gas pressure = 62 psi, temperature difference between columns = 20 °C, temperature program = 25-100 °C at 10 °C·min ⁻¹ , ramp delay = 60 s, with the extra heating applied to the inlet	275
Figure 163: Lavender oil separated on LOC 4. Modulation ratio = 9:1 s, carrier gas pressure = 65 psi, modulator gas pressure = 64 psi, temperature difference between columns = 10 °C, temperature program = 20-120 °C at 2 °C·min ⁻¹ , ramp delay = 20 s	276
Figure 164: A compilation of lavender oil component peaks seen at varying intensities.....	277
Figure 165: A close-up of the spiral primary column of LOC 1.....	282

List of Abbreviations

The following table describes the significance of various abbreviations and acronyms used throughout the thesis. The page on which each one is defined or first used is also given

Abbreviation	Meaning	Page
A	The Eddy Diffusion term	80
ACE	Atmospheric Chemistry Experiment	39
AED	Atomic emission detector	155
ATMOS	Atmospheric Trace Molecule Spectroscopy	39
B	The Longitudinal Diffusion term	80
BTEX	Benzene, toluene, ethylbenzene and xylene	124
C	The Mass Transfer term	80
CFCs	Chlorofluorocarbons	32
CI	Chemical ionization	129
CLRTAP	Convention on Long-range Transboundary Air Pollution	41
COC	Cool-on-column	97
COTS	Commercial off-the-shelf	161
CQ	Component qualification	132
CRISTA	CRyogenic Infrared Spectrometers and Telescopes for the Atmosphere	39
CRM	Certified reference material	135
CVAO	Cape Verde Atmospheric Observatory	38
DAQ	Data acquisition device	220
d_f	Stationary phase film thickness	74
DQ	Design qualification	132
DRIE	Dry Reactive Ion Etching	162
DVT	Design verification testing	131
ECD	Electron capture detection/detector	67
EI	Electron impact	128
EPA	The US Environmental Protection Agency	49
EPC	Electronic pressure control	96
FAAM	Facility for Airborne Atmospheric Measurements	39

FID	Flame ionisation detection/detector	57
FPD	Flame photometric detector	96
GC	Gas chromatography	2
GC-FID	Gas chromatography-flame ionisation detection	57
GC-MS	Gas chromatography-mass spectrometry	57
GCxGC	Comprehensive two-dimensional gas chromatography	2
GOME	Global Ozone Monitoring Experiment	39
H	Height equivalent to a theoretical plate	78
HPLC	High performance liquid chromatography	63
I.D.	Internal diameter	74
IQ	Installation qualification	130
LC	Liquid chromatography	64
LIDAR	Light Detection And Radar	40
LiGA	Lithographie, Galvano-formung, Abformung	164
LOC	Lab-on-a-chip	187
LOD	Limit of detection	131
LOQ	Limit of quantitation	132
LOSU	Level of scientific understanding	35
LTCC	Low temperature cofired ceramic	164
MDL	Method detection limits	252
MEMS	Micro-Electro-Mechanical Systems	160
MOPITT	Measurements of Pollution in the Troposphere	39
MOZAIC	Measurement of OZone and water vapour by Airbus in-service aircraft	39
MS	Mass spectrometry/mass spectrometer	57
MTBF	Mean time between failures	131
m/z	Mass to charge ratio	128
N	Number of theoretical plates/separation efficiency	74
NAEI	National Atmospheric Emissions Inventory	40
NCD	Nitrogen chemiluminescence detector	140
NDACC	Network for the Detection of Atmospheric Composition Change	39
NEMS	Nanoelectromechanical systems	155
NMVOC	Non-methane volatile organic compounds	49
NPD	Nitrogen phosphorous detector	96
NPL	The National Physical Laboratory	24

OEM	Original equipment manufacturer	131
OQ	Operational qualification	130
PCB	Polychlorinated biphenyls	122
PEG	Polyethylene glycol	110
PID	Photoionization detector/detection	2
PLOT	Porous-layer open tubular GC columns	108
PM	Particulate matter	41
POCP	Photochemical Ozone Creating Potential	56
PQ	Performance qualification	130
PVT	Programmed vaporization temperature	97
r	Radius	74
RF	Radiative Forcing	35
RSD	Relative standard deviation	134
SAW	Surface acoustic wave	161
SCD	Sulphur chemiluminescence detector	155
SFC	Supercritical fluid chromatography	64
SHIVA	Stratospheric Ozone: Halogen Impacts in a Varying Atmosphere	39
S:N	Signal-to-noise ratio	136
SVOC	Semi-volatile organic compounds	122
TCD	Thermal conductivity detector	122
TDU	Thermal desorption unit	94
TEOM	Tapered Element Oscillating Microbalance	45
TOF MS	Time-of-flight mass spectrometer	155
UARS	Upper Atmosphere Research Satellite	39
UNECE	United Nations Economic Commission for Europe	41
UV	Ultraviolet	32
VOC	Volatile organic compound(s)	2
WCOT	Wall-coated open tubular GC columns	108
WHO	The World Health Organization	44
1D	One-dimensional	143
2D	Two-dimensional	24
α	The selectivity factor	75
β	Phase ratio	74

Preface

This PhD thesis represents a culmination of experimental work and learning that has taken place over a period of almost four years (2008 – 2012). It contains the results of research undertaken within the Atmospheric Chemistry Research Group at the Department of Chemistry of the University of York. This research was funded by the National Physical Laboratory (NPL), the Defence Science and Technology Laboratory (DSTL), the Natural Environment Research Council (NERC), the Yorkshire Enterprise Fellowship (YEF) Scheme, and the Chemical and Biological Knowledge Base Programme of the National Measurement Office.

The field of gas chromatography, including column technology, is generally considered a mature science. This belief has led to a relatively small amount of new and active research being conducted in this area, in comparison to other analytical techniques. Instead, work based on the use of commercially available products for new applications is much more commonly reported.

This body of work details the development of a miniaturised, planar two-dimensional (2D) GCxGC of novel design, describing original column coating and solvent evaporation processes, innovative software control, and presenting the first ever successful 2D plots generated on a glass, microfabricated device of its kind. Sections of the work have been published in the *Journal of Chromatography A* under the title “Microfabricated Planar Glass Gas Chromatography with Photoionization Detection”^[1], and in *LCGC Europe* as “Lab-on-a-Chip GC for Environmental Research”^[2].

The idea of a portable GCxGC device came about as a result of the field-work experiences of my PhD supervisor, Professor Alastair Lewis, and colleagues. As experts in the field of Atmospheric Chemistry, they often partake in field campaigns in environments that can be considered exotic, remote, and largely challenging. Transporting bulky, heavy scientific instruments with high power consumption to areas of the world where electricity is often limited is fraught with logistical infeasibilities. Thus, measurement of atmospheric compounds of interest at sites, such as the humid tropical jungles of Borneo or the desolate snowy plains of Antarctica, generally first consists of taking a vast

number of samples, which are then extracted and/or analysed on return to the analytical laboratory. This could be weeks after the initial sampling took place. A means of reliable real-time monitoring and on-site, direct and immediate analysis would eliminate the issues faced with regards to the homeward transport of the collected samples, the potential for leakage and general loss of sample, reactions within the sampling vessel, and the disappointment realised after hours or even days of laboratory analysis only to find a complete lack of the analytes of interest.

The construction of the device manifold, to be described, and the software control system was achieved with the help of Dr Christopher Rhodes, whose electronic skills and LabVIEW knowledge proved priceless and seemingly limitless. The glass chips were manufactured by a small team of experts in the field of glass microfluidic devices, led by Philip Homewood, at the Dolomite Centre. Further collaborative and concurrent work was conducted with and by scientists, including Robin Grenfell, Brian Goody, Alice Harling, Paul Brewer, Gergely Vargha and Martin Milton, at NPL. Many other people contributed to the overall success of this work, in particular my supervisor, Professor Alastair Lewis, Dr Jacqueline Hamilton, Professor Keith Bartle, Dr Samuel Edwards, Richard Lidster and Steve Andrews, all of whom proved to be invaluable sources of advice, practical help, encouragement, support and friendship.

The task of preparing this thesis has, thus, been to extract from these, (oftentimes) shared activities a coherent body of work, and one that I can call my own. My primary role within the overall project has been focused on the areas that affect chromatographic success, i.e. column coating, solvent evaporation, modulation to achieve two-dimensional separation, method development and general chromatographic optimisation and development using the glass devices. On Dr Rhodes' departing of the research group, my role was expanded to include electronic and software related work as well. This thesis emulates the above, with the central theme being chromatography and the work done to perfect this.

As this project encompassed a number of different and broad areas of science, a background to the main subject areas are provided by the first four chapters.

The first chapter gives detail on atmospheric chemistry – what it is, why it is an essential scientific field, and the overall challenges faced within it. The second chapter focuses on the principles of chromatography as an analytical technique, with particular focus on gas chromatography. This chapter examines the important factors that require careful consideration when developing an analytical method and much of what is described here formed the basis or the drive of the experimental work. Chapter 3 follows the evolution of the established technique of GC to two-dimensional gas chromatography, indicating how this comprehensive technique has the separating power to resolve hundreds and even thousands of peaks in very complex samples, such as air. Finally, in Chapter 4, a thorough literature review is provided on instrument and GC miniaturisation, allowing for the discernment of where and how the developed device “fits in” within the field. The remaining chapters detail and present the experimental thinking, processes and results of the lab-on-a-chip GCxGC project. The experimentation recounted is not reported in the chronological order in which it was conducted, but has rather been written in a fashion to allow an understanding of the various steps that took place and the thought processes behind them.

References

1. Lewis, A.C., et al., *Microfabricated planar glass gas chromatography with photoionization detection*. *Journal of Chromatography A*, 2009. **1217**(5): p. 768-774.
2. Halliday, J., et al., *Lab-on-a-Chip GC for Environmental Research*. *Lc Gc Europe*. **23**(10): p. 514-+.

Acknowledgements

I would like to start by thanking my supervisor, Professor Ally Lewis. I appreciate all the help, advice, support and encouragement you have provided over the years. I will always be grateful to you for this amazing opportunity – I can't even imagine how different my life would be if I hadn't been so won over by your enthusiasm for the project that I didn't even think twice about starting over in a new country.

I would also like to thank Dr Jacqui Hamilton. Not only have you been an invaluable source of knowledge and ideas, but your friendship and the personal support you've provided have made a massive impact on me.

Thanks goes to Dr Chris Rhodes for all the practical and electronic work he did for the project. Without you this project would never have even started, never mind come to completion. Thank you also to Dr Sam Edwards for his electronics work and (more importantly) for keeping me entertained during the long hours in the lab.

To my fellow PhD students and the Post-Docs who "looked after us", thank you for the wild nights, the laughs, the impromptu lab "experiments", and for being there with me every step of the way. Particular thanks go to Richard Lidster, Steve Andrews and Shalini Punjabi for brainstorming sessions and work-related support. Overall, a big thank you goes to Richard, Steve, James, Kelli, Sam, Shalini, Marvin, Martyn, Rosie, Xiaobing, Ruth, Katie, Jimmy, Mustafa, and Sarah for making "work" so much fun.

To Kyle and Keegan, thank you for being the most supportive siblings anyone could ever wish for (and for being my best friends!). I know you are (probably) the only people to read this thesis who don't actually *have* to read it, and I can't express enough how grateful I am for your proofreading services (and yes, I will return the favour!). You two have kept me sane through this process, and have always made sure I didn't dissolve into a big puddle of stress. Thank you to my baby sister Josie as well for always bringing a smile to my face.

An enormous thank you goes to my amazing Mom and Dad. Your love, patience, encouragement, understanding and will for me to succeed has motivated me to become the person I am today and to achieve all that I have. I genuinely would not have survived this without you. I love you both very much.

To Chris, thank you for being my knight in shining armour. Thank you for looking after me and loving me. Thank you for all the massages, cups of coffee and words of encouragement. You have been so patient these last few months. I can't wait to properly start our life together! We have so much to look forward to.

My beautiful hairy babies, Millie and Alfie (and Tofu and Mylo), thank you for always being able to make me smile and always being ready for a cuddle! Your lovely puppies are the best things to have happened to me yet.

To Brian and Denise, thank you for seeing this through with me. Without your visits, phone calls, texts and emails I would have been lost. I promise there will be much more visiting now and face-to-face conversations again. Your friendship means the world to me, and I hope I can provide you both with the love and support through your good and bad times that you have always provided me.

There are so many more people to thank, and two pages of writing is not enough to summarise my gratitude to everyone who has helped in any way, big or small, in making this project a success.

Thank you!

Author's Declaration

I, Jaydene Halliday, declare that, except where explicit reference is made to the contribution of others, this thesis is the result of my own work. It is being submitted for the degree of Doctor of Philosophy at the University of York. It has not been submitted for any other degree or examination at the University of York or any other institution.

Jaydene Halliday
York, September 2012

1.0 The Atmosphere

1.1 The Composition of the Atmosphere

The Earth's atmosphere contains several different layers, as illustrated in Figure 1. These can be defined according to air temperature as follows:

1. The troposphere (decreases from $\sim 15\text{ }^{\circ}\text{C}$ to $-55\text{ }^{\circ}\text{C}$)
2. The stratosphere (increases from $\sim 55\text{ }^{\circ}\text{C}$ to $-5\text{ }^{\circ}\text{C}$)
3. The mesosphere (decreases from $\sim -5\text{ }^{\circ}\text{C}$ to $-90\text{ }^{\circ}\text{C}$)
4. The thermosphere (increases from $\sim -90\text{ }^{\circ}\text{C}$ to $1,500\text{ }^{\circ}\text{C}$)
5. The exosphere (day time = $1,500\text{ }^{\circ}\text{C} +$; night time = absolute zero)^[8].

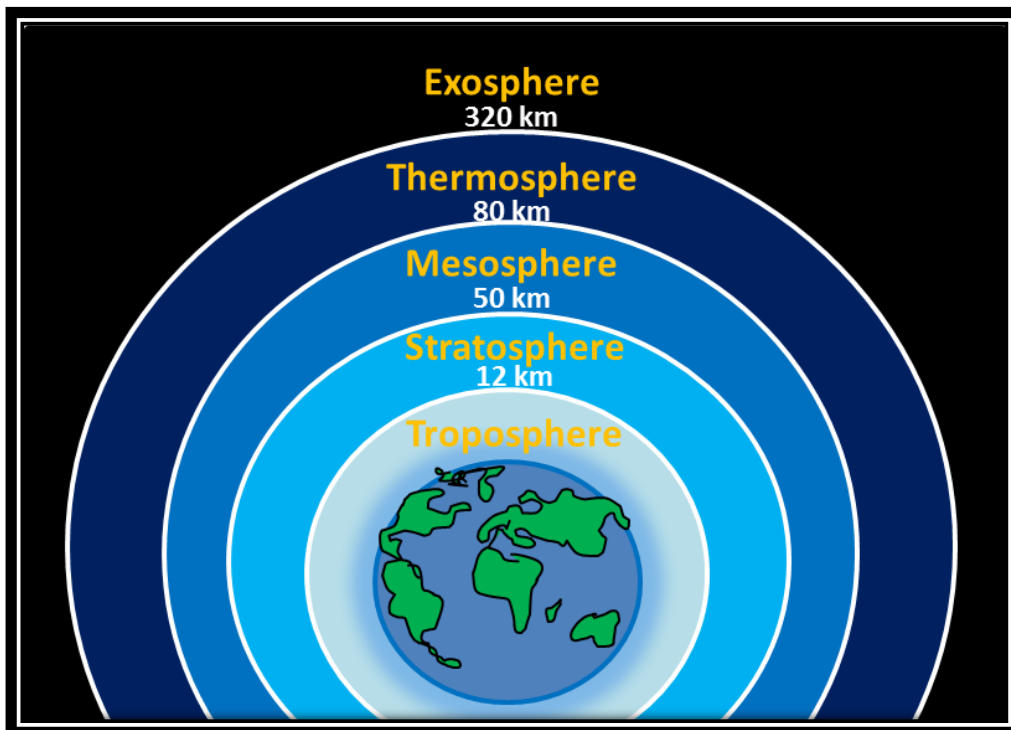


Figure 1: The Earth's atmosphere

The earth's atmosphere is composed of a very thin, well mixed layer of the gases listed in Table 1.

1.1.1 The Troposphere

The troposphere is the lowest portion of Earth's atmosphere, and is the region in which we live and into which chemical compounds are generally emitted as a result of human activities. It contains approximately 75% of the atmosphere's mass and 99% of its water vapour and aerosols^[10].

Table 1: Composition of pure dry air^[11]

Constituent Gas	By Mass (%)	By Volume (%)	Molecular Weight
Nitrogen (N₂)	75.51	78.09	28.02
Oxygen (O₂)	23.14	20.95	32.00
Argon (Ar)	1.3	0.93	39.94
Carbon Dioxide (CO₂)	0.05	0.03	44.01
Neon (Ne)	1.2×10^{-3}	1.8×10^{-3}	20.18
Helium (He)	8.0×10^{-4}	5.2×10^{-4}	4.00
Krypton (Kr)	2.9×10^{-4}	1.0×10^{-4}	83.7
Hydrogen (H₂)	0.35×10^{-5}	5.0×10^{-5}	2.02
Xenon (X)	3.6×10^{-5}	0.8×10^{-5}	131.3
Ozone (O₃)	0.17×10^{-5}	0.1×10^{-5}	48.00
Radon (Rn)	-	6.0×10^{-18}	222.00

It is also the layer where the majority of the world's weather takes place. The troposphere extends from the Earth's surface to the tropopause at 10-18 km and it is deeper in the tropical regions and shallower near the poles. The troposphere is characterised by generally decreasing temperature with increasing altitude from an average of 289 K at ground level to 210-215 K at the tropopause^[9]. Pressure decreases monotonically, with increasing altitude, from an average of 1,012 mbar at the Earth's surface to 140 mbar at the tropopause.

The lowest km or so of the troposphere contains the planetary boundary layer and inversion layers, with vertical mixing between the boundary and inversion layers and the free troposphere above them being hindered.

The transfer of energy between the surface of the Earth and the atmosphere is controlled by the processes of conduction, convection and radiation. Ocean currents also play a significant role in transferring this heat towards the poles, and contribute to the development of many types of weather phenomena.

1.1.2 The Stratosphere

The stratospheric ozone layer is the planet's natural sunscreen. Unfortunately, it has thinned during the past few decades because of the rise in atmospheric pollutants, such as chlorofluorocarbons (CFCs). This has allowed more ultraviolet (UV) radiation to reach many parts of the planet's surface since the 1970's. However, other forms of pollution have helped to shield Earth from UV rays.

Using an atmospheric radiation model, Gunnar Myhre of the University of Oslo and colleagues found that since 1750 pollutants such as sulphate, soot particles, sulphur dioxide (SO₂) and nitrogen dioxide (NO₂) have actually reduced the amount of UV light reaching some industrialised regions by as much as 20%^[12]. By scattering or absorbing UV light, such pollution may be masking some of the effects of ozone depletion.

Molecular oxygen (O₂) and ozone (O₃) in the stratosphere absorb UV radiation below ≤ 290 nm, therefore only solar radiation of wavelength ≥ 290 nm is transmitted through the stratospheric ozone layer into the troposphere and impacts the Earth's surface. Any depletion of stratospheric ozone allows shorter wavelength radiation to be transmitted through the stratosphere into the troposphere leading to increased photodissociation rates in the troposphere and not yet fully understood effects on tropospheric chemistry.

Because of the presence of high mixing ratios of O₃ in the stratospheric ozone layer, with a peak mixing ratio of $\sim 10 \times 10^{-6}$, there is net transport of O₃ by eddy diffusion from the stratosphere into the troposphere^[9]. In addition to this net downward transport of O₃ from the stratosphere, O₃ is formed photochemically in the troposphere from the interactions of VOCs and nitrogen oxides (NO_x) in the presence of sunlight. These sources of tropospheric O₃ are balanced by in situ photochemical destruction and by dry deposition at the earth's surface.

The result of downward transport of stratospheric ozone, in situ formation and destruction, and dry deposition at the Earth's surface is the presence of ozone in the "clean" natural troposphere. Ozone mixing ratios at "clean"

remote sites at ground level are in the range $(10^{-40}) \times 10^{-9}$ and tend to increase with increasing altitude^[9].

1.1.3 The Mesosphere

The mesosphere starts at a height of 50 km above the Earth's surface and extends to approximately 85 km high. It is flanked on either side by the mesopause, which is the boundary between the mesosphere and the thermosphere above it, and the stratopause below. It is an important area of the atmosphere because of the chemistry which occurs there, and the ionization of molecular O_2 and atomic O causing them to release electrons. This ionization is mainly due to incoming solar radiation and only takes place during the day. As with the troposphere, the mesosphere is mostly comprised of nitrogen and oxygen, as well as some minor gas constituents, such as ozone. O_3 reaches a maximum of concentration low in the stratosphere, resulting in a maximum of solar heating near the stratopause. Due to the low levels of ozone in the mesosphere, temperatures in this region of the atmosphere decrease significantly with altitude as less heating occurs due to UV absorption. Also, trace concentrations of CO_2 found in the mesosphere have a cooling effect as it radiates any heat into space. The top portion of the mesosphere is the coldest part of the Earth's atmosphere, with temperatures of $-90\text{ }^\circ\text{C}$ and lower being reached^[13]. Beyond this atmospheric layer temperatures rise again as a result of reduced radiative cooling combined with heating by absorption of short wavelength, i.e. $< 180\text{ nm}$, UV radiation by O_2 , O atoms and N_2 ^[14]. A feature of the mesosphere is that it exhibits both turbulence and atmospheric waves due to the decrease in temperature coupled with the low density of the air. This results in important mixing and transport of both biogenic and anthropogenic atmospheric chemicals, with rapid migration, often in less than six months, to any latitude^[15].

1.1.4 The Thermosphere

The thermosphere extends from the mesopause at about 90 km to 500–1,000 km above the Earth, where it meets the thermopause. Despite featuring extremely low air density, and being the area in which both the space shuttle and the International Space Station orbit the Earth, this atmospheric layer is considered part of the Earth's atmosphere. As previously mentioned, temperatures climb sharply in the thermosphere below altitudes of

approximately 300 km. After this point, temperatures plateau, maintaining a steady level with increasing altitude. Extreme temperatures ranging from about 500 °C up to 2,000 °C or even higher are seen in this layer of the atmosphere. Daytime temperatures tend to be about 200 °C – 500 °C hotter than at night, depending on solar activity. Collisions occur so infrequently between gas particles from the thermosphere and above that they become separated based on the types of chemical elements they contain. Energetic UV and X-ray photons from the sun also break apart molecules in the thermosphere, where atomic oxygen (O), atomic nitrogen (N), and helium (He) are the main components of air.

Much of the X-ray and UV radiation from the sun is absorbed in the thermosphere. When the sun is very active and emitting more high energy radiation, the thermosphere gets hotter and expands. Because of this, the height of the thermopause varies. High-energy solar photons also tear electrons away from gas particles in the thermosphere, creating electrically-charged ions of atoms and molecules. Earth's ionosphere, composed of several regions of such ionized particles in the atmosphere, overlaps with and shares the same space with the electrically neutral thermosphere. Moving ions, dragged along by collisions with the electrically neutral gases, produce powerful electrical currents in some parts of the thermosphere^[16]. Charged particles (electrons, protons, and other ions) from space collide with atoms and molecules in the thermosphere at high latitudes, exciting them into higher energy states. Those atoms and molecules shed this excess energy by emitting photons of light, which we see as colourful auroral displays, i.e. the Southern and Northern Lights^[17].

1.1.5 The Exosphere

The exosphere is wedged between the thermopause below it, also sometimes known as the exobase, and the vacuum of outer space above. The air in this layer is so thin that there is debate as to whether or not it can be considered a part of Earth's atmosphere, especially as it does not possess a clear upper boundary. One definition of the exosphere specifies it to extend to the point where radiation pressure from sunlight exerts a stronger force on hydrogen atoms than the pull of the Earth's gravity. This is around 190,000 km or approximately halfway to the moon^[18].

1.2 Atmospheric chemistry

Atmospheric chemistry is a multidisciplinary branch of atmospheric science, which studies the composition of the Earth's atmosphere, as well as other planets, changes induced by biogenic and anthropogenic processes, the emission, transport and deposition of atmospheric chemical species, the rates and mechanisms of chemical reactions taking place in the atmosphere, and the effects of atmospheric species on human health, the biosphere and climate. Research in this field may include environmental chemistry, physics, meteorology, computer modelling, oceanography, geology, volcanology and climatology, amongst other disciplines.

There are various reasons as to why the composition and chemistry of the atmosphere are important. One of the most significant is the interactions that take place between the atmosphere and living organisms. The composition of the Earth's atmosphere changes regularly as a result of natural processes such as lightning, volcanic emissions and bombardment by solar particles from corona, and also as a result of human activity, much of which is associated with our increasing use of fossil fuels as an energy source for things such as heating, transportation, and electric power production. These changes alter the energy balance of the climate system and are drivers for climate change. They affect absorption, scattering and emission of radiation within the atmosphere and at the Earth's surface. Unfortunately, not all of these changes produce positive results and many, including acid rain and photochemical smog formation, toxic air pollution, ozone depletion, increases in greenhouse gases and global warming, can be harmful to human health, crops and ecosystems^[19, 20]. The resulting positive or negative changes in energy balance due to these factors are expressed as radiative forcing (RF), which is used to compare warming or cooling influences on global climate. Figure 2 shows the global average radiative forcing in 2005 for CO₂, CH₄, N₂O and other important agents and mechanisms, along with the current assessed level of scientific understanding (LOSU)^[6].

It is the job of the atmospheric chemist to seek to understand the causes of the above problems by studying the photochemistry of the molecular constituents of air, the formation and properties of airborne particles, cloud processing of materials, transport and dispersion of chemical tracers, and biogeochemical

cycles. Through this they are able to obtain a theoretical understanding of the atmospheric problems faced and can develop instruments and models for studying the atmosphere. This allows for the devising and testing of possible solutions, and often results in changes, for the better, to government policy.

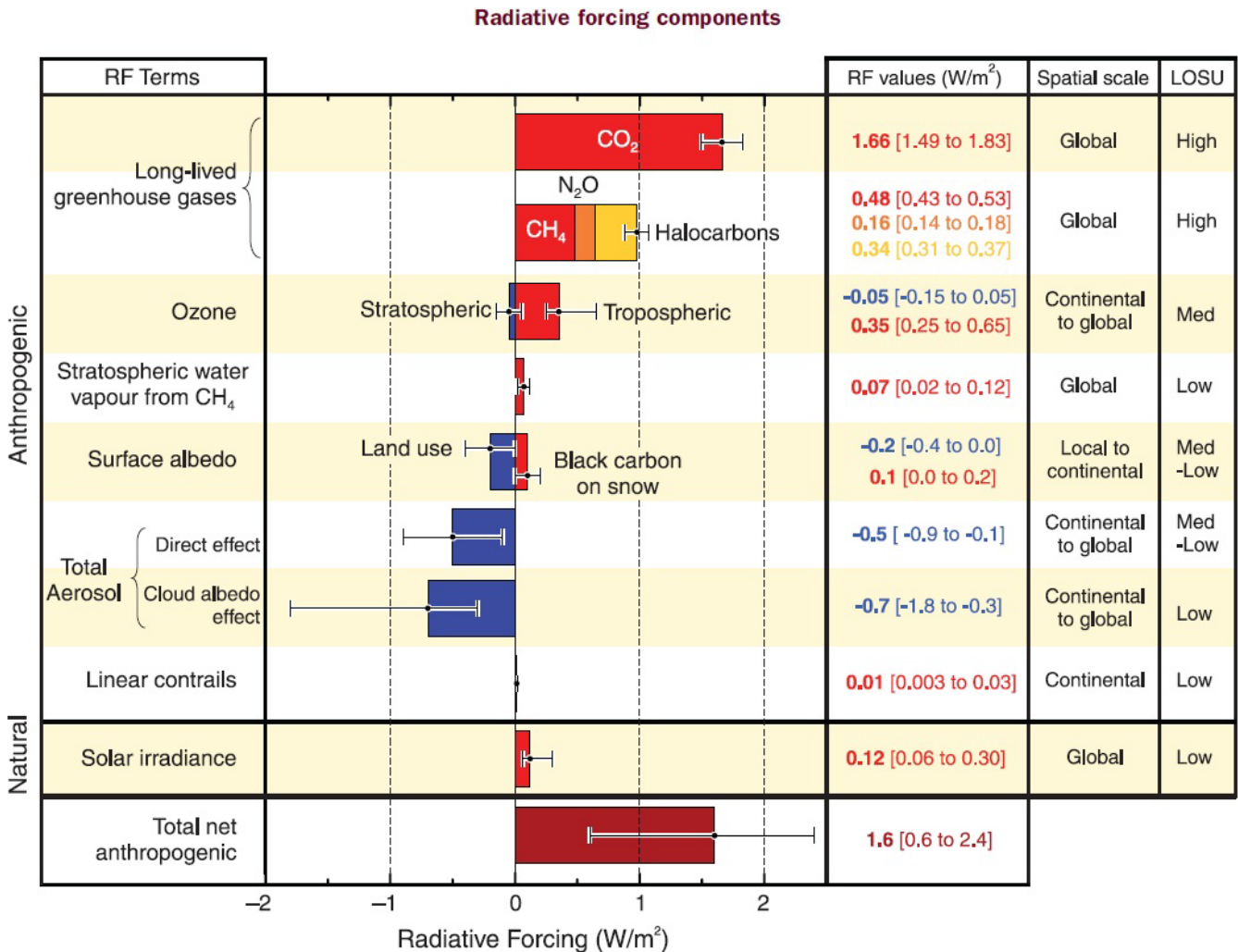


Figure 2: Global average radiative forcing in 2005 for CO₂, CH₄, N₂O and other important agents and mechanisms, together with the typical geographical extent (spatial scale) of the forcing and the assessed level of scientific understanding (LOSU)^[6]

1.2.1 The History of Atmospheric Chemistry

The field of atmospheric chemistry could be considered relatively new, with increasing attention being paid to it since the advent of the industrial revolution and increase in atmospheric pollution and the various environmental problems that has induced. The first scientific studies of atmospheric composition began in the 18th century, with Joseph Priestly^[21], Antoine Lavoisier^[22] and Henry Cavendish^[23] being the first to make

measurements of the composition of the atmosphere. Interest shifted towards trace constituents with very small concentrations in the late 19th and early 20th centuries, with one of the most important discoveries, that of ozone, being made by Christian Friedrich Schönbein in 1840^[24]. The 20th century saw an increase in the consideration of how the concentrations of trace gases in the atmosphere have changed over time and the chemical processes which create and destroy compounds in the air.

Finally, in 1995, the importance of atmospheric chemistry was acknowledged when the atmospheric scientists Paul Crutzen, Mario Molina and Frank Sherwood Rowland were awarded the Nobel Prize in Chemistry^[25].

In the 21st century the focus is, yet again shifting. Rather than concentrating on atmospheric chemistry in isolation, the focus is now on seeing it as one part of a single system with the rest of the atmosphere, biosphere and geosphere. An important driver for this is the link between chemistry and climate, such as the effects of the changing climate on the recovery of the ozone hole and vice versa, and the interaction of the composition of the atmosphere with the oceans and terrestrial ecosystems.

1.2.2 Atmospheric Chemistry Methodology

The central elements in atmospheric chemistry are observation (field measurements and remote sensing), atmospheric modelling and laboratory studies of gases, aerosols, clouds and precipitation, isotopes, radiation, dynamics, biosphere interactions, and hydrosphere interactions. Progress in the field is generally driven by interactions between these components, allowing them to form an integrated whole.

1.2.2.1 Observations

Observations of atmospheric chemistry are essential. The need for detailed, repeated, and global scale observations of the chemical composition of the atmosphere is driven by the quest to increase scientific understanding of the multitude of chemical and physical processes in the earth's atmosphere. Those observations having no obvious explanation stimulate new modelling and laboratory studies, allowing atmospheric chemists to establish the

atmosphere's composition in ever-increasing detail, and hence follow and, importantly, understand its changes^[26].

Routine observations of chemical composition give an idea of changes in atmospheric composition over time. An important example of this is the Keeling Curve, which is a series of measurements showing the on-going change in concentration of CO₂ in the Earth's atmosphere from 1958 to the present day. The graph is based on continuous measurements taken at the Mauna Loa Observatory in Hawaii, and showed the first significant evidence of rapidly increasing CO₂ levels in the atmosphere, a product of fossil fuels burning^[5]. These very precise measurements resulted in global concern over the build-up of CO₂ in the atmosphere, eventually leading to the tracking of greenhouse gases worldwide.

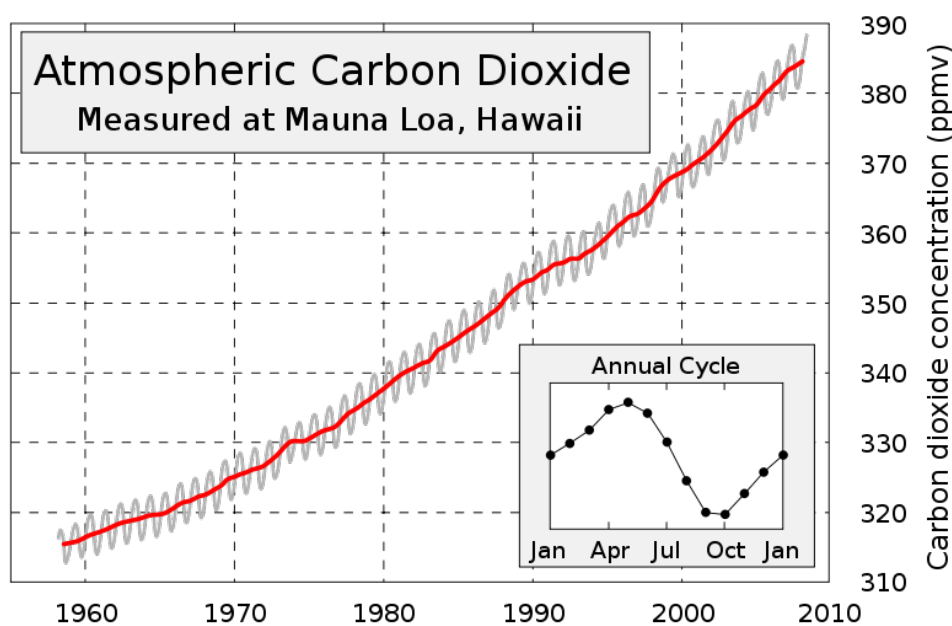


Figure 3: The Keeling Curve: Atmospheric CO₂ concentrations as measured at Mauna Loa Observatory^[5]

In order to make observations of, for example, the transport and transformation of organic pollutants, detailed field measurements of atmospheric composition are first required. Atmospheric chemistry field work directly probes the atmosphere, utilising various instruments which could be located:

- In ground-based observatories, such as that on Mauna Loa or at the Cape Verde Atmospheric Observatory (CVAO)^[27]

- On mobile platforms, such as the UK's Facility for Airborne Atmospheric Measurements (FAAM)^[28] and MOZAIC (Measurement of OZone and water vapour by Airbus in-service aircraft)^[29]
- On ships, such as that used during the Stratospheric Ozone: Halogen Impacts in a Varying Atmosphere (SHIVA) project^[30].

The term remote sensing is used to describe the science of observing and measuring an object without coming into direct contact with it, such as by way of:

- Balloons, such as those used by the Network for the Detection of Atmospheric Composition Change (NDACC)^[31] and Ozone Sonde Observations of Syowa Station^[32]
- Satellites, e.g. the Atmospheric Chemistry Experiment (ACE)^[33], the Upper Atmosphere Research Satellite (UARS)^[34], the Global Ozone Monitoring Experiment (GOME)^[35] and Measurements of Pollution in the Troposphere (MOPITT)^[36]
- Space shuttle platforms, e.g. the Atmospheric Trace Molecule Spectroscopy (ATMOS) experiment^[37] and Cryogenic Infrared Spectrometers and Telescopes for the Atmosphere (CRISTA)^[38].

Instruments used for this kind of work can be divided into two types, i.e. passive and active.

Passive instruments detect natural energy that is reflected or emitted from the observed scene, thus, the radiation that is sensed is that which has been emitted by the object being viewed or reflected by the object from a source other than the instrument itself. The most common external source of radiation sensed by passive instruments is reflected sunlight. Examples of passive remote sensors that are used by scientists include radiometers, spectrometers^[26], and spectro-radiometers.

Active instruments, on the other hand, provide their own energy, or electromagnetic radiation, which is used to illuminate the object or scene being observed. A pulse of energy is sent from the sensor to the object. The reflected or backscattered radiation is then measured by the instrument. As with passive remote sensors, many different types of active remote sensors

are used, including radars, scatterometers, Light Detection And Radar (LIDAR), and laser altimeters^[39, 40].

1.2.2.2 Atmospheric Modelling

Computer models are used to synthesise and test theoretical understanding of atmospheric chemistry. Numerical models solve the differential equations governing the concentrations of chemicals in the atmosphere. Atmospheric modelling and analysis scientists are responsible for providing a sound scientific and technical basis for regulatory policies to improve ambient air quality. Predictive atmospheric models are developed and evaluated on all spatial and temporal scales for assessing changes in, for example, air quality and air pollutant exposures. Comprehensive Eulerian air quality models are used to account for many of the major processes in the atmosphere that are considered key in determining the distributions and levels of the atmospheric chemical species. This is accomplished through detailed simulation of various physical and chemical processes such as horizontal and vertical transport, diffusion, emissions, deposition, chemistry, and cloud processes^[41-43].

1.2.2.3 Laboratory Studies

Atmospheric laboratory work covers many different areas, from the development of new instruments and improving current techniques, as demonstrated in this body of work, to analysing samples collected on field campaigns; from simulating the various reactions of certain atmospheric chemicals in smog chambers^[42] to predicting products and determining thermodynamic data such as Henry's Law coefficients^[44].

1.3 Atmospheric Pollutants of Concern

United Kingdom air quality is generally considered as being good. It has improved considerably over the last ten or so years. Tighter controls on pollutant emissions have resulted in the air over the UK being cleaner today than at any time since before the industrial revolution^[45]. The UK National Atmospheric Emissions Inventory (NAEI)^[46] compiles estimates of atmospheric emissions from UK pollution sources such as cars, trucks, power stations, industry and agricultural activities. The NAEI is continually improved and used to produce estimates of UK emissions on an annual basis. This information is reported annually to the European Commission and the United

Nations Economic Commission for Europe (UNECE), as required in the National Emission Ceilings Directive and the protocols under the Convention on Long-range Transboundary Air Pollution (CLRTAP)^[47, 48]. While, greenhouse gases are most active high in the atmosphere, in terms of air quality, the concentration of pollutants closer to the ground is the most important factor. Nevertheless, long-range transboundary air pollution is a phenomenon that occurs when air pollutants travel long distances. Along the way they chemically react in the atmosphere, resulting in the production of other pollutants. This effect culminates in air pollution problems, not only in the local areas where the pollutants are initially released, but also in areas a long way from the source.

Despite the significant reductions achieved, air pollution still causes considerable harm to both public health and the natural environment, and combative action needs to be ongoing, especially in built-up urban cities. Estimates indicate that air pollution reduces life expectancy in the UK by an average of six months, with estimated equivalent health costs of up to £20 billion each year^[45].

The main pollutants of concern in the UK include particulate matter (PM₁₀, PM_{2.5} and PM₁), oxides of nitrogen (NO_x), oxides of sulphur (SO_x), ammonia (NH₃), VOCs, and ground level O₃. Besides the damaging effects of short and long-term exposure to air pollution, ranging from premature deaths caused by heart and lung disease to worsening of asthmatic conditions, emissions of sulphur, nitrogen, and ammonia can also be deposited to land and water causing either acidification, or nutrient enrichment, i.e. eutrophication. This results in damage to biodiversity in both semi-natural environments and upland rivers and lakes. Ozone on the other hand, can lead to direct damage to crops and vegetation, affecting ecosystem function and resulting in loss of crop yields. Emissions of VOCs, NO_x, and sulphur compounds lead to a complex series of chemical and physical transformations which result in such effects as:

- The formation of O₃ in urban and regional areas, as well as in the global troposphere
- Acid deposition

- The formation of secondary particulate matter through gas/particle partitioning of both emitted chemical compounds and the atmospheric reaction products of VOCs, NO_x, SO₂, and organo-sulphur compounds.

Road transport, large fuel-burning plants such as power stations, and agriculture are key sources for many of these pollutants, and often of climate change-causing greenhouse gas emissions too. Links between air quality and climate change actions are critical, and many of the actions to mitigate against climate change will also reduce air pollution in the long term.

1.3.1 Particulate Matter (PM)

The most dangerous air pollutant in terms of health effects is particulate matter (PM). PM is a mixture of solid particles and liquid droplets, and can include dust, dirt, soot, and smoke. There are three sizes of particles that cause particular concern, i.e. PM₁₀, PM_{2.5} and PM₁. PM₁₀ describes “coarse” particles with a diameter of 2.5 – 10 μm. To put this into perspective, PM₁₀ particles are one-seventh the width of a human hair^[1], as illustrated in Figure 4. These particles are composed of aluminosilicate and other oxides of crustal elements. Major sources include fugitive dust from roads, industry, agriculture, construction and demolition, and fly ash from fossil fuel combustion. The lifetime of PM₁₀ is from minutes to hours, and its travel distance varies from <1 km to 10 km^[49].

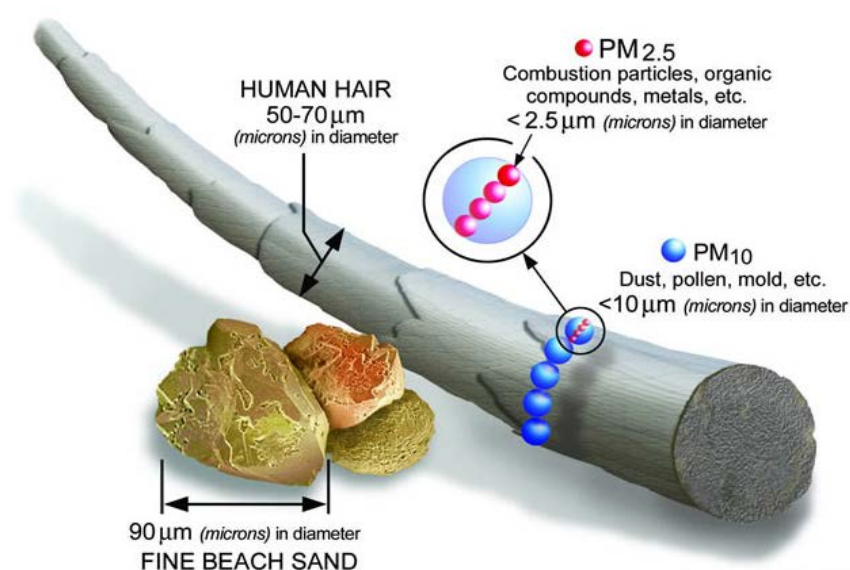


Figure 4: The size of particle pollution^[1]

Finer particles, those smaller than $2.5\ \mu\text{m}$ in diameter, are designated $\text{PM}_{2.5}$. These are the major cause of reduced visibility or haze seen in many parts of the country and can be subdivided into two different types, namely primary and secondary particles.

Primary particles are those that are emitted directly into the atmosphere from combustion processes, i.e. from vehicle exhausts or chimneys, construction sites, unpaved roads, and fields. These are generally very small, often less than $1\ \mu\text{m}$ in diameter (i.e. ultrafine particulate matter or PM_1).

Secondary particles are those which are formed in the atmosphere (as shown in Figure 5) by complicated reactions between other pollutants, and are composed of various combinations of sulphate compounds, nitrate compounds, carbon compounds, ammonium, hydrogen ions, organic compounds, metals (Pb, Cd, V, Ni, Cu, Zn, Mn, and Fe), and particle bound water.

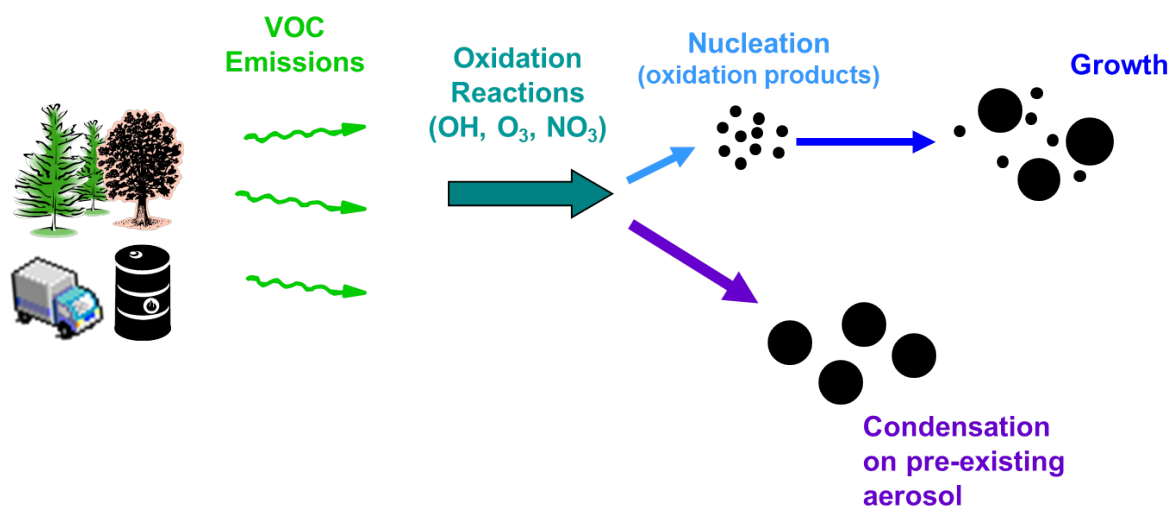


Figure 5: Schematic of secondary particulate matter/secondary organic aerosol formation

These are generally less than $2.5\ \mu\text{m}$ in diameter, but the size tends to vary depending on humidity. Their lifetime is from days to weeks and travel distance ranges from $100\ \text{km}$ to $>1,000\ \text{km}$ ^[50].

Table 2: Components of particulate matter

Precursors of Primary PM	Sources
Sodium Chloride (NaCl)	Sea salt
Elemental carbon	Black carbon (soot) formed during high temperature combustion of fossil fuels, e.g. coal, natural gas, oil, biomass fuels
Trace metals	Generated by metallurgical processes, such as steel making or by impurities in fuels, e.g. lead, cadmium, nickel, chromium, zinc, manganese
Minerals	Found in coarse dusts from quarrying, construction and demolition work, e.g. aluminium, silicon, iron, calcium
Precursors of Secondary PM	Sources
SO ₂	Formed by combustion of sulphur-containing fuels, e.g. coal
NO _x	Formed by combustion of fuels used in power generation, domestic heating, traffic
NH ₃	Emitted from agricultural sources, livestock waste
VOCs	Aromatic compounds, e.g. benzene and toluene, are generated by traffic and solvents Monoterpenes are emitted from vegetation, especially conifers and heathers

The World Health Organization (WHO) advises there is no safe exposure level to PM^[51]. Adverse effects on cardiorespiratory health leading to hospitalization and even premature mortality have been shown to be associated with even relatively low particulate levels, although the most serious health problems are among those susceptible groups with pre-existing lung or heart disease and/or the elderly and children. The detrimental impact of particles is most likely due to their small size, which allows them to deeply penetrate the lung. PM can also be absorbed into the bloodstream.

Particulate matter levels can vary according to the weather, time of year, and location, with exposure most likely to occur in the summer, when the sun and

hot temperatures react with pollution to form smog. UK estimates indicate that the short-term exposure to the levels of PM₁₀ experienced in 2002 led to 6,500 deaths and 6,400 hospital admissions being brought forward that year^[51], although it is not possible to know by what length of time those deaths were brought forward.

Measurements of the concentration of particulate matter in air, such as those shown in Figure 6, are made by recording the mass of particulate matter in one cubic metre of air, using the units micrograms per cubic metre ($\mu\text{g}\cdot\text{m}^{-3}$). Size-selective inlets are used to exclude particles greater than 10 μm from any analysis conducted as the air quality objectives are framed in terms of the concentration of PM₁₀. Any particulate matter is deposited on a filter, which is then weighed to determine the mass of particulate matter that was in that volume of air. The reference measurement method for the EU is known as the Tapered Element Oscillating Microbalance (TEOM) method. Here, a TEOM filter is mounted on a constantly vibrating tapered glass tube. Particles collect on the filter resulting in a slowing down of the vibration. This change in vibration is then very precisely measured without the need to stop sampling, thus giving a continuous measurement of the amount of particulate matter being collected^[51].

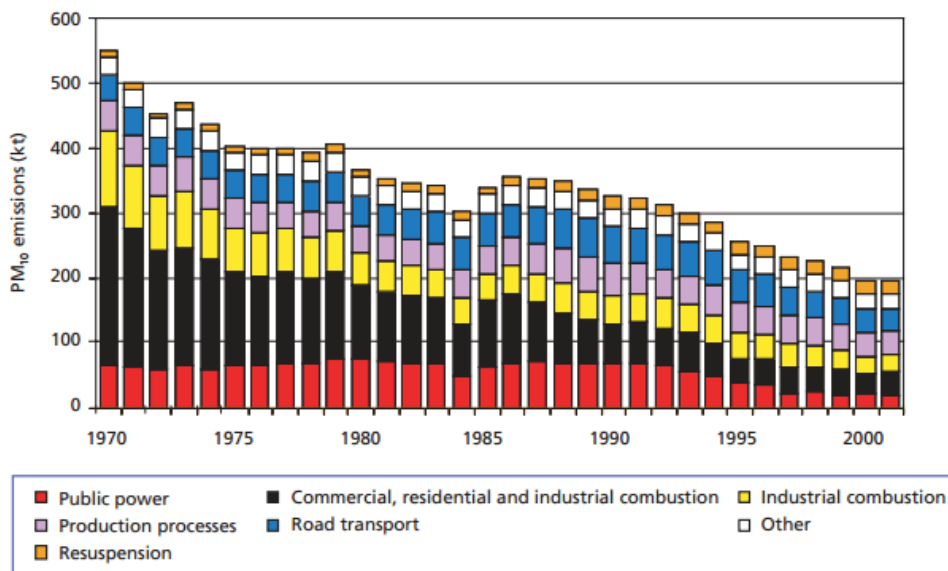


Figure 6: PM₁₀ emissions in kilotonnes in the UK by source from 1970 to 2001^[7]

1.3.2 Ammonia (NH₃)

Emissions of NH₃ are involved in the following processes:

- Acidification
- Nitrification
- Eutrophication
- Secondary particulate matter formation.

Agriculture, and in particular cattle and other livestock, is the prominent source of NH₃ emissions, accounting for 89% of ammonia emissions in 2009^[3], as illustrated by Figure 7.

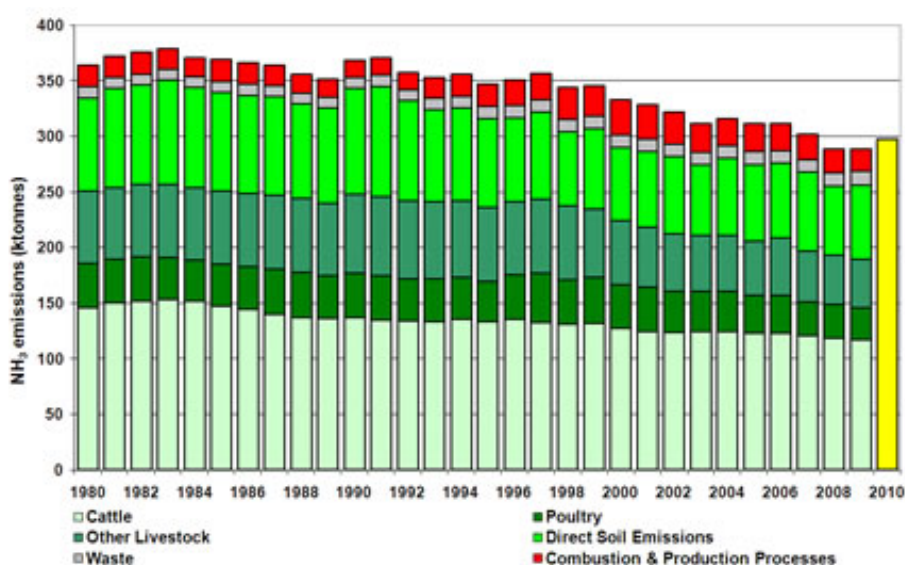


Figure 7: Ammonia emissions from 1980 to 2009^[3]

1.3.3 Sulphur Dioxide (SO₂)

SO₂, along with particulate matter, is involved in the formation of winter-time smog. Sulphur dioxide also has adverse health effects causing nerve stimulation in the lining of the nose and throat, resulting in irritation, coughing and chest tightness. Asthma sufferers are particularly sensitive to SO₂ concentrations^[52].

SO₂ can result in the formation of sulphuric acid (H₂SO₄) in the atmosphere, which is a major component of aerosols and an important contributor to acid deposition. Sources of SO₂ to the atmosphere include emission from combustion, smelters, volcanoes, and oxidation of oceanic dimethylsulphide ((CH₃)₂S) emitted by phytoplankton. About 75% of total sulphur emission to

the atmosphere is anthropogenic^[53]. In 2009, fuel combustion accounted for more than 92% of UK SO₂ emissions, with the largest contribution being from power stations, accounting for 40% of the total in 2009^[2]. Figure 8 below shows the emissions of SO₂ from 1970 to 2009.

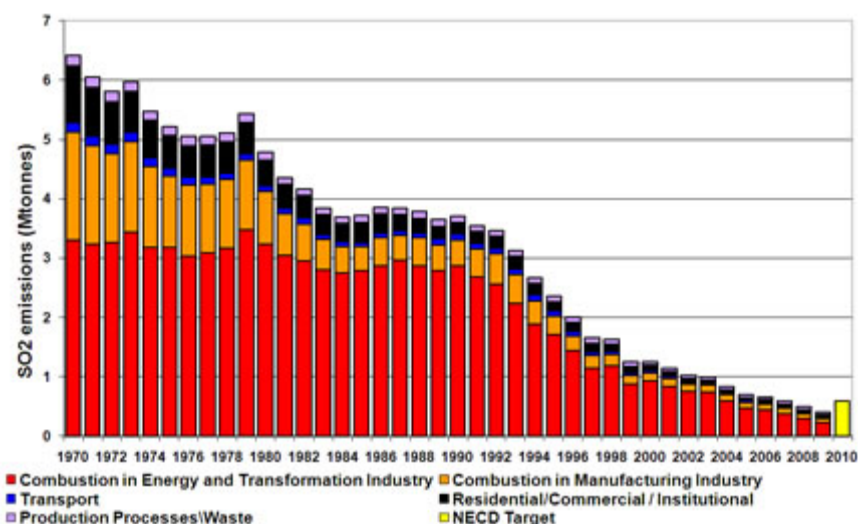


Figure 8: Emissions of SO₂ from 1970 to 2009^[2]

1.3.4 Nitrogen Oxides (NO_x)

Nitrogen oxides consist of nitric oxide (NO) and nitrogen dioxide (NO₂), and are formed when N₂ combines with O₂. These compounds are referred to as NO_x as they are rapidly inter-converted^[54]. Their lifespans in the atmosphere range from one to seven days. NO is rapidly oxidized to N₂O in air. N₂O is a greenhouse gas that absorbs light and leads to the yellow-brown haze sometimes seen hanging over cities. It is one of the important components of smog. NO_x are corrosive and hazardous to health, with exposure to high industrial levels of NO and NO₂ resulting in collapse, burning and swelling of tissues in the throat and upper respiratory tract, difficulty breathing, throat spasms, fluid build-up in the lungs, and even genetic mutations and death^[55]. NO_xs are also one of the precursors for photochemical ozone formation, and they contribute to wet and dry deposition of nitrogen in areas both close to and remote from sources.

Nitrogen oxides are produced in combustion processes, partly from nitrogen compounds in the fuel, but mostly by direct combination of atmospheric oxygen and nitrogen in flames. NO_xs are produced naturally by lightning,

which oxidizes atmospheric N_2 to NO_x , and also, to a small extent, by microbial processes in soils, for example, nitrification oxidizes ammonia to NO_2 or NO_3 , and biological growth and decay. Biomass burning, as in forest and grassland fires, also oxidizes organic nitrogen to produce NO_x ^[56].

Man-made or anthropogenic emissions of nitrogen oxides dominate total emissions in Europe, with the UK emitting about 2.2 million tonnes of NO_2 each year. Of this, about 25% is from power stations, 50% from motor vehicles, with vehicles travelling at high speeds contributing most, and the remaining 25% from other industrial and domestic combustion processes. Of the nitrogen oxides emitted, most is nitric oxide, some is nitrous oxide and less than 10% is nitrogen dioxide^[4]. The amount of nitrogen dioxide emitted varies with the temperature of combustion; as temperature increases so does the level of nitrogen dioxide.

Unlike emissions of sulphur dioxide, emissions of nitrogen oxides are only falling slowly in the UK, as evidenced by Figure 9, as emission control strategies for stationary and mobile sources are offset by increasing numbers of road vehicles.

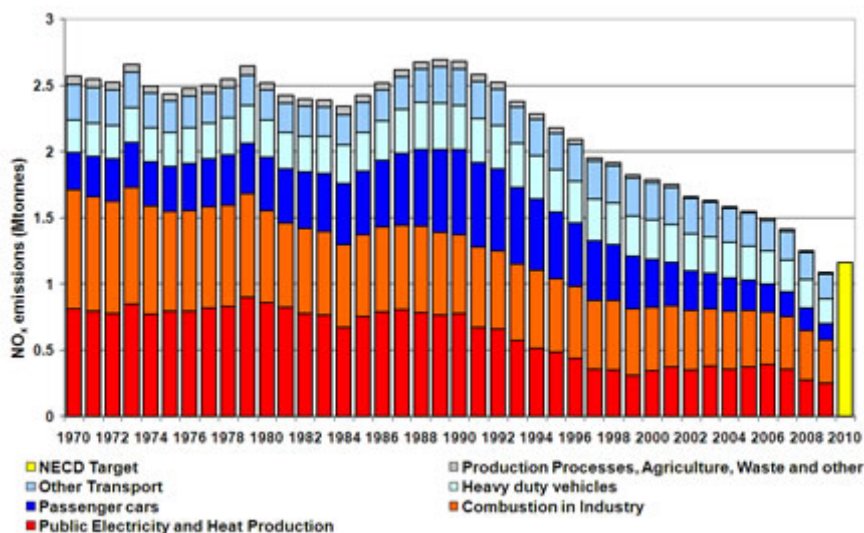


Figure 9: Emissions of NO_x from 1970 to 2009^[4]

1.3.5 Volatile Organic Compounds (VOCs)

A vast range of chemicals are emitted and processed in the atmosphere, and VOCs are a critical subset. They include:

- Alkanes (or paraffins)
- Alkenes (or olefins)
- Saturated and unsaturated alkyl halides
- Carbonyls
- Alcohols
- Aromatic and halogenated aromatic hydrocarbons.

WHO defines VOCs as organic compounds sampled on a solid sorbent and having a lower boiling point limit of 50–100 °C and an upper boiling point limit of 240–260 °C^[57]. The U.S. Environmental Protection Agency (EPA) defines them as those C₂–C₁₀ substituted and unsubstituted hydrocarbons with a vapour pressure greater than 0.1 mm·Hg (0.01 kPa) at 25 °C^[57].

VOCs are emitted from either biogenic, or natural, sources or anthropogenic, or man-made sources. In the UK it is estimated that less than 5% of the VOCs emitted into the atmosphere, i.e. 2.3 million tonnes per year, expressed in terms of carbon, are emitted from vegetation. The remainder originates from transport and vehicle emissions (both exhaust and evaporative), which have been shown to heavily contribute to urban VOC levels, solvent use and other industrial processes, such as the manufacture and use of petroleum products, biomass burning, landfills, sewage treatment plants^[57, 58]. The above measurements include only non-methane volatile organic compounds (NMVOC). Methane, whilst being a volatile hydrocarbon, is present in the atmosphere from natural sources at much larger concentrations than other VOCs, and so is generally considered separately. The largest emissions of individual VOCs are of the following:

- Butane
- Toluene
- Pentane
- Propane
- Ethanol
- 'White spirit'.

Alkanes account for approximately 50% of gasolines, and 50% of NMVOCs in vehicle exhaust and in ambient air in urban areas^[59].

Biogenic emissions account for over 90% of total VOCs entering the atmosphere^[57]. They consist principally of isoprenoids (or terpenoids), namely isoprene (a C₅ hydrocarbon) and monoterpenes (C₁₀ hydrocarbons

such as α -pinene, menthol, and camphor) as well as various aldehydes, ketones, organic acids, and alcohols. Because approximately 10% of ozone production appears to be due to isoprene chemistry, factors affecting emissions of isoprene (e.g. solar radiation, leaf temperature and duration of low temperature episodes) have been given particular attention. Algae and plankton release a variety of halocarbons found in marine emissions, including methyl iodide, methyl bromide, methyl chloride, dibromomethane and bromoform. One of the largest sources of chlorine in the stratosphere is methyl chloride, thought to arise principally from natural sources.

VOCs have always been the subject of analysis due to their role and importance in atmospheric chemistry. However, a clear understanding of the role of these compounds in the photo-oxidation mechanism, their distribution, variation with time, and health hazards requires long-term monitoring. Short term studies provide only limited information about the state of atmosphere at a specified time and location.

The monitoring and control of the emission of VOCs into the atmosphere is important for a number of reasons. Many VOCs, such as benzene, 1,3-butadiene, and formaldehyde^[60], cause serious health problems in the form of toxic, carcinogenic, and mutagenic effects. Studies have shown that VOCs contribute to sick building syndrome, and that they may account for 35–55% of outdoor air cancer risk. As well as the adverse effects of direct VOC emissions, VOCs also heavily contribute to secondary effects, such as the formation of ground-level tropospheric photochemical ozone, the enhancement of the global greenhouse effect, and the depletion of the stratospheric ozone.

Tropospheric ozone is a secondary photochemical pollutant resulting primarily from the reaction of VOCs with NO_x ^[43] in the presence of sunlight. It is a major component of smog and has adverse effects on human health, vegetation and materials.

Different VOCs can produce vastly different amounts of ozone. Ethene (C_2H_4), for example, can produce over 14 times more ozone than ethane (C_2H_6) under the same conditions. While much is known about the general chemical

reactions of the most-abundant VOCs in the atmosphere, there is still some uncertainty concerning the chemistry of many, less-abundant VOCs, including their exact chemical products and subsequent reactions of these products. Approximately 87% of the nearly 800 explicit compounds for which reactivities are available are estimated as being “uncertain”^[42].

1.3.6 Tropospheric Ozone (O₃)

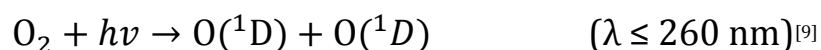
There are two main types of tropospheric ozone, i.e. O₃ which occurs naturally at ground-level in low concentrations and O₃ that is a result of anthropogenic activities. The first is formed by biogenic hydrocarbon emissions released by plants and soil, and also comprises small amounts of migrated stratospheric ozone. Natural ozone formation is of such low levels that it is not considered a threat to the health of humans or the environment.

However, the opposite is true for the latter type of ozone. O₃ differs from the majority of other pollutants in that it is not directly emitted into the atmosphere. Rather, tropospheric ozone is formed by the interaction of sunlight, particularly ultraviolet light, with hydrocarbons or VOCs and NO_x, which are emitted as described above. The amount of ozone near the earth's surface has more than doubled since 1900, due to human emission of ozone precursors, NO, NO₂, and VOCs.

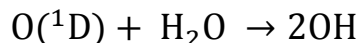
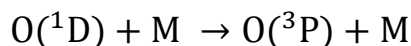
The ozone found in the stratosphere shields us from harmful UV radiation, however, direct exposure to this irritating, reactive molecule results in damage to forests and crops, as well as materials such as nylon, rubber, fibres, paints and textile dyes, amongst others. It also destroys living tissue, and so is hazardous to human health.

The formation of stratospheric ozone is the result of the photolysis of atmospheric oxygen into atomic oxygen in the presence of ultraviolet radiation from the sun, as follows:

Equation 1

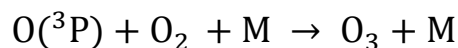


O(¹D) atoms either react with water vapour to generate OH radicals or are deactivated to ground-state oxygen, O(³P) atoms^[9]:

Equation 2**Equation 3**

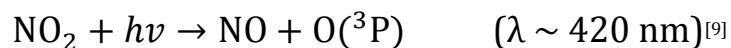
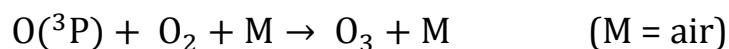
Where M = N₂ or O₂.

O(³P) can then bond with O₂ to form ozone:

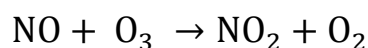
Equation 4

Where M = air.

Ozone can also be formed photochemically by the photolysis of NO₂ to give NO and an O atom, which then combines with molecular O₂ as follows^[52]:

Equation 5**Equation 6**

This occurs during the day, in the presence of hydrocarbons and UV light. The ozone then rapidly reacts with nitric oxide to create nitrogen dioxide and oxygen. This process, known as the Chapman Cycle, is illustrated in Figure 10.

Equation 7

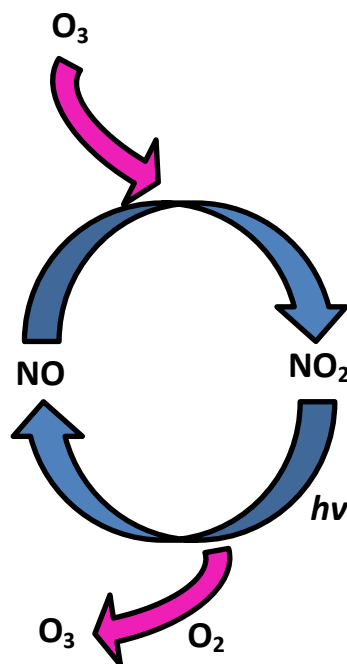
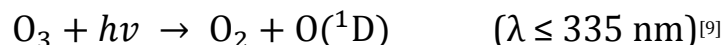


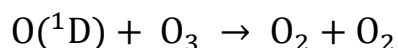
Figure 10: Schematic of the reactions involved in an NO-to-NO₂ conversion and O₃ formation in an NO-NO₂-O₃ system in the absence of VOCs^[9]

This process occurs naturally and means that during daytime hours a photoequilibrium (dependent on the amount of sunlight) exists between NO, NO₂ and O₃, with no net formation or loss of O₃^[9]. Eventually, NO₂ is oxidised to nitric acid (HNO₃) which is either absorbed directly at the ground, is converted into nitrate-containing particles, or dissolves in cloud droplets. At night, different oxidation processes convert NO₂ to nitrates. Upper atmospheric sunlight can also split ozone into oxygen atoms and oxygen molecules. Excited oxygen atoms can react with other ozone molecules, destroying them and creating two new oxygen molecules.

Equation 8



Equation 9



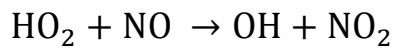
Thus, under natural conditions a balance exists between the creation and destruction of ozone molecules in the stratosphere.

1.3.6.1 Formation of Tropospheric Ozone

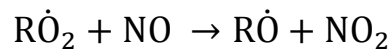
In the troposphere, ozone formation is also via the splitting of molecules by sunlight, as well as a number of other reaction pathways.

In the presence of VOCs, however, the formation of intermediate radicals results. These HO₂ and RÖ₂ radicals react with NO, converting it to NO₂:

Equation 10



Equation 11



This then photolyzes to form O₃. This overall process results in the net formation of ozone, as evidenced by Figure 11. Net photochemical formation of tropospheric O₃ versus net photochemical loss of O₃ is, therefore, dependent on the NO concentration, and is determined by the rate of the

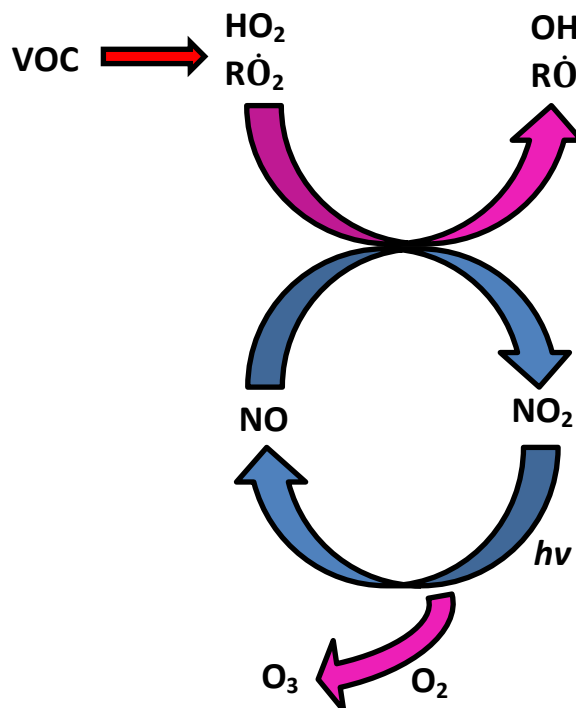
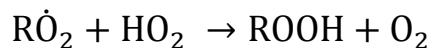


Figure 11: Schematic of the reactions involved in NO-to-NO₂ conversion and O₃ formation in an NO-NO₂-O₃ system in the presence of VOCs^[9]

reaction of the HO₂ and R \dot{O} ₂ radicals with NO, compared to those for reactions of the R \dot{O} ₂ radical with the HO₂ radical:

Equation 12

A general VOC degradation/transformation reaction scheme is illustrated in Figure 12.

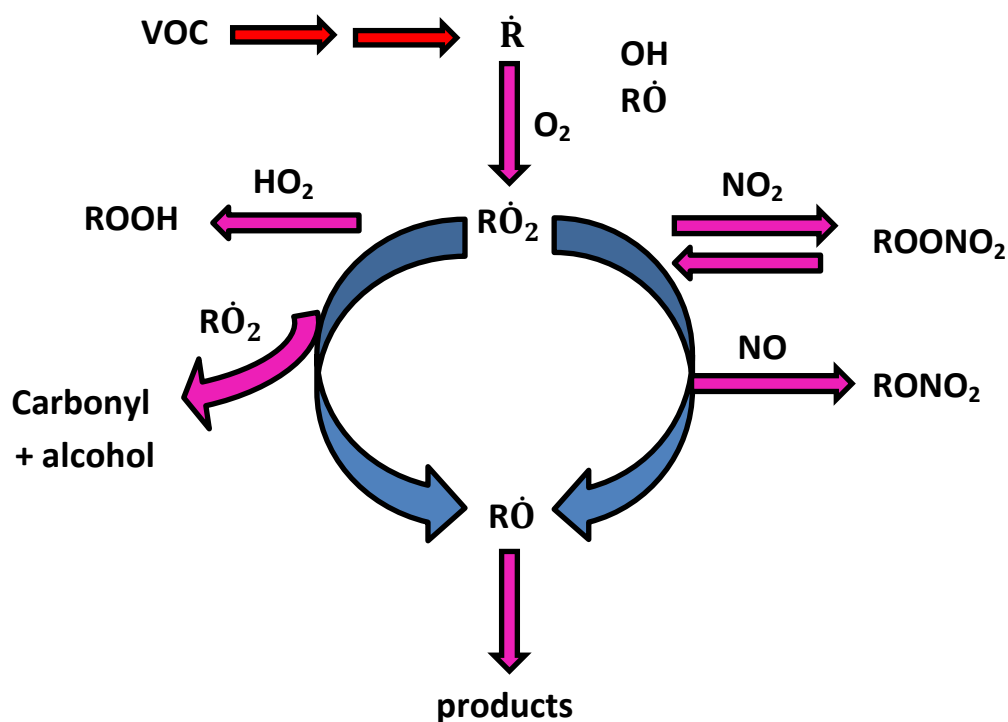
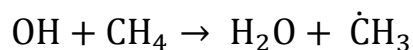
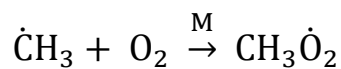
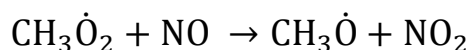
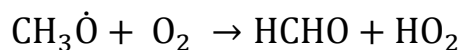
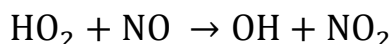


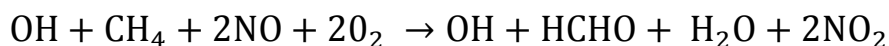
Figure 12: A typical VOC degradation scheme^[9]

The simplest VOC degradation scheme is that for methane. The tropospheric degradation of methane in the presence of NO leading to first-generation products is as follows:

Equation 13**Equation 14**

Equation 15**Equation 16****Equation 17**

This gives a net equation of:

Equation 18

Thus, it is clear to see that the only way to reduce ozone is to reduce the emissions of its precursors. As such, VOC monitoring and research towards the understanding of the degradation and transformation reactions of VOCs within the troposphere is vital. This research allows for the ranking of individual VOCs by their photochemical ozone creating potential (POCP)^[61], and enables prioritization of time, money and efforts with regard to the analysis of VOCs of importance.

1.4 A Summary

In order to establish a clear understanding of each of the above detailed compounds in terms of their distribution, variation with time, mechanisms, and, importantly, the health hazards they pose, a mixture of long and short term monitoring of the atmosphere is required. To date, control strategies for ozone precursors, NO_x, and VOCs have contributed to the reduction in emissions of these compounds, and consequently in the overall reduction of observed peak ozone concentrations at monitoring sites throughout the UK^[62].

The challenge, however, is still to detect trace amounts of VOCs and other atmospheric pollutants in complex matrices, such as air, with sufficient sensitivity. Generally, pre-concentration of the analytes of interest on a

sorbent material is used, followed by the separation and detection of the compounds via gas chromatography-flame ionisation detection (GC-FID) or gas chromatography-mass spectrometry (GC-MS), after thermal desorption or solvent extraction. Gas chromatography is the most widely used chromatographic technique for environmental and atmospheric analyses, and its use has been reported in countless journal articles across the world, with just a select few being referenced here^[57-60, 63, 64].

1.5 References

1. *Particulate Matter (PM)*. 2012 03/02/2012 [cited 2012 06/02/2012]; Available from: <http://www.epa.gov/pm/basic.html>.
2. *Sulphur dioxide*. 2012 2012 [cited 2012 06/02/2012]; Available from: http://naei.defra.gov.uk/pollutantdetail.php?poll_id=8.
3. *Ammonia*. 2012 2012 [cited 2012 06/02/2012]; Available from: http://naei.defra.gov.uk/pollutantdetail.php?poll_id=21&issue_id=1.
4. *Nitrogen Oxides*. 2012 2012 [cited 2012 07/02/2012]; Available from: http://naei.defra.gov.uk/pollutantdetail.php?poll_id=6&issue_id=1.
5. Simmon, R. *The Keeling Curve*. 2005 2011 [cited 2011 19/11/2011]; Available from: <http://earthobservatory.nasa.gov/IOTD/view.php?id=5620>.
6. Bernstein, L., et al, *Climate Change 2007: Synthesis Report*, A. Allali, et al, Editor. 2007, IPCC: sPAIN.
7. *PM₁₀ (particulate matter < 10 um)*. 2012 2012 [cited 2012 06/02/2012]; Available from: http://naei.defra.gov.uk/pollutantdetail.php?poll_id=24&issue_id=1.
8. Finlayson-Pitts, B.J., Pitts, J. N., *Chemistry of the Upper and Lower Atmosphere*. 1999, London: Academic Press. 969.
9. Atkinson, R., *Atmospheric chemistry of VOCs and NOx*. *Atmospheric Environment*, 2000. **34**(12-14): p. 2063-2101.
10. *Atmosphere*. 2011 01/01/2011 [cited 2011 09/10/2011]; Available from: http://www.meteoblue.com/fr_FR/content/449.
11. Saha, K., *The Earth's Atmosphere: Its Physics and Dynamics*. 2008, Germany: Springer.
12. *Atmospheric science: Industrial UV shield*. *Nature*, 2009. **462**(7270): p. 141-141.

13. Russell, R. *The Mesosphere*. 2008 17/07/2008 [cited 2011 08/09/2011]; Available from: <http://www.windows2universe.org/earth/Atmosphere/mesosphere.html>.
14. *Mesosphere and Mesopause*. 2011 2011 [cited 2011 08/09/2011]; Available from: <http://www.atoptics.co.uk/highsky/hmeso.htm>.
15. *Mesosphere*. 2011 2011 [cited 2011 08/09/2011]; Available from: <http://library.thinkquest.org/21418/spacee/Mesos.htm>.
16. Russell, R. *The Thermosphere*. 2008 28/07/2008 [cited 2011 08/09/2011]; Available from: <http://www.windows2universe.org/earth/Atmosphere/thermosphere.html>.
17. *Thermosphere - Overview*. 2011 2011 [cited 2011 08/09/2011]; Available from: <https://spark.ucar.edu/shortcontent/thermosphere-overview>.
18. *Exosphere - Overview*. 2011 2011 [cited 2011 08/09/2011]; Available from: <https://spark.ucar.edu/shortcontent/exosphere-overview>.
19. UCLA. *What is Atmospheric Chemistry*. [cited 2011 03/12/2012].
20. Wayne, R.P., *Chemistry of Atmospheres: An Introduction to the Chemistry of the Atmospheres of Earth, the Planets, and their Satellites*. 3rd ed. 2000, Oxford: Oxford University Press. 775.
21. Scratch, L.S. *Joseph Priestly*. 2012 2012 [cited 2012 04/01/2012]; Available from: <http://www.chemistryexplained.com/Pl-Pr/Priestley-Joseph.html>.
22. Scratch, L.S. *Antoine Lavoisier*. 2012 [cited 2012 04/01/2012]; Available from: <http://www.chemistryexplained.com/Kr-Ma/Lavoisier-Antoine.html>.
23. Scratch, L.S. *Henry Cavendish*. 2012 [cited 04/01/2012 2012]; Available from: <http://www.chemistryexplained.com/Bo-Ce/Cavendish-Henry.html>.
24. Britannica, E. *Christian Friedrich Schonbein*. 2012 2012 [cited 2012 04/01/2012]; Available from: <http://www.britannica.com/EBchecked/topic/528052/Christian-Friedrich-Schonbein>.
25. Nobelprize.org. *The Nobel Prize in Chemistry 1995*. 2012 18 August 2012 [cited 2012 04/01/2012]; Available from: http://www.nobelprize.org/nobel_prizes/chemistry/laureates/1995/.
26. Harrison, R.M., et al., *Measurement and modelling of air pollution and atmospheric chemistry in the UK West Midlands conurbation: Overview of*

- the PUMA Consortium project*. Science of the Total Environment, 2006. **360**(1-3): p. 5-25.
27. Carpenter, L.J., et al., *Seasonal characteristics of tropical marine boundary layer air measured at the Cape Verde Atmospheric Observatory*. Journal of Atmospheric Chemistry, 2010. **67**(2-3): p. 87-140.
 28. Highwood, E.J., et al, *Aerosol scattering and absorption during the EUCAARI-LONGREX flights of the Facility for Airborne Atmospheric Measurements (FAAM) BAe-146: can measurements and models agree?* Atmos. Chem. Phys., 2012. **12**(15): p. 7251-7267.
 29. Logan, J.A., et al., *Changes in ozone over Europe: Analysis of ozone measurements from sondes, regular aircraft (MOZAIC) and alpine surface sites*. Journal of Geophysical Research-Atmospheres, 2012. **117**.
 30. Aschmann, J., et al., *Modeling the transport of very short-lived substances into the tropical upper troposphere and lower stratosphere*. Atmospheric Chemistry and Physics, 2009. **9**(23): p. 9237-9247.
 31. Hendrick, F., et al., *NDACC/SAOZ UV-visible total ozone measurements: improved retrieval and comparison with correlative ground-based and satellite observations*. Atmospheric Chemistry and Physics, 2011. **11**(12): p. 5975-5995.
 32. Solomon, S., et al, *Four decades of ozonesonde measurements over Antarctica*. Journal of Geophysical Research, 2005. **110**(1): p. 1-15.
 33. Bernath, P.F., *Atmospheric chemistry experiment (ACE): Mission overview*, in *Earth Observing Systems IX*, W.L. Barnes and J.J. Butler, Editors. 2004, Spie-Int Soc Optical Engineering: Bellingham. p. 146-156.
 34. Ahmad, S.P., J.E. Johnson, and C.H. Jackman, *Atmospheric products from the Upper Atmosphere Research Satellite (UARS)*, in *Chemistry, Dynamics and Layered Structures of the Atmosphere*, T.A. Blix and J. Lastovicka, Editors. 2003, Pergamon-Elsevier Science Ltd: Kidlington. p. 2105-2110.
 35. Carboni, E., *GOME aerosol optical depth retrieval over ocean: Correcting for the effects of residual cloud contamination*. Atmospheric Environment, 2006. **40**(36): p. 6975-6987.
 36. Ho, S.P., et al., *A global comparison of carbon monoxide profiles and column amounts from Tropospheric Emission Spectrometer (TES) and*

- Measurements of Pollution in the Troposphere (MOPITT)*. Journal of Geophysical Research-Atmospheres, 2009. **114**.
37. Chang, A.Y., et al., *A comparison of measurements from ATMOS and instruments aboard the ER-2 aircraft: Halogenated gases*. Geophysical Research Letters, 1996. **23**(17): p. 2393-2396.
38. Offermann, D., et al., *Cryogenic Infrared Spectrometers and Telescopes for the Atmosphere (CRISTA) experiment and middle atmosphere variability*. J. Geophys. Res., 1999. **104**(D13): p. 16311-16325.
39. *Remote Sensing of the Atmosphere*. 2012 2012 [cited 2012 05/02/2012]; Available from: <http://en.ilmatieteenlaitos.fi/atmospheric-remote-sensing>.
40. Wiscombe, W. *Remote Sensing: Absorption Bands and Atmospheric Windows*. 2012 2012 [cited 2012 05/02/2012]; Available from: http://earthobservatory.nasa.gov/Features/RemoteSensing/remote_04.php.
41. *Atmospheric Modeling and Analysis*. 2011 26/10/2011 [cited 2012 05/02/2012]; Available from: <http://www.epa.gov/AMD/>.
42. Luecken, D.J. and M.R. Mebust, *Technical challenges involved in implementation of VOC reactivity-based control of ozone*. Environmental Science & Technology, 2008. **42**(5): p. 1615-1622.
43. Aliwell, S.R. and R.L. Jones, *Measurements of tropospheric NO₃ at midlatitude*. Journal of Geophysical Research-Atmospheres, 1998. **103**(D5): p. 5719-5727.
44. Ji, C., et al., *Measurement of Henry's Law Constants Using Internal Standards. A Quantitative GC Experiment for the Instrumental Analysis or Environmental Chemistry Laboratory*. Journal of Chemical Education, 2008. **85**(7): p. 969.
45. *The Air Quality Strategy for England, Scotland, Wales and Northern Ireland*. 2007, DEFRA: UK.
46. *Emissions of Air Pollutants in the UK*. 2012 2012 [cited 2012 05/02/2012]; Available from: <http://naei.defra.gov.uk/index.php>.
47. *Reducing air pollutant emissions*. 2011 13/04/2011 [cited 2012 05/02/2012]; Available from: <http://www.defra.gov.uk/environment/quality/air/air-quality/emissions/>.

48. Derwent, R.G., et al., *Analysis and interpretation of the continuous hourly monitoring data for 26 C2-C8 hydrocarbons at 12 United Kingdom sites during 1996*. Atmospheric Environment, 2000. **34**(2): p. 297-312.
49. *Particulate Matter*. Tox Town 05/01/2012 [cited 2012 06/02/2012]; Available from: http://toxtown.nlm.nih.gov/text_version/chemicals.php?id=21.
50. Fierro, M., *Particulate Matter*. 2000, Pima County Department of Environmental Quality.
51. Pilling, M., ApSimon, H., Carruthers, D., Carslaw, D., Colville, R., Derwent, R., et al., *Particulate Matter in the United Kingdom: Summary*. 2005, Department for the Environment, Food and Rural Affairs.
52. *WHO Air quality guidelines for particulate matter, ozone, nitrogen dioxide and sulphur dioxide*. 2005, World Health Organisation (WHO).
53. *Atmospheric Chemistry*. 2008 2008 [cited 2012 07/02/2012]; Available from: <http://www.ecomii.com/science/encyclopedia/atmospheric-chemistry>.
54. *Nitrogen Oxides (NO_x)*. 2010 08/11/2010 [cited 2012 07/02/2012]; Available from: http://www.apis.ac.uk/overview/pollutants/overview_NOx.htm.
55. *Nitrogen Oxides*. Tox Town 2012 03/01/2012 [cited 2012 07/02/2012]; Available from: http://toxtown.nlm.nih.gov/text_version/chemicals.php?id=19.
56. Carslaw, N., et al., *Simultaneous observations of nitrate and peroxy radicals in the marine boundary layer*. Journal of Geophysical Research-Atmospheres, 1997. **102**(D15): p. 18917-18933.
57. Wang, D.K.W. and C.C. Austin, *Determination of complex mixtures of volatile organic compounds in ambient air: an overview*. Analytical and Bioanalytical Chemistry, 2006. **386**(4): p. 1089-1098.
58. Martins, E.M., G. Arbilla, and L.V. Gatti, *Volatile Organic Compounds in a Residential and Commercial Urban Area with a Diesel, Compressed Natural Gas and Oxygenated Gasoline Vehicular Fleet*. Bulletin of Environmental Contamination and Toxicology, 2010. **84**(2): p. 175-179.

59. Atkinson, R., J. Arey, and S.M. Aschmann, *Atmospheric chemistry of alkanes: Review and recent developments*. *Atmospheric Environment*, 2008. **42**(23): p. 5859-5871.
60. Hopkins, J.R., A.C. Lewis, and P.W. Seakins, *Analysis and applications of measurements of source dominated hydrocarbon concentrations from the PUMA campaigns in June/July 1999 and January/February 2000 at an urban background site in Birmingham, UK*. *Atmospheric Environment*, 2005. **39**(3): p. 535-548.
61. Altenstedt, J., Pleijel, K., *POCP for individual VOC under European conditions*. 1998, IVL Swedish Environmental Research Institute: Goteborg. p. 1-48.
62. Hopkins, J.R., et al., *An observational case study of ozone and precursors inflow to South East England during an anticyclone*. *Journal of Environmental Monitoring*, 2006. **8**(12): p. 1195-1202.
63. Bottenheim, J.W., et al., *Alkenes in the Arctic boundary layer at Alert, Nunavut, Canada*. *Atmospheric Environment*, 2002. **36**(15-16): p. 2585-2594.
64. Qin, Y., et al., *C2-C10 nonmethane hydrocarbons measured in Dallas, USA-Seasonal trends and diurnal characteristics*. *Atmospheric Environment*, 2007. **41**(28): p. 6018-6032.

2.0 Chromatography

2.1 The History of Chromatography

The origin of the term 'chromatography' can be traced back to 1906, when the Russian botanist Mikhail Tswett first used it to describe the separation that occurred when solutions of chlorophylls, xanthophylls, and other plant pigments were passed through glass columns of finely divided calcium carbonate or alumina using petroleum ether. The separated species appeared as coloured bands on the column, inspiring him to name the technique chromatography by fusing the Greek words chroma, meaning 'colour', and graphein, meaning to 'write'. However, as Tswett went on to detail in his published work, "*...it is obvious that the adsorption phenomena described are characteristic not only for chlorophyll pigments; it is evident that different coloured and colourless compounds follow the same regularities.*"^[1, 2]

Since the early 20th Century, the applications of chromatography have grown explosively, with the two main categories of chromatography being Gas Chromatography (GC) and High Performance Liquid Chromatography (HPLC). This mammoth growth can be attested to a number of things, including the development of several new types of chromatographic techniques, as well as the mounting need by scientists for better approaches to characterising complex mixtures. Chromatography, as a whole, has evolved into an extremely powerful separation tool that finds application to all branches of science.

Chromatography can be characterized in two ways, based upon the following:

1. The physical means by which the stationary phase and mobile phases are brought into contact. An example of this would be column chromatography. Here the stationary phase is held in a narrow tube through which the mobile phase is forced under pressure. Planar chromatography would be a second example. In this instance, the stationary phase is supported on a flat plate. The equilibria upon which these two types of chromatography are based are identical and the theory developed for column chromatography is readily adapted to planar chromatography.

2. The types of mobile and stationary phases, and the kinds of equilibria involved in the transfer of solutes between phases.

The latter is a more fundamental classification of chromatographic methods, and there are three general categories of chromatography within it, i.e.

- Liquid chromatography (LC)
- Gas chromatography (GC)
- Supercritical-fluid chromatography (SFC).

As implied by their names, the mobile phases in the three techniques are liquids, gases and supercritical fluids, respectively.

In all chromatographic separations the sample is transported in a mobile phase, which is then forced through an immiscible stationary phase fixed in place in a column or on a solid surface. The two phases are chosen to enable the sample components to distribute themselves between the mobile and stationary phase to varying degrees. Slow movement with the flow of mobile phase is achieved for those components that are strongly retained by the stationary phase, whilst components that are weakly held by the stationary phase travel rapidly. The differences in mobility observed result in sample components separating into discrete bands or zones that can then be analysed qualitatively and/or quantitatively^[3].

2.2 Gas Chromatography

The invention of GC as an analytical technical was pioneered by A.T. James and A.J.P. Martin, who, in 1952, reported the separation of methylamines, and later volatile fatty acids, by partition chromatography, using nitrogen gas as the mobile phase, silicone oil/stearic acid supported on diatomaceous earth as stationary phase, and a test tube containing indicator solution for detection. The determination was by discontinuous titration ^[2, 4, 5]. This work was based on a visionary proposal by Martin and his colleague R.L.M. Synge in a 1941 publication in which he states, "*... the mobile phase need not to be a liquid but may be a vapour Very refined separations of volatile substances should therefore be possible in a column in which permanent gas is made to flow over gel impregnated with a non-volatile solvent*"^[6]. This same work, which later won the authors the 1952 Nobel Prize for Chemistry, also anticipated the

separation of chiral compounds and isotopes, as well as predicting HPLC by stating the desirability of using very small particles for the stationary phase^[7].

The 1950s saw GC spread into research institutes, academic and university laboratories, as well as in heavy industry and public health laboratories^[2].

Table 3: A classification of chromatographic techniques

General Classification	Specific Method	Stationary Phase	Type of Equilibrium
Liquid Chromatography (LC) (mobile phase: liquid)	Liquid-liquid, or partition	Liquid adsorbed on a solid	Partition between immiscible liquids
	Liquid-bonded phase	Organic species bonded to a solid surface	Partition between liquid and bonded surface
	Liquid-solid, or adsorption	Solid	Adsorption
	Ion exchange	Ion exchange resin	Ion exchange
	Size exclusion	Liquid interstices of a polymeric solid	Partition/sieving
Gas Chromatography (GC) (mobile phase: gas)	Gas-liquid	Liquid adsorbed on a solid	Partition between gas and liquid
	Gas-bonded phase	Organic species bonded to a solid surface	Partition between liquid and bonded surface
	Gas-solid	Solid	Adsorption
Supercritical-Fluid Chromatography (SFC) (mobile phase: supercritical fluid)		Organic species bonded to a solid surface	Partition between supercritical fluid and bonded surface

Petrochemical labs, facing the challenge of analysing complex hydrocarbon mixtures, recognized the importance of GC almost immediately. The analytical controls of the time could no longer keep up with the new processes in petroleum refining, and gas chromatography provided the essential solution

to the problems faced by this industry by providing a simple and sensitive method for the analysis of volatile compounds^[8, 9].

The next big step in the evolution of GC was the invention of capillary columns. Martin first suggested the use of capillary columns at a meeting in 1956, however, the idea was independently realised and demonstrated by Marcel Golay in 1957^[10]. Soon after this, Desty and co-workers, who had already made major contributions to the development of GC in the UK, constructed the first glass capillary drawing machine^[11]. Glass proved to be a more practical material for the construction of capillary columns in comparison to its predecessors, copper, cupronickel, stainless steel, and nylon. This was because it resulted in less adsorption of analytes onto the column wall. Glass was, however, not without its disadvantages. The most noticeable drawback being difficulties in everyday use, as these columns were both fragile and inflexible. 20 years of development followed on various methods of coating glass capillaries, with a number proving to be quite effective, such as etching the surface with acid. 1979 saw the introduction of fused-silica capillary columns by Dandeneau and Zerenner^[7, 12]. These flexible columns were based on fibre optic technology and were coated directly after drawing with polymer heat-resistant coatings^[13]. The debut of these columns saw the start of modern gas chromatography as it is known today.

GC analytes of interest are generally organic compounds which are volatile enough to be vaporised at a temperature (usually) below 400 °C, and stable enough to not decompose at this temperature. Analytes will thus typically have a significant vapour pressure below 250 °C, and a molecular weight under 500 Da. Only about 20% of known organic compounds can be analysed by gas chromatography without prior treatment^[14]. Problem analytes could have one or more of the following properties:

- **Thermal lability:** These analytes decompose in the hot GC system.
- **High molecular weight:** These are subject to discrimination due to their lower volatility.
- **Trace concentration:** These analytes are difficult to detect, particularly in dirty samples.
- **High activity:** These can be irreversibly adsorbed or broken down within the system.

In general, these compounds require more care when choosing and optimising the analytical system.

Derivatization to increase volatility is a common pre-step to many GC analyses. It involves chemically altering an analyte to impart favourable chromatographic behaviour. Low volatility may result from the size of a molecule and the resultant large dispersion forces holding it together. Smaller molecules may have a low volatility due to the strong intermolecular attractions between polar groups. Polar samples tend to adsorb on the active surfaces of the column walls and the solid support. By masking or eliminating the presence of polar OH, NH, and SH groups, derivatization can yield dramatic increases in volatility. The technique can also be used to decrease volatility, thus allowing analysis of very low molecular weight compounds, aiding in the separation of sample peaks from the solvent peak, increasing the detectability of compounds such as steroids and cholesterol, increasing stability to prevent thermal decomposition, and enhancing sensitivity for Electron Capture Detection (ECD) by introducing halogenated substituents^[15, 16]. While, derivatization serves to accentuate the differences in the sample compounds to facilitate the chromatographic separation, it can be cumbersome and introduces the possibility of quantitative errors.

Typical subjects of derivatization include alcohols, phenols, amines, amides, and carboxylic acids. Types of derivatization include:

- *Silylation*, which readily volatilizes the sample, and is the most prevalent method used
- *Alkylation*, which is generally used as the first step to further derivatizations or as a method of protection of certain active hydrogens
- *Acylation*, which is a method commonly used to add fluorinated groups.

2.3 Principles of Chromatography

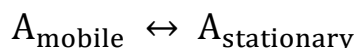
There are two approaches that can be taken to explain the separation process that occurs within a gas chromatographic column:

- 1. Plate theory:** This theory was proposed in 1941 by Martin and Synge, and was based on an analogy with distillation and counter current extraction.
- 2. Rate theory:** This was proposed in 1956 by J.J. van Deemter, and accounts for the dynamics of a separation.

2.3.1 The Partition Coefficient (K)

In plate theory, the chromatographic column is treated as though it were a static system in equilibrium. Each analyte will exhibit an equilibrium between the mobile phase and the stationary phase, such as that shown below for a solute species A.

Equation 19



The equilibrium constant (K) for this reaction, also known as the partition coefficient, is defined as:

Equation 20

$$K = \frac{C_S}{C_M}$$

Where:

- C_S = the molar concentration of the solute in the stationary phase
- C_M = its molar concentration in the mobile phase.

Ideally, K is constant over a wide range of solute concentrations.

Figure 13 shows a typical chromatogram for a sample containing a single analyte. The time it takes after sample injection for the analyte peak to reach the detector is called the retention time (t_R). The small peak on the left is for a species that is not retained by the column. This could be from either the sample or the mobile phase. The dead time (t_M) is the time it takes for the unretained species to reach the detector.

Table 4: Typical GC Applications

Pharmaceutical Industry

- Analysis of residual solvents in raw materials and finished products
- Urine drug screens for barbiturates and underivatized drugs
- Ethylene oxide analysis in sterilized products, such as sutures

Foods/Flavours/Fragrances

- Quality testing
- Solvents testing
- Fingerprinting of fragrances for characterization

Petrochemical

- Natural gas analysis
- Gasoline characterization
- Fraction quantitation
- Analysis of aromatics in benzene
- Mapping of oil reserves
- Tracing of reservoirs

Chemical/Industrial

- Determination of product content
- Determination of purity
- Monitoring production processes
- Detection of organic acids, alcohols, amines, esters, and solvents.

Environmental

- Detection of pollutants such as pesticides, fungicides, herbicides, purgeable aromatics
- Monitoring of stack and waste emissions
- Monitoring of water discharges

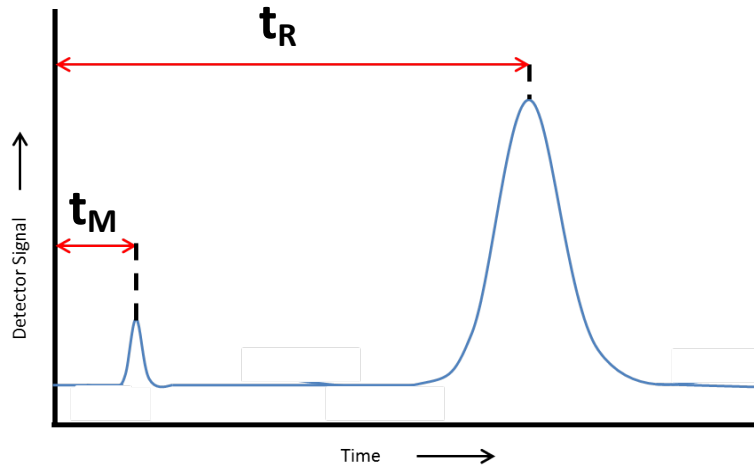


Figure 13: A typical chromatogram for a two-component mixture where the small peak on the left represents a species that is not retained on the column

The dead time is also equivalent to the time required for an average molecule of the mobile phase to pass through the column.

The average linear rate of solute migration (\bar{v}) is:

Equation 21

$$\bar{v} = \frac{L}{t_R}$$

Where:

- L = the length of the column in metres (m).

Similarly, the average linear rate of movement \bar{u} of the molecules of the mobile phase is:

Equation 22

$$\bar{u} = \frac{L}{t_M}$$

In order to relate the retention time of a solute to its distribution constant, its migration rate is expressed as a fraction of the velocity of the mobile phase:

Equation 23

$$\bar{v} = \bar{u} \times \text{fraction of time solute spends in mobile phase}$$

This fraction, however, also equals the average number of moles of a solute in the mobile phase at any instant divided by the total number of moles of that solute in the column:

Equation 24

$$\bar{v} = \bar{u} \times \frac{\text{moles of solute in mobile phase}}{\text{total moles of solute}}$$

As:

- moles of solute in mobile phase = $C_M V_M$
- moles of solute in stationary phase = $C_S V_S$

Therefore:

Equation 25

$$\bar{v} = \bar{u} \times \frac{C_M V_M}{C_M V_M + C_S V_S} = \bar{u} \times \frac{1}{1 + C_S V_S / C_M V_M}$$

An expression for the rate of solute migration as a function of its distribution constant and as a function of the volumes of the stationary phase and mobile phase can then be derived by substitution of Equation 20 into the above equation, giving^[3]:

Equation 26

$$\bar{v} = \bar{u} \times \frac{1}{1 + K V_S / V_M}$$

2.3.2 The Retention Factor (k')

The retention factor, or capacity factor is a means of measuring the retention of an analyte on the chromatographic column^[17]. For a solute A, the capacity factor k'_A is defined as:

Equation 27

$$k'_A = \frac{K_A V_S}{V_M}$$

Where K_A is the distribution constant for the species A. Substitution of the above equation into Equation 26 yields:

Equation 28

$$\bar{v} = \bar{u} \times \frac{1}{1 + k'_A}$$

It is possible for k'_A to be derived from a chromatogram. This can be done by substituting Equation 21 and Equation 22 into Equation 28 to give:

Equation 29

$$\frac{L}{t_R} = \frac{L}{t_M} \times \frac{1}{1 + k'_A}$$

This can be rearranged to give:

Equation 30

$$k'_A = \frac{t_R - t_M}{t_M}$$

k' values of approximately 10 or over are not ideal as the sample is highly retained and will spend a significant amount of time interacting with the stationary phase. This generally means that elution times are long, and the peaks may be broad and over resolved. Thus, increasing retention above a k' value of 10 only provides minimal increases in resolution. A low k' value of 1 or less implies peaks are eluted too rapidly with no time for separation.

The optimum region is $2 < k' < 10$, and the most effective and convenient way to alter and control the retention factor of a peak is to adjust the temperature of the mobile phase. The retention factor decreases as temperature increases, with an inversely proportional relationship:

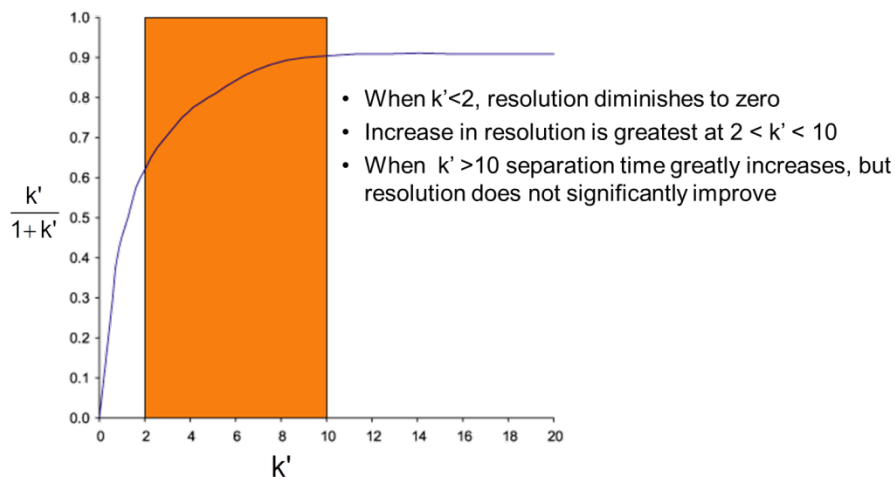


Figure 14: Effect of k' on resolution

Equation 31

$$\ln k' \propto \frac{1}{T}$$

Thus, decreasing the temperature results in a decrease in the relative amount of analyte in the mobile phase and an increase in the retention factor and retention time. This is described by the Clausius-Clapeyron and Van't Hoff equations shown below:

Equation 32: The Clausius-Clapeyron Equation

$$\log p^0 = \frac{-\Delta H}{2.3 RT} + \text{const.}$$

Equation 33: The Van't Hoff Equation

$$\frac{d \ln k}{dT} = \frac{\Delta H}{RT^2}$$

Where:

- p^0 = analyte vapour pressure at a given absolute temperature, T (K)
- ΔH = enthalpy of vapourisation at absolute temperature, T (K)
- R = the gas constant, i.e. $8.314472 \text{ J}\cdot\text{K}^{-1}\cdot\text{mol}^{-1}$

The Clausius-Clapeyron Equation shows that as temperature decreases, the analyte vapour pressure also decreases $\left(\frac{-1}{T}\right)$. As the analyte vapour pressure decreases it partitions more readily into the stationary phase and is retarded in the column longer, hence its retention factor and retention time increases^[18].

The Van't Hoff Equation indicates that as temperature is increased the natural logarithm of the retention factor increases, which is a direct proportionality between retention and temperature^[19].

Other variables that affect the retention factor include the chemical nature of the stationary phase, which will be discussed in more detail further on, as well as the ratio between the amounts of carrier and stationary phase inside the GC column, i.e. the phase ratio (β). These parameters, however, involve changing the GC column and are, therefore, less convenient than temperature for changing retention factor.

2.3.3 Phase Ratio (β)

The term phase ratio (β) is used to describe the relationship between column radius (r), or internal diameter (I.D.), and film thickness (d_f), as they are related to separation efficiency (N). Phase ratio can be calculated using the following equation:

Equation 34

$$\beta = \frac{r}{2d_f} = \frac{\text{I.D.}}{4d_f}$$

The phase ratio of a column is effectively a measure of the stationary phase to mobile phase ratio at any point in the column.

As:

Equation 35

$$K = \frac{C_S}{C_M} = k'\beta = k' \left(\frac{r}{2d_f} \right)$$

It is clear that increasing the phase ratio will result in decreased analyte retention. Inversely, if the phase ratio is decreased, analyte retention will increase. The phase ratio can be increased/decreased by increasing/reducing the column internal diameter or increasing/decreasing the film thickness respectively. Decreasing the phase ratio will also result in an increase in column capacity.

The table below shows some common phase ratios for various combinations of film thickness and internal diameter:

Table 5: Common phase ratios

Column I.D. (μm)	Film Thickness (mm)			
	0.10	0.25	0.50	1.0
0.10	250	100	50	25
0.25	625	250	125	63
0.32	800	320	160	80
0.53	1325	530	265	133

It is possible to change column diameter or film thickness to obtain a specific effect, such as an increase in efficiency, without changing retention time. This can be accomplished by proportionate changes in both column diameter and film thickness. Reducing the column internal diameter would lead to increased analysis time at constant pressure and temperature. However, reducing the stationary phase film thickness would result in the phase ratio remaining approximately constant, and the net result of a more efficient separation within the same timescale as the original separation.

Generally, for low boiling point compounds a low phase ratio is best, whereas for higher boiling point compounds a higher phase ratio is desirable.

2.3.4 The Selectivity Factor (α)

The selectivity or separation factor (α) defines the ability of the chromatographic system to chemically distinguish between sample components. It is usually measured as a ratio of the capacity factors of the two

peaks in question and can be visualised as the distance between the apexes of two peaks.

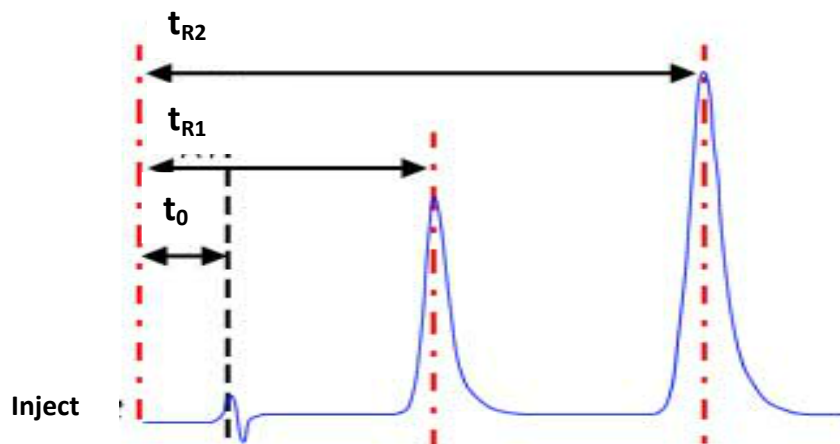


Figure 15: Selectivity factor

Equation 36

$$\alpha = \frac{k'_2}{k'_1} = \frac{t_{R2} - t_0}{t_{R1} - t_0}$$

Selectivity values between the peak of interest and the preceding peak are quoted. A high α value is indicative of a good separation between the apexes of each peak. The selectivity between separated peaks will always be greater than 1.0, as being equal to 1.0 would imply that the two peaks are co-eluting. The greater the selectivity value, the further apart the apexes of the two peaks. An increase of selectivity to above 1.0 results in a substantial improvement of

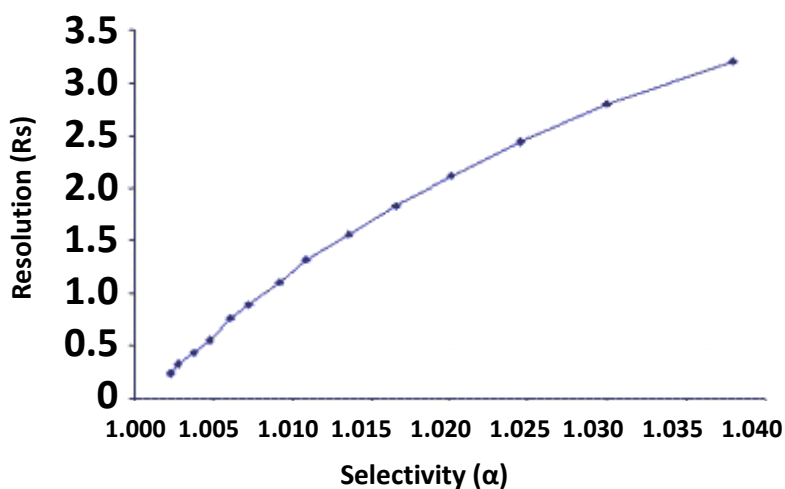


Figure 16: Resolution as a function of selectivity

resolution. Selectivity is dictated by the stationary phase chemistry, the column temperature, and the phase ratio. Small changes in selectivity lead to large changes in resolution, thus changing the selectivity of a system provides an excellent means of optimising the chromatographic resolution. In fact, a 4% increase in selectivity results in a resolution increase of over one order of magnitude.

Table 6: Parameters capable of altering selectivity

Parameter	Usage
Oven Temperature and Ramp Rate	<ul style="list-style-type: none"> Less predictable than other parameters but highly convenient
Stationary Phase	<ul style="list-style-type: none"> The most powerful way to alter selectivity in GC analysis
Phase Ratio (β)	<ul style="list-style-type: none"> Alters the distribution constant of analyte molecules, which affects the selectivity of a separation

2.3.5 The Efficiency Factor (N)

The column efficiency of a gas chromatography column is gauged by the number of theoretical plates (N) it possesses. The concept of a plate was derived from an analogy of Martin and Synge who likened column efficiency to fractional distillation, where the column is divided into "theoretical plates". Each plate is the distance over which the sample components achieve one equilibration between the stationary and mobile phase in the column. Therefore, the more theoretical plates available within a column, the more equilibrations are possible, and the better quality the separation. Efficiency may be calculated by determining the ratio of the retention time and the width of the peak of interest.

Equation 37

$$N = \left(\frac{t_R}{\sigma}\right)^2 = 16 \left(\frac{t_R}{w_b}\right)^2 = 5.54 \left(\frac{t_R}{w_h}\right)^2$$

The measurement of σ can be made at different heights on the peak. At the

base of the peak w_b is 4σ , so the numerical constant is 4^2 or 16. At half height, w_h is 2.354σ and the constant becomes 5.54. The width at half-height is more easily measured than the width at the base, as it overcomes problems associated with peak tailing and non-baseline resolved peaks. GC separations are primarily driven by the efficiency of the columns used, and columns with high plate numbers are considered to be more efficient than columns with a lower plate count. This is because they will have a narrower peak at a given retention time than a column with a lower N number. This means that less peak separation, i.e. lower α , is required to completely resolve narrow peaks. The biggest contributor to lower efficiency, and hence band broadening, is usually the column itself. The column length, whether it is packed or capillary, the film thickness, internal diameter and the quality of either the column packing or column coating, all play a part in determining the column efficiency. Several other factors also need to be taken into account, including:

- Injection volume
- Dead volumes in the injector or detector, especially the column couplings
- Flow rate
- Type of carrier gas used.

The number of theoretical plates per metre ($N \cdot m^{-1}$) is often calculated in order to compare columns run under the same temperature conditions and with the same peak retention. However, results are only valid for isothermal temperature conditions, as temperature programs result in highly inflated, inaccurate plate numbers. Another condition is that the retention factor of the test solute used to calculate the plate number is greater than 5.

A second measure of column efficiency is the height equivalent to a theoretical plate (H), calculated using the equation shown below. The shorter each theoretical plate, the more plates are contained within any length of column, thus the more plates per metre, the higher the column efficiency.

Equation 38

$$H = \frac{L}{N}$$

Figure 17 demonstrates that an increase in resolution follows an approximately straight line as efficiency is increased. Doubling the efficiency will only result in an increase of the resolution factor by a factor of $\sqrt{2}$, i.e. 1.42, and will also mean a doubling of the analysis time and the cost of the column.

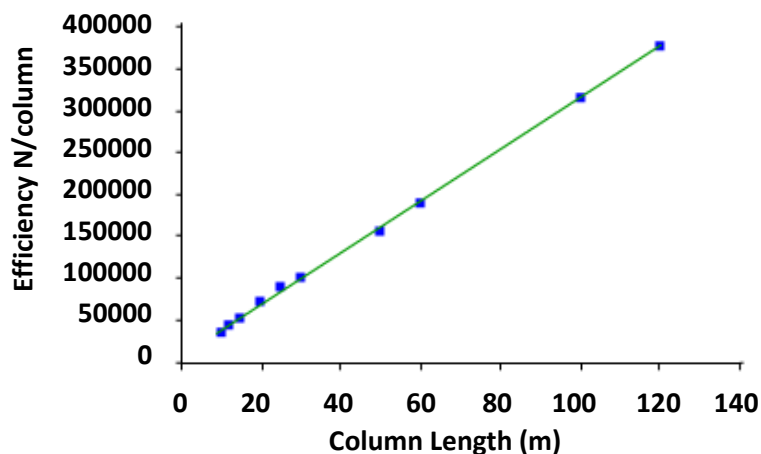


Figure 17: Resolution as a function of efficiency

2.3.6 Band Broadening

Band broadening is a phenomenon that reduces the efficiency of a GC separation leading to reduced resolution and poor chromatographic performance. This is problematic in terms of both the quality of the separation obtained and the accuracy with which sample components can be quantified. The degree of band broadening naturally increases with the age of the chromatography column being used, but strategies exist to slow these processes and to optimise column and instrument performance to ensure maximum efficiency and, hence, minimum band broadening.

Table 7: Typical column efficiency measures for a standard 30 m polydimethylsiloxane column

Column I.D. (mm)	N·m ⁻¹	N·columns ⁻¹
0.10	10,000	300,000
0.20	4,500	135,000
0.32	3,200	96,000
0.53	1,500	45,000

In 1956, J.J. van Deemter derived an equation that included the main factors contributing to column band broadening relevant to packed GC and LC columns. He described the individual terms, A, B and C, and also derived a composite curve which related plate height (H) to linear velocity (\bar{u}) of the mobile phase flowing through the column.

2.3.6.1 The van Deemter Equation

The van Deemter Equation is shown below:

Equation 39

$$H = A + \frac{B}{\bar{u}} + C\bar{u}$$

Where:

- A = The Eddy Diffusion term
- B = The Longitudinal Diffusion term
- C = The Mass Transfer term
- \bar{u} = The linear velocity of the mobile phase in mm·sec⁻¹.

Since plate height is inversely proportional to plate number, a small value indicates a narrow peak, which is the desirable condition. Thus, each of the

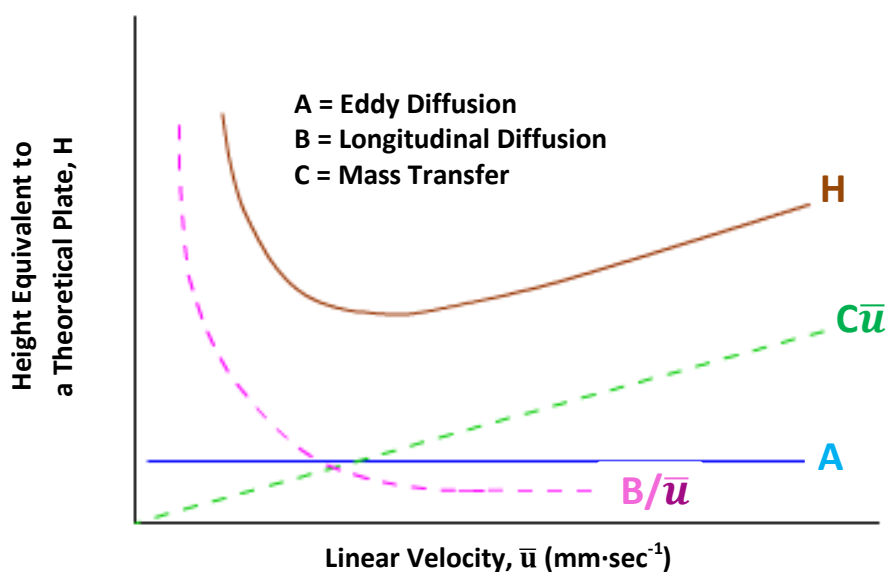


Figure 18: A van Deemter plot for a packed column illustrating the relationship of A, B, and C with linear velocity, and the corresponding effect on H

three constants, A, B, and C, should be minimised in order to maximise column efficiency.

Eddy Diffusion, A

The first of the factors relating to band broadening is that of Eddy Diffusion, i.e. the A term. The A term accounts for the fact that an analyte molecule within a band of analytes can take one of many paths through a packed column. These multiple paths arise due to inhomogeneities in column packing and the particle size of the packing material. The length of these pathways can differ significantly, thus, the residence time in the column will vary for molecules of the same species. This multiple path effect tends to make the band of analytes broader as it moves through the column. The Eddy Diffusion term in the van Deemter equation essentially reflects the quality of column packing, and is directly proportional to the diameter of the particles making up the packing.

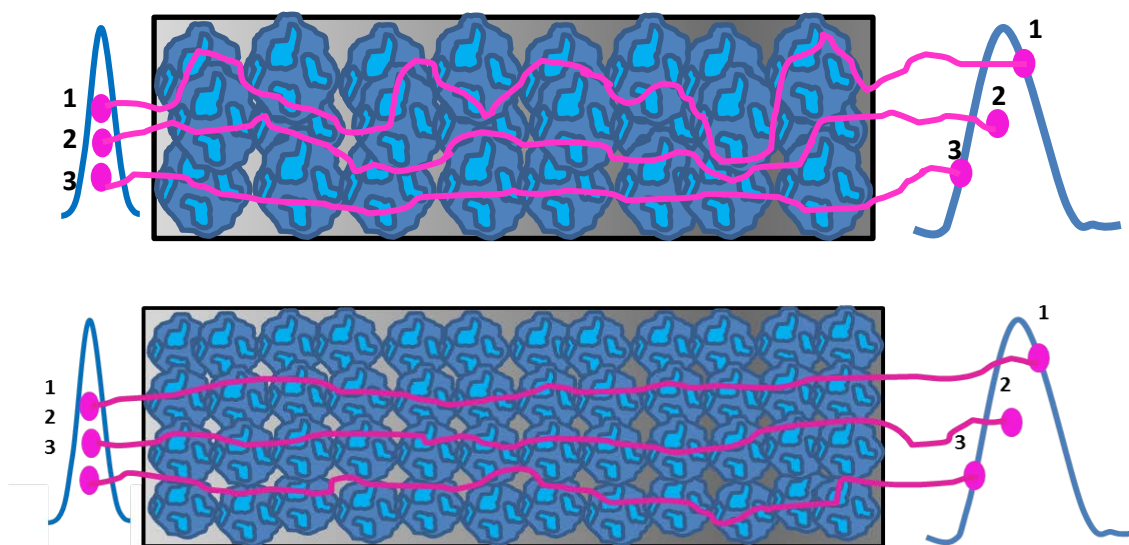


Figure 19: A comparison of Eddy Diffusion occurring within a column with large packing particles, as well as one with small packing materials

Eddy Diffusion can be minimised by:

- Selecting tightly packed columns
- Using smaller stationary phase particles
- Using particles with a narrow size distribution.

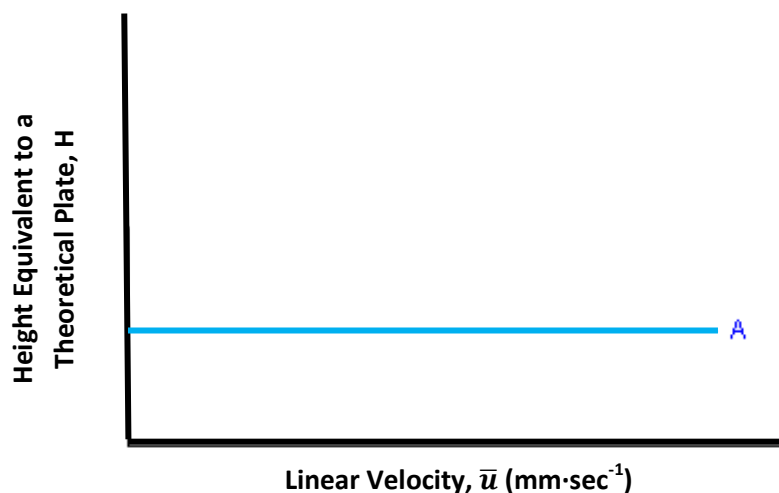


Figure 20: The effect of the A term on the height equivalent to a theoretical plate at given linear velocities

Longitudinal Diffusion, B/\bar{u}

A band of analyte molecules contained in a fluid or gaseous mobile phase will disperse in every direction due to the concentration gradient at the outer edges of the band. This process of the analyte band broadening is referred to as Longitudinal Diffusion. Solutes diffuse from the concentrated centre of a zone to the more dilute regions ahead and behind the zone centre, i.e. toward and away from the direction of flow of the mobile phase. The diffusion process is random in nature, resulting in a concentration curve that is Gaussian in form^[17]. The extent of the sample plug diffusion is directly related to the length of time that the solute band remains in the column, i.e. the longer a column, the longer the sample will stay within it and the more diffuse it will become. The consequence of this is a broader resulting peak. This time is inversely proportional to the mobile phase velocity, indicating that the dispersion will also be inversely proportional to the mobile phase velocity.

Longitudinal diffusion also occurs in all areas of the GC system where internal volumes are larger than necessary, for example:

- Injection liners that are too large
- Non-optimised splitless injection conditions
- Columns incorrectly installed in the injector and/or the detector.

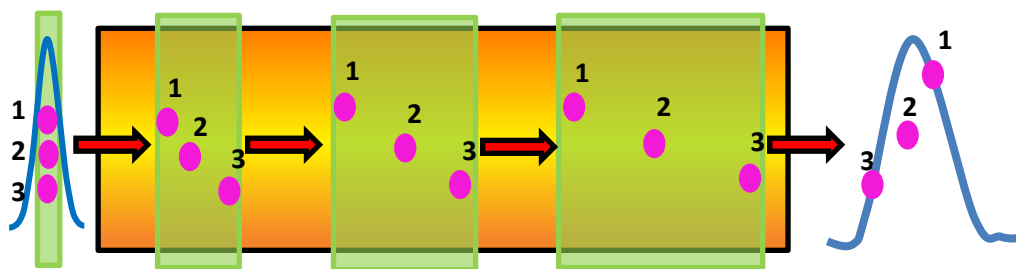


Figure 21: A schematic illustration of longitudinal diffusion

As longitudinal diffusion has a much larger effect at low mobile phase velocity or flow, using high linear velocity, will reduce its band broadening effects.

Longitudinal diffusion can be minimised by:

- Using shorter or small I.D. columns
- Using higher mobile phase flow rates
- Ensuring the inlet liner and temperature are appropriate
- Ensuring the column is properly installed into the injector and detector
- Using carrier gas with a low diffusion coefficient.

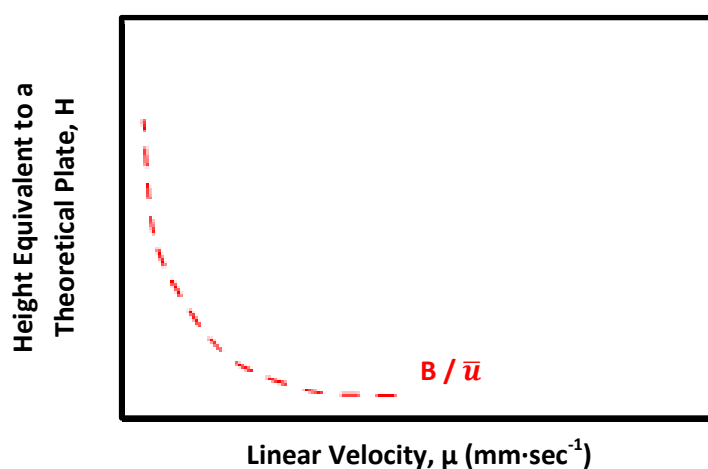


Figure 22: Effect of longitudinal diffusion on height equivalent to a theoretical plate at given linear velocities

Mass Transfer, $C\bar{u}$

The C term in the van Deemter equation relates to the mass transfer of the solute in the mobile phase or the stationary phase. During passage through a column, the analyte molecules are constantly and reversibly transferring from the mobile phase to the stationary phase. This process, however, is not instantaneous, and a certain amount of time is required for the molecules to

diffuse through the mobile phase to the interface before entering the stationary phase.

On injection into the column, any molecules near the stationary phase will enter it immediately. Those molecules some distance away will travel for a period of time before encountering the stationary phase. As the mobile phase is constantly flowing forward, the molecules that remain in it are quickly swept along the column, whilst the molecules that entered the stationary phase slowly diffuse through it. When the faster moving molecules finally reach the interface, they enter the stationary phase a considerable distance ahead of the molecules still within it. This process repeats itself throughout the length of the column, with the analyte band in the mobile phase being propelled along the column by the mobile phase, and analyte molecules at the front of the band partitioning into the stationary phase and those at the rear of the band partitioning out. The faster this process happens, the narrower the resulting peak width.

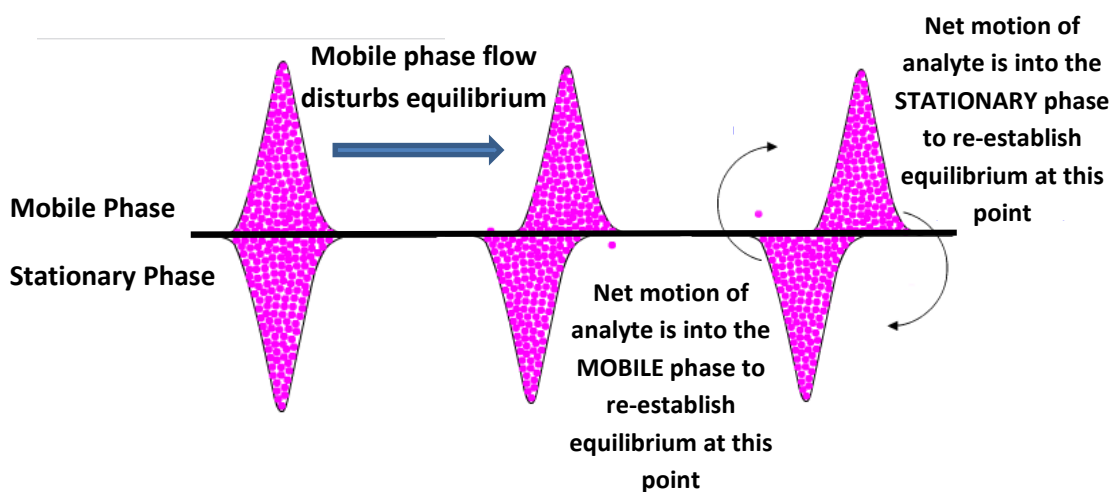


Figure 23: An illustration of mass transfer

Stationary phase mass transfer can be minimised by:

- Using thin stationary phase films
- Using temperature programming to ensure all analytes elute within a reasonable time ($k' < 20$)

Mobile phase mass transfer effects can be minimised by:

- Using small internal diameter columns, thus reducing the mass transfer distances.

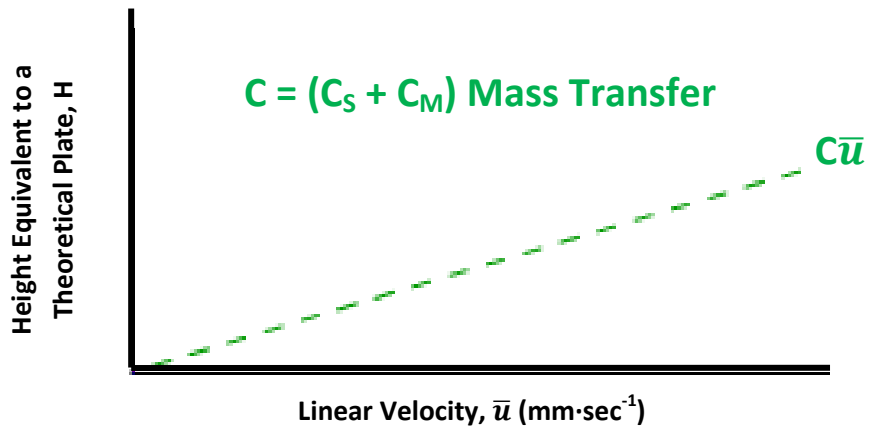


Figure 24: The effect of mass transfer on height equivalent to a theoretical plate for given linear velocities

2.3.6.2 The Golay Equation

In 1958, Golay described a similar relationship to deal with capillary gas chromatography columns, which contain no packing material and therefore do not possess an Eddy Diffusion or A term. The Golay equation contains only three functions. One describing dispersion from longitudinal diffusion and two describing dispersion from the resistance to mass transfer in the mobile and stationary phases, respectively^[17, 20].

Equation 40

$$H = \frac{B}{\bar{u}} + (C_s + C_m)\bar{u}$$

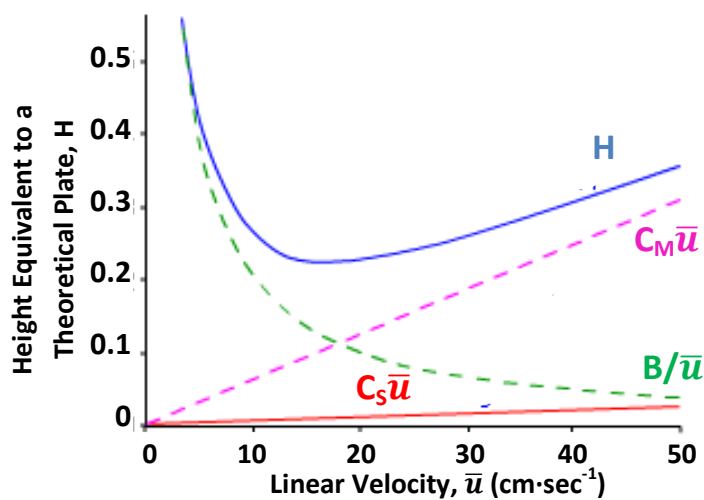


Figure 25: A Golay Plot showing the relationship between C_m , C_s , and B with linear velocity, and the effect these factors have on H , within a capillary column

2.3.7 Chromatographic Resolution

The most important thing in chromatography is to obtain the optimum resolution in the minimum time. The resolution (R_s) of a column provides a quantitative measure of its ability to separate two analytes. Column resolution is defined as:

Equation 41

$$R_s = \frac{\Delta Z}{\frac{W_A}{2} + \frac{W_B}{2}} = \frac{2\Delta Z}{W_A + W_B} = \frac{2[(t_R)_B - (t_R)_A]}{W_A + W_B}$$

Baseline resolution usually occurs at an R_s value of 1.5. Values greater than 1.5 indicate visible baseline between the peaks, whilst a value of less than 1.5 indicates that there is some degree of co-elution. A resolution value of 1.5 or greater ensures that the area or height of each peak may be accurately measured. The identification of specific peaks by their retention times becomes more certain as resolution increases.

2.3.7.1 The Fundamental Resolution Equation

A mathematical relationship exists between the resolution of a column (R_s), the retention factor (k'_A and k'_B) for two solutes, the selectivity factor (α), and the number of plates (N). For two solutes A and B having retention times that are close enough to one another to assume that:

Equation 42

$$W_A = W_B \approx W$$

Equation 41 then takes the form:

Equation 43

$$R_s = \frac{(t_R)_B - (t_R)_A}{W}$$

Equation 36 permits the expression of W in terms of (t_R) and N , which can then be substituted into the above equation to give:

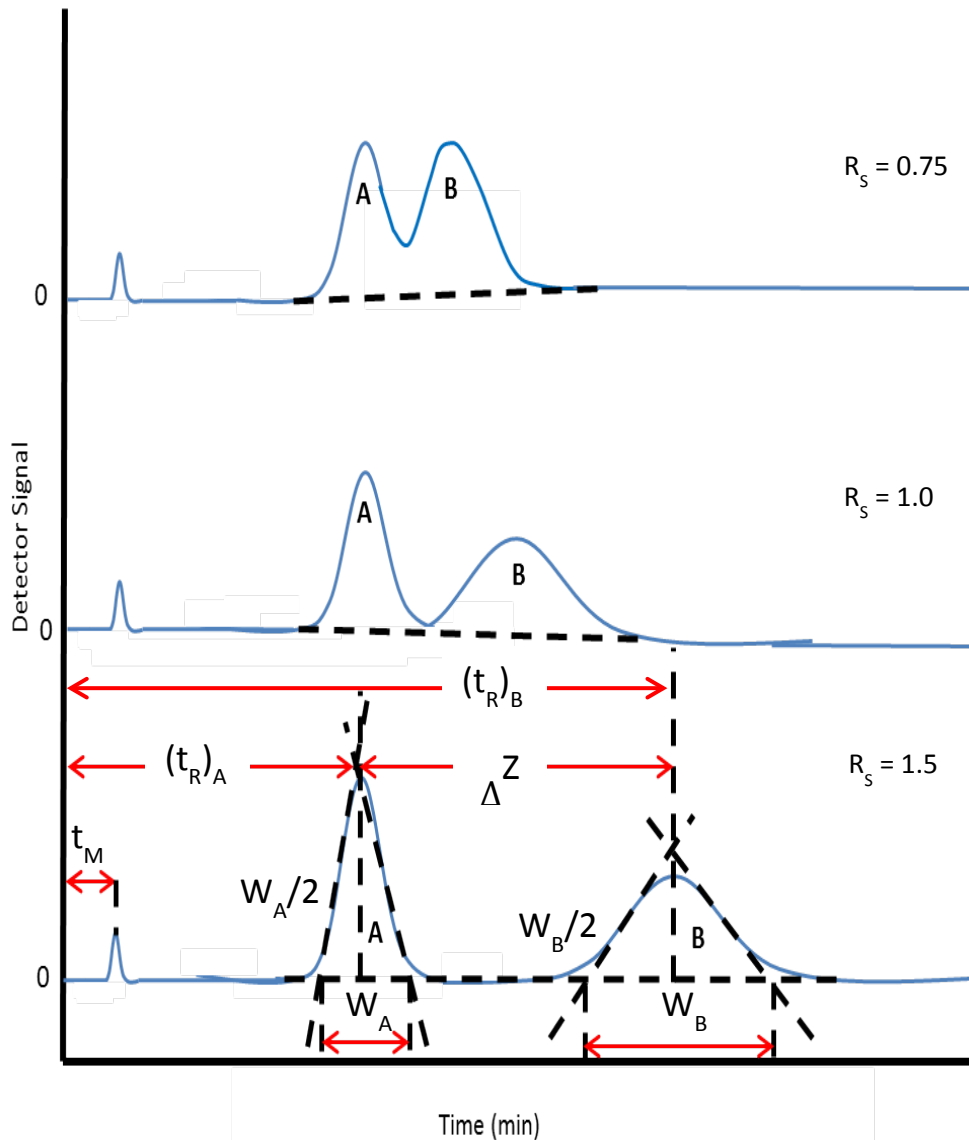


Figure 26: Separation at three resolutions

Equation 44

$$R_S = \frac{(t_R)_B - (t_R)_A}{(t_R)_B} \times \frac{\sqrt{N}}{4}$$

Substituting Equation 30 and rearranging leads to an expression for R_S in terms of the retention factors for A and B, i.e.:

Equation 45

$$R_S = \frac{k'_B - k'_A}{1 + k'_B} \times \frac{\sqrt{N}}{4}$$

As:

Equation 46

$$\alpha = \frac{k'_B}{k'_A}$$

It is possible to eliminate k'_A from Equation 46 by substituting the above equation and rearranging to give the following:

Equation 47

$$R_s = \frac{1}{4}\sqrt{N} \times \frac{\alpha - 1}{\alpha} \times \frac{k'_B}{1 + k'_B}$$

This can be simplified further when this equation is applied to a pair of solutes whose distribution constants are similar enough to make their separation difficult. Thus, when $K_A \approx K_B$, it follows from Equation 9 that $k'_A \approx k'_B = k'$, and from the equation below that $\alpha = 1$.

Equation 48

$$\alpha = \frac{K_B}{K_A}$$

This results in the Fundamental Resolution Equation:

Equation 49

$$R_s = \underbrace{\frac{1}{4}\sqrt{N}}_{\text{Efficiency}} \times \underbrace{\alpha - 1}_{\text{Selectivity}} \times \underbrace{\frac{k'}{1 + k'}}_{\text{Retention}}$$

The above equation highlights how resolution is affected by efficiency, selectivity and retention.

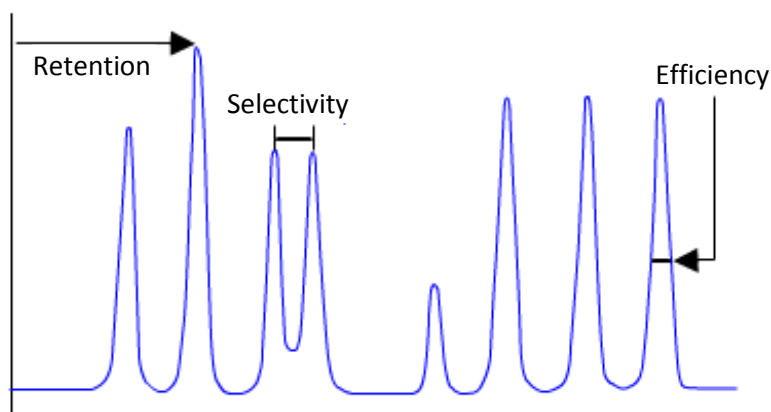


Figure 27: The main factors effecting resolution

2.4 The Gas Chromatograph

Since the technique was first introduced in 1951, GC instrumentation has continuously evolved. Most modern commercial GC systems operate in the following way:

1. An inert carrier gas, also known as the mobile phase, is supplied from a gas cylinder or gas generator to the GC where the pressure is regulated using manual or electronic (pneumatic) pressure controls.
2. The flow controller provides precise control of the carrier gas into the GC system.
3. The regulated carrier gas is supplied to the inlet and subsequently flows through the column and into the detector.
4. The sample is injected into the injection port, which is usually heated, via an autosampler or by manual injection. The sample is then volatilised and a representative portion is carried onto the column by the carrier gas.
5. The sample is separated inside the column by differential partitioning of the analytes between the mobile and stationary phases, as described. This is based on relative vapour pressure and solubility in the immobilised liquid stationary phase.
6. The column oven controls the GC column temperature. The oven heats rapidly to give excellent thermal control, and is cooled using a fan and vent arrangement.
7. On elution from the column, the carrier gas and analytes pass into a detector which responds to some physico-chemical property of the analyte and generates an electronic signal measuring the amount of analyte present.

- The signal is then amplified and sent to the data system, which converts the electrical signals produced by the detector into a chromatogram. The data system can also be used to perform various quantitative and qualitative operations on the chromatogram^[3, 18, 21].

A critical factor in GC analysis is that all components in the flow path of the sample, i.e. inlet, column oven, column and detector, are set to an appropriate temperature to allow all sample compounds to move through the system in the gas phase.

2.4.1 The Carrier Gas Supply

Modern GCs may require several different gases in order to operate. The function of the carrier gas is to transport vaporised sample onto the GC column, through the column and into the detector without reacting with the analyte molecules. The nature of the gas required is dictated by the type of inlet, column and detector system used. The main criteria, however, are that it is of high purity, is suitably inert to not react with the stationary phase or the sample components, and that it is appropriate for the type of detector used. Different carrier gas types are suited to either packed or capillary GC columns due to the variation in linear velocity of the carrier through the columns of different internal diameter (typically 0.32 mm for capillary columns and 4 mm

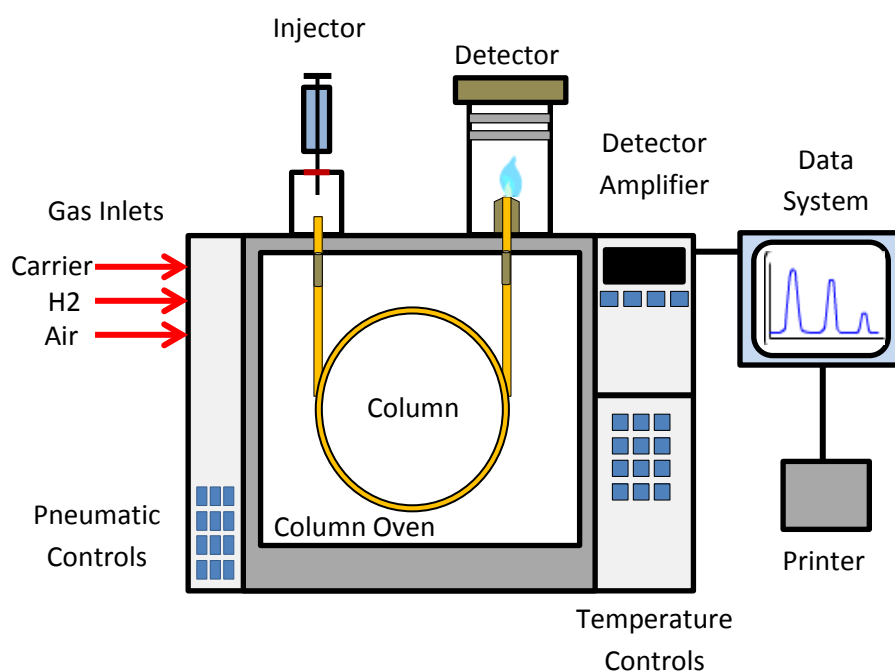


Figure 28: A typical gas chromatograph

for packed columns). Three of the most commonly used carrier gases are helium (He), nitrogen (N₂) and hydrogen (H₂).

Helium can be used for either packed or capillary columns, and is the most commonly used carrier gas for the latter. Nitrogen, on the other hand, is commonly used for packed columns but less frequently used in capillary column GC. Hydrogen carrier gas is only used for capillary GC. Despite having combustion potential, it is becoming more and more commonly used for a number of reasons, which will be looked at in more detail next.

Two main factors determine a carrier gas' ability to affect the efficiency of a chromatographic separation, i.e.:

1. **Diffusivity:** This provides a measurement for the diffusion speed of a solute vapour in a given gas.
2. **Viscosity:** This provides a measurement of the resistance of a liquid or gas to flow.

The diffusivities of helium and hydrogen are similar. However, nitrogen has a diffusivity value that is approximately four times lower.

Table 8: Relevant characteristics of carrier gases^[22]

Carrier Gas	Viscosity at 50 °C (kg·s ⁻¹)·m ⁻¹	Diffusivity – butane, 100 °C (m ² ·s)
Hydrogen	9.4	6.10x10 ⁻⁶
Helium	20.8	5.5x10 ⁻⁶
Nitrogen	18.8	1.5x10 ⁻⁶

The diffusion speed of the solute in the carrier gas determines the speed of chromatography. The slower the mobile phase velocity, the more often a solute molecule can diffuse from the stationary phase surface into the gas stream and back into the stationary phase, and the better the separation^[21]. However, a slow carrier gas flow rate can result in band broadening through longitudinal diffusion. It is for this reason that it is preferable to operate at the optimum gas velocity, as at this velocity, the maximum number of contacts are made with the stationary phase with a minimum amount of band broadening in the gas phase. Since diffusion in hydrogen and helium is much faster than in

nitrogen, for both radial and longitudinal diffusion, GC analyses conducted with either H₂ or He are 2-3 times faster than those conducted with N₂ as carrier gas.

The second major factor that differentiates the various typical carrier gases is viscosity. The viscosity of a gas is determined by its molecular weight and by temperature. Increasing either will result in an increase in viscosity.

A carrier gas' viscosity determines the inlet pressure required for a given velocity. High inlet pressures strongly compress the gas in the column inlet, which can cause a variety of problems. As indicated by Figure 14, efficiency suffers when the gas velocity is below the optimum velocity, as a result of excessive longitudinal diffusion. It also worsens again beyond the optimum, as a result of insufficient radial diffusion.

As shown in the plot, nitrogen has the lowest height equivalent to a theoretical plate value as it is the most viscous of the stationary phases. As its viscosity minimises longitudinal diffusion, using nitrogen carrier gas will give the most efficient separation of the three gases. However, the minimum point on the curve corresponds to a relatively low linear velocity. Whilst this is suitable when using packed GC columns with large internal diameter, it results in unacceptably long run times for capillary columns. In comparison, hydrogen and helium both show optimum efficiencies at higher linear velocities. This implies that it is possible to achieve separation efficiency that is comparable to that produced by nitrogen, but at a faster flow rate, resulting in desirable shorter analysis times.

Hydrogen carrier can be reactive, an example of which being the catalytic hydrogenation of unsaturated molecules at high inlet temperatures. However, it costs less than helium, with hydrogen generators being used to produce very high purity gas. Additionally, hydrogen displays a curve which indicates that a range of high linear velocities can be used to achieve chromatographic separations, resulting in fast analyses without any compromise in separation efficiency.

Another carrier gas, besides nitrogen, that is used with packed columns is

argon. This gas is particularly useful in H₂ and He analyses. Argon/methane carrier gas mixtures have also been used in isothermal ECD applications. Air may also be used as a carrier gas under certain conditions, usually with portable or on-site chromatographs^[23].

The management of a constant supply of gases to a GC is crucial to keep the instrument functional. It is particularly important to avoid any interruption in carrier gas flow, as if the supply fails whilst the column is heating, it may undergo irreparable damage.

Two stage pressure regulators are used with gas cylinders to reduce the pressure from the cylinder to a desired line or working pressure. It is essential for the carrier gas to be clean in order to prolong the lifetime of the GC column. This also allows for a less noisy baseline and good peak shape. Detector gases are also susceptible to impurities, and these can lead to increased background signal, baseline noise and reduced sensitivity.

Oxygen, moisture and hydrocarbons are three commonly encountered contaminants. It is possible for O₂ and moisture to enter the gas stream through permeation of tubing and fittings. Both of these are known to degrade the column stationary phase through oxidation, drastically reducing column lifetimes. Oxygen also reduces ECD performance, whilst the performance of MS detectors can be affected by the presence of water. Hydrocarbons can appear from grease and lubricating oils within tubing, causing ghost peaks, increasing baseline noise and, again, reducing detector sensitivity^[24].

Gas contamination is reduced by the use of gas purifiers, or traps, fitted along the carrier gas transfer lines before they reach the GC instrument.

2.4.2 Preconcentration

The preconcentrator concentrates analytes of interest before injection onto the analytical column. A preconcentrator tube can be used with a pump to sample air in the field, or it can be used in-line with sample injection onto the GC system. Any VOCs present in the sample will flow through the preconcentrator's adsorbent bed and, subsequently, stick to its particles, accumulating over the sampling period as illustrated in Figure 29.

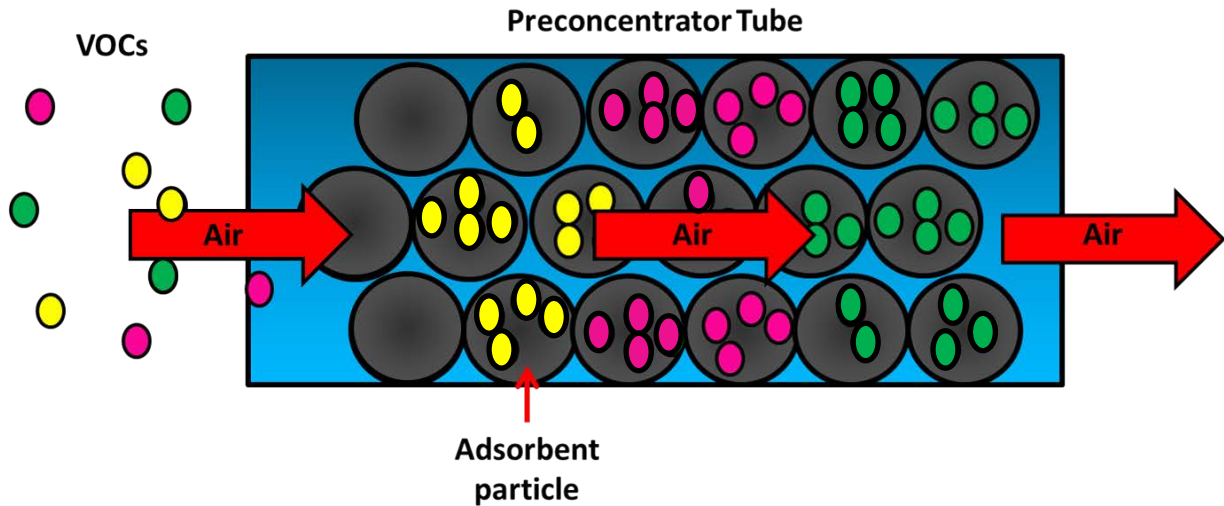


Figure 29: An illustration of the adsorption process of a preconcentrator

If used on location, the tube is manually removed from the pump after sampling, its ends are capped to prevent VOC diffusion out of the tube, and the trapped sample is transferred back to the laboratory for analysis. Here, it is loaded into a thermal desorption unit (TDU) attached to a GC. The TDU automatically loads the preconcentrator tube into a preheated block. The adsorbents desorb, as shown in Figure 30, and a high flow rate carrier gas is flushed through the tube injecting the concentrated sample components onto the chromatographic column. A split inlet and a cryofocusing trap are generally used to narrow the plug width and sample mass, resulting in a larger N value.

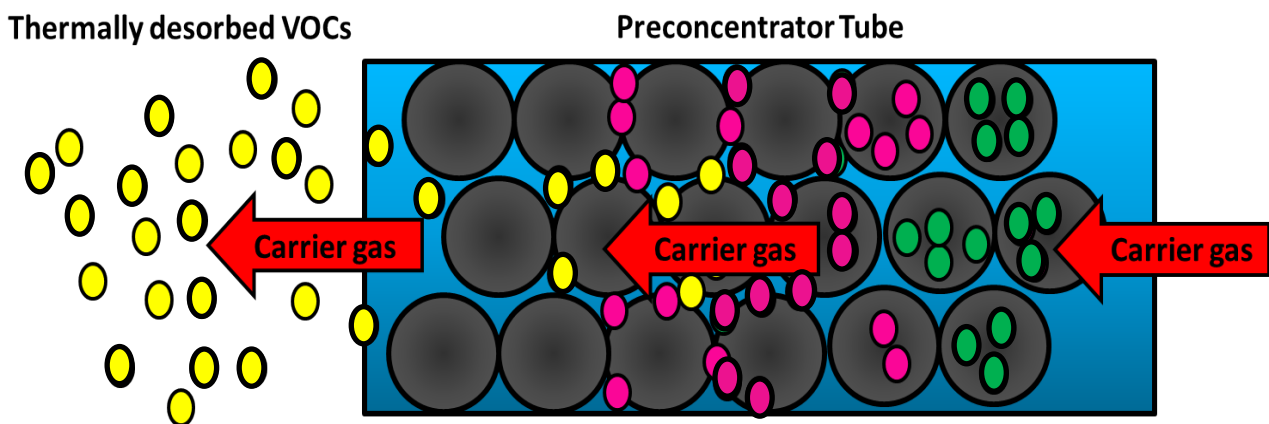


Figure 30: An illustration of the thermal desorption process of a preconcentrator

2.4.3 Flow Control

In the past, control of the gases required to run a GC was done manually, through a combination of on-off valves, forward and back-pressure regulators, needle valves and mass-flow-control regulators. Shown below is a typical schematic for the manual pressure control of a split/splitless inlet.

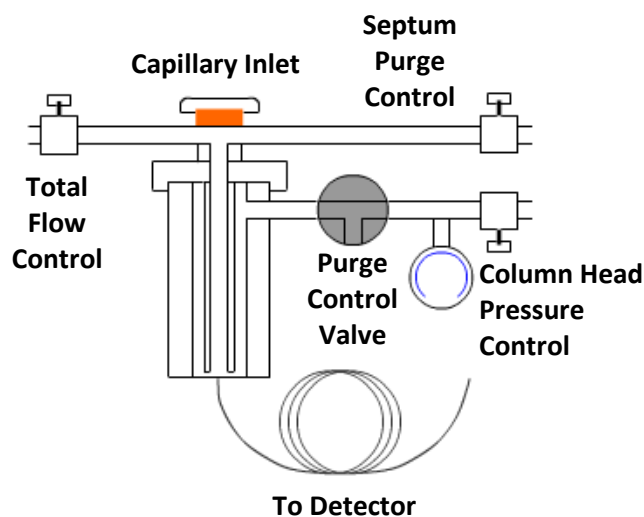


Figure 31: A typical manual split/splitless inlet

In this instrument there are several gas flow paths that are regulated using manual valves as follows:

- **Total flow control:** this valve is used to regulate the total amount of carrier gas entering the GC from the gas supply line.
- **Septum Purge Control:** a valve used to regulate the proportion of the total flow allowed to pass through the septum purge line (the flow is back pressure regulated as the valve is after the septum).
- **Column head pressure control:** a valve that controls the backpressure and hence flow of gas through the column. A pressure gauge reads the column head pressure.
- **Split flow:** the split flow is the difference between the total flow and the sum of the column flow and septum purge flow. Once the column flow is set, the split flow is adjusted by altering the total flow controller^[21].

All flows are measured manually using either a soap bubble flow meter or an electronic flow meter at the detector, septum purge vent, or split vent. The

only visible indicator of pressure is the column head pressure gauge. Detector gases would be controlled using manual valves in much the same fashion as that described for the above inlet.

Today, modern gas chromatographs are fitted with electronic pressure control (EPC) systems, where a microprocessor is used to set, monitor and control pressures via proportional valves, pressure and flow sensors. EPC allows for a constant pressure or a constant flow rate of carrier gas by monitoring the gas pressures and flow rates that, in turn, control electronic regulators. With Constant Pressure Mode, the head pressure is held constant throughout the GC run. When temperature is increased for a column with constant pressure on the inlet, the average flow rate in the column will decrease owing to increased viscosity of the gas mobile phase in a proportional but nonlinear manner. This ultimately results in lower column efficiency and unacceptably long retention times for more highly retained analytes. As well as that, when using Mass-Flow sensitive detectors, such as an FID, nitrogen phosphorous detector (NPD) or flame photometric detector (FPD), the reduction in column flow rate has the added disadvantage of changing the chromatographic baseline. This leads to a steadily rising or falling baseline position, and can make integration of the peaks in the chromatogram both difficult and irreproducible^[25].

Constant Flow Mode is preferred as the EPC will ramp carrier gas head pressure linearly in-line with the oven temperature program, ensuring that the carrier gas flow rate through the GC column is the same regardless of the oven temperature^[9]. This results in a flatter baseline, better peak shape and shorter elution times for more highly retained analytes. With the commercialization of flow programming, it is now possible to achieve highly reproducible flows^[23].

2.4.4 Sample Injection

The function of the sample inlet is to allow the introduction of a sample into the gas chromatograph in an accurate, reproducible manner. The vaporized sample should be a true representation of the overall sample and, unless specifically desired, should be injected without chemical change as a narrow band onto the chromatographic column. Failure to achieve this will significantly reduce the separation capability of the GC column. This makes

sample introduction one of the most important steps of a GC analysis. General requirements for GC inlets are that they:

- Do not cause more band broadening than the analytical column
- Allow a representative sample to be injected with good accuracy and precision
- Ensure the composition of the injected sample is representative of the original sample
- Do not allow discrimination to occur, based on differences in boiling point, polarity or concentration
- Do not cause the analyte to alter through thermal or catalytic degradation
- Are applicable to trace analysis as well as to undiluted samples.

Various inlets are available, including multimode, split/splitless, purged packed, cool-on-column (COC), programmed vaporization temperature (PVT), and volatiles interface, and often a GC may have more than one inlet. The type of analysis being performed, the type of sample being analysed, and the column being used all need to be considered when deciding upon which of the above inlets to use.

Before being transported onto the column, solid and liquid samples need to first be converted to the gas phase. Samples already in the gas phase need to be efficiently diverted onto the column, whilst avoiding any potential condensation en-route. The primary aim of gas, liquid and solid sampling techniques is to ensure that a representative and homogeneous aliquot of the sample is delivered to the column. For optimum column efficiency, the sample should not be too large, and should be introduced quickly as a 'plug' of vapour, as slow injection of large samples causes band broadening and loss of resolution.

Gas sampling methods generally require the entire sample to be in the gas phase at the conditions under which sampling occurs. Gas sampling can include the use of canisters, gas tight bags, gas tight syringes, and valves. If samples are mixtures of gases and liquids, either heat and/or pressure is employed to ensure that the entire sample is in the gaseous form.

Liquids are traditionally sampled by syringe. This can either be done manually, or in conjunction with an automatic liquid sampler. As the volatile liquid is introduced into the heated inlet, the sample is rapidly vapourised, transferred into the gas phase and subsequently swept onto the GC column. If the liquid is not particularly volatile, it is possible to use special GC inlets such as COC or PTV to overcome any volatility issues.

Solid sampling is not as common as gas and liquid sampling. Solid samples are generally first dissolved in suitable volatile liquid, before an aliquot of the solution is injected into the inlet. For volatile species that are entrained in solid matrices, analytes are usually driven out of the solid, often by increasing the solid's surface area by, for example, micronisation, followed by strong heating. The sample is then purged with the carrier gas forcing the volatile components into the headspace of the vial above the solid sample. Volatile components of the sample partition between the gas and sample phases, usually reaching equilibrium. A portion of the volatiles in the gas phase is then flushed into a sample loop, the contents of which are injected into the GC system, or directly into the GC column. Headspace injection is also applicable to liquid samples^[26].

The major benefit of headspace injection is that caustic and non-volatile sample components are eliminated prior to injection. This reduces the possibility of damage to the column and/or system inlet. The drawback, however, is that analyte sensitivity, particularly for compounds of low volatility, tend to be low and peaks are broader than with liquid sample injections. The use of a purge and trap system can counteract this by concentrating volatile components in the headspace prior to injection into the GC system. Here, volatile analytes move from the headspace onto a selective sorbent where they are concentrated, while other volatile components of the matrix pass through. Analytes are then thermally desorbed and pass into the GC column^[27].

The split/splitless inlet is the most commonly used for capillary GC. As the name suggests, it can be operated in two modes, either split or splitless. The injection principle of the split/splitless inlet is outlined below:

- A syringe containing the sample is used to pierce a rubber septum. Septa are used to isolate the inlet from atmospheric pressure, and hence maintain an increased pressure inside the inlet, whilst the injection is made. It is important to ensure that the syringe is deactivated with respect to the target analytes and will not absorb sample components. Various needle point styles are available for manual and autosampler injection, and for use with different septa styles^[24].
- The septum purge gas reduces the number of contaminant compounds which are outgassed from the septa at elevated temperatures. It does this by flowing across the underside of the septum and flushing the outgassing products to waste via the septum purge gas outlet. The septum purge gas also helps to prevent contamination of the underside of the septum by sample components that may overspill from the inlet liner during injection, thus reducing carryover from injection to injection. Typical septum purge gas flows are in the region of 2-5 ml·min⁻¹.
- The sample is rapidly introduced into the metal body of the inlet, which is usually surrounded by a radiative heating material into which a heating element is placed. A homogeneous heating profile over the whole length of the injector body is required to ensure that cold spots are not created, as less volatile analytes may condense at these points and foul the inlet liner or other components.
- The sample liquid rapidly volatilises to the gaseous form and is constrained within a glass liner of fixed volume. There are many varieties of liner for particular applications and injection modes, and these will be covered shortly. The liner also allows for sample vapour splitting, as well as offering an inert surface which can help to reduce the degree of analyte degradation or adsorption in the inlet.
- The split valve, or split line gas outlet, is used to discard some or all of the liner contents.
- The position of the capillary column within the inlet is of vital importance. The column tip is the position at which the sample vapour splitting will occur. Failure to properly site the column within the liner can lead to increased sample discrimination, as well as incorrect and irreproducible split ratios.

2.4.4.1 Split Injection

Split injection is conventionally used for analyses where the sample concentration is high and the amount of analyte reaching the capillary column needs to be reduced. Capillary columns have limited sample capacities and so can otherwise be easily overloaded. In split injection the valve is constantly in the open position and the gas flow is regulated to determine the fraction of the sample vapour that is discarded relative to that which reaches the capillary column.

This type of injection ensures that the sample is rapidly volatilised and transferred to the capillary column, hence ensuring a narrow analyte band^[28]. For this reason initial column temperatures for split injection tend to be higher than the boiling point of the sample solvent. The ratio of gas flows between the capillary column and the split flow line, i.e. the split ratio, gives a measure of the volume fraction of the sample vapour that will enter the column. The magnitude of the split ratio will depend on the concentration of the sample injected and the capacity of the capillary column used. During method development and optimisation, the split ratio is usually adjusted

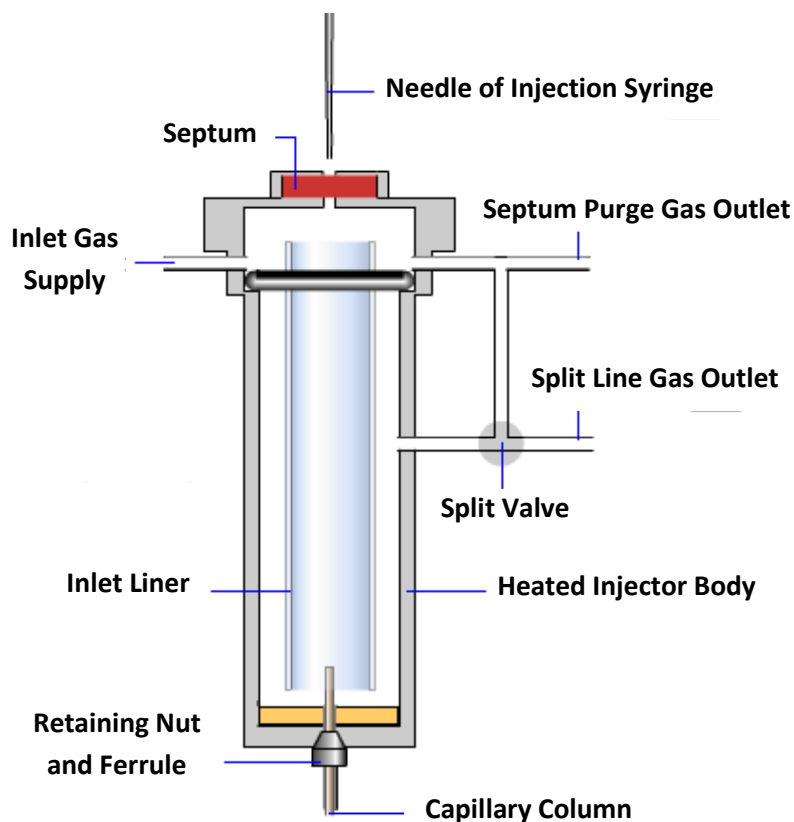


Figure 32: Typical split/splitless inlet

empirically to obtain a good balance between analytical sensitivity and peak shape. If the split ratio is too low peak shape will be broad and may show the fronting behaviour associated with overloading. On the other hand, if it is too high, too little sample will reach the column and the sensitivity of the analysis will decrease as peak areas decrease. Generally, split ratio has an approximately linear relationship with analyte peak area. This means that halving the split should result in a halving of the resultant peak area.

2.4.4.2 Splitless Injection

Splitless injection is analogous to split injection in many ways. The hardware used for splitless injection is almost identical to the split injector and most manufacturers will use the same inlet for both split and splitless injection. Just as with split injection, the sample is introduced into a hot inlet using a sample syringe where it is rapidly injected and volatilised. Initially, the valve is closed to ensure all analyte is transferred to the capillary column. The transfer of the sample vapour, diluted with carrier gas, from the inlet is much slower compared to split injection. The sample vapours are trapped, or condensed, on the head of the analytical column using a low initial oven temperature. This keeps chromatographic bands as narrow as possible. The split line is then opened after an optimised period of time in order to discard residual solvent and sample vapours from the inlet^[29].

Table 9: A comparison of split and splitless injection

	Split Injection	Splitless Injection
Advantages	Narrow solute peaks	Narrow analyte peaks
	Suitable for qualitative analysis	Suitable for both qualitative and quantitative analysis
	Minimizes the solvent effect	
Disadvantages	Requires rather high concentration of analyte	Broad solvent peak
	Makes quantitative analysis more complex	Retention times depend on solvent evaporation speed
	Not suitable for very expensive or toxic compounds	Solvent affects the shape of the peaks

2.4.4.3 Liners for Split/Splitless Injection

Liners are the centrepiece of the inlet system in which the sample is evaporated and brought into the gas phase. Choosing the appropriate liner for a specific application is an important task, as liners help to direct the volatile components of an injected sample onto the column. The liner has many functions which include:

- To constrain the volatilised components of the sample
- To allow the sample to be split through excess sample and carrier escaping from the liner outlet
- To cause mixing of the sample vapours with the carrier
- To prevent involatile material from fouling the GC column
- To avoid analyte thermal degradation
- To decrease the potential for inlet discrimination.

The three liner characteristics that must be considered for each application are:

- Liner volume
- Liner treatments or deactivation
- Any liner design features that might affect carrier gas flow through the inlet or sample vaporization^[30].

As discussed, the elevated temperatures used in the inlet vaporize the liquid sample to a gas for transfer to the head of the column. This phase transition is accompanied by a very significant volume change. The volume of the resulting vapour must be of the appropriate size to fit within the volume of the liner. If the volume is too great for the liner, reproducibility and sensitivity can be compromised, due to backflash and loss of the sample into the septum purge or split lines. Backflash also frequently results in sample carryover.

Another problem that may be encountered is that of active sites on liners, which may adsorb sample components and cause peak tailing, with potential loss of sensitivity and reproducibility. Hence, liners are generally made of deactivated glass.

There are a variety of liners available, including straight, tapered, packed and cup-splitter types. Liners may also contain packing material, such as glass or

quartz wool, and beads. These can provide good mixing of the sample within the liner, and can act as a filter for contaminants, such as crumbling septa pieces. They also provide sites of activity and so care needs to be taken when choosing a liner to ensure it is correct for the type of sample you are analysing and the functional groups of active compounds within it.

Table 10: A comparison of popular liner types

Liner Type	Advantages	Disadvantages
Straight	Cost-effective	Risk of flash-back
	Easy to clean	Risk of analyte discrimination
Tapered	Low analyte activity	More expensive
	Low risk of flash-back	
Packed	Enhanced sample mixing and vaporization	May absorb analytes leading to peak broadening
	Traps non-volatiles	May contribute to analyte decomposition
Cup-Splitter	Low risk of analyte discrimination	Difficult to clean
	Enhanced resolution	More expensive

If liners are not changed on a regular basis or if the correct liner is not used, one or more of the following issues may arise:

- Peak shape degradation
- Solute discrimination
- Poor reproducibility
- Sample decomposition
- Ghost peaks^[31].

2.4.4.4 Injection Volume

The nature and volume of the sample solvent injected into the split/splitless inlet will have a major impact on the accuracy and reproducibility of quantitative analysis, as well as on the chromatographic peak shape. As the injection is made, the sample solvent rapidly volatilises and expands into the

gas phase. The total volume of the gas should be able to be constrained within the volume of the inlet liner; otherwise the excess gas will spill over into the inlet gas supply and septum purge lines. The temperature in these lines rapidly decreases, and the sample solvent vapour can recondense, depositing analyte onto the inner walls of the tubing. When the next overloaded injection is made, the sample solvent from this injection will again backflash into the gas lines. This process results in carry-over and reduced quantitative accuracy and reproducibility^[21].

The inlet pressure and temperature govern the expansion volume of the sample solvent, as does the natural expansion coefficient of the solvent itself. Expansion volumes can be predicted, allowing the volume of solvent that may be safely injected into an inlet liner of known volume to be calculated.

2.4.4.5 Sample Discrimination

Sample discrimination occurs when sample components do not move onto the column at the same time. This leads to a non-representative sample entering the analytical column compared to the original sample. One of the sources of sample discrimination is the residence time of the syringe needle being too short for higher boiling and less volatile analytes. This results in the analyte condensing on the cold inner and outer surfaces of the needle before it is withdrawn from the inlet. Some less volatile analytes may never properly volatilise and the sample passes the head of the capillary column as a mixture of sample vapour and non-uniform liquid droplets. The consequence of this phenomenon is that late eluting peaks, in particular, will be broad and have poor resolution and sensitivity. There are, however, several approaches to solving the problem, including:

- Optimising liner geometry and packing materials to promote sample mixing and volatilisation
- Optimising the injection routine (filled needle, hot needle, solvent flush, air flush, sandwich method, etc.)
- Improving instrument design to reduce fluctuations in split flow.

In general, the least amount of discrimination is obtained if the injection is performed as rapidly as possible. For this reason, fast autosamplers generally give less discrimination than manual injection.

2.4.5 Nuts and Ferrules

The capillary column is held in the lower part of the GC inlet using a fitting into which the column nut and ferrule are screwed. The column nut secures the GC column to the inlet and the ferrule seals the opening in the nut where the column is inserted. It is important that the correct type of ferrule is used, of which there are three main types:

1. Graphite
2. Vespel
3. Vespel/Graphite

Table 11: A comparison of ferrule types

Ferrule Type	Advantages	Disadvantages
Graphite	Easy to use	Soft, easily deformed or destroyed
	Stable seal	Possible system contamination
	Higher temperature limit	Not for use with GC/MS transfer lines
Vespel or Vespel/Graphite	Mechanically robust	Flows at elevated temperature
	Long lifetime	Must retighten frequently, prone to leakage
		Polymer bleed problematic with some detectors (NPD and ECD)

Graphite ferrules are the easiest to use. They are leak-free, universal for most systems, and have the highest temperature limits of up to 450 °C. As these ferrules are soft, they easily conform to column outside diameters and different types of instrument fittings, however, they can flake or fragment upon removal, causing particles to lodge in the injector or detector sleeves. They also do not hold a seal under vacuum and so are not suited to mass spec detection. Vespel/Graphite ferrules (85% vespel, 15% graphite), on the other hand, are hard and so must match the column and fitting dimensions closely to seal properly. In addition, because they can deform during initial heating, they

need to be retightened or leakage will occur. Vespel/Graphite ferrules do not fragment though, and can be reused many times. Vespel is a high-temperature polyimide based material which is very hard. While the vespel/graphite composites have lower temperature limits than purely graphite ferrules, up to 350 °C, they are preferred by mass spectroscopists as they give particulate free, tight and reliable connection, thus preventing contamination of the ion source and maintaining their seal under vacuum. 100% vespel ferrules are easy to remove and reuse, but are only used for isothermal GC operation up to 280 °C^[3, 21].

Using the wrong ferrule or one that is worn-out can result in inconsistent and unreliable chromatography, as well as causing leaks. This allows air and other contaminants to enter the instrument through the column seal, causing major interference with column and detector performance^[30].

2.4.6 GC Columns

The coiled, tubular gas chromatographic column is located within a temperature-controlled oven. Generally, one end of the column is attached to the inlet, while the other end is attached to the detector. Columns vary in length, diameter, and internal coating.

The column may arguably be considered the key component of a gas chromatograph, as it is here that the separation takes place. However, it is important to note that the total variance of a separation (σ_T) will conform to principles of error propagation and be a sum of variances from the injector (σ_i), column (σ_c), detector (σ_d), and data system (σ_{ds}), i.e.

Equation 50

$$\sigma_T = \sqrt{\sum (\sigma_i + \sigma_c + \sigma_d + \sigma_{ds})}$$

Thus, each of these components contributes to the overall efficiency of a GC separation and merits individual attention^[23].

Two general types of columns are encountered in gas chromatography, packed and open tubular, or capillary. Capillary columns are the more efficient of the two types. Their high separating power is primarily due to their longer length and thin stationary phase films. There is a trade-off for attaining this high separating power. Column capacity, i.e. the mass of individual solutes that can be injected into the columns in ng, for every narrow bore 0.18 mm capillary column is limited to about 100 ng per component and increases to 1,000-2,000 ng for megabore (0.53 mm) columns. By comparison, the capacity for packed columns is considerably higher, on the order of 10,000 ng.

2.4.6.1 Packed Columns

Packed GC columns can be either glass or stainless steel. They represent one of the original types of GC columns and are typically assembled by the end-user. Glass columns are favoured when thermally labile materials are being separated, such as essential oils and flavour components. Stainless steel columns, however, are used as they can easily tolerate the elevated pressures necessary for long packed columns, which glass cannot. Before packing, glass columns are generally treated with an appropriate silanizing reagent to eliminate the surface hydroxyl groups, which can be catalytically active or produce asymmetric peaks. Stainless steel columns are usually washed with dilute hydrochloric acid, then extensively with water followed by methanol, acetone, methylene dichloride and n-hexane. This washing procedure removes any corrosion products and traces of lubricating agents used in the tube drawing process. Columns are then packed by placing a piece of deactivated glass wool at one end of the tube to keep the silica based stationary phase within the tubing as it is slowly poured into the opposite end. The pellicular solid particles are typically carbon or diatomaceous earth, and are typically between 30/40 mesh and 100/120 mesh. These will previously have been coated with the chosen stationary phase. A vacuum is then applied at the end of the tubing to remove the solvent that was used to prepare the stationary phase gel. Subsequently, the tubing is capped off with a piece of deactivated glass wool. The smaller the particle size the higher the column efficiency. A typical packed GC column will be between 2 and 4 m in length with an internal diameter of between 2 and 4 mm^[32].

To date, the vast majority of gas chromatography has been carried out on packed columns. This situation is, however, changing rapidly, with packed columns being replaced by the more efficient and faster capillary columns. Packed columns do, however, still have some features that can be advantageous in that they can accept high sample loading and can give a greater analytical dynamic range.

2.4.6.2 Capillary Columns

Capillary columns differ from packed columns in that the stationary phase is coated on the inner wall, either as a thin film, i.e. wall-coated open tubular (WCOT), or impregnated into a porous layer which is then coated on the inner wall, i.e. porous layer open tubular (PLOT). PLOT columns act as molecular sieves for the retention of room temperature or permanent gases, such as O₂, CO, CO₂, SO₂, NO₂, and NO.

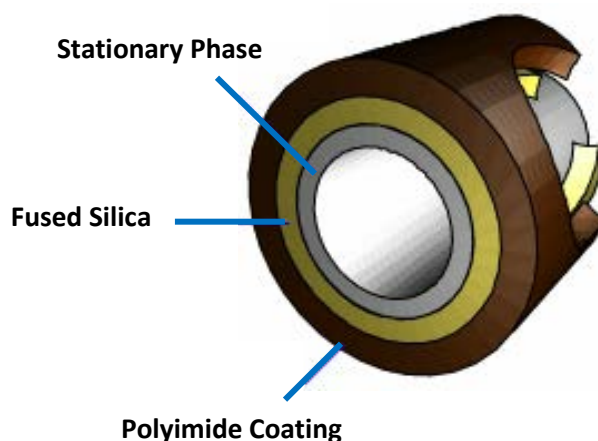


Figure 33: Typical cross-section of a wall coated open tubular (WCOT) capillary

As previously mentioned, Dandenau and Zerenner introduced flexible fused silica capillary columns using the quartz fibre drawing technique. They found that coating the capillary tube with a polyimide polymer immediately after drawing prevented moisture coming in contact with the surface and thus stabilized the tube and prevented stress corrosion. As with packed columns, surface treatment is necessary to reduce adsorption and catalytic activity, as well as to make the surface sufficiently wettable to coat with the selected stationary phase. The treatment may involve washing with acid, silanization and other types of chemical treatment, including the use of surfactants.

Deactivation procedures used for commercial columns are kept highly proprietary.

Open tubular columns are coated internally with a liquid stationary phase or with polymeric materials that can be polymerized to form a relatively rigid, internal polymer coating. Column stability depends on the stability of the stationary phase film which, in turn depends on the constant nature of the surface tension forces that hold it to the column wall. These surface tension forces can be reduced by exposure to oxygen, extreme heat or reactive chemicals, resulting in the film suddenly breaking up, i.e. stationary phase bleed. This shows as a consistent disturbance in chromatogram baseline signal resulting from compound elution at elevated temperatures. Stationary phase bleed can be overcome by in-situ cross-linking of unsaturated groups in the stationary phase molecule by means of free-radical initiators, such as peroxides or azo compounds, to yield elastomers^[10].

The majority of columns commercially available have undergone extensive crosslinking between the stationary phase and the polymer backbone, i.e. the column wall itself. This crosslinking gives extended temperature stability, extremely low bleed levels and longer column lifetimes. Whenever a column is first installed it will show some bleed due to oxygen exposure. Therefore, it is important to condition any column following installation at the maximum isothermal temperature to be used until bleed levels stabilize.

Table 12: Comparison of wall-coated capillary, support-coated capillary and packed columns

	Wall-Coated Capillary	Support-Coated Capillary	Packed
Length (m)	10 – 100	10 – 50	1 – 5
Internal diameter (mm)	0.1 – 0.8	0.5 – 0.8	2 – 4
Liquid film thickness (μm)	0.1 – 1	0.8 – 2	10
Capacity per peak (ng)	<100	50 – 300	10,000
Resolution	High	Moderate	Low

As well as displaying increased separation efficiency in comparison to packed columns, capillary columns also work at lower temperatures and achieve much better separation in equal times.

Stainless steel clad silica columns can be used for separations that require temperatures of over 400 °C. High temperature fused silica columns are also available from a number of suppliers. These have special, and proprietary, polyimide coatings which give extended high temperature stability without the need for using the specialist metal columns mentioned above.

2.4.7 Stationary Phases

The stationary phase is an organic polymeric liquid that is either coated on or covalently bonded to the silica interior surface of the column via silyl-ether linkages. The choice of the appropriate column for a given separation depends on the chemical nature of the analyte, the sample matrix, the solvent, and especially on the nature of the molecular interactions between analyte and stationary phase. The first stationary phases for GC were a varied collection of hydrocarbon and silicone oils, greases, esters, and polymers. Today the majority of GC stationary phases are based on a crosslinked polysiloxane backbone with appropriate pendant groups, such as CH₃, Ph, CH₂-CH₂-CH₂-CN, CF₃. The pendant group may also be tailored for a steric separation. A number of wax, or polyethylene glycol (PEG), phases, as well as cyano phases, are also popular.

The selection of the correct stationary phase is one of the most critical parameters in the success of any GC method. As the interaction of the analyte molecules with the mobile phase is almost negligible, the column temperature and the interaction of the analyte with the stationary phase will govern the selectivity of the separation [33].

2.4.7.1 Stationary Phase Selectivity

In choosing an appropriate GC stationary phase it is generally accepted that the principle of 'like dissolves like' holds well, and that to separate polar analytes a polar stationary phase is required, and vice versa.

All covalently bonded molecules will share electrons between the bonded atoms. The greater the difference in electron affinity, or electronegativity, between atoms in a covalent bond the more polar the bond. Thus, a non-polar covalent bond will have a uniform distribution of electron charges between the atoms. The simplest non-polar covalent bonds exist in homonuclear diatomic species such as Cl_2 (Figure 34) or H_2 . In this type of molecule there is no permanent localised electrical charge build up, instead electrons are shared uniformly within the molecule.

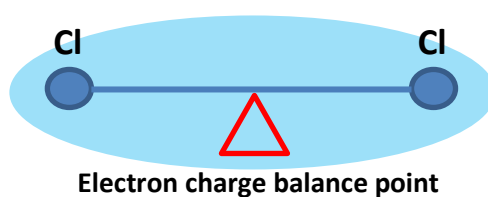


Figure 34: Cl_2 - non-polar bond. The electron charge cloud is uniformly spread in this homonuclear diatomic molecule

Alternatively, a polar bond displays a non-uniform electron distribution cloud. This typically occurs when two non-metal atoms which are more than two positions apart in the periodic table, are involved in the bond. A typical example of HCl is shown in Figure 35.

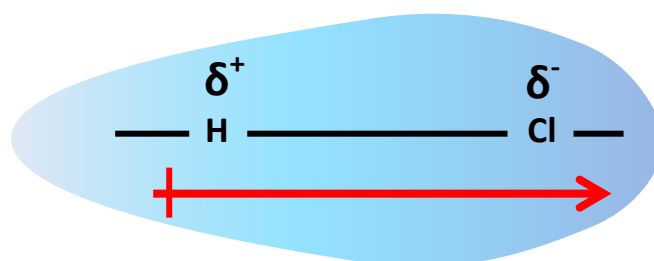


Figure 35: HCl - polar bond. Electrons spend more time drawn towards chlorine

The red arrow head shown under the molecule indicates the direction of highest negative charge and indicates that the molecule has a dipole moment, i.e. it is polarised, with a pair of relatively positive and negative centres^[34].

Electronegativity is an index that relates the relative attraction an element has for electrons within a covalent bond. It is possible to predict the presence of a

dipole moment within a molecule by comparing the electronegativity of the bonded atoms. For example, when the electronegativity value between two atoms differs by more than 0.5 units the bond is likely to be polar, unless a high degree of molecular symmetry is present.

The skill of stationary phase selection lies in knowing (or empirically discovering), the degree of polarity required to avoid overly long retention times whilst still obtaining a satisfactory separation. When separating compounds of intermediate polarity or where the analytes are a mixture of polar and non-polar compounds, further knowledge of the retentivity and selectivity of each phase is required. The three main mechanisms of interaction are dispersion, dipole (including dipole - induced dipole), and hydrogen bonding.

Table 13: Polarity and its relationship with electronegativity^[35]

Bond	Electronegativity Difference	Polarity
C - H	2.5 - 2.1 = 0.4	Non-polar
C - O	3.2 - 2.5 = 1.0	Polar
C - F	4.0 - 2.5 = 1.5	Very polar (around the limit at which covalent and ionic bonds are differentiated)
C - N	3.0 - 2.5 = 0.5	Polar
O - H	3.5 - 2.1 = 1.4	Very polar
C - S	2.5 - 2.5 = 0	Non-Polar

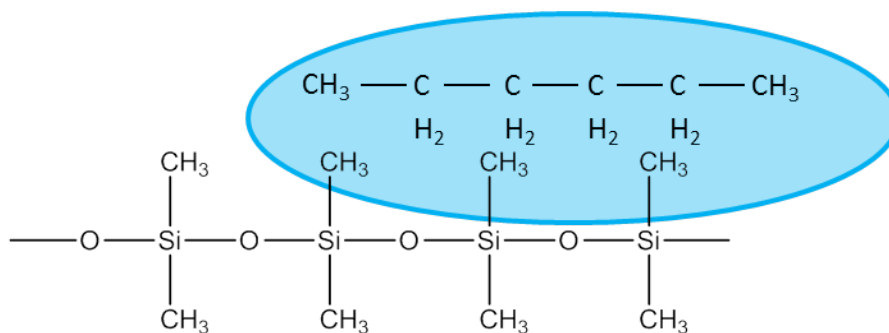


Figure 36: Non-polar analyte interacting with a non-polar stationary phase

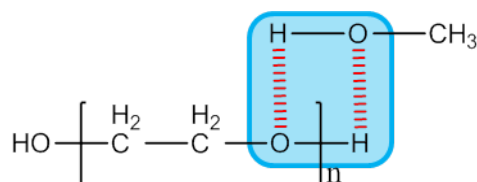


Figure 37: Polar analyte interacting with a polar stationary phase

Dispersive Interactions

Dispersive interactions are nonpolar and give rise to separations based on analyte volatility. Analyte boiling point can be used as an indicator of analyte volatility. In general, the more volatile an analyte is, i.e. the lower its boiling point, the less retained it will be and the earlier it will elute from a column with a predominantly dispersive stationary phase. Dispersive interactions are caused by charge fluctuations that occur throughout a molecule, arising from electron/nuclei vibrations. The fluctuations are random in nature and are essentially a statistical effect. Every molecule has a number of arrangements of nuclei and electrons having dipole moments that fluctuate. This results in an overall molecular charge of zero. However, at any instant in time, the dipoles are capable of interacting with other instantaneous dipoles of other molecules. Dispersive forces are ubiquitous and must arise in all molecular interactions. They can, themselves, occur in isolation, but are always present even when other types of interaction dominate. Examples of interactions that are exclusively dispersive are those between hydrocarbons. The lower molecular weight hydrocarbons are liquids and not gases due entirely to the dispersion forces that act between the hydrocarbon molecules^[21, 33].

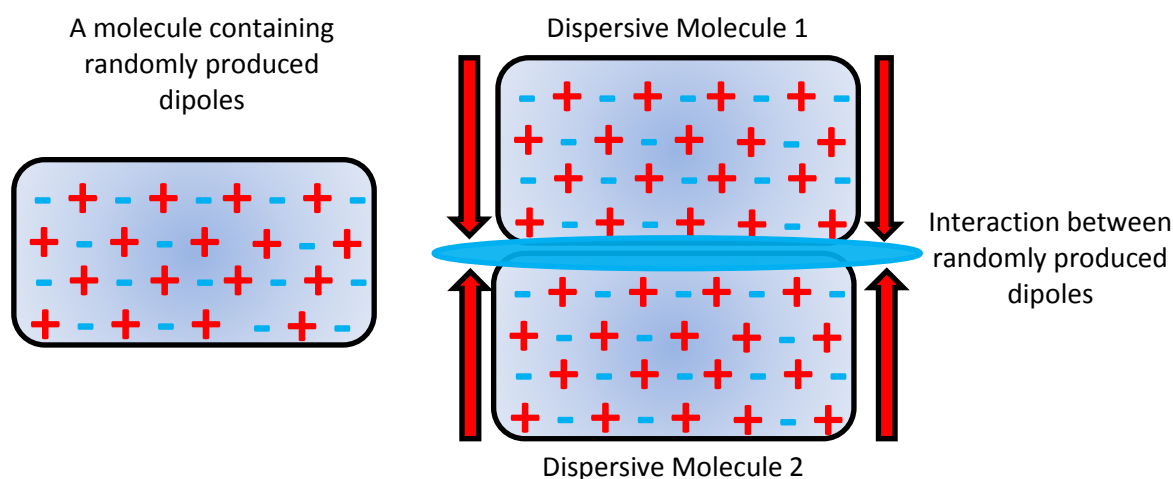


Figure 38: Dispersive interactions

Dipole Interactions

There are two distinctive classes of dipole-dipole interaction:

1. Those between two species containing a permanent dipole, i.e. dipole – dipole interactions
2. Those between a molecule possessing a permanent dipole and a polarisable molecule, i.e. dipole - induced dipole interactions.

Dipole-dipole interactions can be very strong and occur between molecules with permanent dipoles. Examples of this type of interaction occur between alcohols, esters, ethers, amines, amides, and nitriles. As well as the dipole interaction, there will also be a contribution to the intermolecular attraction from the dispersive interaction; however, the strength of the dipole-dipole interaction will far exceed any dispersive interactions that occur^[21, 33].

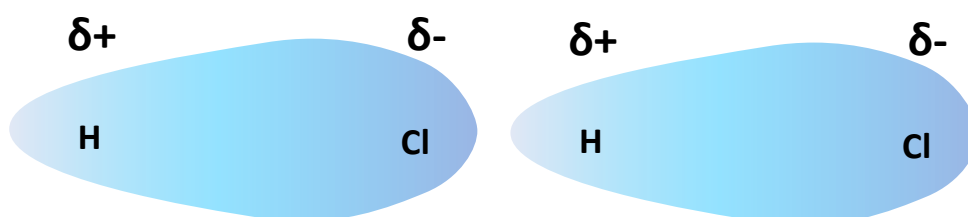


Figure 39: Dipole-dipole interaction between two HCl molecules

Dipole-induced dipole interactions occur when a molecule containing a permanent dipole approaches a molecule that is polarisable. Most commonly these molecules would contain pi-electron systems, i.e. aromatic or unsaturated compounds. The strength of this interaction lies between dispersive and dipole-dipole interactions. Again these interactions will occur alongside any purely dispersive interaction that occurs between the molecules.

Hydrogen Bonding

Hydrogen bonding is a special case of a dipole-dipole interaction in which the dipoles associated with the hydroxyl groups (usually) of two molecules come into close proximity. Hydrogen bonding interactions are very strong compared to dispersive interactions and, in the extreme, the dipole-dipole interaction energy can approach that of a chemical bond, an example being the association of water with methanol^[21, 33].

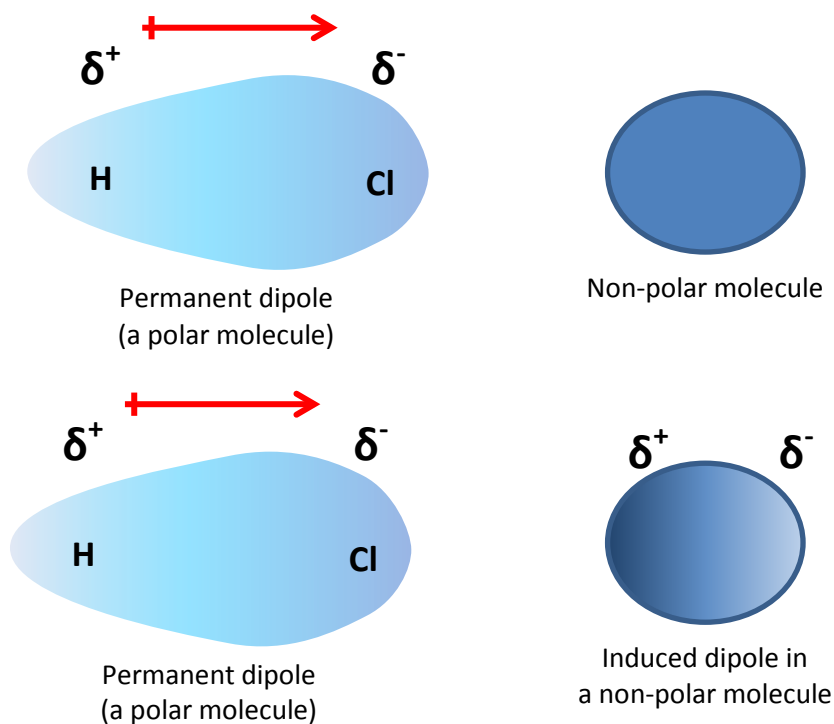


Figure 40: Dipole-induced dipole interaction between permanent dipole and induced dipole

As with dipole interactions, even when molecules are undergoing hydrogen bonding, there is still an underlying weak dispersive interaction occurring simultaneously.

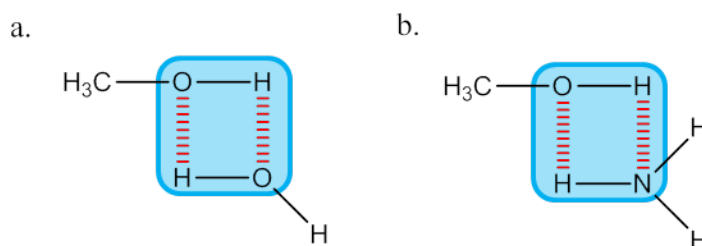


Figure 41: a. Hydrogen bonding interaction between methanol and water, and b. between methanol and ammonia

Table 14: Interaction Energies

Interaction	Typical Energy of Interaction ($\text{kJ}\cdot\text{mol}^{-1}$)
Dispersive	$\ll 1$
Dipole-Induced Dipole	1
Dipole-Dipole	3.3
Hydrogen Bonding	19

2.4.7.2 Polysiloxane Stationary Phases

The methyl modified polysiloxane phases are the most commonly used as they offer a wide range of selectivity, rapid equilibration and high temperature stability. Standard polysiloxanes are characterized by the repeating siloxane backbone. Each silicon atom contains two functional groups. The type and amount of the groups distinguish each stationary phase and its properties. The most basic polysiloxane is the 100% methyl substituted. When other groups are present, the amount is indicated as the percent of the total number of groups. For example, a 5%-(di)phenyl-95%-(di)methyl polysiloxane contains 5% phenyl groups and 95% methyl groups. The phenyl-methyl modified phases have increasing polar selectivity with higher percentage of phenyl groups.

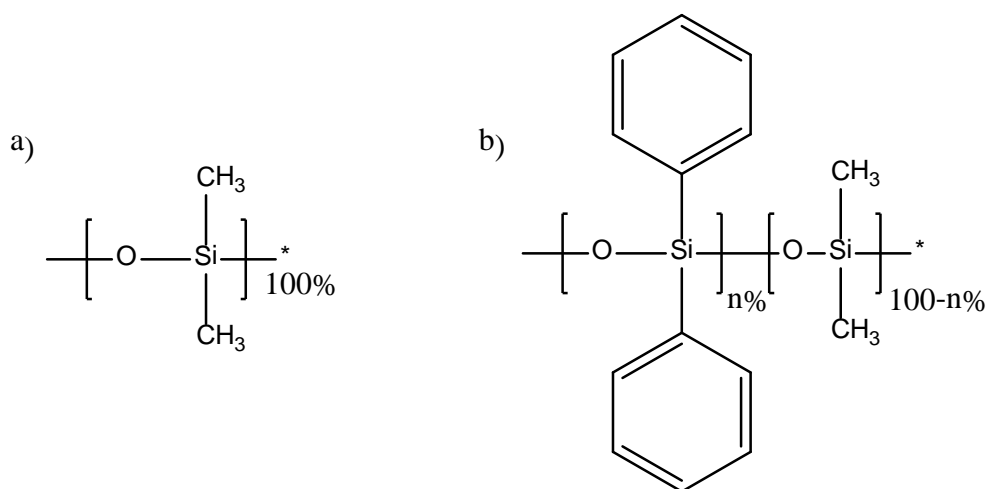


Figure 42: a) 100%-Dimethylpolysiloxane; b) Phenyldimethylpolysiloxane, where the monomer n typically equals 5%, 35% or 50%. A higher percentage of the functional monomer, n, indicates a higher degree of interaction

The primary chemical interactions which occur between phenyl modified stationary phases and analytes are Van der Waals forces and pi orbital stacking. The phenyl groups incorporated into these stationary phases act as pi-pi and H-bonding acceptors.

The 100% dimethylpolysiloxane phases are particularly popular for applications where separations are solely based on boiling points and hydrophobic interactions. The 5%-phenyl phases are the most widely used for GC analysis because of their combination of hydrophobic and aromatic

selectivities. The higher percentage phenyl columns, i.e. 35% and 50%, are generally used where aromatic selectivity is most critical. Compounds commonly analysed using phenyl phases include:

- Alkaloids
- Phenols
- Metabolites
- Pharmaceuticals

There are also 5%-phenyl columns which have an arylene matrix and provide slightly different selectivity in comparison to the other 5%-phenyl phases due to the difference in its structure.

Table 15: Polysiloxane phases

Phase	100% Dimethylpolysiloxane	Phenyl- dimethylpolysiloxane
Predominant Interactions	<ul style="list-style-type: none"> • Dispersive 	<ul style="list-style-type: none"> • Dispersive • Induced Dipole
Primary Applications	<ul style="list-style-type: none"> • Boiling point separations • Hydrocarbon analysis 	<ul style="list-style-type: none"> • Aromatic/aliphatic mixtures

2.4.7.3 Cyano phases

The cyano phases represent the third major type of GC stationary phase functionality. These phases give medium polarity selectivity with increased polarity the higher the cyano content. The cyano phases have temperature limits comparable to those of the PEG phases. 2 common cyano phases are 6%-cyanopropylphenyl-94%-dimethylpolysiloxane and 14%-cyanopropylphenyl-86%-dimethyl-polysiloxane. The naming of this group of phases differs to the before-mentioned. For example, 14% cyanopropylphenyl-dimethylpolysiloxane contains 7% cyanopropyl, 7% phenyl, and 86% methyl. As the cyanopropyl and phenyl groups are on the same silicon atom, their amounts are summed. Cyano phases give unique selectivities for a wide range of compounds due to the combination of hydrophobic, H-bonding, pi orbital and dipole interactions.

Table 16: "Cyano" Dimethylpolysiloxane phases

Phase	Cyanopropylphenyl-dimethylpolysiloxane
Predominant Interactions	<ul style="list-style-type: none"> • Dispersive • Dipole • Hydrogen bonding
Primary Applications	<ul style="list-style-type: none"> • Functionalised molecules

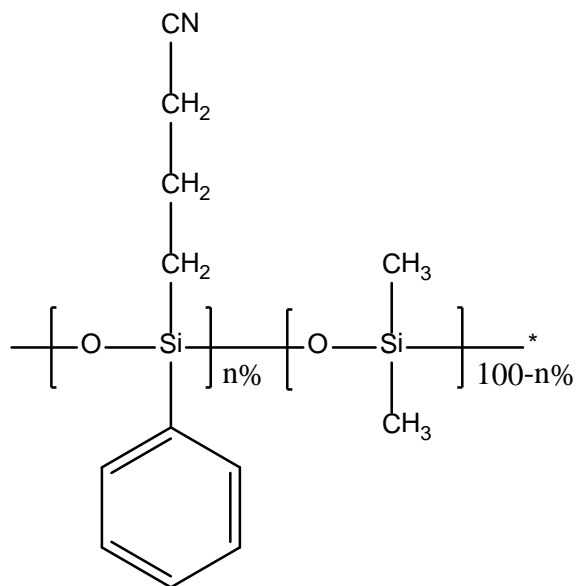
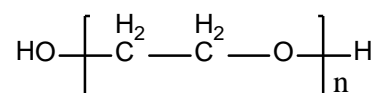


Figure 43: Cyanopropylphenyl-dimethylpolysiloxane, where *n* typically equals 6%, 14% or 50%

2.4.7.4 Polyethylene Glycols

Polyethylene glycols are widely used as stationary phases. These phases represent the most polar of the GC phases. PEGs have the ability to interact with polar functionalities on compounds via H-bonding and dipole-dipole interactions. The thermal stability of PEG phases is much less than that of the phenyl modified phases. Examples of compounds commonly analysed by PEG phases included:

- Alcohols
- Solvents
- Basic compounds
- Small organic acids
- Fatty acids

**Figure 44: Polyethylene glycol or wax stationary phase**

Also available from a number of column suppliers are PEG or wax phases that are 100% aqueous stable. These are made of a lower molecular weight polymer that has a liquid character at a lower temperature than the original wax phase. The unique bonding of the lower molecular weight PEG polymer allows it to be used with 100% aqueous samples without inconsistencies from injection to injection, and also gives better selectivity for low boiling point compounds.

Acid modified PEG phases (modified with nitroterephthalic acid) are also available which give unique selectivities for free fatty acids. The name of most PEG phases of this type is FFAP. Base modified polyethylene glycol stationary phases are also available for the analysis of basic compounds. Strong acids and bases often exhibit peak tailing for standard columns. pH modified stationary phases, such as these, may decrease the amount of tailing for strong acids or bases.

Table 17: Glycol (wax) phases

Phase	Polyethylene Glycol
Predominant Interactions	<ul style="list-style-type: none"> • Dispersive • Dipole • Hydrogen bonding
Primary Applications	<ul style="list-style-type: none"> • Polar compounds

Table 18: Stationary phase interaction summary

Phase	Dispersion	Dipole	H-Bonding
Methyl (-CH₃)	Strong	None	None
Phenyl (-C₆H₅)	Strong	None	Weak
Cyanopropyl (-C₃H₆CN)	Strong	Strong	Moderate
PEG (-OCH₂CH₂O-)	Strong	Strong	Moderate

2.4.7.5 PLOT Columns: Gas-Solid Stationary Phase Selection

PLOT columns are capillaries in the conventional sense but the inner wall of the capillary is coated with small, solid porous particles using a binder. The sample compounds undergo a gas-solid adsorption/desorption process with the stationary phase, and, as the particles are porous, size exclusion and shape selectivity processes also occur.

The most common PLOT column stationary phases include various derivatives of styrene, aluminium oxides and molecular sieves. These columns are very retentive, and are used to obtain separations that are very difficult with conventional stationary phases. PLOT columns are used primarily for the separation of highly volatile liquids and permanent gases without the need for cryogenic or sub-ambient cooling of the GC oven. Separations that would require column temperatures well below ambient temperatures, even with thick film capillary columns, can be obtained at ambient temperatures or above using PLOT column technology^[36].

2.4.7.6 Packed Columns: Stationary Phase Selection

As previously described, packed GC columns contain a particulate adsorbent onto which the stationary phase is coated. Packed columns were for many years the most popular, and, for a significant period of time, the only option for gas chromatography. This has meant that over 1,000 stationary phases and supports have been invented, far too many to be detailed within the confines of this work. The main reason for there being so many more stationary phase types for packed columns in comparison to capillary, is due to the inherent lack of efficiency of packed columns. This makes selectivity of the stationary phase extremely important.

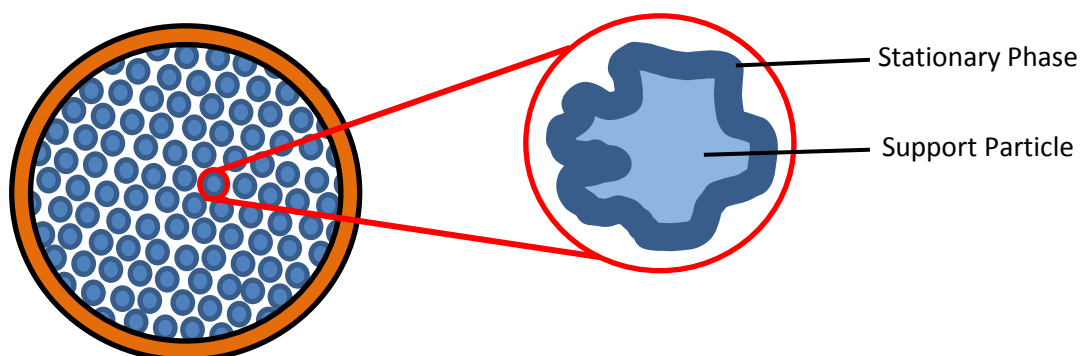


Figure 45: A typical packed GC column, detailing a solid particle coated in stationary phase

2.4.8 The Column Oven

Column temperature is an important variable that must be controlled to a few tenths of a degree for precise work. Liquids or solids must be converted to a vapour state and then be maintained as a vapour throughout a GC separation. Therefore, most gas chromatographs are equipped with ovens to keep the column at a temperature suitable for the analysis. Exceptions are those chromatographs that are used in separating simple gases such as light hydrocarbons or permanent gases. Early gas chromatographs were equipped with isothermal ovens. The optimum column temperature depends upon the boiling point of the sample and the degree of separation required. Roughly, a temperature equal to or slightly above the average boiling point of a sample results in a reasonable elution time. For samples with a broad boiling range, it is often desirable to employ temperature programming, whereby the column temperature is increased either continuously or in steps as the separation proceeds. Today, temperature programmed ovens allow separations of chemicals spanning a range of vapour pressures in a single analysis.

Conventional ovens consist of a resistive wire coil that radiates into the inner volume of the oven. Heat from the resistive wire source is spread, ideally in an even manner, throughout the oven volume using a fan attached to an electric motor. A thermistor or thermocouple inside the oven is part of regulating the oven temperature via the amount of heat released by the heating element. This is controlled by the power delivered to the element and a feedback circuit to control and program the oven temperature. Efforts to create isothermal conditions, i.e. no thermal gradients inside the oven volume, are essential for reproducible chromatography^[23].

2.5 GC Detectors

Detectors identify the presence of compounds as they exit the column. As each separated compound enters the detector from the column, an electrical signal proportional to the amount of compound detected is generated. This signal is generally sent to a data analysis system, such as Agilent's ChemStation, where it shows up as a peak on a chromatogram.

A variety of detectors for gas chromatographs are available. The most widely used detectors in GC have been the flame ionization detector (FID), the

thermal conductivity detector (TCD), the electron capture detector (ECD), and the mass spectrometer (MS). Other common commercially available detectors include the photoionization detector, and the nitrogen–phosphorus detector.

The ideal detector for gas chromatography has the following characteristics:

- Adequate sensitivity
- Good stability and reproducibility
- A linear response to solutes that extends over several orders of magnitude
- A temperature range from room temperature to at least 400 °C
- A short response time that is independent of flow rate
- High reliability and ease of use
- Similarity in response to all solutes or, at least, a highly predictable and selective response toward one or more classes of solutes
- Nondestruction of sample^[3].

2.5.1 The Flame Ionization Detector (FID)

The FID is the most widely used GC detector. The column effluent exiting the column enters the stainless steel jet, which is situated inside a cylindrical electrode system and surrounded by a high flow of air to support combustion, where it mixes with hydrogen gas and air, i.e. the oxidant. It then moves up to the detector head where it burns in an oxy-hydrogen flame producing ions in the process. These ions are collected and form a small current that becomes the signal. The collector electrode is biased about +300 V relative to the flame tip and the collected current is amplified by a high impedance circuit. Since water is produced in the combustion process, the detector must be heated to at least 125 °C to prevent condensation of water and high boiling samples^[14, 37].

Most FIDs run at 250 °C or hotter. The FID is sensitive to almost all molecules that contain hydrogen carbon bonds, including aromatic and chlorinated VOCs, petroleum constituents, semi-volatile organic compounds (SVOC) and polychlorinated biphenyls (PCBs). Detection is in the low ppb to high ppt range. Inorganic compounds are not detectable by FID^[13].

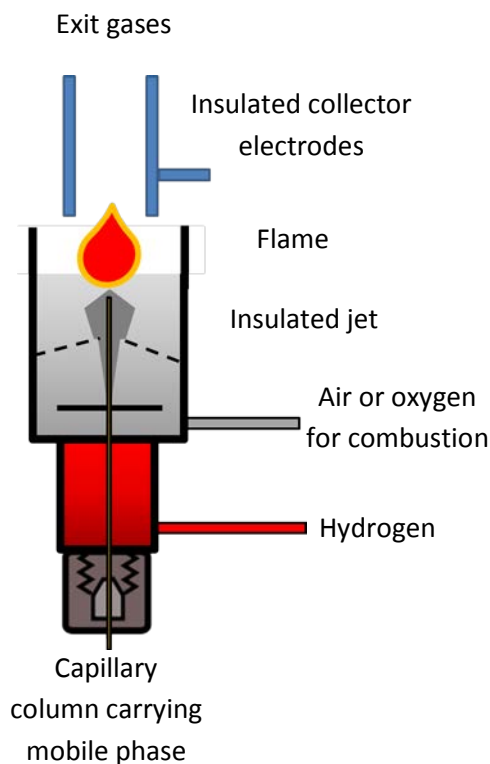


Figure 46: The FID sensor

2.5.2 The Photoionization Detector (PID)

A PID consists of an ultraviolet lamp, ranging in energy from 9.5 to 11.7 eV, mounted on a low-volume flow-through cell. Each constituent of the sample will pass through the cell, where the UV lamp emits suitably high photons to energize and ionize sample components that have an ionization potential less than or equal to its own. Photoionization occurs when an atom or molecule absorbs a photon of sufficient energy to release an electron and form a positive ion. The resulting ions are collected at positively charged electrodes, where the change in current is measured. The type of PID lamp used determines the peak photon energy that can be generated:

- Xenon = 9.6 eV
- Deuterium = 10.2 eV
- Krypton = 10.6 eV
- Argon = 11.7 eV^[38].

Argon lamps, thus, can be used to detect the largest range of volatile compounds, while Xenon lamps are generally used to increase selectivity.

The PID is more selective than the FID, and is able to detect certain inorganic vapours, as well as aromatic and chlorinated VOCs, and petroleum constituents, including benzene, toluene, ethylbenzene and xylene (BTEX). Detection levels are in the low ppb to high ppt range. Unlike the FID, the PID is a non-destructive detector and can be used in series before other detectors. Using multiple detectors extends the range of compounds that can be detected in one analysis. Other advantages include that the PID offers very fast response, high accuracy, and good sensitivity. It is also the most efficient and inexpensive type of gas detector, and is capable of giving instantaneous readings and monitoring continuously^[39, 40].

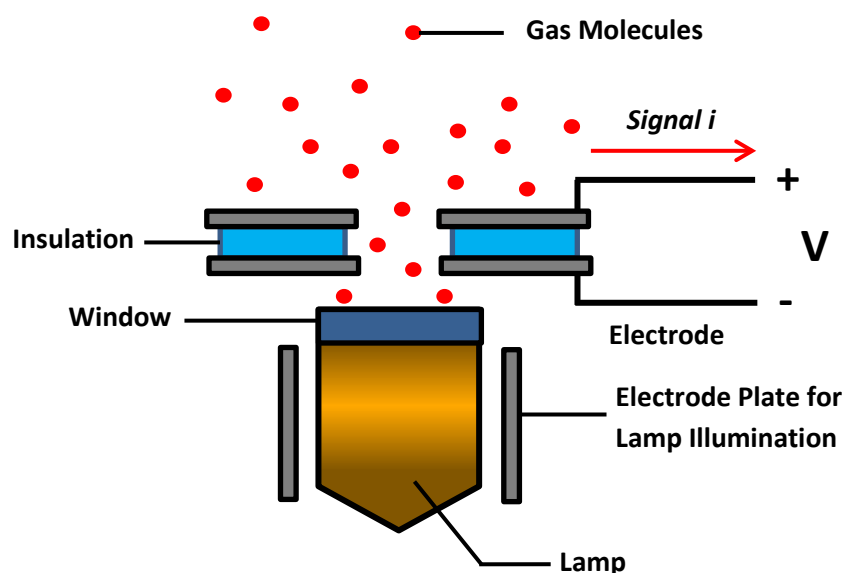


Figure 47: A typical photoionization detector configuration

Table 19: FID vs PID

	FID	PID
Advantages	Good sensitivity	Non-destructive
	Large linearity	Simple
	Ruggedness	Does not require extra gases
	Nearly universal in detection	Portable
Disadvantages	Destructive	Non-selective among organic vapours below ionization potential of lamp
	Complex instrumentation requiring hydrogen	Affected by high humidity

2.5.3 The Electron Capture Detector (ECD)

The ECD is a selective detector capable of providing very high sensitivity for compounds that capture electrons, including halogenated materials such as pesticides and polychlorinated biphenyls. For this reason, one of its primary uses is in pesticide residue and environmental analysis^[14]. Other electronegative functional groups include peroxides, quinones, and nitro groups. This detector is also an ionization-type detector; however, it varies from the before mentioned by detecting samples based on a decrease in the level of ionization, rather than an increase. The column effluent is passed over over a radioactive ^{63}Ni beta emitter. These negatively charged β particles are drawn toward the positive electrode. When they collide with and ionize the make up gas more electrons are produced. This results in a constant standing current between a pair of electrodes. When an electronegative analyte is eluted from the column and enters the detector, it captures some of the free electrons. This results in a marked decrease in the standing current, giving a negative peak, as the negative ions formed have slower mobilities than the free electrons and are, hence not collected by the anode^[3]. The major drawback of ECD is the necessity to use a radioactive source which may require a license or at least regular radiological testing. A newer innovation is an ECD operated with a pulsed discharge so that it does not require a radioactive source. The ECD is also easily contaminated and prone to problems^[25]. Detection levels are again in the low ppb to ppt range, and like the PID, it is a non-destructive detector.

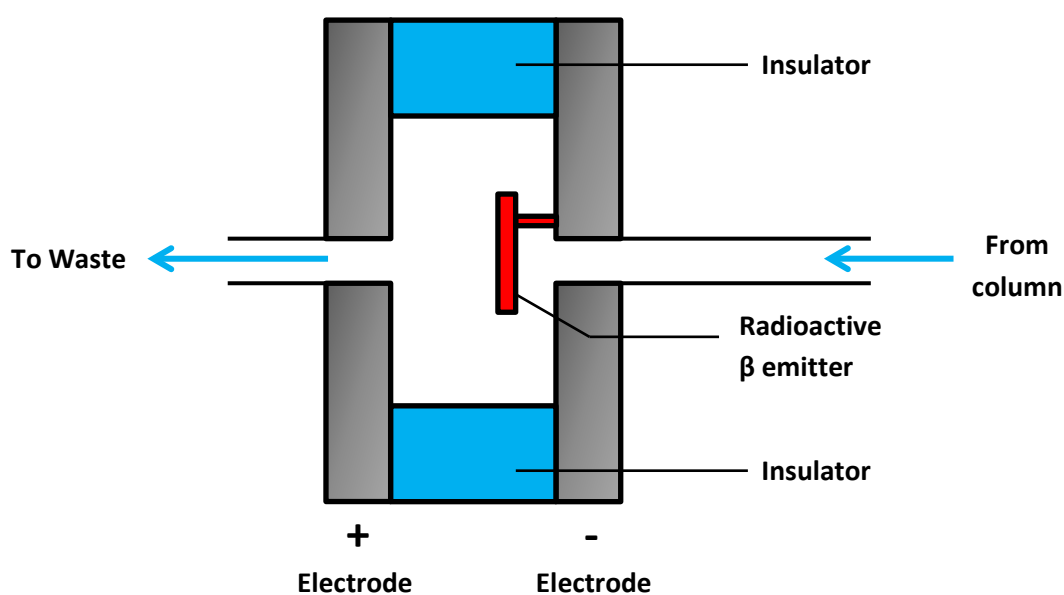


Figure 48: A schematic of an electron capture detector

2.5.4 The Thermal Conductivity Detector (TCD)

The TCD was one of the first detectors used in conjunction with gas chromatography, and they remain popular, particularly for packed columns and inorganic analytes, such as H_2O , CO , CO_2 , and H_2 . As the TCD measures the thermal conductivity of analytes in the mobile phase in comparison to the thermal conductivity of the pure mobile phase, it is classed as a differential detector. As a comparison needs to be made at least two cell cavities are required, although cells with four cavities are more common. These are drilled into a metal block, typically constructed of stainless steel. Each cavity contains a high resistance tungsten or a tungsten-rhenium alloy filament, incorporated into a Wheatstone Bridge circuit^[14]. A temperature differential is created by passing a DC current through filaments, heating them above the temperature of the cell block, and thus creating a temperature differential. When only the pure mobile phase passes over all four of the elements, the bridge circuit is balanced with a zero control, however, when an analyte elutes the thermal conductivity of the gas mixture in the two sample cavities decreases as their filament temperatures increase. This results in a significant increase in the resistance of the filaments causing a voltage to develop across opposite corners of the bridge making it unbalanced. Subsequently, the voltage is

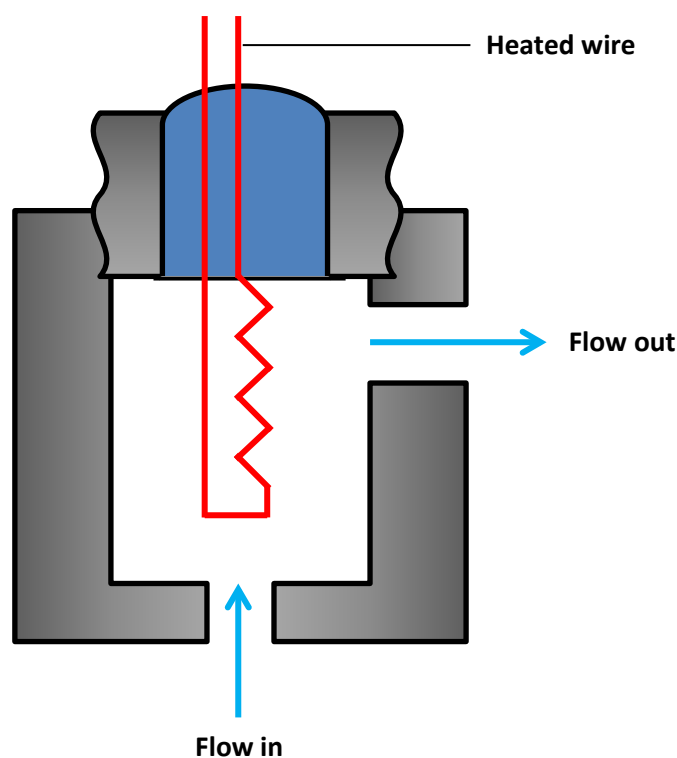


Figure 49: A schematic of a thermal conductivity detector

dropped across an attenuator before all or part of it is fed to a recorder, integrator, or other data system^[3]. The carrier gas used with the TCD must have a thermal conductivity that is very different from the samples to be analysed, so the most commonly used gases are helium and hydrogen, which have the highest thermal conductivity values. Overall, the TCD is a rugged, universal detector with moderate sensitivity. Like the PID, it is non-destructive. It has a limited target analyte list, however, and can only detect gaseous compounds in the ppm range. For this reason it is not used for trace analysis.

2.5.5 The Nitrogen-Phosphorous Detector (NPD)

The NPD is a highly sensitive but very specific detector, giving a strong response to phosphorous, nitrogen and some halogen containing compounds. This detector is similar to the FID, except that the hydrogen gas flow rate is reduced and an electrically heated thermionic rubidium or caesium bead contained inside a small heater coil is positioned just above the jet orifice to receive the column effluent. The bead is heated by passing a current through the coil. Analyte molecules exiting the column collide with the hot bead. Any nitrogen or phosphorous containing molecules partially combust and are adsorbed on the surface of the bead. This adsorbed material reduces the work function of the surface and, as a consequence, the emission of electrons is increased. The discharged ions are attracted to a collector electrode and an electronic amplifier is used to transmit the signal to the data processing system. If the detector is to respond to both nitrogen and phosphorus, then a minimum hydrogen flow is employed to ensure that the gas does not ignite at the jet. In contrast, if the detector is to respond to phosphorus only, a large flow of hydrogen can be used and the mixture burned at the jet. Unfortunately, the response of the detector seriously deteriorates with time, and the bead must be replaced fairly regularly if the detector is in continuous use^[13].

The NPD is destructive and capable of detection in the ppb range. It is typically used in analysis for organophosphorus pesticides and herbicides. In addition, it may be used in analysis of nitroaromatics, i.e. explosives^[41].

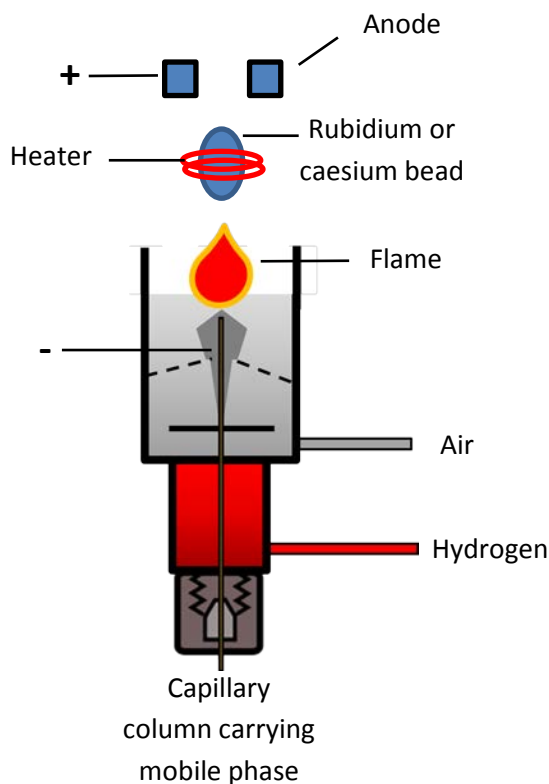


Figure 50: The Nitrogen Phosphorous Detector

2.5.6 The Mass Spectrometer (MS)

The MS detector is, in many cases, the most valuable GC detector type as it is a universal detector with the added benefit of being able to distinguish co-eluting compounds based on differences in their molecular weight or mass to charge ratio (m/z)^[42]. This makes the mass spectrometer a very powerful, useful, and popular detector to use in combination with a gas chromatograph.

As previously described for the before mentioned techniques, analyte molecules must first be ionized to enable detection. A number of ionization techniques exist for MS. The oldest, most common and most simple is electron impact (EI). Here ionization is achieved by impact of a highly energetic (70 eV) electron beam. Column effluent passes into a heated ionization source at low vacuum. Electrons are drawn out from a tungsten filament by a collector voltage of 70 eV. This voltage, which is applied to the filament, defines the energy of the electrons. The high energy electrons then strike the neutral analyte molecules, usually resulting in a loss of an electron and, thus, ionization and fragmentation^[43]. This ionization technique produces almost exclusively positive ions:

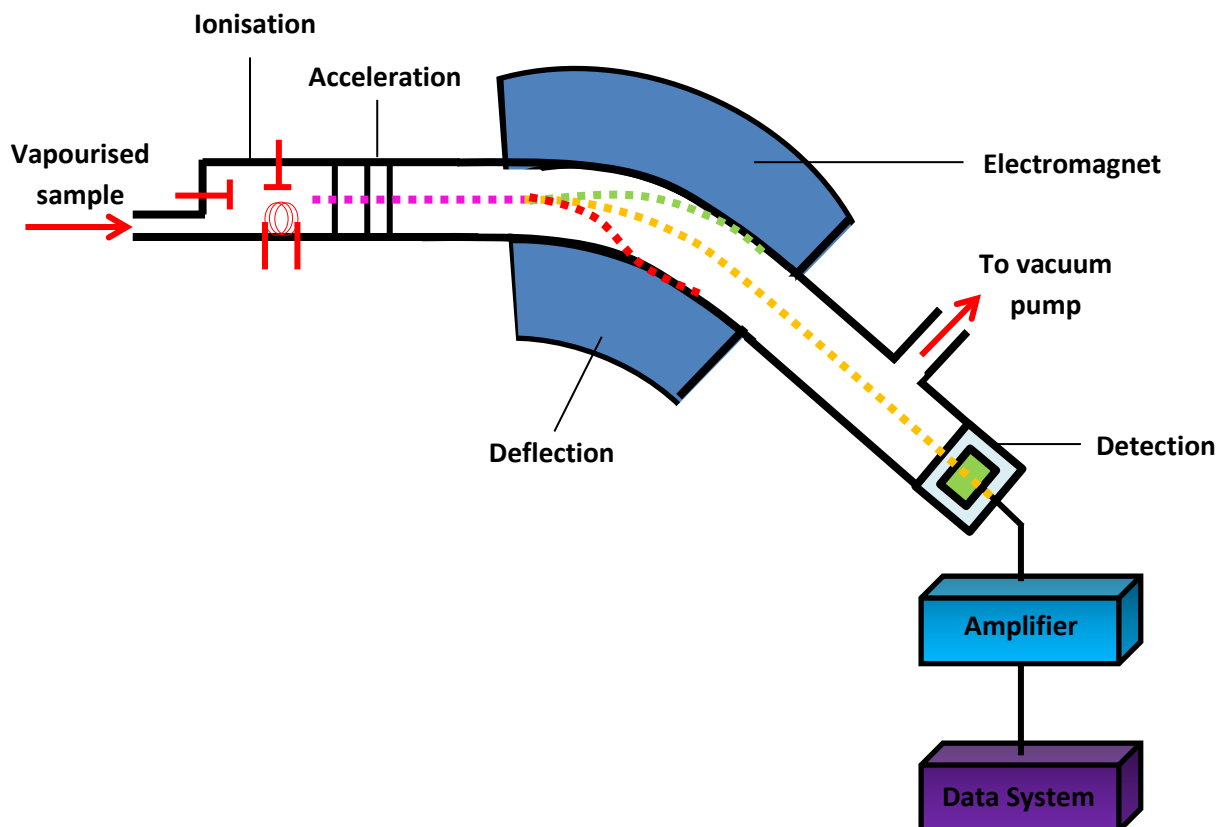
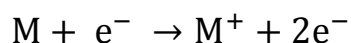


Figure 51: A schematic of a magnetic sector mass spectrometer

Equation 51



Where M = the mass of the analyte of interest.

Another ionization technique commonly used in GC-MS is chemical ionization (CI). In CI, a reagent gas, such as methane, is admitted to the ion chamber where it is ionized. This produces a cation which undergoes further reactions to produce secondary ions. These secondary ions then serve as a reagent to gently ionize the sample. This process generally results in less fragmentation and, thus, a simpler mass spectrum. The major MS peaks that normally result are:

- (M + 1)
- (M)
- (M - 1)
- (M + 29)^[3, 14]

After ionization, the charged particles are repelled and attracted by charged lenses into the mass analyser. Here the ionic species are separated by their mass-to-charge ratio by either magnetic or electrical fields. Typical mass analyzers for GC-MS are quadrupoles or ion traps. Other analyzers are single-focusing magnetic sector, double-focusing magnetic sector, and time of flight.

Table 20: Detector Summary^[44-46]

Detector	Dynamic Range	Dependency
FID	10^7	Mass
PID	10^6	Concentration
ECD	10^4	Concentration
TCD	10^5	Concentration
NPD	10^4	Mass
MS	$10^4 - 10^7$	Mass

2.6 The Data Acquisition System

The overall purpose of separation is to allow for the qualification and quantitation of the individual components of a mixture. Qualitative analysis identifies the solute or solutes present in a mixture, while quantitative analysis determines how much of a substance or substances is present in a mixture. In order to make sense of the raw information gained from the separation and subsequent detection processes, a data acquisition system is required.

Such a system is generally comprised of two basic components. The function of the first is to amplify and convert the analogue signal from the detector into digital data. The second component is typically a computer with a suitable software program installed. This receives and stores the digitized signal, and allows results to be easily retrieved and replayed.

2.7 Validation and Calibration

Methods used in analytical chemistry require validation. It is essential for these methods to be evaluated and tested to ensure that they produce valid results suitable for their intended purpose.

Examples of potential purposes include, but are not limited to, the following:

- Determination of how much of a particular compound or product is present in a sample
- Determination of whether or not a compound or product meets specifications
- Determination of whether or not a compound or product meets regulatory requirements
- Surveillance of an environment to determine the presence and amount of a component, contaminant, or a nutrient
- Identification of a particular compound or product and/or its components.

Validation, therefore, is the process of demonstrating or confirming the performance characteristics of a method of analysis. Determinations of the following set of validation parameters are generally required for qualitative methods:

- Specificity/selectivity
- Limit of detection (LOD)
- Precision
- Stability.

Qualitative methods with a pre-defined threshold concentration for reporting of results require the following additional parameters to also be determined:

- Linearity
- Accuracy (bias) at the threshold concentration
- Precision at the threshold concentration.

Quantitative methods, on the other hand, generally entail the determination of the following:

- Specificity/selectivity
- Limit of detection
- Precision
- Linearity and working range
- Accuracy (bias)
- Recovery
- Uncertainty of measurement
- Stability.

Additional parameters which are desirable, but not always essential, include:

- Lower limit of quantitation (LOQ)
- Ruggedness
- Robustness.

Before a method can be validated, it first must be relatively well developed, optimized, and stabilized. Another requirement is that it has been applied to some practical test samples with acceptable results.

System validation normally precedes method development. All systems and equipment that may affect the efficacy, quality and/or recording of the end product/result require the following qualification steps^[47]:

1. Design Qualification (DQ):

This step demonstrates that either a proposed design or an existing commercially available design will satisfy all pre-agreed user requirements. Before construction or procurement of a design, satisfactory execution of the DQ is essential.

2. Component Qualification (CQ):

The purpose of this step is to ensure that all auxiliary components are manufactured to the correct design criteria.

3. Installation Qualification (IQ):

IQ is necessary to show that the equipment not only meets all specifications, but is correctly installed with all required components and documentation needed for continued operation in place.

4. Operational Qualification (OQ):

This step demonstrates the correct operation of all facets of the equipment.

5. Performance Qualification (PQ):

PQ gives an indication that the process or equipment performs as intended in a consistent manner over time.

Design verification testing (DVT) is performed before the above detailed system validation. DVT takes place after prototyping and involves the comprehensive testing of all product specifications, interface standards, original equipment manufacturer (OEM) requirements, and diagnostic commands. Within the overall process of DVT, the following tests are performed^[48]:

1. Functional testing (including usability)
2. Performance testing
3. Climatic testing
4. Reliability testing
5. Environmental testing
6. Mechanical testing
7. Mean time between failures (MTBF) prediction
8. Compliance and regulatory testing
9. EMC testing and certification
10. Safety certification

Design refinement is generally performed either following this step or concurrently. During this stage of the design process, engineers revise and improve the design to meet performance and design requirements and specifications^[48].

As well as the above instrument based validation steps, any computer and software system developed and used alongside the hardware system would also require its own validation process. The overall aim is the development of a suitably designed system capable of providing a high degree of assurance that every step, process, and change has been thoroughly evaluated before its implementation.

2.7.1 Specificity (Selectivity)

Specificity allows measurement of the ability of a method to identify and quantify the analyte of interest in the presence of other interfering substances which may be found within the overall sample. Examples of such interferences include impurities, degradants and, often, the matrix itself. In order to determine the specificity of a method, known standards should be tested in a matrix as close to the matrix of the sample itself, with the inclusion of any

materials which may be encountered in the sample. Selectivity is concentration-dependent and should be determined at the low end of the calibration range^[49]. The purpose of this validation step is to ensure that the effects of impurities, cross-reacting substances, etc., which may be present in the matrix are known and accounted for.

2.7.2 Quantitative Analysis – The Calibration Curve

Quantitative chromatographic analysis generally consists of the preparation of a series of standard solutions containing a known amount of the analyte of interest. The instrument response for each is measured, with a five-point calibration being typical. Measurement of the peak areas or peak heights of the resulting chromatograms are then taken and plotted as a function of concentration. This then allows for an estimate of the amount of actual analyte present in a sample based on comparison of either the sample peak's height or area with that of one of the standards.

A calibration curve can verify the proper functioning of an analytical instrument, and gives an indication of the following^[50]:

- Linearity
- Regression equation
- Calibration/Working range
- Limit of Detection
- Limit of Quantification
- Correlation efficient R^2

2.7.3 Linearity

The linearity of an analytical procedure is defined as its ability, within a given range, to obtain results which are directly proportional to the concentration of analyte in the sample^[51]. A high correlation coefficient (R^2) of 0.99 or greater is often recommended as a criterion of linearity. As evidenced in the graphs above, all three standard curves had R^2 values of over 0.99 indicating good linearity.

A linear calibration graph takes the general form:

Equation 52

$$y = mx + c$$

Where:

- c = the intercept of the line with the y-axis
- m = the slope or tangent.

In an ideal world, the intercept value would be zero, as, in theory, when no analyte is present no instrument response is expected. However, this is rarely found to be the case in practice. Interactions, interferences, noise, contaminations and other sources of bias result in a baseline value above zero. Thus, the intercept (c) can be considered as the signal of the blank sample of the standard series.

The slope (m) gives an indication of the sensitivity of the overall method, with a steeper slope correlating to a more sensitive method^[51].

2.7.4 Repeatability and Reproducibility

Repeatability conditions occur when analyses are performed by the same analyst on the same day with the same instrument in the same laboratory. Reproducibility conditions are represented by any variation from these conditions, such as the analyses taking place on different days, using different instruments, or being performed in different laboratories.

Precision and accuracy together determine the total error of the analysis. Both require examination under repeatability and reproducibility conditions.

2.7.5 Precision

Precision is a measure of the closeness of the analytical results obtained from a series of replicate measurements of the same measure under the conditions of the method. It reflects the random errors which occur in a method.

Precision is usually expressed as the variance, standard deviation or coefficient of variation of analytical results obtained from independently

prepared quality control standards^[51]. As precision is concentration dependent, it should be measured at different concentrations within the working range. 20% is considered an acceptable precision value at lower concentrations; however, a better value is generally expected for higher concentrations.

The standard deviation (σ) is calculated from the square root of the variance (σ^2) as follows:

Equation 53

$$\sigma = \sqrt{\frac{1}{N} \sum_{i=1}^N (x_i - \bar{x})^2} = \sqrt{\sigma^2}$$

Where:

- σ = the standard deviation
- x_i = each value of the dataset
- \bar{x} = the arithmetic mean of the data
- N = the total number of data points.

Under a normal distribution, \pm one standard deviation encompasses 68% of the measurements and \pm two standard deviations encompasses 96% of the measurements^[52].

The relative standard deviation (RSD), or coefficient of variance, is used to compare the uncertainty between different measurements of varying absolute magnitude. The RSD is calculated from the standard deviation (σ), and is commonly expressed as a percentage (%):

Equation 54

$$\% \text{ RSD} = \left(\frac{\sigma}{\bar{x}} \right) \times 100\%$$

2.7.6 Accuracy

Accuracy is a measure of the extent to which test results generated by the method and the true value agree. Any difference seen is due to systematic method and laboratory error. It is usually expressed as a percentage. A number of techniques exist to determine the accuracy of a method.

1. Comparison of the method results with results from an established reference method.
2. Comparison of the true value as supplied with a control sample or certified reference material (CRM), i.e. a sample of known concentration, with the measured value.
3. Comparison of a blank sample matrix of interest spiked with a known concentration with the method determined value^[51].

Absolute error (E_A) is calculated by:

Equation 55

$$E_A = \text{True Value} - \text{Indicated Value}$$

This value is then used to determine the relative error (e_R) of the system:

Equation 56

$$e_R = \frac{E_A}{\text{True Value}}$$

This then allows for the calculation of accuracy:

Equation 57

$$\% \text{ Accuracy} = (1 - e_R) \times 100\%$$

The accuracy of the system and the method was not determined here; however, had there been more time available it would have been examined.

2.7.7 Limit of Detection (LOD)

The lowest analyte concentration that can be detected and identified, but not necessarily quantitated, with a given degree of certainty is known as the limit of detection^[51]. The LOD is also the lowest concentration that can be distinguished from the background. As with the determination of accuracy, more than one technique exists for the determination of the LOD. All methods require the analysis and comparison of the signal-to-noise ratio (S:N) of blank samples and samples with known low concentrations of analyte. The purpose of these examinations is to establish the minimum concentration at which the analyte can be reliably detected. A minimum S:N ratio of 3:1 is widely accepted for estimating the detection limit^[51].

2.7.8 Limit of Quantitation (LOQ)

An analytical procedure's LOQ is the lowest amount of analyte in a sample which can be quantitatively determined with suitable precision and accuracy. Typically a signal-to-noise ratio of 10:1 can be used to estimate this value in much the same way as LOD is estimated^[51].

2.8 References

1. Ettre, L.S. and K.I. Sakodynskii, *Tswett, M.S. and the Discovery of Chromatography .1. Early Work (1899-1903)*. *Chromatographia*, 1993. **35**(3-4): p. 223-231.
2. Smolkova-Keulemansova, E., *A few milestones on the journey of chromatography*. *Hrc-Journal of High Resolution Chromatography*, 2000. **23**(7-8): p. 497-501.
3. Skoog, D.A., Holler, F. J., Nieman, T. A. , *Principles of Instrumental Analysis*. Fifth Edition ed. 1998, USA: Brooks/Cole Thomson Learning.
4. James, A.T. and A.J.P. Martin, *Gas-Liquid Partition Chromatography - The Separation and Micro-estimation of Volatile Fatty Acids from Formic Acid to Dodecanoic Acid*. *Biochemical Journal*, 1952. **50**(5): p. 679-690.
5. Brinkman, U.A.T. and H.-G. Janssen, *50 years of gas chromatography*. *TrAC Trends in Analytical Chemistry*, 2002. **21**(9-10): p. 545-546.
6. Martin, A.J.P. and R.L.M. Synge, *A new form of chromatogram employing two liquid phases I. A theory of chromatography 2. Application to the*

- micro-determination of the higher monoamino-acids in proteins.* Biochemical Journal, 1941. **35**: p. 1358-1368.
7. Adlard, E.R., *50 years of gas chromatography.* Chromatographia, 2003. **57**: p. S13-S18.
 8. Ettre, L.S., *Chromatography: the separation technique of the 20th century.* Chromatographia, 2000. **51**(1-2): p. 7-17.
 9. Bartle, K.D. and P. Myers. *History of gas chromatography.* in *Meeting of the Royal-Society-Chemistry.* 2001. Leeds, England: Elsevier Science London.
 10. Berezkin, V.G. and E.N. Viktorova. *Changes in the basic experimental parameters of capillary gas chromatography in the 20th century.* in *25th International Symposium on Capillary Chromatography.* 2002. Riva Del Garda, Italy: Elsevier Science Bv.
 11. Desty, D.H., J.N. Haresnape, and B.H.F. Whyman, *Construction of Long Lengths of Coiled Glass Capillary.* Analytical Chemistry, 1960. **32**(2): p. 302-304.
 12. Bente, P.F., E.H. Zerenner, and R.D. Dandeneau, *Silica Chromatographic Column,* U.S. Patent, Editor 1979, Hewlett-Packard Company: USA.
 13. Scott, R.P.W., *Capillary Columns,* 2003, Library4Science: England.
 14. McNair, H.M., Miller, J. M., *Basic Gas Chromatography, Techniques in Analytical Chemistry.* 1997, Canada: John Wiley & Sons, Inc. 193.
 15. Knapp, D.R., *Handbook of Analytical Derivatization Reactions.* 1979, New York: John Wiley and Sons.
 16. Blau, K. and G. King, *Handbook of Derivatives for Chromatography.* 1979, London: Heyden & Sons Ltd.
 17. Scott, R.P.W., *Principles and Practice of Chromatography,* 2003, Libraryforscience, LLC. p. 106.
 18. McNair, H.M. and J.M. Miller, *Basic Gas Chromatography.* Second Edition ed. 2011, New Jersey: John Wiley and Sons. 256.
 19. Wilson, I.D. and C.F. Poole, *Handbook of Methods and Instrumentation in Separation Science.* Vol. Volume 1. 2009, Canada: Academic Press. 866.
 20. Golay, M.J.E., *Gas Chromatography.* 1958, London: Butterworths.
 21. Hinshaw, J.V. *Theory and Instrumentation of GC.* 2011 [cited 2012 02/01/2012]; Available from: www.chromacademy.com/gc-training.asp.

22. Grob, K. *Carrier Gases for GC*. 2010 2012 [cited 2012 03/01/2012]; Available from: www.restek.com/Technical-Resources/Technical-Library/Editorial/editorial_A017.
23. Eiceman, G.A., *Instrumentation in Gas Chromatography, Encyclopedia of Analytical Chemistry*. 2000, London: John Wiley & Sons Ltd.
24. Agilent, *Maintaining your Agilent GC and GC/MS Systems*.
25. Scott, R.P.W., *Principles and Practice of Chromatography*, 2003, Library4Science.
26. Poole, C.F., *The Essence of Chromatography*. 2003, Amsterdam, The Netherlands: Elsevier Science B.V. 927.
27. Hinshaw, J.V. *Headspace Sampling*. Headspace Sampling 2011 01/10/2011 [cited 2011 04/12/2011]; Available from: <http://www.chromatographyonline.com/lcgc/article/articleDetail.jsp?id=747878>.
28. Grob, K. and H.P. Neukom, *Dependence of the Splitting Ratio on Column Temperature in Split Injection Capillary Gas-Chromatography*. *Journal of Chromatography*, 1982. **236**(2): p. 297-306.
29. Grob, K., *Peak Broadening or Splitting caused by Solvent Flooding after Splitless or Cold On-Column Injection in Capillary Gas-Chromatography*. *Journal of Chromatography*, 1981. **213**(1): p. 3-14.
30. Technologies, A., *GC Inlet Resource Guide*, 2001: USA.
31. Grob, K. and C. Wagner, *Procedure for Testing Inertness of Inserts and Insert Packing Materials for GC Injectors*. *Hrc-Journal of High Resolution Chromatography*, 1993. **16**(8): p. 464-468.
32. Scott, R.P.W., *Gas Chromatography*, 2003, Library4Science, LLC. p. 92.
33. Abraham, M.H., C.F. Poole, and S.K. Poole, *Classification of stationary phases and other materials by gas chromatography*. *Journal of Chromatography A*, 1999. **842**(1-2): p. 79-114.
34. Turner, D. and R.E. Majors. *It's All About Selectivity*. 2012 01/02/2012 [cited 2012 04/03/2012]; Available from: <http://www.chromatographyonline.com/lcgc/Features/Its-All-About-Selectivity/ArticleStandard/Article/detail/756793>.
35. Education, P. *Bond Polarity and Electronegativity*. 2010 [cited 2012 04/08/2012]; Available from: <http://wps.prenhall.com/wps/media/objects/3311/3391006/blb0805.html>.

36. Vickers, A.K., *A "Solid" alternative for analysing oxygenated hydrocarbons - Agilent's new capillary GC PLOT column*. Lc Gc Europe, 2007: p. 8-8.
37. Scott, R.P.W., *Gas Chromatography*, 2003, Library4Science, LLC.
38. *Introduction to Photolonisation Detection*. 2010 April 2010 [cited 2011 23 November 2011]; Available from: www.alphasense.com/pdf/PID/AAN_301-04.pdf.
39. *Photoionization Detector (PID) HNU*, 1994, United States Environmental Protection Agency.
40. Chou, J., *Hazardous Gas Monitors - A Practical Guide to Selection, Operation and Applications*. 1999, New York: McGraw-Hill. 258.
41. EPA, *Determinative Chromatographic Separations*, 2003, Environmental Protection Agency: USA. p. 1-66.
42. Llamas, A.M., C.B. Ojeda, and F.S. Rojas, *Process analytical chemistry - Application of mass spectrometry in environmental analysis: An overview*. Applied Spectroscopy Reviews, 2007. **42**(4): p. 345-367.
43. Miller, J.M., *Chromatography Concepts and Contrasts*. Second Edition ed. 2005, New Jersey: John Wiley & Sons, Inc.
44. VWR. *Specifications*. 2012 2012 [cited 2012 02/08/2012]; Available from: https://us.vwr.com/stibo/hi_res/8425265.pdf.
45. Wong, P.S.H., et al, *Ion Trap Mass Spectrometry*. Current Separations, 1995. **16**(3): p. 8.
46. Scientific, R. *GC Volatiles Systems*. 2010 2012 [cited 2012 14/07/2012]; Available from: <http://www.rtf-scientific.com/files/vph.PDF>.
47. *European Commission Enterprise Directorate-General: Qualification and Validation*. 2000 01/01/2000 [cited 2012 03/01/2012]; 15:[11]. Available from: http://ec.europa.eu/health/files/pharmacos/docs/doc2001/feb/annexe15_en.pdf.
48. Silverman, M. *Reliability Services in the Prototype Phase, Design Verification Testing (DVT)*. 2004 01/01/2012 [cited 2012 03/01/2012]; Available from: http://www.opsalacarte.com/Pages/reliability/reliability_prot_dvt.htm.
49. *European Medicines Agency, Validation of Analytical Procedures: Text and Methodology*. 1995 01/06/1995 [cited 2012 03/01/2012]; Available from:

http://www.ema.europa.eu/docs/en_GB/document_library/Scientific_guideline/2009/09/WC500002662.pdf.

50. EPA, *Calibration Curves: Program Use/Needs*. 2010 01/10/2010 [cited 2012 03/01/2012]; Available from: <http://www.epa.gov/fem/pdfs/calibration-guide-ref-final-oct2010.pdf>.
51. *Analytical Detection Limit Guidance & Laboratory Guide for Determining Method Detection Limits*. 1996 01/04/1996 [cited 2012 03/01/2012]; Available from: <http://www.iatl.com/content/file/LOD%20Guidance%20Document.pdf>.
52. Tissue, B.M. *Measures of Precision*. 2000 01/07/2012 [cited 2012 03/07/2012]; Available from: <http://www.files.chem.vt.edu/chem-ed/data/precision.html>.

3.0 Two-Dimensional Gas Chromatography

As evidenced in the previous chapter, gas chromatography is a flexible, relatively simple technique with widespread applications. While conventional GC, in combination with FID or MS, has been used in many studies to measure atmospheric VOCs, it often fails to separate components in particularly complex samples, such as air, to a satisfactory degree. This is because most atmospheric samples contain such a degree of closely eluting peaks of both analytes and matrix components that the peak capacity in only one chromatographic dimension (1D) is greatly exceeded. The result can be severe peak overlap and/or unresolved regions, leading on to difficulties in identification and inaccuracy in quantification^[1]. Lewis, et al. (2000)^[4], in one of the most important applications of GCxGC, illustrated the separation of more than 500 chemical species of VOCs from urban air samples in one run. The strong difference in abundance between components was shown to completely mask numerous air pollutants with relatively lower mixing ratios within the apparent baseline noise observed in GC-MS. This effectively rendered them invisible on a conventional chromatogram^[4, 5]. Many of these previously undetected aliphatic, carbonyl and aromatic components proved to be very reactive ozone precursors, intermediate products of photochemical reactions, and tracers of specific processes. Thus, researchers may have previously underestimated the contribution of some of these VOCs to urban air pollution, and, despite their individual abundances being low, quantification of these species may be of importance for understanding atmospheric processes, such as ozone formation.

In comprehensive 2D GC, each peak separated on the first column (the first dimension) is sliced and fully transferred for further separation into the second column (the second dimension). Usually, the first column contains a non-polar stationary phase, and the second column a polar stationary phase. This combination allows components to be independently separated, first according to their volatility, and then according to their polarity.

3.1 Multidimensional Gas Chromatography (GC-GC)

Historically, the peak capacity problem in conventional gas chromatography was dealt with through the implementation of a technique referred to as

“heart-cutting”. Deans illustrated this technique via the so-called “Deans switch” fluidic valve in 1968, when he diverted a specific section of a GC chromatogram into a second column of different polarity^[6]. Schomburg went on to demonstrate how this could be achieved for capillary columns^[7].

Heart-cutting or multidimensional GC entails a complex and unresolved portion of the main column effluent being collected and subsequently injected to a second column, which is coated with a stationary phase of different selectivity. This process subjects the analytes of interest to an additional separation. The individual fractions need to be small in order to not lose the separation already obtained. While this approach does increase the resolution of the selection portion of the 1D chromatogram, difficulties are encountered when the analytes of interest are scattered throughout the first-dimension chromatogram and when discovery of unknowns is the ultimate aim. Overall, the technique lacks the power of a comprehensive two-dimensional technique, in which the entire sample is subjected to all dimensions of the separation and any subsequent separation dimension preserves the separation achieved in all previous dimensions.

3.2 Comprehensive Two-Dimensional GC (GCxGC)

Two-dimensional chromatography was suggested by Martin in 1944^[8]. A considerable increase in peak capacity is achieved if a mixture to be analysed is subjected to two coupled separations with different separation mechanisms. Comprehensive two-dimensional gas chromatography is a technique that is ideally applied to the separation of complex mixtures of volatile and semi-volatile compounds. The technique is considered comprehensive as all of the analyte mass from the first column is transferred to the second column. Thus, all compounds are subjected to two different separation mechanisms. The other interesting aspect of a comprehensive, as opposed to a heart-cut technique is that the 2D separation is completed in the run time of the first separation. In addition, highly structured 2D chromatograms are often obtained, which facilitate fingerprinting and allow for provisional identification of unknowns.

GCxGC was pioneered by John Phillips in the early 1990s^[9]. Since its introduction, it has become known as a versatile technique that can be applied

to essentially all GC-amenable complex samples and analyte classes for the following purposes:

1. **Target-compound analysis.** This type of analysis is devoted to a limited number of compounds in a complex matrix.
2. **Group type analysis.** Here, the goal is to distinguish and analyse families of compounds.
3. **Fingerprinting (or exhaustive analysis).** The objective here is the classification of a sample in a certain group or category, or the complete analysis of the entire sample^[10].

Table 21: Selected applications of GCxGC

Analyte	Sample
Hydrocarbon (group) type	Gasoline; kerosene; diesel; fire debris; C ₉ olefins
Biomarkers	Crude oil
Oxygenates	Gasoline
S-containing compounds	Diesel; gas oil; kerosene
Alkylphenols	Industrial phenol additive
Flavours and fragrances	Tea; lavender; oregano, bergamot; ginger; ginseng; tea tree; peppermint; brunch extract; sour creams; garlic
PCBs, toxaphene	Standards; enantiomers; cod liver; technical mixtures
Pesticides	Surface water; fruits; vegetables
FAMES	Fish; vegetable oils; mussels
PAHs	Soil; sediment; fly ash
VOCs, aromatics, oxygenates	Air
Racing drugs	Horse/dog urine
Sterols	Faeces
PCBs, dioxins, pesticides	Serum; urine
Wound-induced plant volatiles	Leaves
Nitrosamines	Cigarette smoke
Polyphenols	Wine

3.2.1 Principles of GCxGC Separation

The mechanism of a GCxGC separation involves injection of the sample onto a first chromatographic column, termed the primary column for initial separation, as with 1D GC. Molecules eluting from this column are then trapped or collected by a modulator (also termed an interface), rather than traversing to the detector. This modulator periodically samples or injects its contents, i.e. the entire collected fraction, onto a second column at a known, regular interval, which is typically in the range of 2-6 s. It then collects another fraction of the effluent from the first column, while the previous fraction is undergoing a very fast and independent separation on the second dimension column, before elution to detector, where it is measured. This process of effluent collection and injection repeats itself throughout the entire analysis.

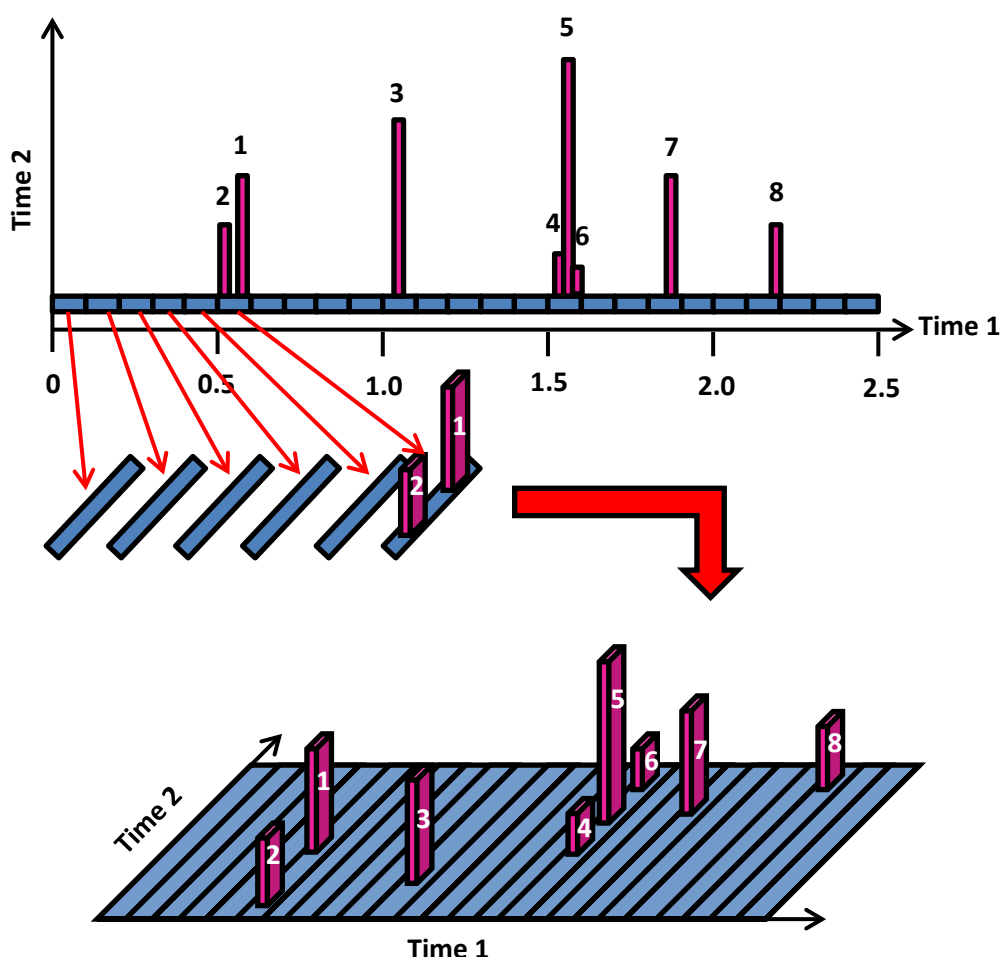


Figure 52: Schematic representing a raw GCxGC chromatogram indicating the positions of individual slices and illustrating how a 3D chromatogram is reconstructed from the raw chromatogram

GCxGC offers many advantages over conventional 1D GC. An important benefit is the very high separation capacity that can be achieved. As a result of the orthogonality, i.e. independent separation mechanisms, of the two separating dimensions to which all constituents of a sample are subjected, the separation power of the GCxGC system is roughly equal to the product of the separation powers of the individual columns. This is what allows for far more compounds to be baseline resolved in a 2D separation plane in comparison to a conventional 1D chromatographic analysis. Not only does the chromatography benefit from enhanced separation of the analytes from each other, but another major advantage is the separation of these analytes from a large part of the interfering background.

GCxGC also boasts improved analyte detectability. This is due to the focusing and compressing effect of the modulator. Since the separation of each modulated fraction on the short second column has to be completed before the next fraction is injected, the second-dimension separation takes only a few seconds. To prevent peak broadening, before injection onto the second column, the modulator focuses the first-column eluate fractions into very narrow pulses with typical widths of approximately 10 ms. The result of this is peak amplitudes that are typically enhanced 20-150 fold, due to the mass conservation in all, except valve-based, modulators^[11]. It is important to note, that such narrow peaks demand very high data acquisition rates of up to 200 Hz. Noise is also, thus, proportionately more prominent. This means that, despite the considerable peak enhancement, improvement of the limits of detection (LODs) are generally more modest, i.e. 5-10 fold.

A further advantage of GCxGC is the generation of structured or ordered chromatograms. This feature has proven very helpful for identification purposes, especially due to the complexity of the majority of GCxGC chromatograms. Those compounds having the same basic structure of containing the same functional group, i.e. members of the same chemical class, have been shown to exhibit a related second-dimension retention time. As a consequence, such classes of compounds are exhibited as bands or clusters, which can easily be recognised in the 2D GCxGC plane. Compounds are further distributed, within each of these clusters, according to their number of carbon

atoms and/or the number and length of the alkyl chains attached to the functional groups. It has been found that compounds with higher boiling points have correspondingly higher first dimension retention times. Compounds that are more polar or polarisable, on the other hand, exhibit higher second dimension retention times^[12]. This structuring facilitates the identification of unknown compounds and the comparison of complex atmospheric samples.

3.2.2 GCxGC Instrumentation

The GCxGC instrument itself is very similar to a conventional GC, and most 2D GC set-ups are the result of the modification of a conventional gas chromatograph. Consequently, the instrumental components utilized in GCxGC are mostly the same as in 1D GC. A block diagram of the typical GCxGC set-up is illustrated below.

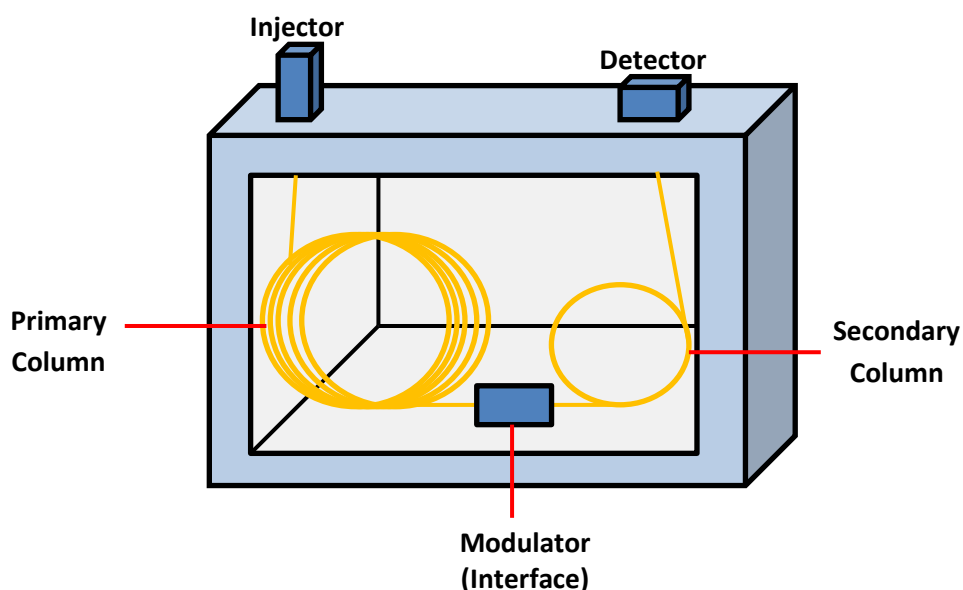


Figure 53: Schematic of a gas chromatogram set up for GCxGC analysis

Important components include the injector, the oven, the columns and the detector. Typically, a longer column coated with a thicker film of a nonpolar stationary phase is installed as the primary column. Its outlet is connected through the modulator to the inlet of the second dimension column, which is coated with a stationary phase of different selectivity^[1].

3.2.2.1 GCxGC Columns

Different compounds obviously undergo different separation mechanisms. For GCxGC analysis any combination of column phase types can be utilised, provided orthogonal separation is facilitated. Typically, however, column sets include a nonpolar first dimension followed by a polar second dimension, as seen in Figure 56 taken from Lewis, et al. (2000)^[4]. This type of arrangement ensures differing retention mechanisms between the columns. The other general requirement is that the second column is shorter and has an internal diameter that is equal to or less than the first column. This ensures that the second column can operate at the required high speed and, hence, complete

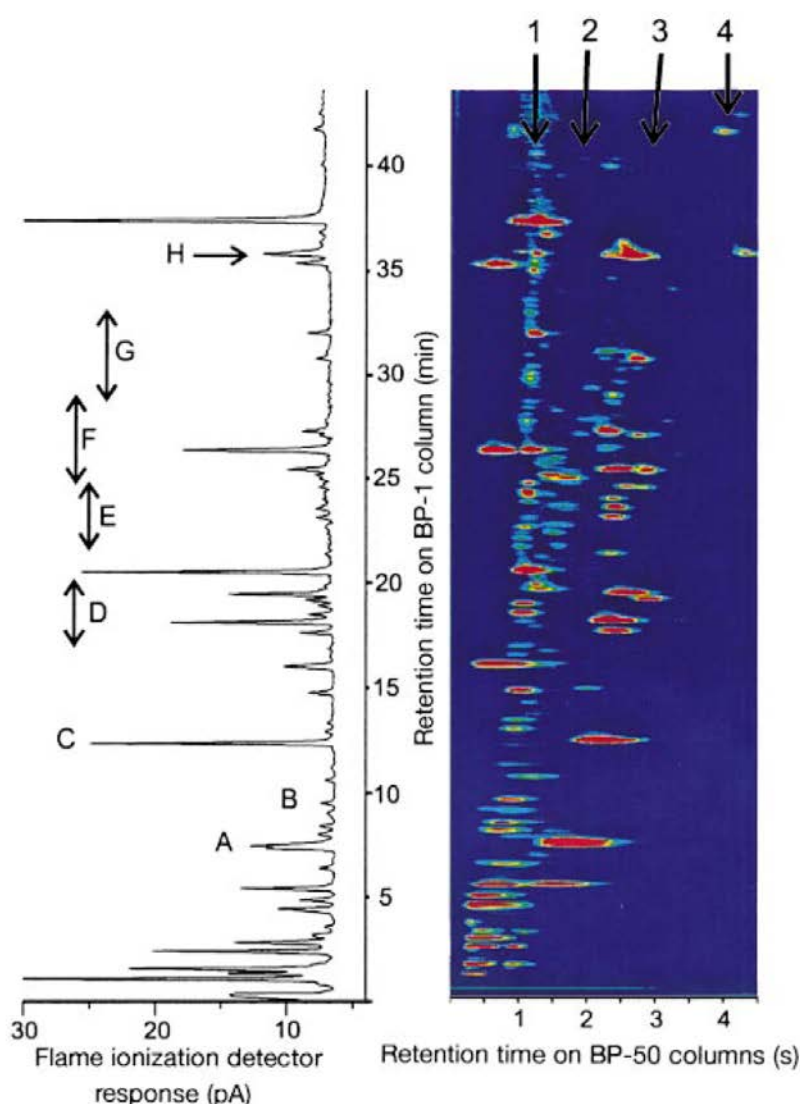


Figure 54: Comprehensive and one-dimensional separations of VOCs in urban air. A. benzene; B. heptane, C. toluene; D. xylenes; E. C₃-benzenes; F. C₄-benzenes; G. C₅-benzenes; H. naphthalene. 1. aliphatic band; 2. carbonyl band; 3. aromatic band; 4. bi-aromatics^[4].

the separation of one injected fraction before the separation of the next fraction is started. Usual primary column lengths are in the order of 20-30 m, while secondary columns are generally 0.5-1 m in length.

The idea that a narrower column should be used in the second dimension has become the conventional wisdom when choosing column sets for GCxGC separations. However, it has been found that overloading of the second dimension is a common feature of such a set up, even when the primary dimension column is not overloaded^[13]. Overloading is the result of the modulator focusing portions of the effluent from the primary column into the very narrow channel of the secondary. This results in reduced peak capacity in the second dimension. Since the amount of second dimension separation space is highly limited, any losses here, including those due to overloading, could seriously impair the performance of the system. Experimentation has shown that this can be avoided by having a secondary column I.D. that is equal to or larger than the first^[13].

On the other hand, narrower columns have significant advantages, most important of which is related to separation speed. It is much easier to obtain a very fast separation in the second dimension with a narrow column. They also provide narrower peaks under conditions of no overload.

When analyzing samples in which the concentrations of the analytes or matrix components are unknown and may be high, logic would suggest that it may be better to use larger diameter columns in the second dimension, as this will lessen the chances and consequences of overloading here. In addition, this may lead to better overall resolution in this second dimension.

Primary dimension separation is generally in the programmed-temperature mode, while the separation on the secondary column is extremely fast and so tends to be performed under essentially isothermal conditions.

3.2.2.2 Modulators

The modulator ensures that the separation is both comprehensive, i.e. the entire sample is subjected to both separation dimensions, and multidimensional, i.e. the separation that is accomplished in one dimension is not lost in the other. The component is positioned at the junction of the dual

column set. Different mechanisms, depending on the modulator, are applied to trap or compress the eluting solutes from the first column and pulse them as narrow peaks of about 0.01 s width to the second. When a given pulse is analysed via the secondary column, the modulator prevents further elution of the solutes at the junction and segments or segregates the solutes into pulsed peaks according to the mechanics of the modulator and the phase and frequency of modulation.

Without a modulator in place to sample the first dimension periodically, bands of analytes separated at the end of the first column, are at risk of recombining in the second column and co-elute at the detector. It is also possible that the bands could change their elution order when they flow unrestricted from one column to the next.

With the addition of a properly configured modulator with an appropriately chosen sampling frequency, the primary column separation will be preserved, as the material the modulator contains is only periodically allowed to enter into the second dimension column thus facilitating GCxGC separation. Each peak eluting from the first dimension should be sampled at least three times across its width^[14].

Numerous modulator designs have been trialled and implemented. The two main types of modulation possible are thermal and fluidic or valve-based modulation.

Thermal Modulation

Thermal modulation allows for the trapping of the analyte mass eluting from the first column in a short segment of capillary column coated with a thick-film stationary phase. A heater rotates over the column trap to desorb, compress and inject the trapped analyte mass into the second column. Different types of thermal modulation have been developed, including ones that enable liquid nitrogen^[15], carbon dioxide or cooled air (cryogenic-jet type modulators) to intermittently blow over a section of the second column to trap the primary column effluent. Following cooling, the column section is rapidly reheated passively from the circulating hot oven air or directly to release the trapped peaks more rapidly. An issue with this type of modulation

is that during the heating stage, any new peak material exiting the primary column will not be trapped and can enter the secondary column along with the already trapped material, resulting in some overlapping and smearing of peak bands^[16].

To counteract this, a second thermal modulator is generally used. Here, the modulators are heated and cooled out of phase with each other. Cooling the first modulator traps peaks at this point. The second modulator is then cooled whilst the first is heated. Thus, while the first modulator is hot, the trapped peaks move to the cooled second modulator zone along with any material that leaks through. On recooling of the first modulator again, the two trapping zones are effectively isolated from each other. The second modulator is then heated, and the trapped peaks are released into the secondary column for separation. Any new material eluting from the first column is trapped inside the still cool first modulator, and so does not enter the second column until the next secondary analysis is ready to start. This scheme effectively isolates the two columns from each other for the purposes of GCxGC^[17].

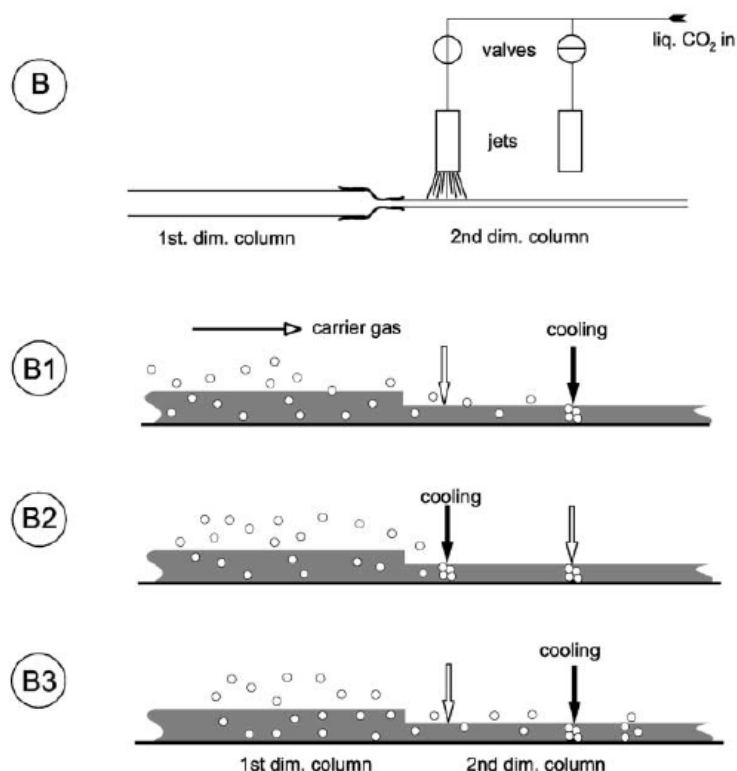


Figure 55: Schematic of dual-jet cryogenic modulation. (B1) Right hand side jet traps analytes eluting from first column; (B2) Right hand side jet switched off, cold spot heats up rapidly and analyte pulse is released into second column; simultaneously, left hand side jet switched on to prevent leakage of first-column material; (B3) next modulation cycle is started^[3].

Cryogenic modulation offers a rapid and reproducible thermal cycle with a resulting high sensitivity through peak sharpening. However, it does have some practical drawbacks, including limited trapping of high-volatility species, freeze out of water in moist samples, ease of portability, and high consumable use if liquid nitrogen is used as coolant.

Valve-Based Modulation

Valve-based modulators can also be used to make GC×GC measurements^[16]. Here, a diaphragm valve is typically used as interface between the two columns. Numerous configurations of this modulation method have been designed, ranging from both columns and the valve being inside the same GC oven, to more recent conformations where a second independently controlled oven houses the valve and the second column. While the former was ideal for mixtures capable of separation under 175 °C (the maximum manufacturer-specified operating temperature for the diaphragm valve due to three O-rings in the interior of the valve), the latter results in a more versatile system to optimize separations on both columns ^[18, 19].

Valve-based comprehensive two-dimensional gas chromatograph is not only compact and robust, but it is also inexpensive. The major drawback of this modulation configuration is the diminished detection sensitivity it can experience, due to only a portion of the effluent from the first column being transferred to the second. However, this loss of sensitivity has now been addressed by the development of total-transfer valve-based GC×GC^[20, 21]. Here, one of the appropriate ports of the high-speed six-port diaphragm valve used as the modulator is simply blocked, resulting in 100% mass transfer from the primary to the secondary column.

The modulation set up used for this project was based on the differential flow modulation first introduced by Seeley et al^[2]. This group used a 2-way, 6-port diaphragm valve, shown in Figure 58, to connect the two columns via a sample loop. Initial designs saw the valve being kept in the sample position for 80% of the time during each modulation period. On actuation of the valve, the sample loop was rapidly flushed to efficiently pass its contents onto the second column. Seeley then went on to produce a differential flow modulator that provided total transfer, resulting in full conservation of material between

columns. This was based on a fluidic switching design, similar to the modulation used for the purposes of this project, and was constructed using a three-way solenoid valve outside the sample path, which controls the direction of sample flow, thus allowing 100% transfer from primary to secondary column^[22]. To eliminate the problems associated with exceeding the maximum temperature limit of the component, the valve could be housed outside the GC oven. A simplified version of this modulator has been adapted by Agilent for commercial use^[23].

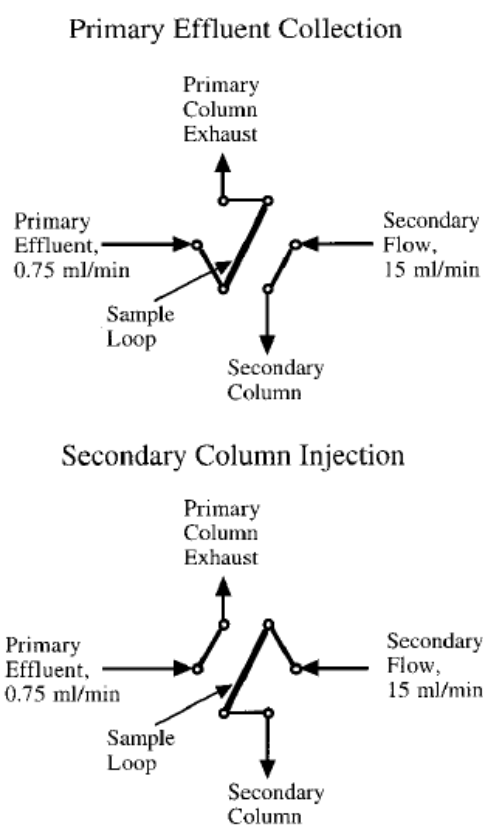


Figure 56: Configuration of Seeley's 6-port modulation valve^[2]

3.2.2.3 GCxGC Detectors

GCxGC analysis requires detectors with a small internal volume, a short rise time and a high data acquisition rate to ensure proper reconstruction of the second-dimension chromatograms. The following detectors have been determined as suitable for GCxGC:

- The flame ionization detector, which has small volumes and acquisition frequencies of 50–300 Hz
- The electron capture detector, with an acquisition frequency of 50 Hz

- The atomic emission detector (AED), with a transfer line adaptation to eliminate the drawback of a mere 10 Hz frequency
- The sulphur chemiluminescence detector (SCD)
- The nitrogen chemiluminescence detector (NCD)^[1].

The above mentioned detectors permit peak recognition, but provide no structural information. To achieve this, a time-of-flight mass spectrometer (TOF MS), which can be operated at high repetition rates of 5–30 kHz, can acquire the fifty or more mass spectra per second which are required for quantification. Fast scanning quadrupole mass spectrometers, with acquisition rates of 33–50 Hz capable of achieving scan ranges of 50–100 mass units, have also recently been shown to perform satisfactorily^[24].

3.2.3 GC×GC Data and Plots

The data produced by GC×GC analysis and the software used to interpret that data differs vastly from that associated with conventional GC. The data system cuts the data arriving at the detector into individual second-dimension chromatograms. It then aligns them into a signal matrix. Two dimensional data is plotted using one independent axis for primary column retention and a second independent axis for secondary-column retention to give a comprehensive two-dimensional chromatogram, which is usually visualised as a 2D colour or contour plot and, occasionally, as a 3D plot^[17, 25].

When a TOF MS detector is coupled to the GC×GC system, an additional dimension is added to the data (that of mass-to-charge ratio). Such highly-structured data are proving to be both incredibly valuable when coupled with novel chemometric techniques, and incredibly challenging to manage and manipulate. GC×GC-TOF MS data cubes containing on the order of 110 million data points per hour for a single sample are not uncommon. Efficient means of sifting through these data to extract useful information is one of the current challenges facing the technique.

In order to derive quantitative information from the data in a GC×GC analysis, the modulated peaks corresponding to the analyte of interest are integrated as usual using the raw data file. The areas of all these peaks are then summed.

3.2.4 The Future of GCxGC

Comprehensive 2-dimensional GC is still a relatively new technique, and since its inception there have been continuous developments in this field. Both conventional GC and GCxGC are robust, reliable, highly sensitive and reproducible tools for environmental and atmospheric gas analysis. Unfortunately, however, despite a high degree of current commercial instrument sophistication, modern GC systems are bulky, power intensive (typically up to 3 kW peak) and require fairly long analysis times. This makes the GC a difficult instrument to operate in remote and challenging locations, such as the Antarctic and the jungles of Borneo. As a result, analyses in such situations are often performed back in the laboratories, far away from the emission source and a long time after the sampling.

There is great potential in this area, therefore, for microfabricated GC systems that are compact, robust and with low power demands. There is particular intrinsic attraction in monolithic GC structures, where all components of the device (injector, column, and detector) are formed in a single fabrication step with benefits for robustness, lack of interconnections, and a structure geometry that is very much easier to heat using planar devices.

3.3 References

1. Panic, O. and T. Gorecki, *Comprehensive two-dimensional gas chromatography (GCxGC) in environmental analysis and monitoring*. Analytical and Bioanalytical Chemistry, 2006. **386**(4): p. 1013-1023.
2. Seeley, J.V., F. Kramp, and C.J. Hicks, *Comprehensive two-dimensional gas chromatography via differential flow modulation*. Analytical Chemistry, 2000. **72**(18): p. 4346-4352.
3. Harynuk, J. and T. Gorecki. *Comparison of comprehensive two-dimensional gas chromatography in conventional and stop-flow modes*. in *28th International Symposium on Capillary Chromatography and Electrophoresis*. 2005. Las Vegas, NV: Elsevier Science Bv.
4. Lewis, A.C., et al., *A larger pool of ozone-forming carbon compounds in urban atmospheres*. Nature, 2000. **405**(6788): p. 778-781.

5. Xu, X., et al., *Comprehensive two-dimensional gas chromatography (GC x GC) measurements of volatile organic compounds in the atmosphere*. Atmospheric Chemistry and Physics, 2003. **3**: p. 665-682.
6. Deans, D., *A new technique for heart cutting in gas chromatography [1]*. Chromatographia, 1968. **1**(1): p. 18-22.
7. Bartle, K.D. and P. Myers. *History of gas chromatography*. in *Meeting of the Royal-Society-Chemistry*. 2001. Leeds, England: Elsevier Science London.
8. Consden, R., A.H. Gordon, and A.J.P. Martin, *Qualitative analysis of proteins: a partition chromatographic method using paper*. Biochemical Journal, 1944. **38**: p. 11.
9. Phillips, J.B. and J. Beens, *Comprehensive two-dimensional gas chromatography: a hyphenated method with strong coupling between the two dimensions*. Journal of Chromatography A, 1999. **856**(1-2): p. 331-347.
10. Vivo-Truyols, G. and P.J. Schoenmakers. *Chemical variance, a useful tool for the interpretation and analysis of two-dimensional chromatograms*. in *29th International Symposium on High Performance Liquid Separations and Related Techniques (HPLC 2005)*. 2005. Stockholm, Sweden: Elsevier Science Bv.
11. Adahchour, M., et al., *Recent developments in comprehensive two-dimensional gas chromatography (GC X GC) I. Introduction and instrumental set-up*. Trac-Trends in Analytical Chemistry, 2006. **25**(5): p. 438-454.
12. Beens, J. and U.A.T. Brinkman, *Comprehensive two-dimensional gas chromatography - a powerful and widely applicable technique*. Analytical and Bioanalytical Chemistry, 2004. **378**(8): p. 1939-1943.
13. Harynuk, J., T. Gorecki, and J. de Zeeuw. *Overloading of the second-dimension column in comprehensive two-dimensional gas chromatography*. in *27th International Symposium on Capillary Chromatography*. 2004. Riva del Garda, ITALY: Elsevier Science Bv.
14. Górecki, T., J. Harynuk, and O. Panic. *Comprehensive Two-Dimensional Gas Chromatography (GCxGC)*. 2010 01/01/2010 [cited 2012 03/01/2012];

Available from: http://www.chem.pg.gda.pl/CEEAM/Dokumenty/CEEAM_ksiazka/Chapters/chapter6.pdf.

15. Pursch, M., et al. *Comprehensive two-dimensional gas chromatography using liquid nitrogen modulation: set-up and applications*. in *1st International Symposium on Comprehensive Multidimensional Gas Chromatography*. 2003. Volendam, Netherlands: Elsevier Science Bv.
16. Fryzinger, G.S., R.B. Gaines, and C.M. Reddy, *GCxGC—A New Analytical Tool For Environmental Forensics*. *Environmental Forensics*, 2002. **3**(1): p. 27-34.
17. Hinshaw, J.V., *Comprehensive two-dimensional gas chromatography*. *Lc Gc Europe*, 2004. **17**(2): p. 86-+.
18. Sinha, A.E., et al., *Comprehensive two-dimensional gas chromatography of volatile and semi-volatile components using a diaphragm valve-based instrument*. *Journal of Chromatography A*, 2003. **983**(1-2): p. 195-204.
19. Sinha, A.E., et al. *Valve-based comprehensive two-dimensional gas chromatography with time-of-flight mass spectrometric detection: instrumentation and figures-of-merit*. in *1st International Symposium on Comprehensive Multidimensional Gas Chromatography*. 2003. Volendam, Netherlands: Elsevier Science Bv.
20. Mohler, R.E., B.J. Prazen, and R.E. Synovec, *Total-transfer, valve-based comprehensive two-dimensional gas chromatography*. *Analytica Chimica Acta*, 2006. **555**(1): p. 68-74.
21. Hamilton, J.F., *Using Comprehensive Two-Dimensional Gas Chromatography to Study the Atmosphere*. *Journal of Chromatographic Science*, 2010. **48**(4): p. 274-282, 10A-11A.
22. Seeley, J.V., et al., *Comprehensive two-dimensional gas chromatography with a simple fluidic modulator*. *American Laboratory*, 2006. **38**(9): p. 24-26.
23. Firor, R.L. *Operation and Applications of Differential Flow Modulation*. 2010 01/10/2010 [cited 2012 03/04/2012]; Available from: http://www.chem.agilent.com/Library/eseminars/Public/Roger_Firor_-_Operation_and_Applications_of_Diff_Flow_Modulation_GC_x_GC.pdf.

24. Beens, J. and U.A.T. Brinkman, *Comprehensive two-dimensional gas chromatography - a powerful and versatile technique*. *Analyst*, 2005. **130**(2): p. 123-127.
25. Marriott, P.J., P. Haglund, and R.C.Y. Ong, *A review of environmental toxicant analysis by using multidimensional gas chromatography and comprehensive GC*. *Clinica Chimica Acta*, 2003. **328**(1-2): p. 1-19.

4.0 GC Miniaturisation

The following chapter gives a detailed literature review of the reported attempts and successes at miniaturising gas chromatography instrumentation^[1].

Miniaturised and microfabricated GC systems are not a new proposition; the first gas chromatograph fabricated in silicon using photolithography and chemical etching techniques was reported in 1975 by Terry, et al. at Stanford University^[6]. The micro-GC consisted of an injection valve and a 1.5 m long column with a depth of 40 μm and a width of 200 μm fabricated on a silicon wafer, with an internally mounted thermal conductivity detector. The spiral column had a rectangular cross-section, and the silicon wafer was hermetically sealed to a Pyrex glass cover plate^[6]. The resolving power of the column was poor in comparison to standard columns of the day. A number of factors contributed to this, not least the difficulty in evenly coating rectangular channels and that the majority of the other GC components were not miniaturized. This resulted in the use of various interconnections between the column and these external components, introducing dead volumes and cold spots, and decreasing performance.

Since that time there has been a great deal of research undertaken to develop silicon fabricated on-chip electrophoresis and liquid chromatography systems, but with chip-based gas chromatography receiving only limited attention.

4.1 Miniaturised Capillary GC Instruments

There are a number of Micro-Electro-Mechanical Systems (MEMS) based GCs currently commercially available, which encompass all instrument components on a smaller scale. Many of these combine conventional drawn capillary narrow bore columns with miniaturised detection and data handling technologies. The Agilent 3000 Micro GC (G2805A: 155 x 364 x 413 mm) provides one- to four-channel micro-GCs using a MEMS TCD detector^[10]. C2V manufacture a handheld micro-GC system (124 x 84 x 60 mm) that, again, uses a MEMS micro-TCD as detector, reporting detection sensitivity at ppm levels^[13]. The shoe-box sized microFAST GC fabricated by ASI Inc. is another example. This uses heated columns to analyse volatile and semi-volatile

compounds with FID detection^[4]. SLS Micro Technology report an instrument (GCM 5000) approximately PDA sized with a footprint of 129 x 65 x 24 mm for analysing ppm levels of permanent gases, such as CO₂, CH₄, and O₂, as well as polar and nonpolar substances. It is equipped with a micro-injector, silicon-glass etched separation column, and a MEMS TCD detector, all of which are integrated with commercial off-the-shelf (COTS) fluidic and electronic modules on a printed circuit board^[8].

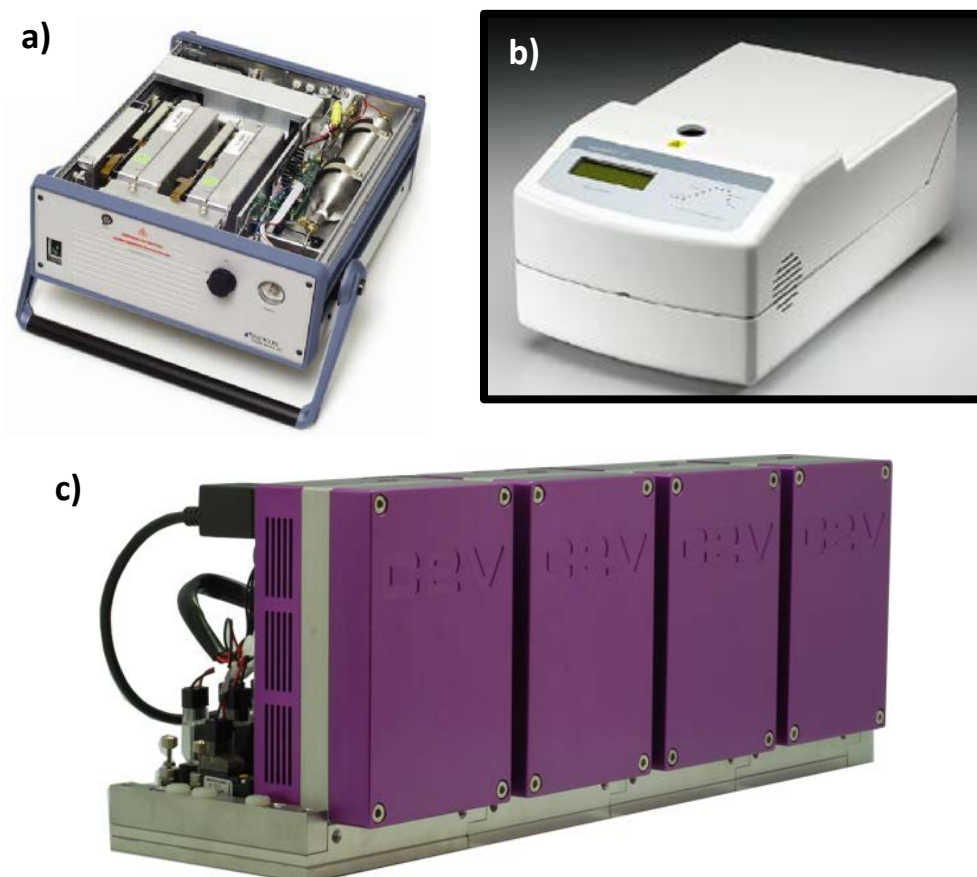


Figure 57: a) The Agilent 3000 Micro GC^[2]; b) The ASI Inc. microFAST GC^[4]; c) The SLS Micro Technology GCM 5000^[8].

4.2 Microfabricated GC Instruments

The μ ChemLab developed by Sandia National Laboratories, is an example of a handheld miniaturized GC instrument for VOC measurement that incorporates a microfabricated etched column. It comprises a preconcentrator consisting of a thin silicon nitride membrane supporting a patterned metal film-heating element, a spiral 1 m long 100 x 400 μ m high aspect ratio GC column on a silicon wafer, and an array of surface acoustic wave (SAW) sensors^[3, 15].

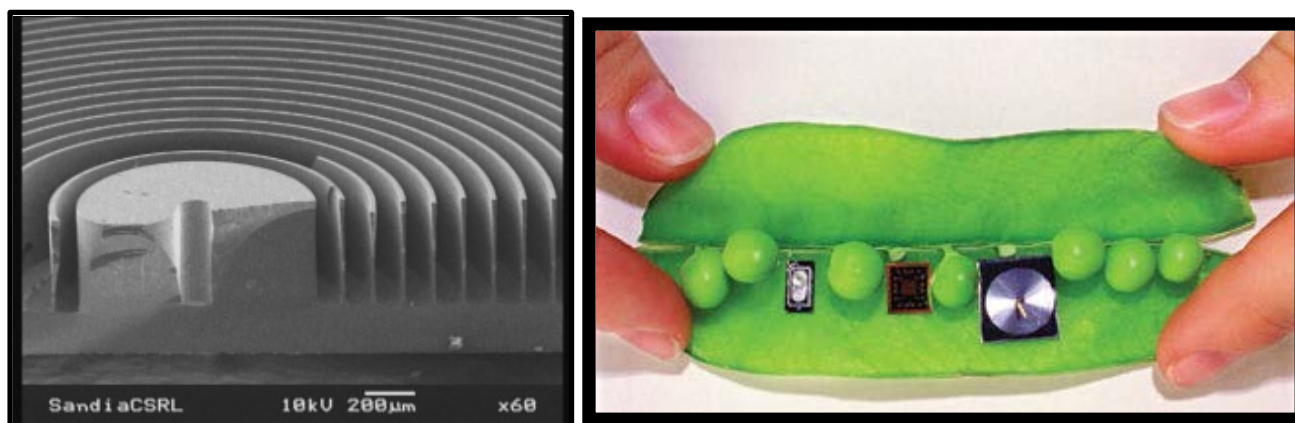


Figure 58: The μ ChemLab developed by Sandia National Laboratories^[3].

Silicon has very much been the favoured substrate to date for microfabricated GC columns, generally manufactured via the Dry Reactive Ion Etching (DRIE) method, followed by a Pyrex cover sheet being anodically bonded to the wafer yielding a sealed GC column. Many silicon examples of micromachined columns can be found in the literature^[7, 16-22], with nonpolar dimethylpolysiloxane and moderately polar trifluoropropylmethyl polysiloxane phases giving columns with between 3,500 and 8,200 plates^[23, 24],

Sanchez, et al. reported the development of a hybrid micro-system to be used for the detection of volatile organic compounds in air^[25]. The rectangular silicon etched column was 2 m long, 50 μm wide and 40 μm deep. This used synthetic air as carrier gas and coupled the micro-column with a SnO_2 gas sensor^[25].

Nishino et al. described a micro-GC that also used a high performance spiral chip column with rectangular cross-section fabricated on a silicon wafer^[21]. In this instance, 35,000 theoretical plates were achieved, with the channel being 8.56 m in length, 200 μm in width and 100 μm in depth. The prototype micro-GC system developed included a split injector, the micro etched column, heater assembly, FID, flow controllers, power circuits and LCD monitor, and was operational in both stand-alone and PC controlled mode^[21].

A micro gas chromatograph comprising a micro-preconcentrator and dual-column pressure- and temperature-programmed separation module, with an

integrated array of nanoparticle-coated chemiresistors acting as detector was reported by Zellers, et al^[26]. This achieved separation of 30 components in 4 minutes with a 3 m DRIE silicon/glass column, and separation of 11 components in 14 seconds with a 25 cm column. Both columns had rectangular cross-sections with a width of 150 μm and a depth of 240 μm ^[26].

4.2.1 Microfabrication Substrates

Although silicon dominates the literature as a substrate, columns have been made in other materials including anodically bonded glass and silicon^[7, 16-18, 20-22, 25], porous silicon^[9], carbon nanotubes^[5], parylene^[11], metal^[12] and ceramic^[14].

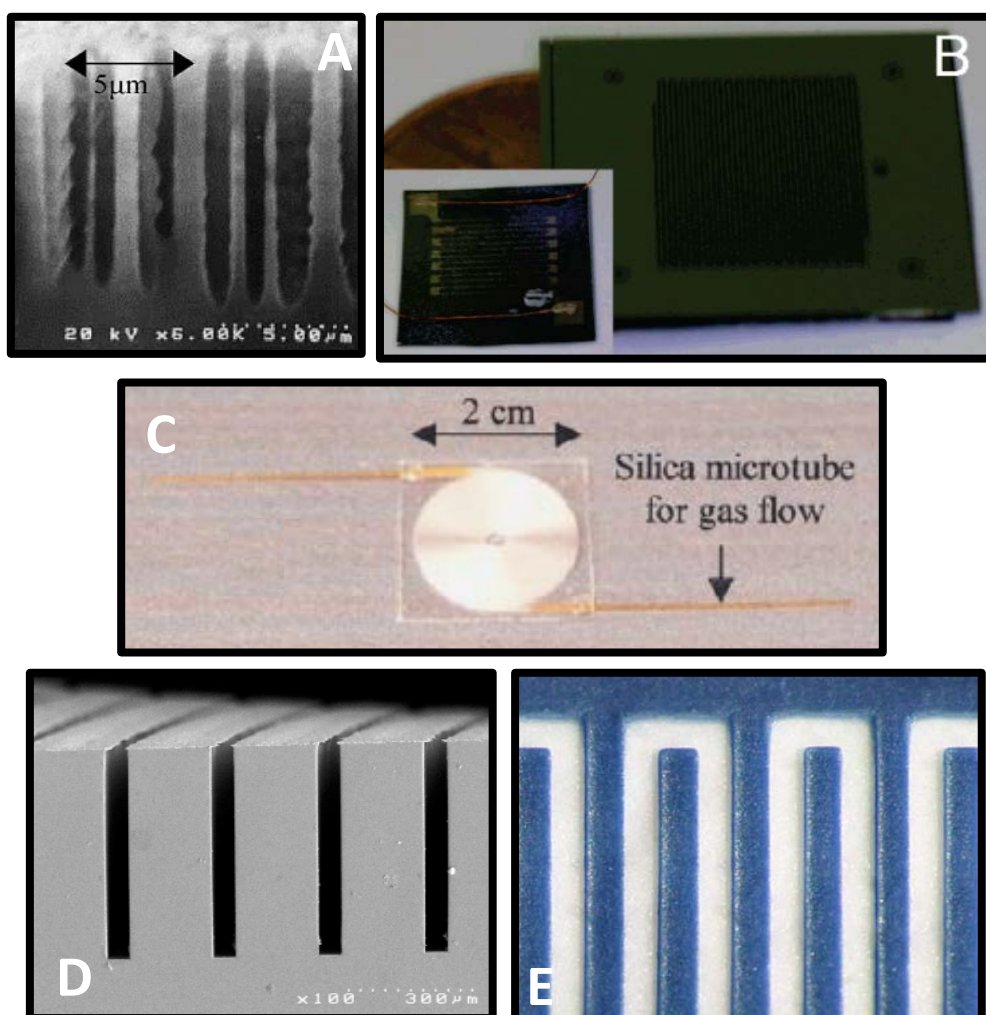


Figure 59: Columns composed of A. Carbon nanotubes^[5]; B. Porous silicon^[9]; C. Parylene^[11]; D. Metal^[12]; E. Ceramic^[14].

In addition, a variety of fabrication techniques have been utilised including deep reactive ion etching, DRIE polymer vapour deposition, stereolithography, silicon bulk micromachining, and Lithographie, Galvano-formung, Abformung (LiGA).

Of GC systems made in other materials, some notable examples include that of Noh, et al. comprising a parylene gas chromatographic column with an embedded heating element^[11]. Parylene is a highly anisotropic crystalline polymer formed by gas phase deposition which allows it to provide a conformal coating to any target structure. Parylene columns are fabricated by first coating the polymer onto a deep reactive ion etched wafer and then thermally bonding this wafer to a parylene coated Pyrex sheet. The spiral column described by this paper had a rectangular cross-section and was 1 m in length, 100 μm in width and 350 μm in depth. The columns yielded good separation results for light compounds on a variety of stationary phases, however, these columns are mainly suited for isothermal operation due to their high thermal capacitance and low thermal conductivity, and this limits their use^[11].

Bhushan, et al. described the fabrication of high aspect ratio nickel microfluidic columns using the LiGA process. The 2 m long, 50 μm wide, 600 μm deep serpentine columns were the separation component of a handheld GC intended for the detection of semi-volatile and volatile compounds. An advantage to using metal columns is their higher thermal conductivity in comparison to silicon-glass substrates^[12, 27].

A ceramic micro-system consisting of a column and micro-FID was reported by Dziurdzia, et al. using photoimageable thick-film technology combined with low temperature cofired ceramic (LTCC)^[14]. The components were integrated onto a single piece of alumina substrate, with the column reported as 4.8 m long, 250 μm wide and 80 μm deep^[14].

4.2.2 Channel Shape

Of the miniaturised devices previously reported, a common feature has been the use of square sided channels to form the separating column. The greatest difficulty associated with column coating is, therefore, in achieving a

uniformly thin layer of the desired thickness right across the cross-section of the column, including the corners. A limitation of rectangular designs is “pooling” of the stationary phase at the column corners producing an uneven thickness of stationary phase. Peak broadening and general degradation of the separation performance may result from analytes spending a longer time in these areas of thicker coating^[28].

Circular cross-sectional channels are able to perform well over a larger range of flow than other reported column shapes, and this increases system design flexibility. Limited numbers of circular channelled microfabricated devices have been reported, notably by Potkay, et al. who reported columns of 1m length and 90 μm diameter with a semi-circular cross-section^[7], and Pai et al. who detailed the use of circular cross-sectional silicon serpentine columns with a 250 μm internal diameter^[29].

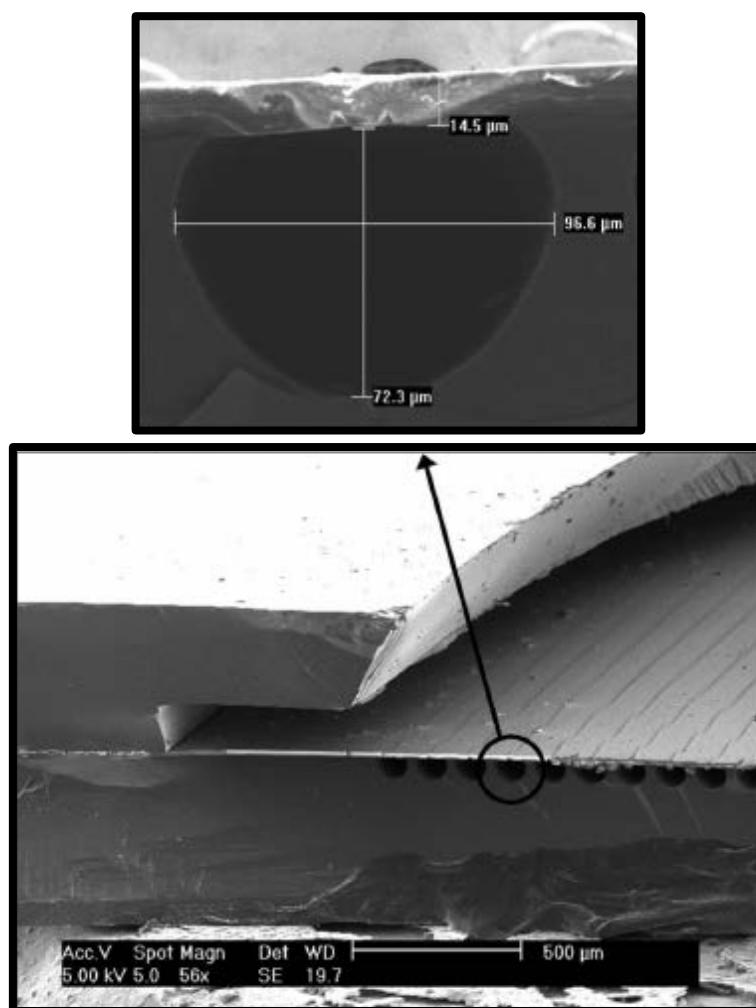


Figure 60: SEM of a side view of Potkay's μGC column^[7].

4.2.3 Miniaturised Detectors

Various detectors have been reported in conjunction with micro-GC systems. TCD is one of the few miniaturized detectors commercially available and has been reported in the literature a number of times^[6, 8, 10, 13]. Other detectors, such as surface acoustic wave devices^[3, 15, 30], differential mobility spectrometers^[18], metal oxide gas sensors^[20, 25], nanoparticle coated chemi-resistors^[26], and carbon nanotubes based ionization detectors^[31], offer promise of miniaturization and integration with columns. Micro-FID has shown results comparable to conventional flame photometric and flame ionization detectors, thus making it also a potentially useful detector when used in combination with a micro-GC system^[32-34].

4.3 Microfabricated GCxGC Systems

While microfabricated GC systems offer one of the faster growing areas of new GC development, microfabrication of GCxGC systems is not, as of yet, as popular a research area. This is for obvious reasons, with a major factor being the slow acceptance of the technique into general analytical laboratories.

Besides the work detailed in this thesis, two other attempts at developing lab-on-a-chip microfabricated GCxGC systems have been reported that are worth noting. The first, reported by Whiting, et al. at Sandia National Laboratories, describes the combination of microfabricated GC columns with pneumatic modulation and microfabricated components. Detection was achieved with nanoelectromechanical (NEMS) resonator mass sensors coated with a chemically-selective polymer to enhance detection of the phosphonate compounds of analytical interest^[35]. This work is still ongoing.

The second report of note, was by Reidy, et al. who refer to the development of a thermally-modulated comprehensive 2D GC system, consisting of a 3 m long nonpolar, polydimethylsiloxane coated first dimension column and a 0.50 m long polar polyethylene glycol second dimension column. Columns were fabricated on 100mm silicon wafers via DRIE. Using a conventional thermal modulator resolution of 14,425 and 5,800 theoretical plates were achieved, respectively, and a 10-component mixture of alkanes and ketones was separated. Replacement of the modulator with a microfabricated device saw the separation of heptane and 2-hexanone^[36].

4.4 The Potential of Microfabrication

Microfabricated GC and GCxGC has the potential of achieving superior performance over traditional instruments. The benefits include, but are not limited to the following:

- Parallel manufacturing for low-cost
- Low power consumption
- Field applicability
- Low solvent requirements
- Small thermal mass allowing for fast temperature programming rates^[5].

Thus, despite the fact that microfabricated columns and GC systems to date have generally struggled to perform at levels comparable to commercial capillary instruments, there is great potential for this continuously evolving technique.

4.5 References

1. Lewis, A.C., et al., *Microfabricated planar glass gas chromatography with photoionization detection*. Journal of Chromatography A, 2009. **1217**(5): p. 768-774.
2. Agilent. *3000 Micro GC*. 2009 [cited 2009 30 July 2009]; Available from: <http://www.chem.agilent.com/en-US/Products/Instruments/gc/3000microgc/Pages/default.aspx>.
3. Lindner, D., *The mu ChemLab (TM) project: micro total analysis system R&D at Sandia National Laboratories*. Lab on a Chip, 2001. **1**(1): p. 15N-19N.
4. *The microFAST GC*. 2010 01/01/2010 [cited 2010 07/08/2010]; Available from: <http://www.analyticalspecialists.com/microfastgc.cfm?s=1001383>.
5. Stadermann, M., et al., *Ultrafast gas chromatography on single-wall carbon nanotube stationary phases in microfabricated channels*. Analytical Chemistry, 2006. **78**(16): p. 5639-5644.
6. Terry, S.C., J.H. Jerman, and J.B. Angell, *Gas-Chromatographic Air Analyzer Fabricated on a Silicon-Wafer*. Ieee Transactions on Electron Devices, 1979. **26**(12): p. 1880-1886.

7. Potkay, J.A., et al., *A low-power pressure- and temperature-programmable micro gas chromatography column*. Journal of Microelectromechanical Systems, 2007. **16**(5): p. 1071-1079.
8. *SLS Micro Technology*. 2010 01/01/2010 [cited 2010 07/08/2010]; Available from: www.sls-micro-technology.de.
9. Lewis, S.E., et al., *Sensitive, selective, and analytical improvements to a porous silicon gas sensor*. Sensors and Actuators B-Chemical, 2005. **110**(1): p. 54-65.
10. *The Agilent 3000 Micro GC*. 2009 01/01/2009 [cited 2010 07/08/2010]; Available from: www.chem.agilent.com/en-us/products/instruments/gc/3000microgc/pages/default.aspx.
11. Noh, H.S., P.J. Hesketh, and G.C. Frye-Mason, *Parylene gas chromatographic column for rapid thermal cycling*. Journal of Microelectromechanical Systems, 2002. **11**(6): p. 718-725.
12. Bhushan, A., et al., *Fabrication and preliminary results for LiGA fabricated nickel micro gas chromatograph columns*. Journal of Microelectromechanical Systems, 2007. **16**(2): p. 383-393.
13. *Data Sheet: C2V-200 micro GC*. 2011 01/01/2011 [cited 2011 05/03/2011]; Available from: <http://www.c2v.nl/products/datasheet.shtml>.
14. Dziurdzia, B., Z. Magonski, and S. Nowak, *A ceramic mini system for the detection of hydrocarbon radicals*. Measurement Science & Technology, 2008. **19**(5): p. 6.
15. *Microsensors and Sensor Microsystems - MicroChemLab*. 2011 26/07/2011 [cited 2011 08/09/2011]; Available from: <http://www.sandia.gov/mstc/MsensorSensorMsystems/MicroChemLab.html>.
16. Reidy, S., et al., *Temperature-programmed GC using silicon microfabricated columns with integrated heaters and temperature sensors*. Analytical Chemistry, 2007. **79**(7): p. 2911-2917.
17. Reston, R.R. and E.S. Kolesar, *Silicon-Micromachined Gas Chromatography System used to Separate and Detect Ammonia and Nitrogen Dioxide .1. Design, Fabrication, and Integration of the Gas Chromatography System*. Journal of Microelectromechanical Systems, 1994. **3**(4): p. 134-146.

18. Lambertus, G.R., et al., *Silicon microfabricated column with microfabricated differential mobility spectrometer for GC analysis of volatile organic compounds*. Analytical Chemistry, 2005. **77**(23): p. 7563-7571.
19. Sanchez, J.B., et al., *Development of a gas detection micro-device for hydrogen fluoride vapours*. Sensors and Actuators B-Chemical, 2006. **113**(2): p. 1017-1024.
20. Lorenzelli, L., et al. *Development of a gas chromatography silicon-based microsystem in clinical diagnostics*. in *8th World Congress on Biosensors*. 2004. Granada, SPAIN: Elsevier Advanced Technology.
21. Nishino, M., et al., *Development of mu GC (Micro Gas Chromatography) with High Performance Micromachined Chip Column*. IEEJ Transactions on Electrical and Electronic Engineering, 2009. **4**(3): p. 358-364.
22. Radadia, A.D., et al., *Partially Buried Microcolumns for Micro Gas Analyzers*. Analytical Chemistry, 2009. **81**(9): p. 3471-3477.
23. Lambertus, G., et al., *Design, Fabrication, and Evaluation of Microfabricated Columns for Gas Chromatography*. Analytical Chemistry, 2004. **76**(9): p. 2629-2637.
24. Lambertus, G. and R. Sacks, *Stop-flow programmable selectivity with a dual-column ensemble of microfabricated etched silicon columns and air as carrier gas*. Analytical Chemistry, 2005. **77**(7): p. 2078-2084.
25. Sanchez, J.B., et al., *A selective gas detection micro-device for monitoring the volatile organic compounds pollution*. Sensors and Actuators B-Chemical, 2006. **119**(1): p. 227-233.
26. Zellers, E.T., et al. *An Integrated Micro-Analytical System for Complex Vapor Mixtures*. in *Solid-State Sensors, Actuators and Microsystems Conference, 2007. TRANSDUCERS 2007. International*. 2007.
27. Bhushan, A., et al. *Fabrication of micro-gas chromatograph columns for fast chromatography*. in *6th Biennial International Workshop on High Aspect Ratio Micro Structure Technology*. 2005. Gyeongju, SOUTH KOREA: Springer.
28. Sumpter, S.R. and M.L. Lee, *Enhanced Radial Dispersion in Open Tubular Column Chromatography*. Journal of Microcolumn Separations, 1991. **3**(2): p. 91-113.

29. Pai, R.S., et al. *Microfabricated gas chromatograph for trace analysis*. in *IEEE Conference on Technologies for Homeland Security*. 2008. Waltham, MA: Ieee.
30. Staples, E.J. and S. Viswanathan, *Detection of Contrabands in Cargo Containers Using a High-Speed Gas Chromatograph with Surface Acoustic Wave Sensor*. *Industrial & Engineering Chemistry Research*, 2008. **47**(21): p. 8361-8367.
31. Modi, A., et al., *Miniaturized gas ionization sensors using carbon nanotubes*. *Nature*, 2003. **424**(6945): p. 171-174.
32. Hayward, T.C. and K.B. Thurvide. *Novel on-column and inverted operating modes of a microcounter-current flame ionization detector*. in *31st International Symposium on Capillary Chromatography*. 2007. Albuquerque, NM: Elsevier Science Bv.
33. Hayward, T.C. and K.B. Thurvide, *Carbon response characteristics of a micro-flame ionization detector*. *Talanta*, 2007. **73**(3): p. 583-588.
34. Thurvide, K.B. and T.C. Hayward, *Improved micro-flame detection method for gas chromatography*. *Analytica Chimica Acta*, 2004. **519**(1): p. 121-128.
35. Whiting, J., et al. *High-speed two-dimensional gas chromatography using microfabricated GC columns combined with nanoelectromechanical mass sensors* in *International Conference on Solid State Sensors and Actuators - Transducers 2009*.
36. Reidy, S., et al. *A Microfabricated Comprehensive Two-Dimensional Gas Chromatography System*. in *Solid-State Sensors, Actuators, and Microsystems Workshop*. 2010. USA.

5.0 Experimental - Benchtop GC-FID

Reported here is the development of a planar microfabricated GC system that uses acid etched borosilicate glass as the working substrate. This device features capillary channels that are circular in cross-section and similar in dimensions to drawn capillary columns. The cost and ease of glass fabrication in this manner is attractive when compared to silicon, allowing two columns to be fabricated within a 95 x 95 mm monolith, also comprising a preconcentrator and additional channels to allow for multidimensional GC. The use of a miniaturised photoionisation detector in conjunction with the glass column is detailed. The overall system displayed an attractive peak capacity and detection limit for VOCs, low power demand and an operating temperature range of 0 to 200 °C without the use of cryogenes.

The following Experimental chapters detail the extensive work conducted to bring the lab-on-a-chip GCxGC instrument from an idea and a design drawing to a working prototype capable of successful two-dimensional separation.

5.1 Commercial Fused Silica Columns

In order for any results achieved using the fabricated glass chip to be significant, a requirement was for them to be compared to what would be expected from a commercial GC system using commercially available GC columns. Thus, initial experimental work conducted was to define a “typical” chromatogram that could be achieved using an industry manufactured GC column of equivalent dimensions to that seen on the microfabricated chip, and with a similar stationary phase chemistry, using a “typical” benchtop GC.

For these purposes, an Agilent HP-5 column of dimensions 30 m x 0.32 mm x 0.25 µm was cut to a length of 7.5 m to match the length of the primary glass etched column. This was then used as a reference throughout column coating experimentation for comparison of results obtained from in-house coated fused silica columns, as well as the coated glass chip column. In addition, the commercial column was used as part of the method development process to determine optimal GC parameters for separation of the various test mixtures used.

Figure 61 is a chromatogram illustrating the quality of results with the commercial column when separating a headspace mixture composed of equal amounts of the following compounds, run on an Agilent 7890A GC:

1. Cyclohexane (boiling point = 80.74 °C)
2. Propyl acetate (boiling point = 102.0 °C)
3. Toluene (boiling point = 110.6 °C)

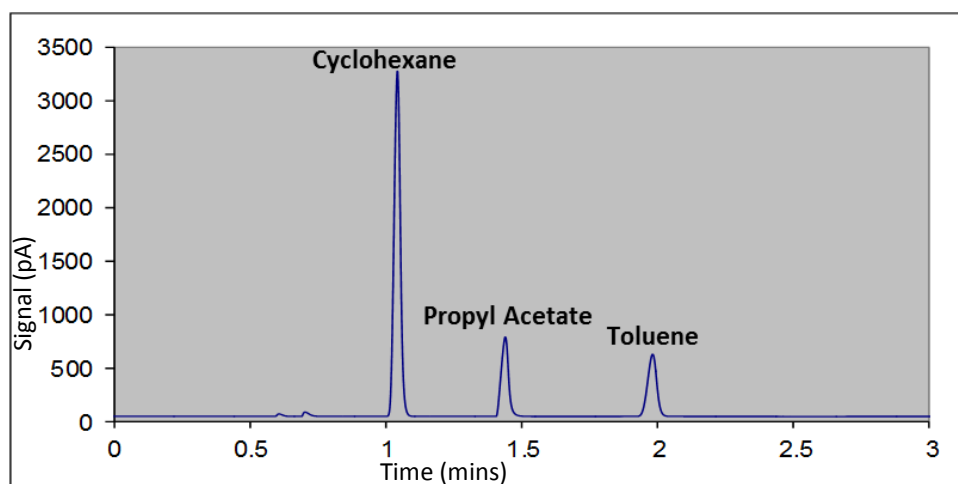


Figure 61: The separation of the headspace vapour of a cyclohexane, toluene and propyl acetate mixture using an Agilent HP-5 0.32 mm x 0.25 µm column cut to a length of 7.5 m

Figure 62 is the result of a liquid injection of the following mixture in isoctane solvent:

1. Tridecane (boiling point = 234.0 °C)
2. Tetradecane (boiling point = 253.0 °C)
3. Pentadecane (boiling point = 270.0 °C)
4. Hexadecane (boiling point = 287.0 °C).

Operating conditions for the above analyses were as follows:

- **Inlet mode:** Splitless
- **Inlet temperature:** 250 °C
- **Carrier gas:** Helium
- **Flow rate:** 6.5 ml·min⁻¹
- **Oven temperature:** 50 °C for 1 min, 50-130 °C at 10 °C·min⁻¹
- **FID temperature:** 250 °C

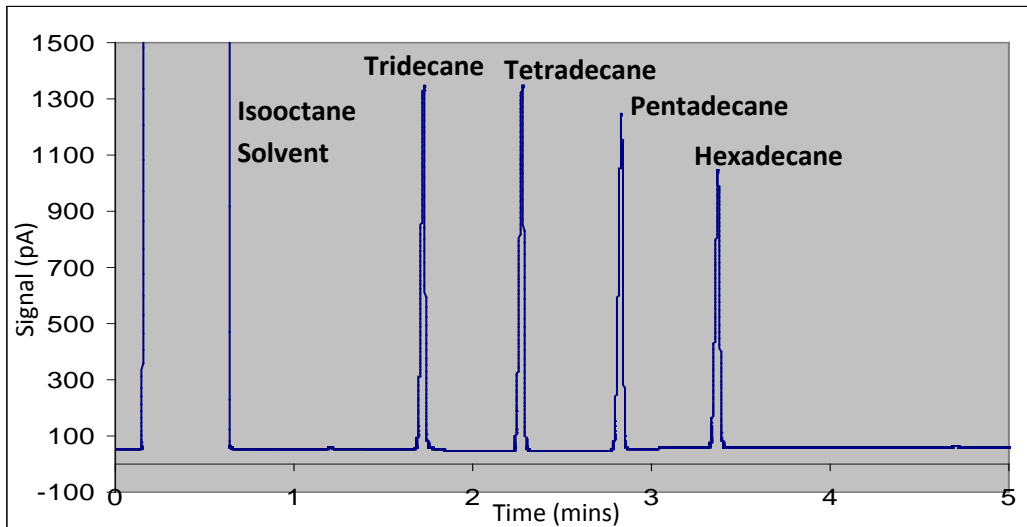


Figure 62: The separation of tridecane, tetradecane, pentadecane and hexadecane using the 7.5 m cut-to-size HP-5 column

5.1.1 Peak Shape

In an ideal world all chromatographic peaks would be symmetrical or Gaussian. However, due to the effects of instrument dead-volume, column loading, and adsorptive effects of the stationary phase and instrument components, peaks often show a fronting or tailing behaviour.

Fronting describes a peak whose front portion (distance A in the Figure 63) is wider or more drawn out than its steeper backside or tail (distance B). Fronting is most frequently caused by overloading the column with sample, and is usually accompanied by a slight shortening of retention time. The more frequent phenomenon of tailing, on the other hand, is the reverse of the above, with the tail of the column being wider than the front. Tailing is generally as a result of strong compound retention by active sites within the chromatographic system^[1].

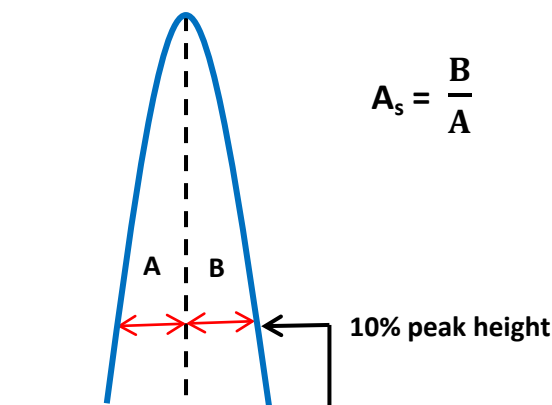


Figure 63: Measurement of peak symmetry




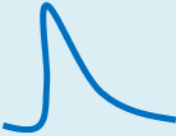
Asymmetrical peaks present a number of problems, including difficulties with regard to:

- Resolution
- Qualification
- Integration
- Quantitation.

As such, limits have been set to define the peak asymmetry beyond which chromatography will be deemed unsuitable. Some examples are shown in the table below for reference.

A number of other factors can also contribute to poor chromatographic peak shape. These include an aging column, dead space in the GC system, and the quality of the cut made to a column, especially on the inlet end. Improperly cut columns lead to peak tailing and loss of efficiency due to the exposure of large amounts of underivatized silanols and the inefficient transfer of analytes from the inlet to the column head. In order to prevent these detrimental effects, columns should be cut at 90° to the column length and should not be jagged.

Table 22: Acceptable and unacceptable peak symmetry values

<p>Excellent $A_s = 1.0 - 1.5$</p> 	<p>Acceptable $A_s = 1.2$</p> 
<p>Unacceptable $A_s = 2$</p> 	<p>Very Poor $A_s = 4$</p> 

5.2 Coating of Deactivated Fused Silica Capillaries

The separation column in a gas chromatograph is often described as the heart of the system. Therefore, successful coating of the column with a suitable stationary phase can be considered one of the most important and difficult tasks in the creation of a lab-on-a-chip GC.

Two primary procedures for the coating of stationary phase as a surface film on capillary columns exist, i.e. dynamic and static coating.

5.2.1 Dynamic Column Coating

To achieve coating via this method, a plug of the stationary phase dissolved in an appropriate solvent is introduced into the opening section of a capillary column sufficient to fill approximately 10% of the column length. The strength of the solution, as well as the physical properties of the surface, the solvent, and the stationary phase itself, all determine the thickness of the final coated film. Pressure is then applied to the front of the column to force the plug through the column at a constant speed of about 2-4 mm per second. Achieving a constant speed is critical to the uniformity of the column coating. When the plug has finally passed through the column, the gas flow is continued for at least a further hour, before being increased to allow the column to be stripped of solvent. Increasing the gas flow before this point can result in forward displacement of the stationary phase solution on the walls of the tube in the form of ripples, and, consequently, a very uneven film. The next

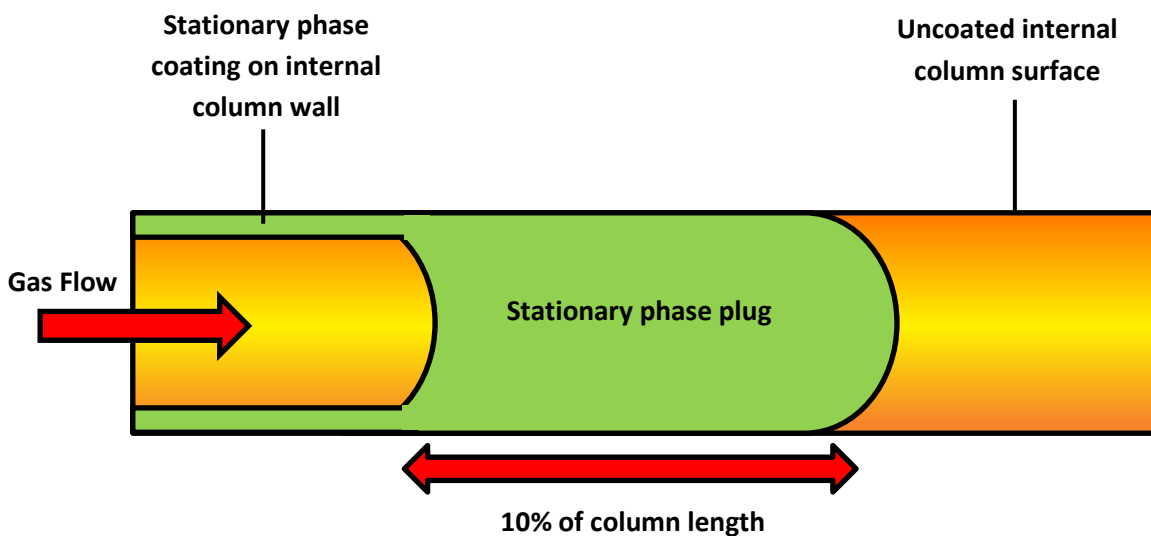


Figure 64: Dynamic capillary column coating

step is to heat the column above the solvent's boiling point, whilst maintaining an increased gas flow, to remove the final traces of solvent^[2].

5.2.2 Static Column Coating

Static coating is the method generally used by industry as it results in a more reproducible and uniform coating of stationary phase. It is achieved by filling the entire length of column with the solution of stationary phase in solvent. One end of the column is then sealed and a vacuum is applied to the other. As the solvent evaporates, the front slowly retreats down the column leaving a coating on the channel walls^[3, 4].

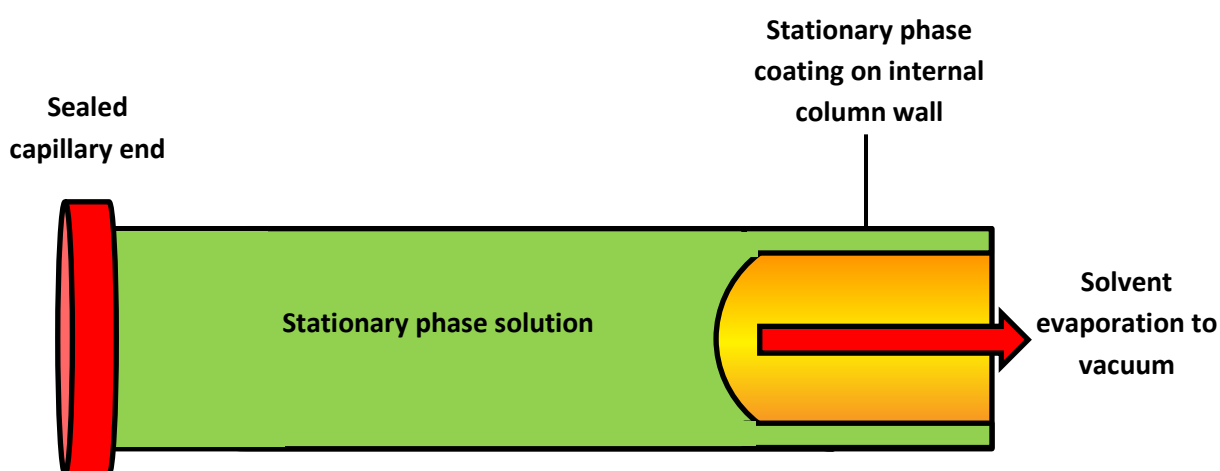


Figure 65: Static capillary coating

5.2.3 Experimental Column Coating Procedure

Neither of the above described procedures can be considered easy, and considerable experience is required to evenly coat capillary columns with a desired stationary phase film thickness. Modern day commercial column manufacturers keep the exact details of column coating highly confidential for obvious reasons. This means that any non-industrial attempts at coating stationary phase onto capillary columns is almost entirely experimental in nature and achieved through trial and error.

OV-101 stationary phase was chosen for these initial coating experiments as this non-polar 100%-dimethylpolysiloxane phase was to be used to coat the primary column of the glass lab-on-a-chip GCxGC.

5.2.3.1 Stationary Phase Preparation for Coating of Fused Silica Columns

A number of stationary phase solutions of varying concentration were prepared for column coating.

For dynamic coating, the % v/v solution required to give a film thickness d_f can be calculated from the Fairbrother-Stubbs equation shown below^[5, 6]:

Equation 58

$$d_f = \frac{cr}{200} \sqrt{\frac{\bar{u}\eta}{\gamma}}$$

Where:

- d_f = film thickness (μm)
- c = concentration (% v/v conc.)
- r = inner capillary radius (μm)
- \bar{u} = velocity of the coating plug ($\text{cm}\cdot\text{s}^{-1}$)
- η = viscosity of the coating solution ($\text{mPa}\cdot\text{s}$)
- γ = surface tension of the coating solution ($\text{mN}\cdot\text{m}^{-1}$)

The viscosity of stationary phase solution can be measured using an automated viscometer or via the Ubbelohde suspended level variation on the U-tube flow method^[7]. Surface tension determinations can be made by measuring the distance the stationary phase solution rises up a length of clean and untreated fused silica tubing with the end immersed in a vial of the solution^[8].

The Fairbrother-Stubbs equation involves the square root of γ . This allows for approximation of the surface tension of the solution to that of the pure solvent without the introduction of significant error. The η values of common stationary phases are widely documented, and so these values were used for film thickness determinations.

For static coating, the % v/v solution required to give a film thickness d_f is determined by a much simpler equation^[3]:

Equation 59

$$c = \frac{2(100)d_f}{r}$$

Table 23: The surface tension and viscosity of common solvents and stationary phases used to coat the columns described in this body of work

Solvent	Surface Tension, γ (mN·m ⁻¹)
Pentane	15.48 ^[9]
Cyclohexane	24.95 ^[10]
Toluene	28.40 ^[10]
Dichloromethane	26.50 ^[10]
Stationary Phase	Viscosity, η (mPa·s)
OV-101	1,500 ^[11]
OV-17	1,300 ^[11]

Once the % v/v has been calculated, this value is multiplied by the stationary phase density (e.g. 0.98 g·cm⁻³ for OV-101) to give the % w/v.

5.2.3.2 Column Stationary Phase Loading

A number of 0.32 mm I.D. deactivated fused silica capillary columns were dynamically and statically coated to a film thickness of 1 μ m in order to determine the ideal conditions for coating of the on-chip column. It was found to be very difficult to keep track of the coating process, due to the lack of visibility caused by the coloured polyimide exterior sheathing the columns. As such, Sudan Blue II dye was mixed into some of the prepared stationary phase solutions to aid in the visualization of the process. It was hoped that the use of this dye would also be able to give an indication of the stationary phase distribution throughout the coated column; however, it was found that the

majority of the dye is removed with the solvent at the evaporation stage, leaving too little dye interacting with the stationary phase itself to allow this.

The apparatus used for column coating was set up as illustrated in the Figure 66. A needle valve controlled the flow of compressed air into the column washing reservoir which was filled with the prepared stationary phase solution. When opened, compressed air filled the reservoir creating a build-up of pressure which in turn pushed the coating solution through the column.

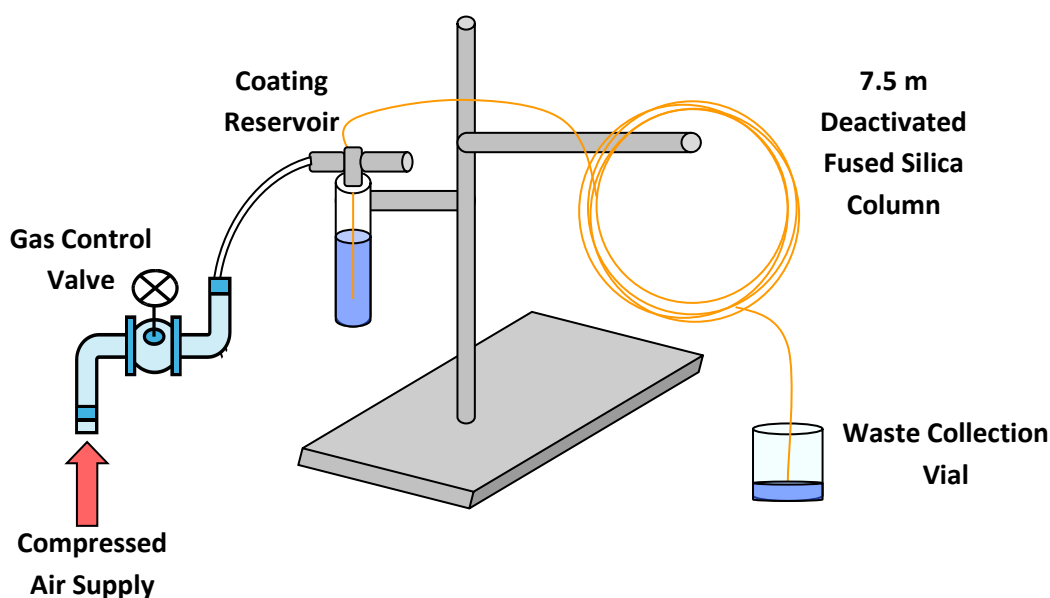


Figure 66: Fused silica column coating setup

A vial placed at the end of the column collected any waste solution. The coating process was conducted at a slow and controlled pace, and, once the column was entirely filled, a stopper was placed at the end. Initially a septum was used for this purpose; however, a secure Valco fitting was found to be more efficient.

5.2.3.3 Solvent Evaporation

Various techniques of solvent evaporation and removal were trialled in order to determine the most effective for static coating.

Evaporation experimentation included placing the filled column into a vacuum desiccator, with one end securely sealed, for an appropriate length of time to ensure complete solvent removal. Another method allowed the direct

attachment of the open column end to a vacuum pump. However, for both of these methods, it was not possible to achieve sufficient control of the evaporation speed, which is an important parameter^[12]. It proved very difficult to find the correct catch point that permitted only the evaporated solvent to be drawn through and out of the column, and not the entire stationary phase solution.

A different attempt involved both ends of the column being attached directly to the vacuum, rather than leaving one end sealed. In this instance, the vacuum proved uneven resulting in solvent evaporation in only one direction and not via both ends moving towards the centre of the column as expected. This method also resulted in evaporation that was far too fast; with evidence of the pentane solvent actually boiling in the column in the form of visible bubbling.

Another, less aggressive method entailed inserting the column into a heated water bath with no vacuum applied. This process proved to be the least successful with no evidence of any evaporation whatsoever taking place, despite a range of increasing temperatures being used over a 30 hour period.

It soon became obvious that the slower the solvent evaporation the better the overall coating. As such, a needle valve was fitted to the vacuum line allowing slow, steady, and controlled solvent removal via either of the first two methods explained.

5.2.4 Removal of Stationary Phase Coating

Not only was the stationary phase coating of the fused silica columns important, but it was also critical to devise a reliable method of removing the coated stationary phase, thus ensuring the reversibility of any coating errors.

It was experimentally determined that removal of stationary phase coating from the columns could be achieved by washing the column with solvent via the same method as column coating. The volume of the column was calculated to be 0.6 ml.

Thus, 6 mls of the solvent, i.e. 10 times the volume of the column, was used to flush the capillary and strip it of coating. The residual solvent was then evaporated by passing air through the column. The complete removal of stationary phase coating could be checked by installation of the column into a GC, followed by the running of a test standard, with a broad, unresolved, unretained peak being the expected result.

Below is an example of one of the “blanked” columns. Only one peak is visible, proving that no retention or resolution of cyclohexane, propyl acetate and toluene took place.

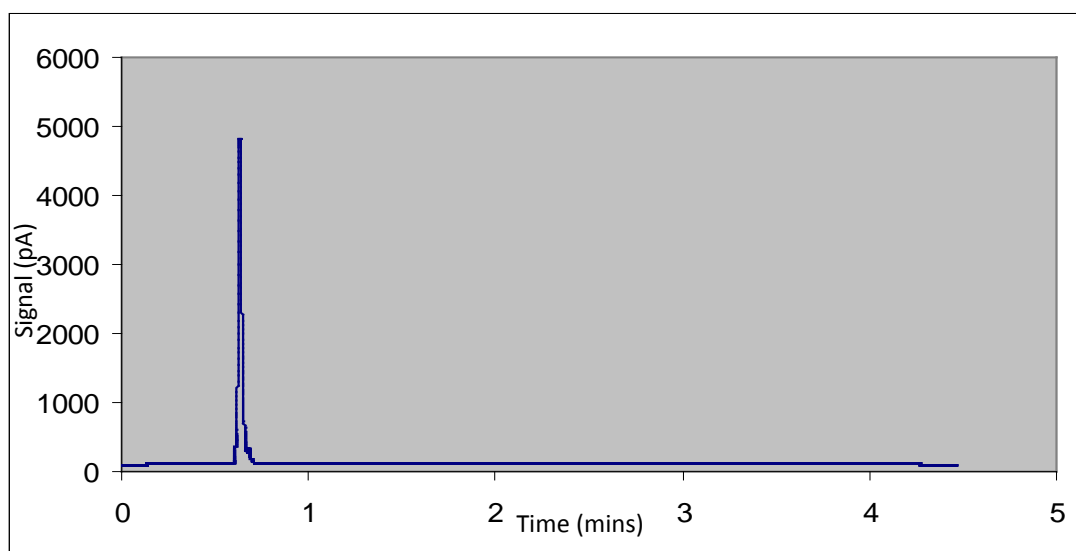


Figure 67: The lack of separation seen between cyclohexane, propyl acetate and toluene when run on a column which has undergone stationary phase removal

5.2.5 Performance Testing of Coated Fused Silica Columns

These initial experiments saw columns coated with an OV-101 stationary phase film thickness of approximately 1 μm . OV-101 is a 100%-dimethylpolysiloxane phase, and was dissolved in pentane to create the coating solution. In order to evaluate the performance of the resulting coated columns, they were set up in an Agilent 7890A GC. The in-house prepared test mixtures previously run on the commercial column were reanalysed on these capillaries in order to establish some sort of comparison. All conditions and parameters were kept the same.

Successful separation of the components was achieved, although peak

retention times had noticeably shifted. This, however, was not unexpected as chromatographic comparisons were being made between results achieved with two different phases (a 100%-dimethylpolysiloxane phase and a 5%-phenyl-95%-dimethylpolysiloxane).

Ideally, a commercial HP-1 column would have been used for these comparisons. However, in terms of phase chemistry, an HP-1, which has a polarity scale value of 5, and an HP-5, which has a polarity value of 8, are not so different as to prevent a basic comparison for the purposes of coating quality determinations.

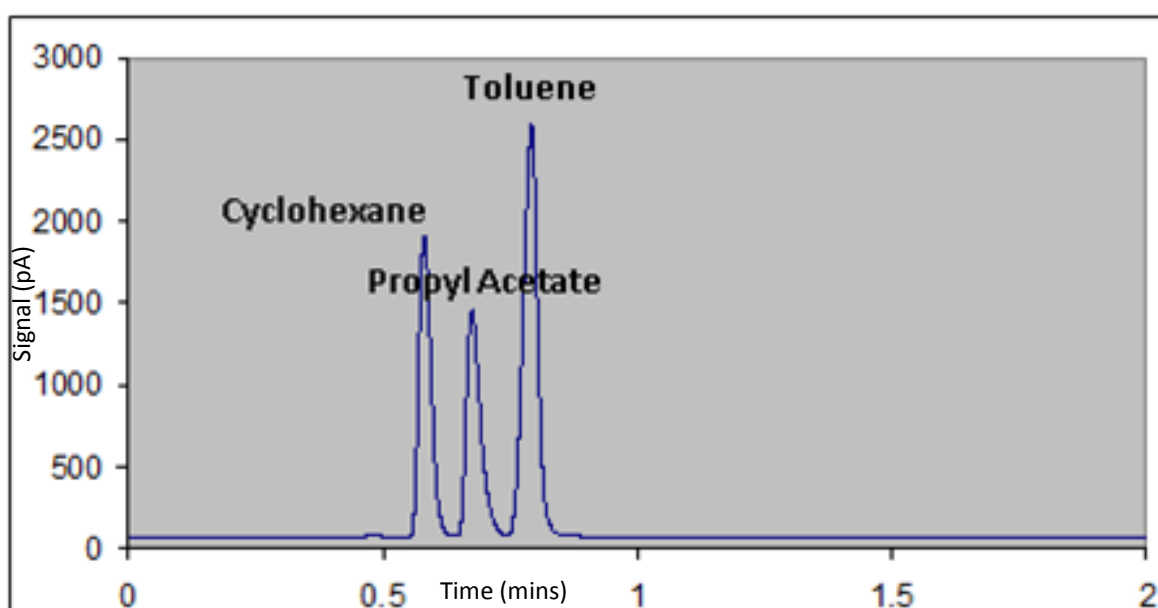


Figure 68: Separation of cyclohexane, toluene and propyl acetate using a 7.5 m x 0.32 mm deactivated fused silica column coated with OV-101 (in pentane) to a film thickness of 1 μ m

5.2.6 Stationary Phase – Solvent Solubility Testing

The following solvents were tested in order to determine which was the most suited for use in the stationary phase solution:

- Pentane
- Dichloromethane
- Cyclohexane
- Toluene.

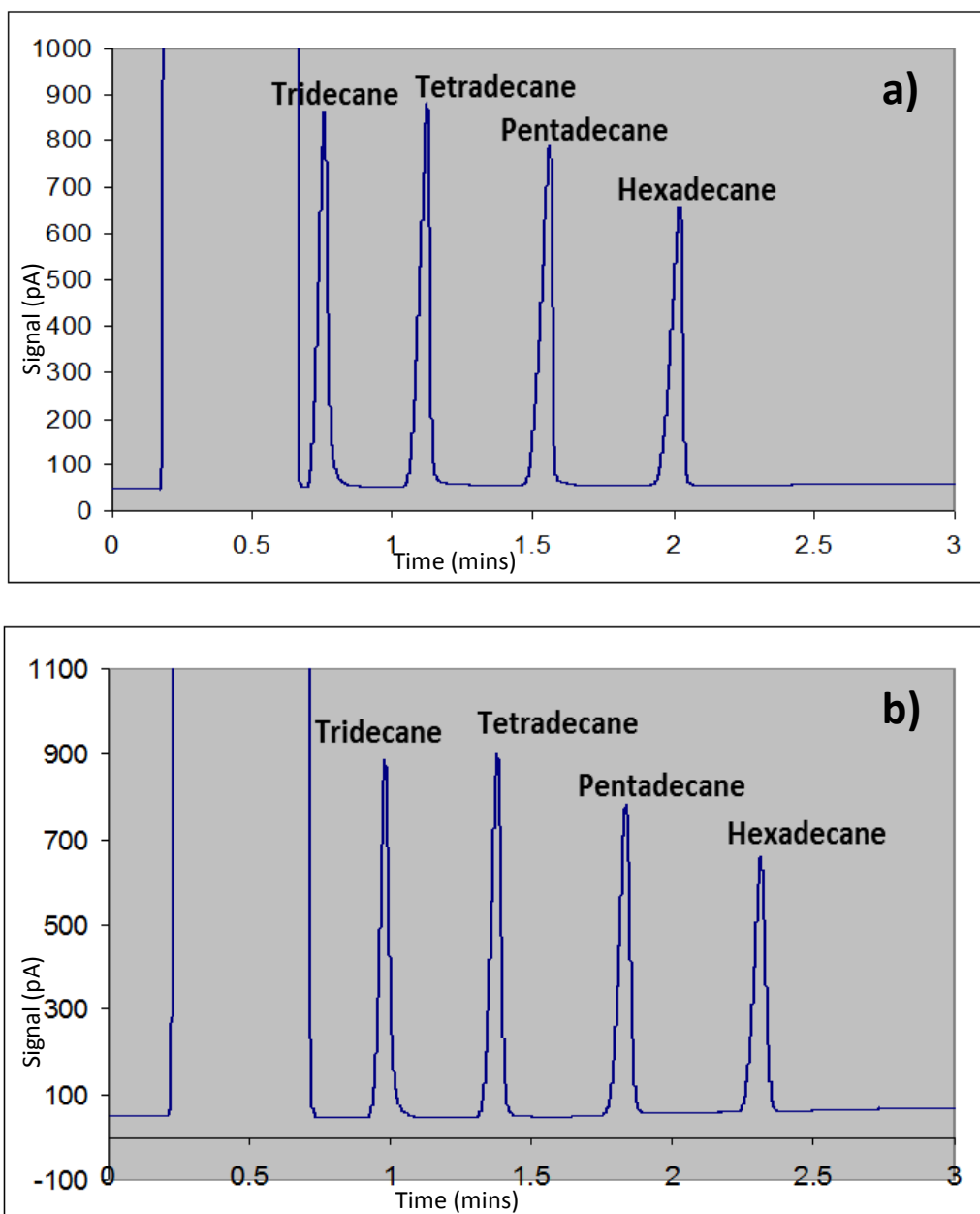


Figure 69: Separation using a 7.5 m x 0.32 mm fused silica column coated to a thickness of 1 μ m with OV-101 in a) dichloromethane; and b) pentane

Pentane not only has the lowest boiling point, thus allowing for the quickest and easiest solvent evaporation, but columns coated using OV-101 dissolved in pentane were found to give better peak shape, retention and separation as illustrated in Figure 69.

Finally, the same 4 component mixture was run on a 7.5 m x 0.32 mm uncoated deactivated fused silica capillary, to prove that the separation seen on the in-house coated columns was, in fact, due to the successful coating of

the columns, and not due to the natural activity of the exposed fused silica walls.

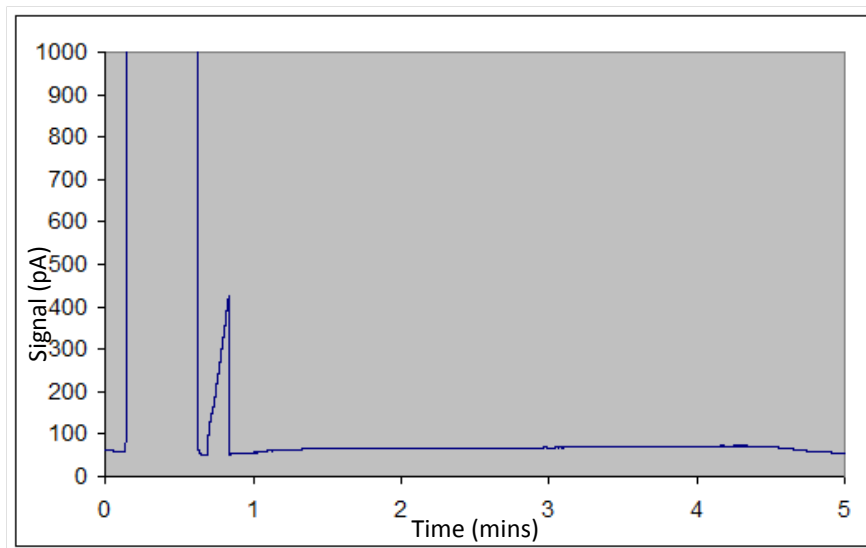


Figure 70: The unresolved, unretained peak achieved using an uncoated 7.5 m x 0.32 mm deactivated fused silica column

Table 24: A comparison of the commercially sourced HP-5 column and the coated OV-101 fused silica column

Parameter	Retention Time, t_R (mins)		Number of Theoretical Plates, N	
Peak	Figure 61 Commercial HP-5	Figure 68 Coated OV-101	Figure 61 Commercial HP-5	Figure Coated OV-101
Cyclohexane	0.3	0.1	1,418.2	88.6
Propyl Acetate	0.7	0.2	1,794.9	319.9
Toluene	1.7	0.3	3,518.1	510.6
Parameter	Retention Time, t_R (mins)		Number of Theoretical Plates, N	
Peak	Figure 62 Commercial HP-5	Figure 69 Coated OV-101	Figure 62 Commercial HP-5	Figure 69 Coated OV-101
Tridecane	1.4	0.5	11,218.5	640.1
Tetradecane	1.98	0.9	21,295.8	8,420.6
Pentadecane	2.5	1.4	34,575.1	4,986.0
Hexadecane	3.1	1.8	51,056.6	16,142.3

As is evidenced by the table above, calculated efficiency for some species is acceptable in comparison to the commercial column, whereas, for other species N is significantly less. The implication here is that columns of only

moderate coating quality were produced. For the purposes of gaining coating experience and determining the feasibility of “DIY” coating, however, this was deemed to be sufficient.

5.3 References

1. Brownlee, R. and J. Higgins, *Peak symmetry as a measure of column performance in high-performance liquid chromatography*. *Chromatographia*, 1978. **11**(10): p. 567-572.
2. Scott, R.P.W., *Capillary Columns*, 2003, Library4Science: England.
3. Bouche, J. and M. Verzele, *A Static Coating Procedure for Glass Capillary Columns*. *Journal of Gas Chromatography*, 1968. **6**(10): p. 501-503.
4. Bingjiu, X. and N.P.E. Vermeulen, *Free Release Static Coating of Glass-Capillary Columns - Static Coating at Elevated Pressure - Theoretical Considerations and Practice*. *Chromatographia*, 1984. **18**(9): p. 520-524.
5. Novotny, M., K.D. Bartle, and L. Blomberg, *Dependence of film thickness on column radius and coating rate in preparation of capillary columns for gas chromatography*. *Journal of Chromatography A*, 1969. **45**: p. 469-471.
6. Blomberg, S. and J. Roeraade, *A Technique for Coating Capillary Columns with a Very Thick-Film of Cross-Linked Stationary Phase*. *Journal of High Resolution Chromatography & Chromatography Communications*, 1988. **11**(6): p. 457-461.
7. Athawale, V.D. and P. Mathur, *Experimental Physical Chemistry*. 2001, New Delhi: New Age International (P) Limited, Publishers. 307.
8. Sugden, S., *The determination of surface tension from the rise in capillary tubes*. *Journal of the Chemical Society, Transactions* 1921. **119**: p. 1483 - 1492.
9. *Surface Tensions*. 2011 01/02/2011 [cited 2011 12/12/2011]; Available from: <http://macro.lsu.edu/HowTo/solvents/Surface%20Tension.htm>.
10. *Surface tension values of some common test liquids for surface energy analysis*. 2006 14/11/2006 [cited 2011 12/12/2011]; Available from: <http://www.surface-tension.de/>.
11. Poole, C.F., *The Essence of Chromatography*. 2003, Amsterdam, The Netherlands: Elsevier Science B.V. 927.

12. Bingjiu, X. and N.P.E. Vermeulen, *Free-release static coating of glass capillary columns: Coating with medium polar and polar stationary phases* Chromatographia, 1984. **18**(11): p. 642-644.

6.0 Experimental – The Glass Lab-on-a-Chip Devices

A number of different glass chip designs were evaluated during the course of this project, each having their own benefits, as well as drawbacks. Glass was chosen as substrate for the microfluidic lab-on-a-chip (LOC) GCxGC for a number of reasons, including that it is:

- Rigid
- Dimensionally stable
- Readily and conveniently available in an appropriate flat form
- Typically cut into rectangular slides.

The biggest advantage of glass over the other potential microchannel substrates previously described is that it allows for the creation of circular channels through the process of isotropic wet etching. Chemical wet etching is popular in MEMS because it can provide a very high etch rate and selectivity.

The borosilicate glass used here is a form of amorphous silicon dioxide (SiO_2), as is the fused silica typically used for commercial GC columns. The major drawback of glass is that it can be brittle. However, the shape and thickness of the glass used for this project gave it significant strength, and, once secured within a suitable reinforced and padded housing, any issue of the fragility of the glass should not be of concern.

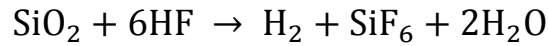
6.1 Fabrication of the Glass Chips

The glass chips were fabricated by the Dolomite Centre, UK, a specialised manufacturer of micro-scaled glass devices. The backbone of all designs evaluated consisted of two 0.5 mm and 2.5 mm thick Schott B270 glass wafers with etched channels bonded together to form a single chip. The chemical etching involved the surface of each half of the glass chip being covered with a chrome and then a photoresist layer. Exposure of the photoresist layer to UV light through a mask outlining the channels causes it to become soluble to the photoresist developer in comparison to the unexposed photoresist which remains insoluble. On removal of the exposed photoresist, an engraved pattern of the channels remains which is subsequently used to etch the

chrome layer. Finally, the glass is wet etched with hydrofluoric acid (HF) solution along these preformed channels.

The HF etching process is controlled to ensure symmetrical, hemi-spherical channels. The reaction that takes place is as follows:

Equation 60



When etching glass with hydrofluoric acid, the resulting shape of the side walls depends on different parameters, i.e.:

- The adhesion between the masking layer and the glass
- The pH of the etch solution
- The temperature of the etch solution
- The amount and type of stirring or agitation^[1].

Agitation is one of the most important parts of the overall process, and is necessary to remove the hydrogen bubbles formed during the reaction, which would otherwise become trapped, creating blockage of the etchant. Figure 71 illustrates the profile of the etch using an isotropic wet etchant with and without stirring of the etchant solution^[2].

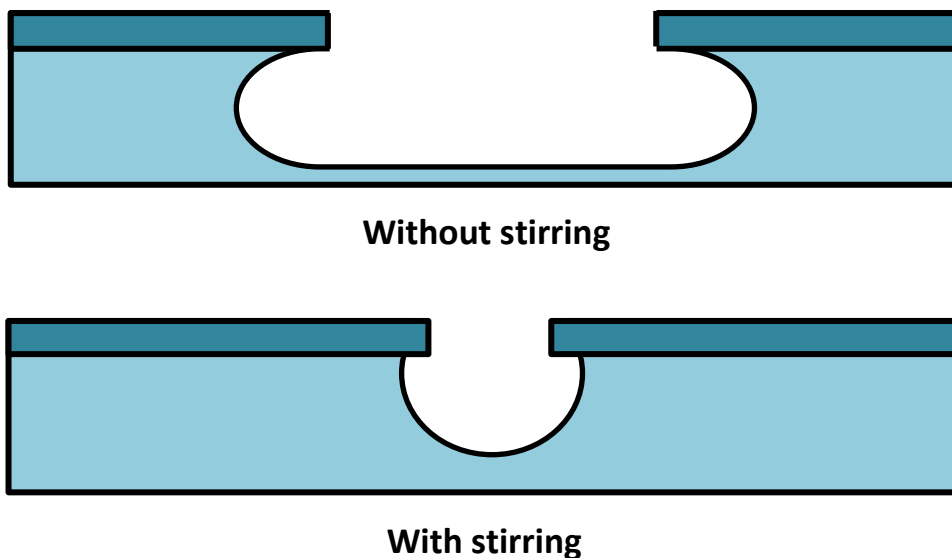


Figure 71: Illustration of the etch profile, with and without stirring, using an isotropic wet chemical etchant

After the photoresist and chrome layers are fully removed the two halves are brought into contact with the channels aligned. The flatness of the glass surfaces results in strong bonding through van der Waals forces. No heating is required and chips fabricated using this process can withstand pressures up to 50 bar.

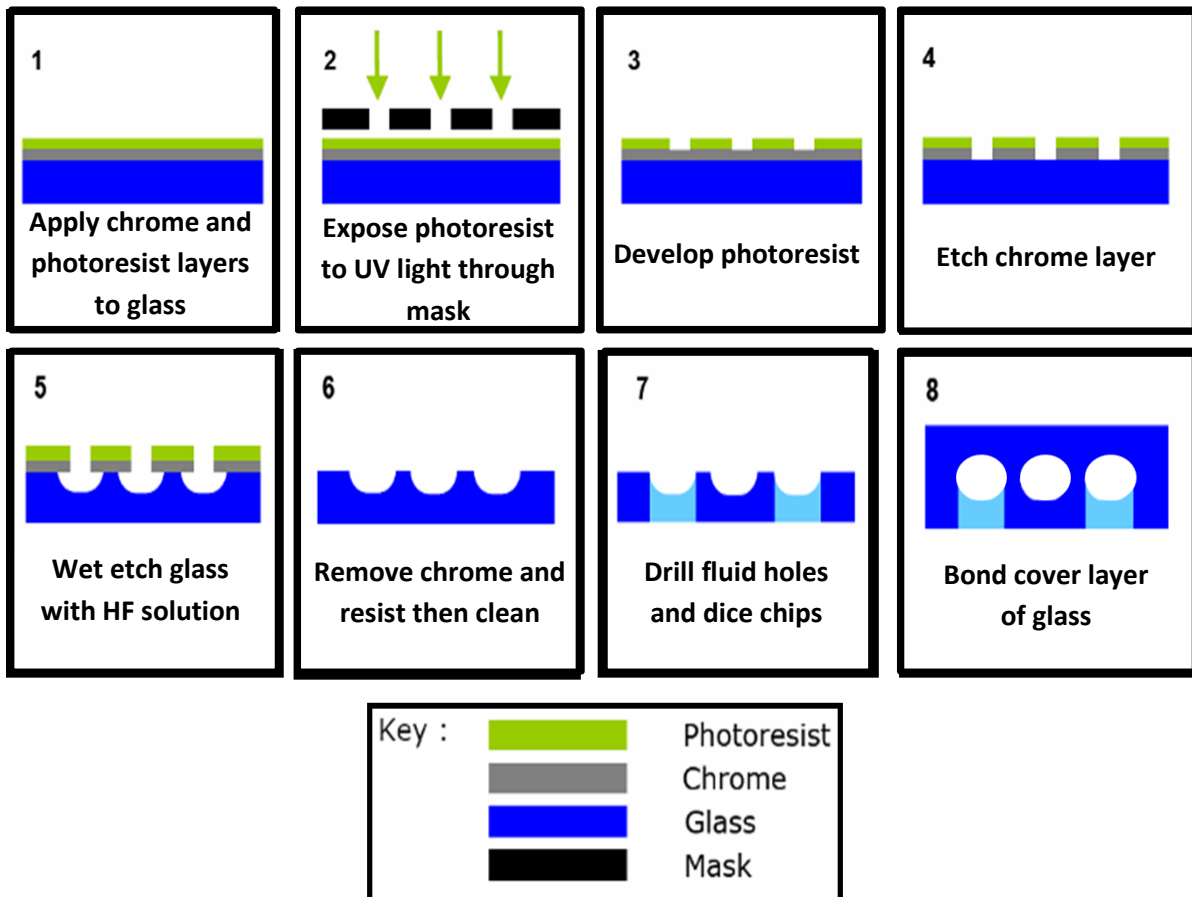


Figure 72: The glass microfluidic lab-on-a-chip GCxGC fabrication process

Figure 73 a) and b) show the cross-section of a portion of one of the glass chips. Images were obtained using an Alicona G4 Infinite Focus microscope and Wild Heerbrugg M400 microscope. Both figures clearly show the uniformity of the column, the accurate alignment of the two halves of glass and that the profile is very close to circular. Measurements of three bores from Figure 73 a) gave internal column diameters of 242, 250 and 248 μm in a chip with a target internal diameter of 250 μm . Figure 73 b) shows how the use of an asymmetric pair of glass thicknesses places the GC channels within a few hundred microns of one surface of the device for direct heating.

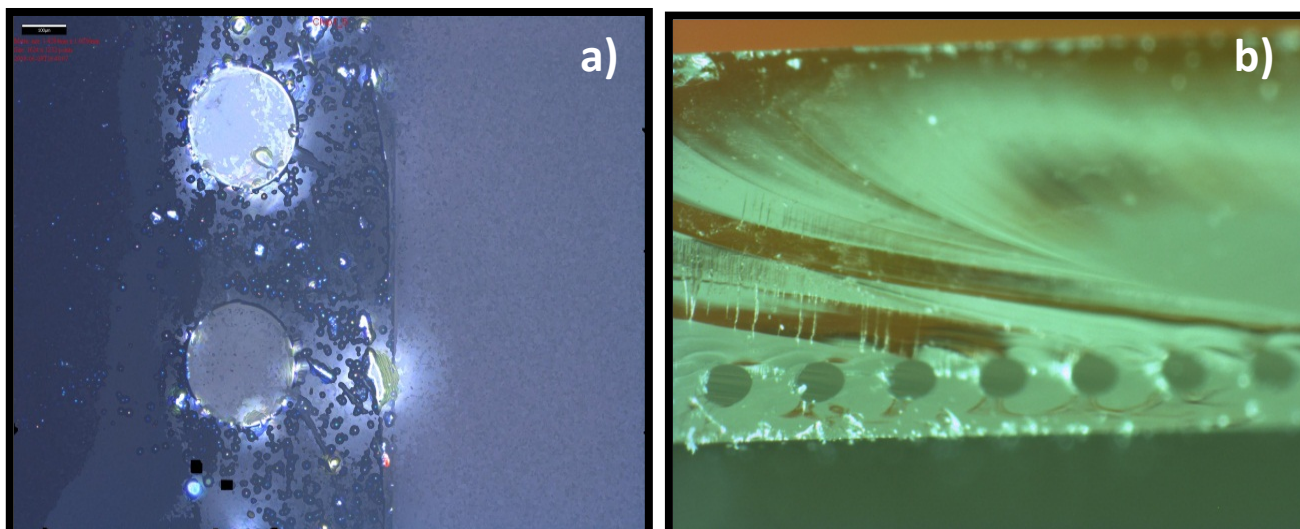


Figure 73: Cross sectional views of a portion of the glass GC chip

Figure 74 shows a magnification of the column spiral, as well as the end section of the etched injection unit, which is 1 mm wide and 0.32 mm deep. This was coupled to the column via a restricting pinch at the injector outlet.

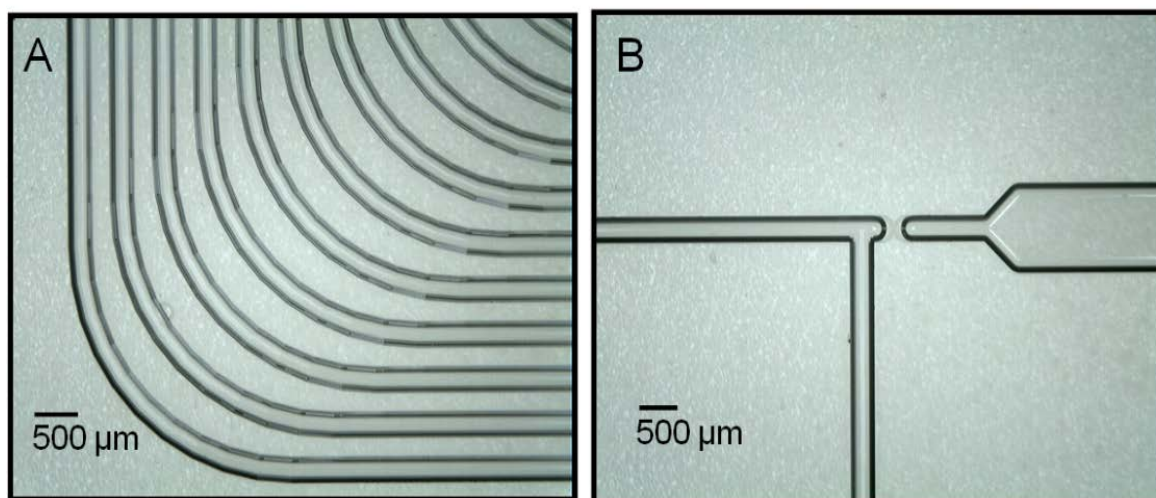


Figure 74: A) Close up image of column turns; B) close up image of injector region coupled to 7.5 m column via a 50 µm restrictor region

6.2 Chip Designs

As discussed, a number of chip designs were investigated during the course of this project. They shall be referred to henceforth as follows:

6.2.1 LOC 1

This chip was the simplest of all designs investigated. As can be seen in the image below, the two columns were completely separate from each other with

no in-built connection. Thus, to achieve sample introduction and subsequent transfer from the 7.5 m x 0.32 mm primary to either the 1.4 m x 0.32 mm secondary column and/or the detector, uncoated deactivated fused silica capillaries were bonded to the chip's various drilled inlet and outlet holes, and attached to the inlet and detector ports of the benchtop GC instrument as appropriate. This modular approach resulted in easier column coating; however significant difficulties were experienced in terms of interfacing the various segments together.

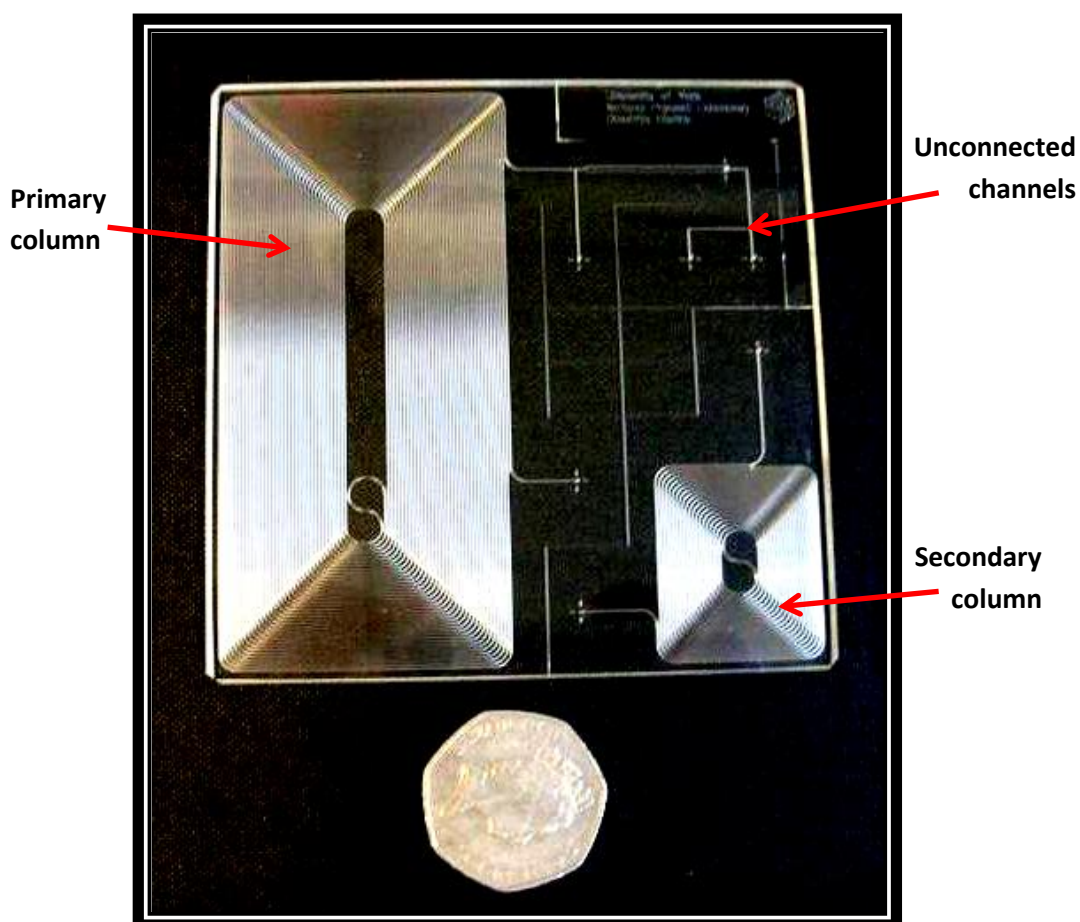


Figure 75: An image of LOC 1 clearly showing both the size of the glass chip in comparison to a regular 50 p coin, and the lack of interconnecting microfluidic channels between the primary and secondary columns

6.2.2 LOC 2

Improvements designed into LOC 2 included a peek edge connector, which provided an easy means of sample introduction and gas pressure modulation in a single connector unit. As well as that, connection of the channels between the primary and secondary columns, modulator and detector allowed for two-

dimensional separation to be achieved. Primary and secondary columns remained 7.5 m and 1.4 m in length, respectively. However, column internal diameter was reduced to 0.25 mm. The modulator collector channel was 120 mm long, 0.5 mm wide and 0.25 mm deep.

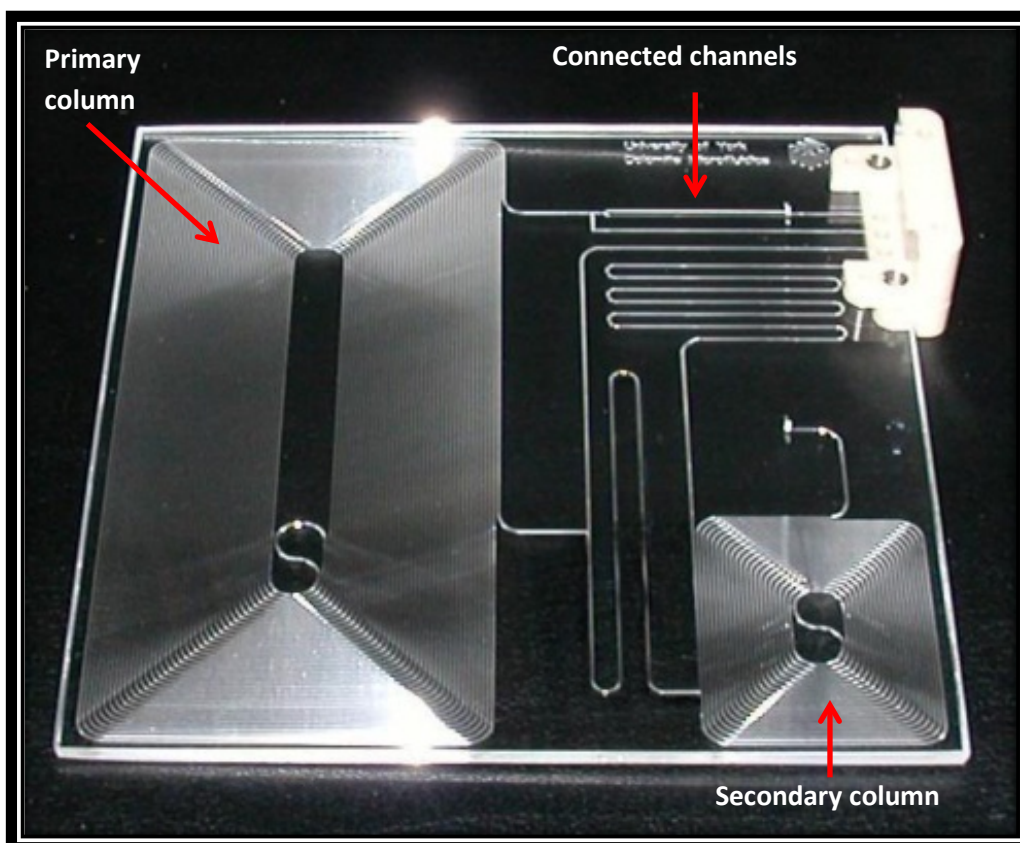


Figure 76: LOC 2, which had a preconcentrating trap, modulator, and inter-connecting channels, as well as an edge connector for easy sample introduction

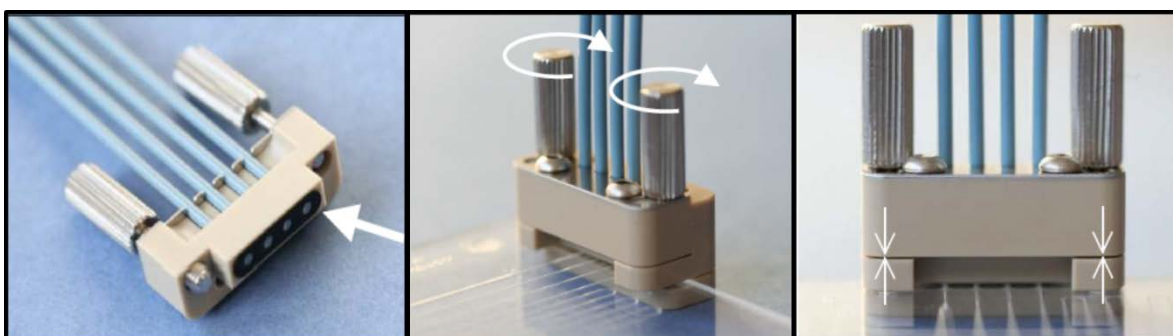


Figure 77: The operation of the edge connector

6.2.3 LOC 3

In this design, two separate chips were fitted per 95 x 95 mm glass wafer by removing the preconcentrator and by reducing the internal diameter of both the primary and secondary columns to 100 μm . Not only did this reduce the

cost of manufacture by creating two GCs on one chip wafer, which were then divided into two, but it also reduced the likelihood of chip breakage by moving the preconcentrator off the chip. The primary column was 8.6 m long and remained spiral. The secondary column was condensed to 110 cm in length, and was changed to a serpentine layout. Finally, the modulator section was changed to 10 cm long, 300 μm wide and 100 μm deep.

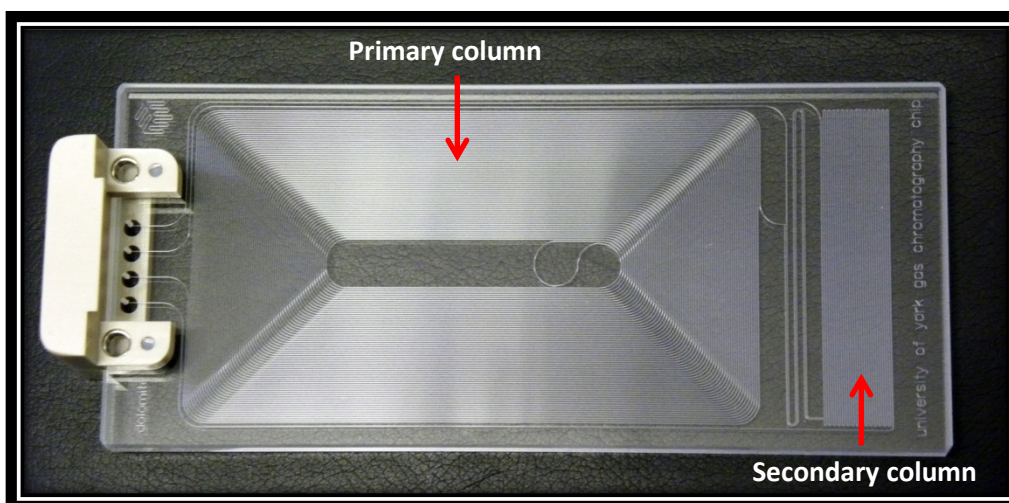


Figure 78: A photo of the reduced LOC 3 chip

6.2.4 LOC 4

Changes applied to this final chip design included that the entire modulator section was moved into the first quarter of the chip, leaving a full quarter for the secondary column to occupy. The extra space this provided and the changing of the column from spiral to serpentine increased this column's length from 1.4 m to 4 m. The internal diameter was also reduced to 180 μm . The primary column remained at a length of 7.5 m with an I.D. of 250 μm . The preconcentrator was completely removed from the chip and the collector length was almost doubled to 200 mm. The two modulator legs were made to be of equal length and internal diameter, the result of which being that either column could be used as primary or secondary.

In the work reported here, the shorter, narrower bore 4 m column was used as primary and the longer, wider bore 7.5 m column as secondary. Finally the detector port or outlet of the secondary column was moved to the edge connector.

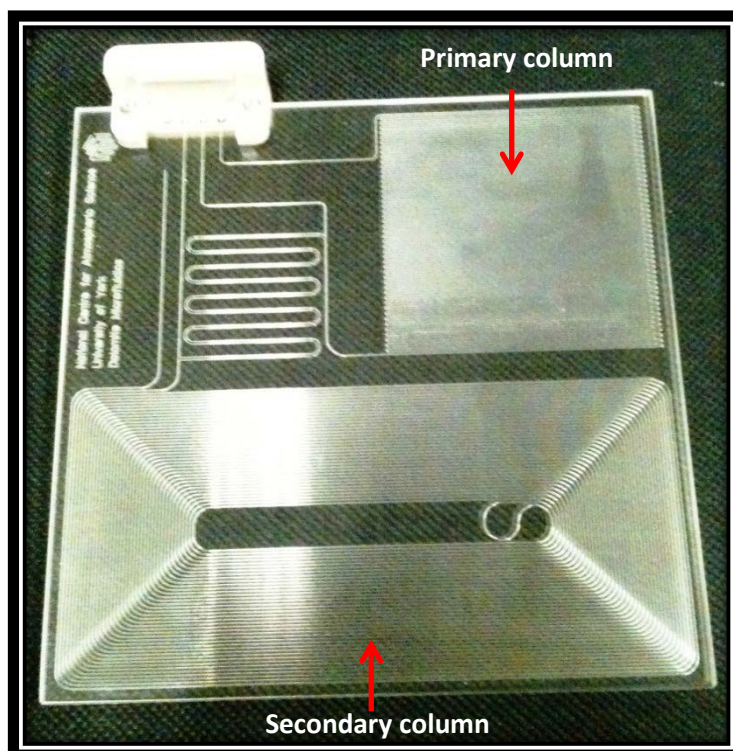


Figure 79: LOC 4 showing the 4 m serpentine primary column, the spiral 7.5 m secondary column, and the relocated and resized modulator channels

6.3 Commercial GC-FID with LOC Column

The coated chips were tested using the fan oven, temperature control, injection and flow control systems of the laboratory gas chromatograph to enable the separation capabilities of the coated glass primary column to be characterised with an established FID.

6.3.1 Chip Connections

Securely bonding the fused silica capillaries to the planar chip in a gas tight fashion was no simple task. Initially epoxy adhesive was used to secure capillaries in place on a spare glass chip. However, this was found to be entirely unsuitable, as it was an irreversible process, thus any capillaries that were accidentally broken could not be easily removed from the glass devices. Hot melt adhesive and Shellac, which is a resin secreted by the female lac bug, were next evaluated for chip bonding potential. Here, the actual process of sealing the capillaries in place was found to be simple and reversible, and the resulting adhesive bonds were able to withstand pressures over 60 psi at low temperatures. However, both had relatively low melting points for GC

analyses, i.e. 100-150°C. This resulted in drooping, shifting capillaries and a substantial threat of channel blockage, again rendering these bonding agents as unsuitable for purpose.



Figure 80: Shellac flakes. These were melted and then used to secure transfer lines to the glass chips during evaluations of bonding agents

As an alternative, high temperature silicone sealant was tested. This sealant was capable of withstanding temperatures of up to 260 °C for continuous operation and 315 °C for intermittent exposure. Again, sealing was unproblematic, and pressure at high rates was sustainable. On heating to 160 °C in the GC oven no issues were encountered. With all the transfer lines connected *except* the line to the detector a flow could be measured, however, on connecting the outlet line to the FID a pressure build-up occurred within the chip that prevented flow, and consequently shut down the instrument. This suggested that the seal produced by the silicone sealant was so efficient in comparison to the aforementioned adhesives that pressures over a certain low threshold were too excessive. This, unfortunately, also ruled out the use of this sealant for connection of capillary columns to the glass microfluidic devices.

At first, the peek edge connector, designed by the Dolomite Centre for use with the chips, seemed the solution to the problem. The major issue experienced with the edge connector, however, was leakage of carrier gas and sample. Being composed of peek, the connector had a continuous use temperature of 100°C. With the chip in the oven of the commercial GC, the peek edge

connector was subjected to frequent and sequential heating to 160 °C followed by cooling to 30°C. This constant heating and cooling resulted in a warping of the peek connector, and, when subjected to pressures of 60 psi and higher, meant that it was unable to hold pressure and subsequently leaked. The simplest means of correcting this was to remove the edge connector entirely from the chip, before reinstallation with a thin wedge of tin foil placed between it and the bottom of the glass chip. This resulted in a retightening of the seal, which would last for a number of temperature gradient runs, before the process would need to be repeated. During one of these adjustments it was noticed that a number of the different edge connectors supplied by the Dolomite Centre came with varying screw lengths. On experimentation, it was determined that the longer screws provided a stronger gas tight seal, and resulted in the edge connector having to be adjusted significantly less frequently than before. Despite the edge connector's limitations, it still provided the best connection between chip and transfer lines.

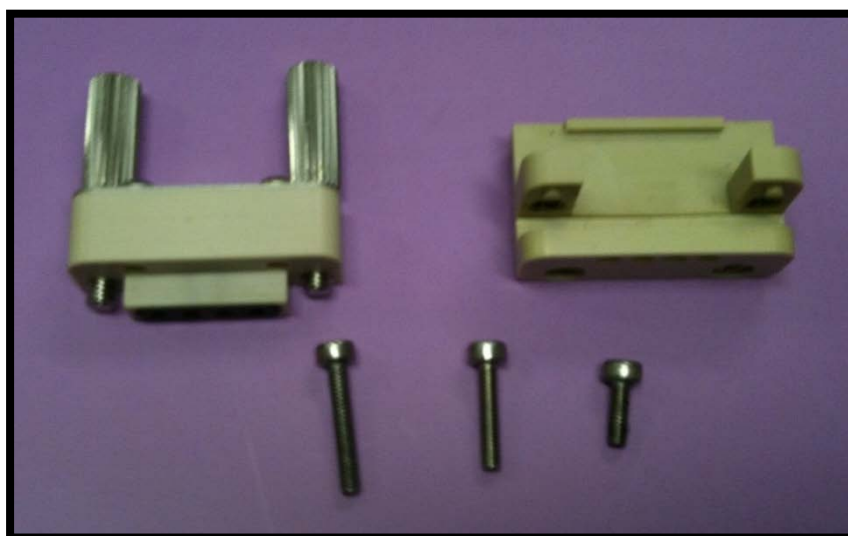


Figure 81: Dismantled view of one of many peek edge connectors used and examples of the varying screw lengths that were observed

6.3.2 LOC 1

LOC 1 was the first glass device to be designed and manufactured for this project. The impracticality posed by the lack of interconnecting channels was soon realised, and LOC 2 was manufactured for comparable interlaboratory evaluation. The majority of the work conducted on LOC 1 took place at the National Physical Laboratory in Teddington by analysts there in conjunction

with the author. All other experimentation described in this body of work was conducted within the Atmospheric Chemistry Laboratories at the University of York by the author and team. Thus, the methods and tools defined in this section vary considerably in comparison to those later detailed.

6.3.2.1 Stationary Phase Coating of LOC 1 Primary Column

The primary column of LOC 1 was statically coated with a 3.8% v/v solution of OV-101 in pentane. The coating process was preceded by a wash step which involved the chip undergoing a number of solvent flushes. Residual solvent was evaporated in a high vacuum, high temperature oven, before the purged chip was allowed to passively cool. It was then weighed on 5 decimal place balance. Coating was performed with a syringe filled with the coating solution. The needle was pushed through a septum, which aided in providing a seal around the inlet. Once coated, the chip was placed inside a vacuum oven with digital temperature control and a vacuum monitor for solvent evaporation. The glass column was left in the oven at room temperature (± 21 °C) for two days with the pressure being maintained between 10 and 40 kPa below atmospheric pressure. The temperature was then increased to 50 °C with a decrease in pressure to 100 kPa below atmospheric. Using this method solvent evaporation was achieved in four days, and was monitored by periodic weighing of the column with a laboratory balance.

Six open vials of pentane were used as a pressure buffer during this solvent evaporation process, and were laid out as shown in the figure below. The saturated vapour of the pentane restricted the vacuum at the start of the process, and served to cool the column. The vials also allowed the vacuum to be maintained at a low enough level to ensure that boiling of the solvent within the column did not take place, as indicated by the absence of boiling in the pentane.

A final weighing confirmed the mass of stationary phase deposited. This gave an accurate indication of how much stationary phase was actually deposited onto the channel walls; however, it unfortunately could not provide an indication of the overall uniformity of the coating. It was calculated that a mass of 11 mg of stationary phase was deposited onto the channel walls, out

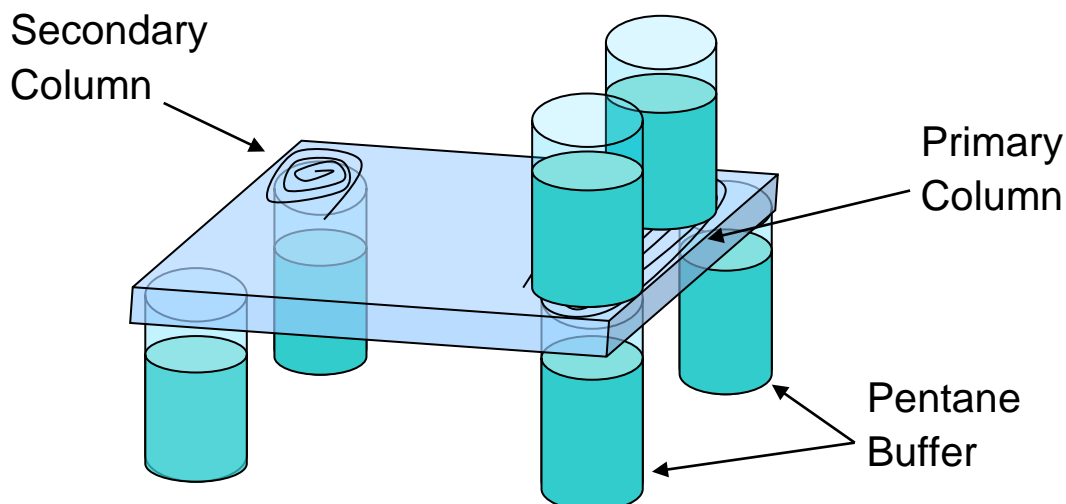


Figure 82: On-chip solvent evaporation using 6 pentane pressure buffer vials

of an expected 13.7 mg, which would be equivalent to a uniform layer of 2 μm in thickness.

6.3.2.2 Performance Testing of LOC 1 Primary Column

As this chip design lacked an edge connector for introduction and exit of the sample, Shellac was used to bond transfer capillaries and split lines into the glass column ports. Using high purity helium as carrier gas, a standard BTEX mixture containing 10 $\mu\text{mol}\cdot\text{mol}^{-1}$ (molar ppm) of the following compounds was injected via a 500 μl gas sample loop:

- Benzene
- Toluene
- M-xylene
- P-xylene
- O-xylene

A second ppm gas mixture of nonane, α -pinene and 3-carene was injected separately onto the Varian 3800 GC system. Automated valve changes were used. The oven was programmed to run at 30 $^{\circ}\text{C}$ for 0.2 min, then ramp at 20 $^{\circ}\text{C}\cdot\text{min}^{-1}$ to 100 $^{\circ}\text{C}$. The switching valve was heated to 170 $^{\circ}\text{C}$. The results achieved are shown below, with good separation between all of the injected components, symmetrical peak shape and elution in 4 minutes. Peak skew is less than 1.8 for all peaks (the majority less than 1.3) and the chromatogram indicates around 2,000 theoretical plates as measured for toluene.

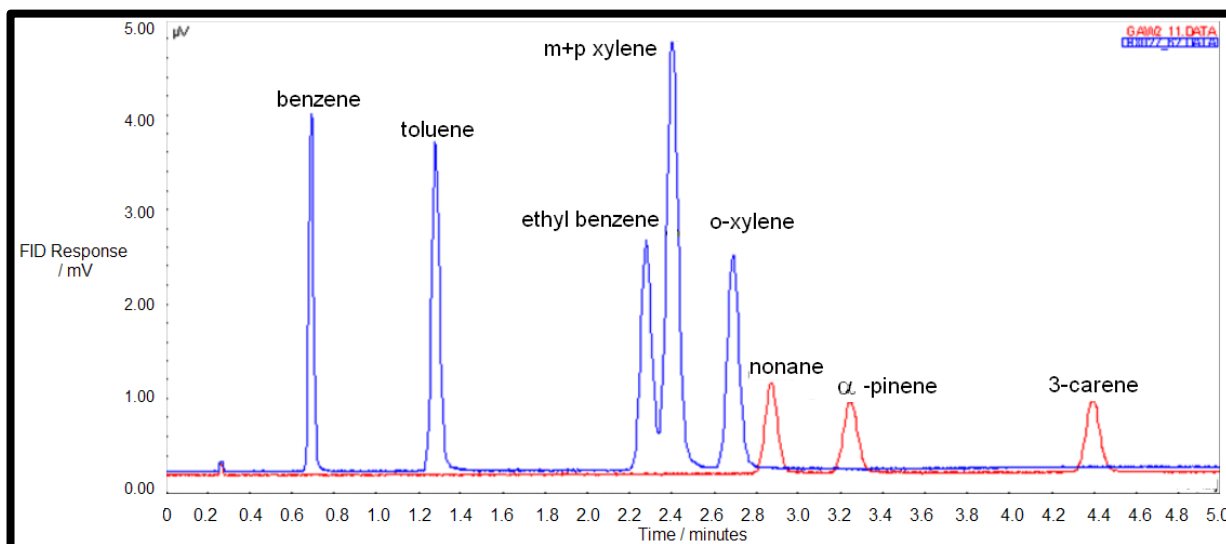


Figure 83: Response of FID (Varian) to injection of the BTEX standard mixture (blue) and a mixture of 2 ppm nonane, alpha-pinene and 3-carene (red) with a 0.5 ml sample loop

6.3.3 LOC 2

Before the primary column on LOC 2 could be coated, the path of flow that would be adopted by the stationary phase solution needed to be determined as this chip had a number of interconnected channels and open ports rather than a single channel with one inlet and one outlet.

6.3.3.1 Flow Path Determinations

In order to determine the best path of flow for coating this on-chip primary column, a number of experiments took place each of which involved introducing dyed pentane onto the column and either drawing it through the column by vacuum or pushing it through using compressed air or a gas-tight syringe.

6.3.3.2 Stationary Phase Coating of LOC 2 Primary Column

Several coating methods were evaluated. The method that gave minimal problems involved blocking the peek tubing transfer lines from the first and fourth drilled chip holes, as well as the preconcentrator and detector holes themselves, before forcing the stationary phase solution through the second peek inlet, onto the column and out towards the third opening. This allowed the primary column to be successfully coated whilst bypassing the preconcentrator and secondary column.

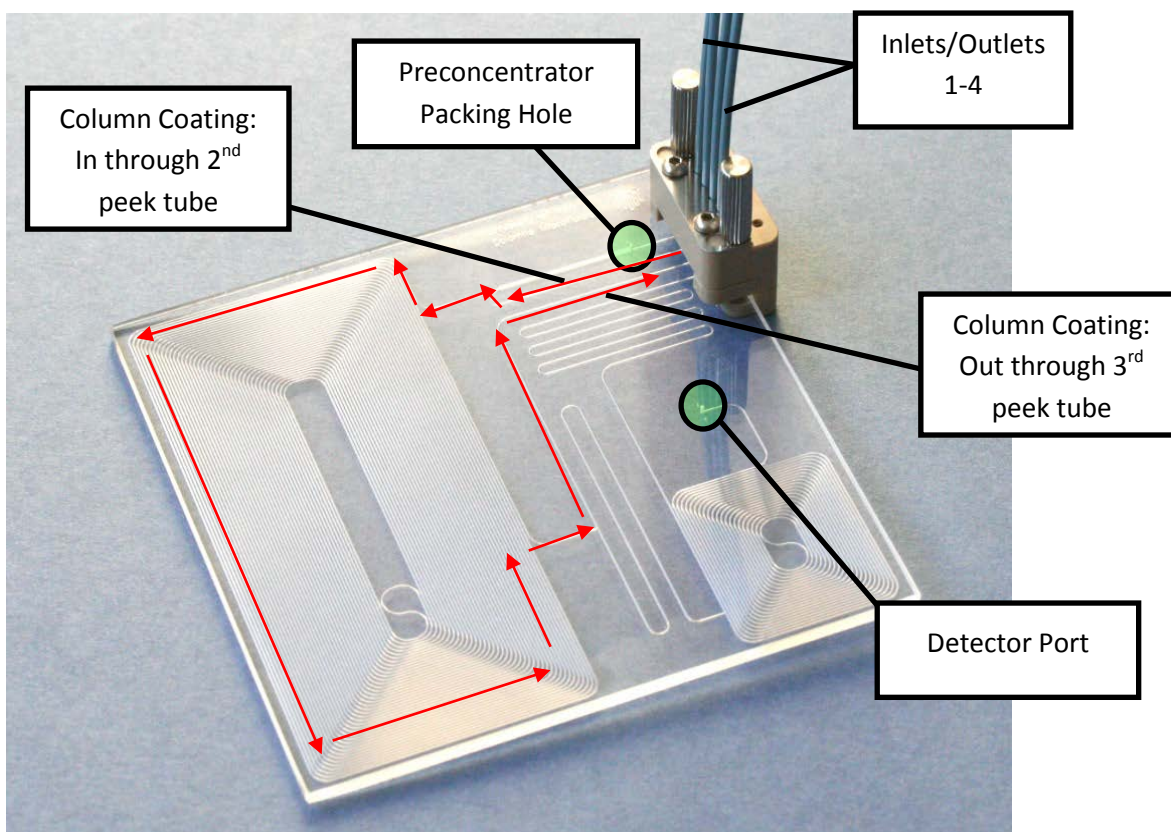


Figure 84: The flow path of the coating solution for LOC

A number of problems were encountered during this coating process, including that both the preconcentrator at the start of the column and the T-junction positioned after the primary column were “firing” air bubbles into the stationary phase plug. These air pockets could potentially affect the coating quality by leaving gaps in the stationary phase film where exposed OH groups on the surface of the glass could interact with sample.

An attempt to discourage this from occurring involved filling the preconcentrator with pentane, thus allowing small plugs of pentane rather than air to be fired into the plug. This diluted the stationary phase solution slightly but, overall, resulted in less of a problem.

Column coating was conducted statically, as previously described, as well as dynamically, using compressed air to push a plug of the stationary phase solution through the 7.5 m x 0.25 mm primary channel of the glass chip via the flow path method detailed above.

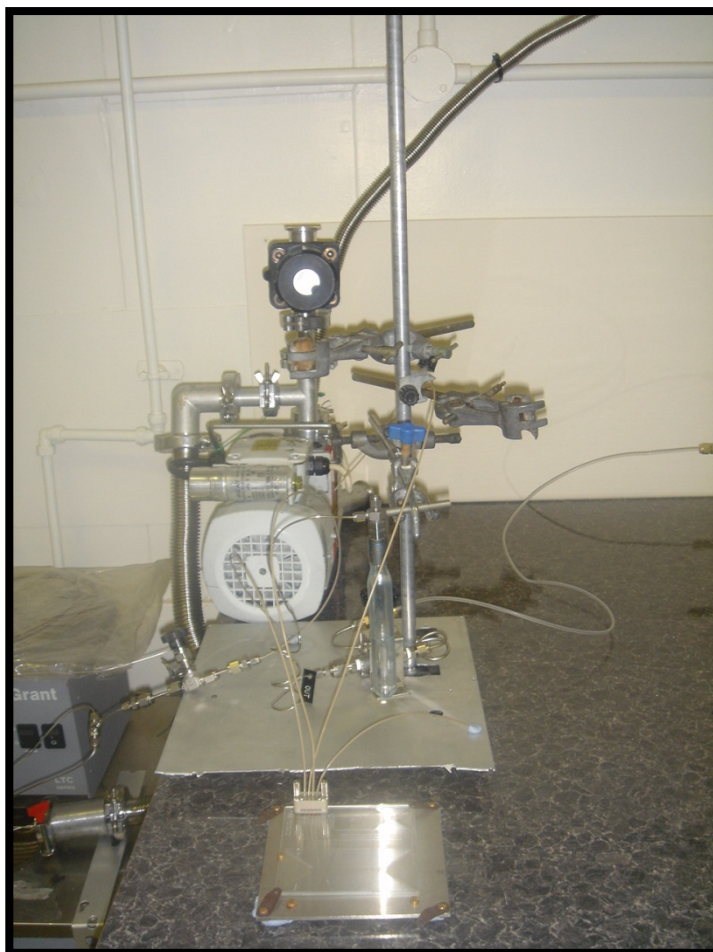


Figure 85: Glass chip column coating set up

Statically coated columns required solvent evaporation, and it was found that it was best achieved by placing the glass device in a vacuum desiccator, set to a constant temperature of 40 °C and with the minimum amount of vacuum applied. This allowed evaporation over a period of ± 36 hours. Alternatively, if available, the vacuum oven set up previously described for the coating of LOC 1 was used.

6.3.3.3 Effect of External Connections on Column Performance

The GC set-up was modified to allow direct attachment of the chip so that the performance of the coated columns could be evaluated. Modification involved using approximate 10 cm lengths of HP-5 commercial column connected from both the injector and detector ports to the peek tubing emerging from the chip (in the 2nd hole and out the 3rd hole, while the 1st and 4th holes were blocked).

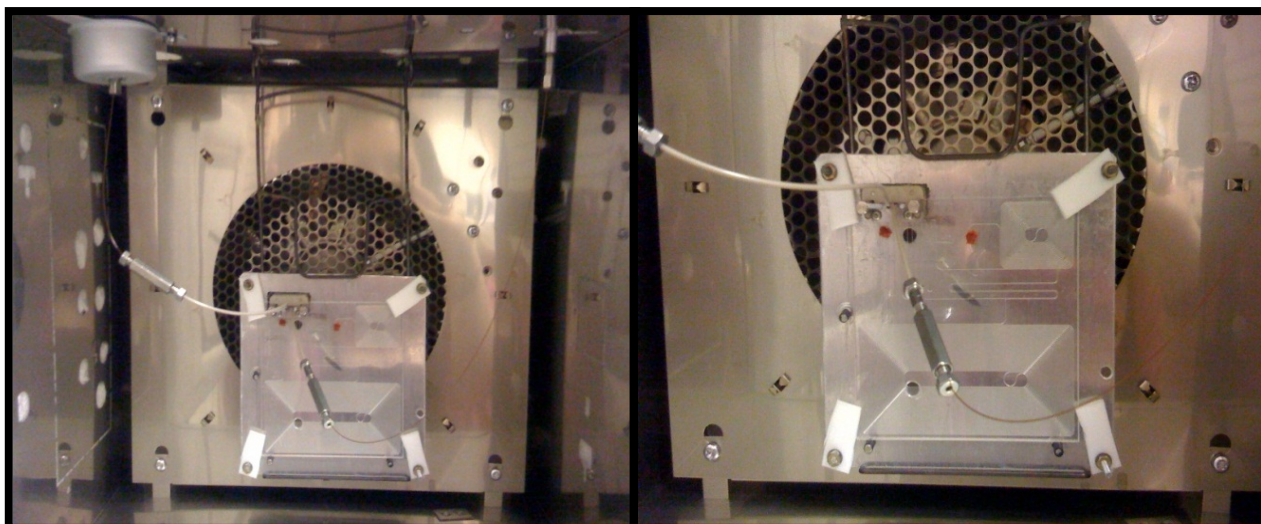


Figure 86: GC set-up to allow direct attachment of glass chip

Before the chip itself was analysed, an experiment was conducted in order to determine whether the lengths of commercial column present in the set-up would affect the chromatography, i.e. would the 10 cm lengths contribute significantly to the chromatographic separation. This was tested by connecting a short length of peek tubing to both the inlet section of the commercial column and the detector section, and by injecting 50 μl of a headspace mixture containing cyclohexane, propyl acetate and toluene onto the GC. Figure 86 resulted, which shows no retention or resolution of the three compounds.

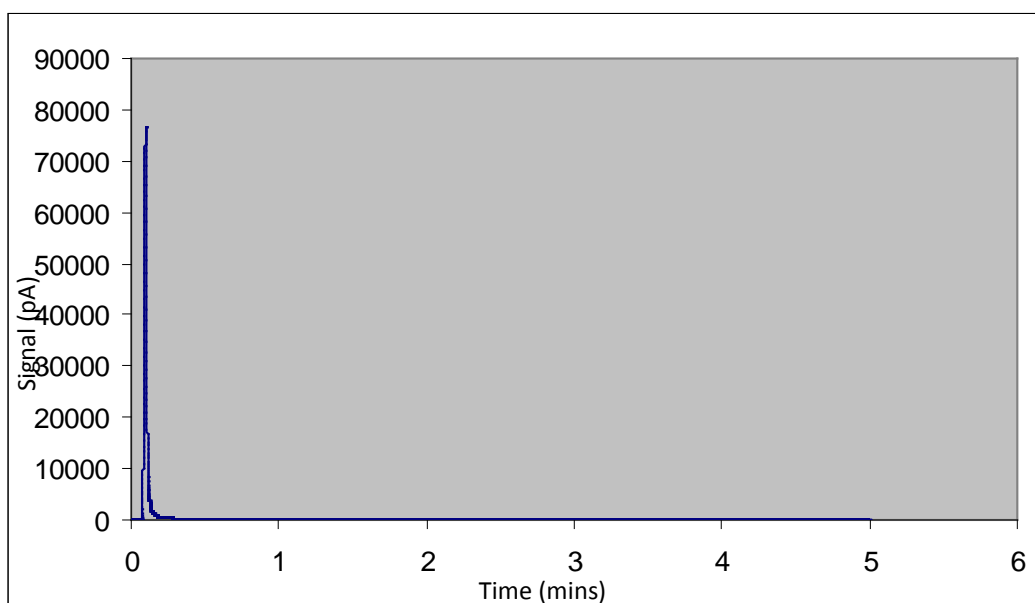


Figure 87: The lack of separation of cyclohexane, propyl acetate and toluene using two 10 cm lengths of HP-5 commercial column and a short length of peek tubing

This, thus, inferred that the lengths of commercial column present in the set-up would not affect the experimental results obtained when using the chip itself.

Next, an experiment was conducted in order to determine whether or not the peek tubing would have a detrimental effect on chromatography. Two separate pieces of peek tubing were connected to the inlet and detector lengths of commercial column, as shown in Figure 88, and the 7.5 m HP-5 commercial column was then connected to these. Again, the above mentioned

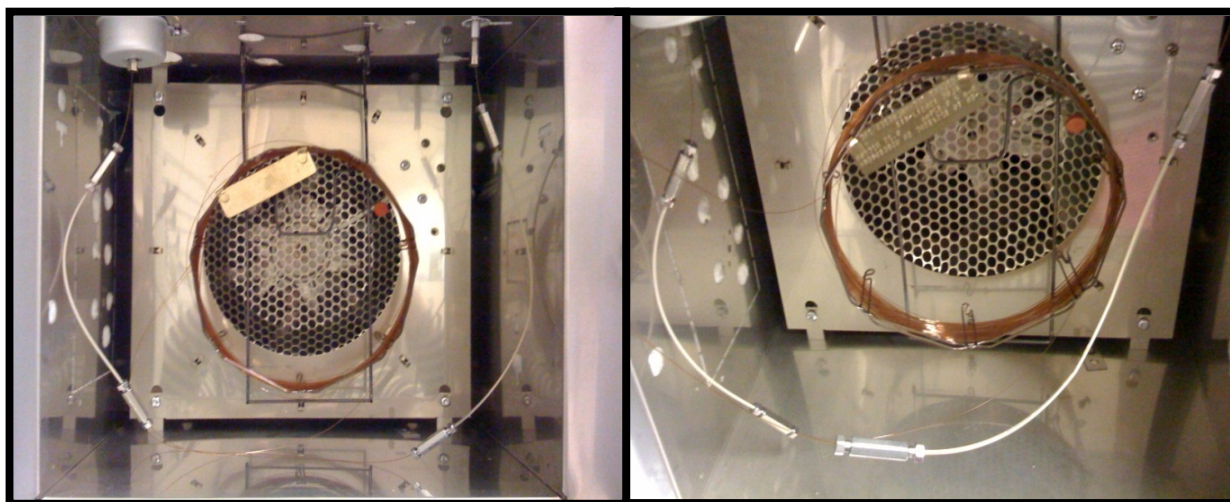


Figure 88: Experimental set-up to determine the effect of the peek tubing on chromatography

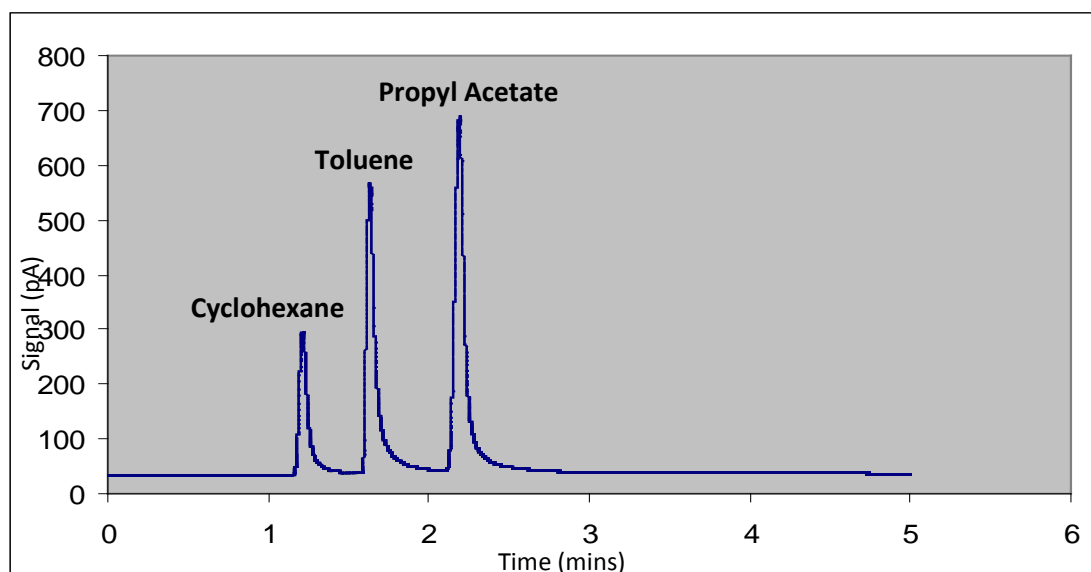


Figure 89: Separation of cyclohexane, toluene and propyl acetate using a 7.5 m x 0.32 mm x 0.25 μ m HP-5 column connected to two lengths of peek tubing

mixture was run and the result is shown below. Separation was achieved successfully, indicating that the effect of the peek tubing interconnections on chromatography can be considered negligible.

6.3.3.4 Dynamic Coating of Glass Chip Primary Columns

Figure 90 shows the result of the primary column dynamically coated with a 2% v/v solution of OV-101 in pentane, which equates to an approximate 1 μm film thickness.

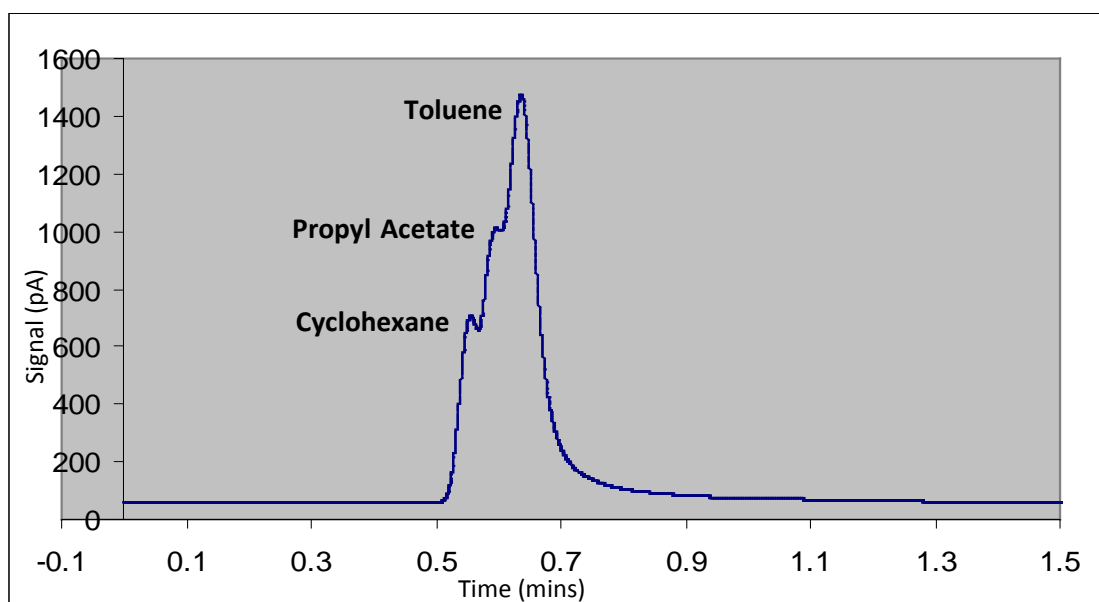


Figure 90: Separation of cyclohexane, propyl acetate and toluene using the 7.5 m x 0.25 mm on-chip primary column coated with a 2% v/v solution of OV-101 in pentane

The same chromatographic result was achieved on analysis of a blank uncoated on-chip column, indicating that a 2% v/v solution is too dilute for adequate coating of the chips. As such, higher concentration stationary phase solutions of 10% and 20% v/v were prepared and used for coating. These resulted in better component separation as illustrated in Figure 91 b) and c). However, despite the use of these higher concentrations, the desired separation was still not being achieved.

6.3.3.5 Static Coating of Glass Chip Primary Columns

It was found that a 2% v/v solution of OV-101 in pentane statically coated onto the chip column gave similar but slightly better chromatographic results

to those obtained by dynamically coating the chip with a 20% v/v solution of OV-101. This is evidenced by Figure 91 d).

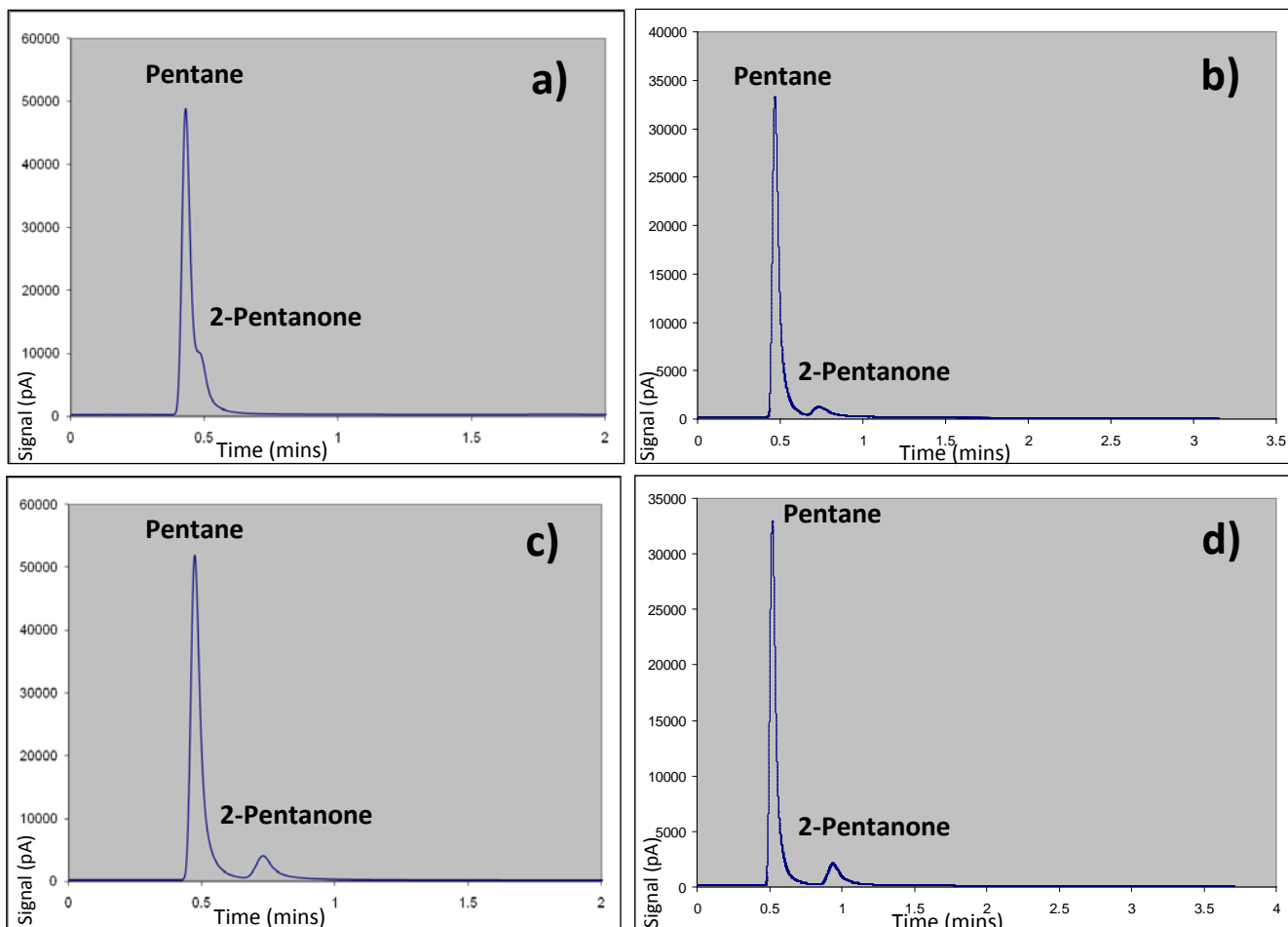


Figure 91: Pentane and 2-pentanone. Primary column coated dynamically with a a) 2% v/v solution of OV-101 in pentane; b) 10% v/v OV-101 in pentane; c) 20% v/v OV-101 in pentane; and d) the separation achieved on a column coated statically with a 2% v/v solution of OV-101 in pentane

6.3.3.6 Effect of Stationary Phase Over-Concentration

The glass column was also statically coated with a 20% v/v solution of OV-101 in pentane for comparison purposes. While Figure 92 shows successful separation and retention, it is clear that there is too much stationary phase present on the column. The excess coating resulted in the formation of pockets or droplets of stationary phase being sporadically positioned throughout the column.

As the sample components came into contact with each of these pockets the flow rate was reduced, resulting in the “jagged” peaks seen in the

chromatogram. The microscopic evidence of these “bubbles” is shown in Figure 93.

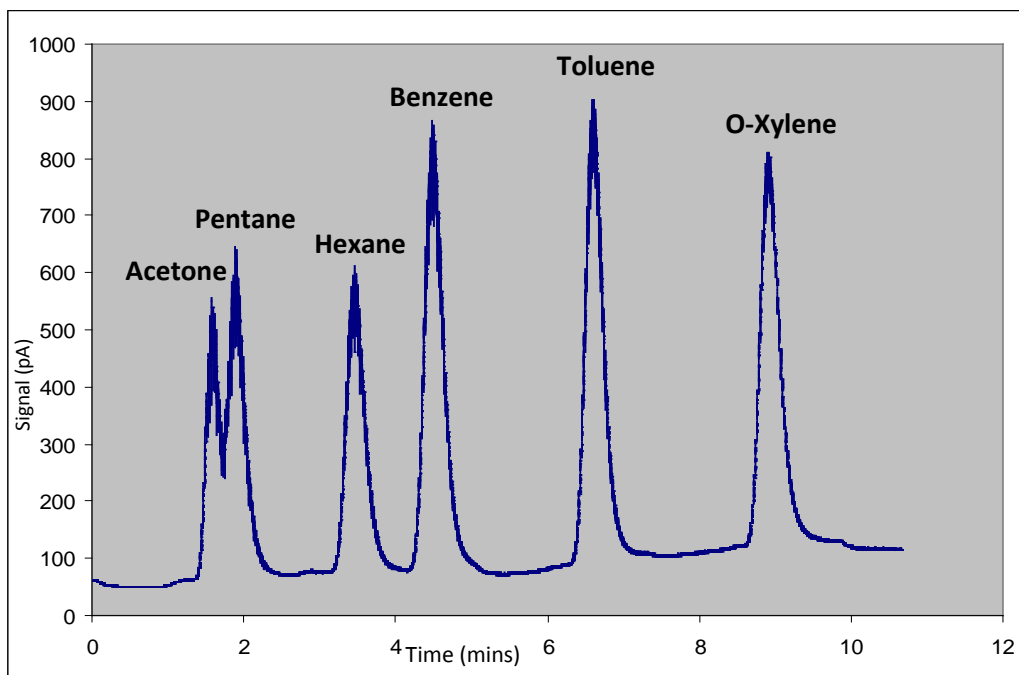


Figure 92: Acetone, pentane, hexane, benzene, toluene and o-xylene. Primary column statically coated with a 20% v/v solution of OV-101 in pentane

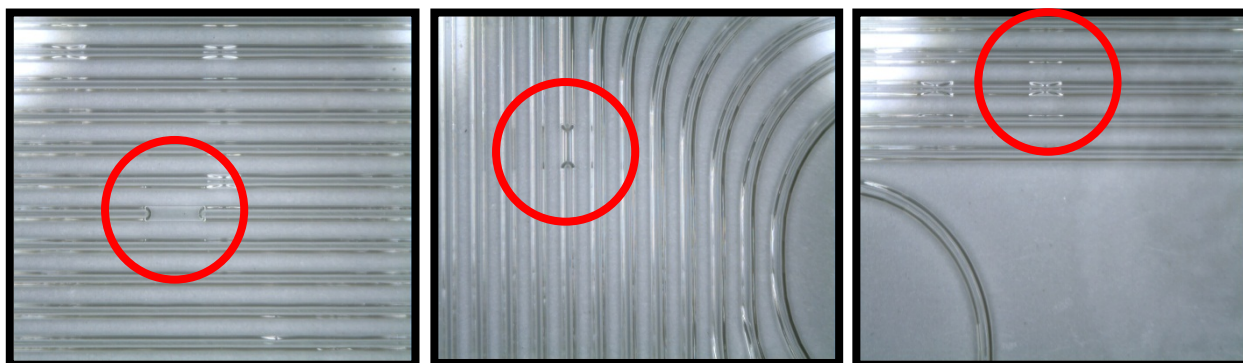


Figure 93: Microscopic evidence of liquid droplets of stationary phase present in microcolumn

6.3.3.7 Dynamic vs. Static Coating

The above work confirmed that static coating is the preferred method of stationary phase film deposition. Not only does static coating allow for a more accurate estimation of film thickness, but, according to available literature, it also generates thinner, more uniform films in comparison to dynamic coating due to the lack of axial motion of the stationary phase during deposition^[3]. In terms of the experimental work conducted here, not only did static coating

provide better resolution and peak shape, but it was also found that a less concentrated stationary phase solution was required. This was important as extreme column bleed was experienced with the use of more highly concentrated silicone stationary phase films. Leached coating material is known to combust in FIDs, resulting in the formation of white silica powder. This then deposits on the surfaces within the detector causing noisy chromatograms, random spikes and poor detector sensitivity. As well as the above, a significant amount of down time is experienced for detector cleaning and conditioning between runs.

Figures 94 and 95 allow comparison of the separation of a more complex 7 component mixture achieved using a column coated dynamically with a 20% v/v solution of OV-101 in pentane, and a statically coated 2% v/v solution of OV-101 in pentane.

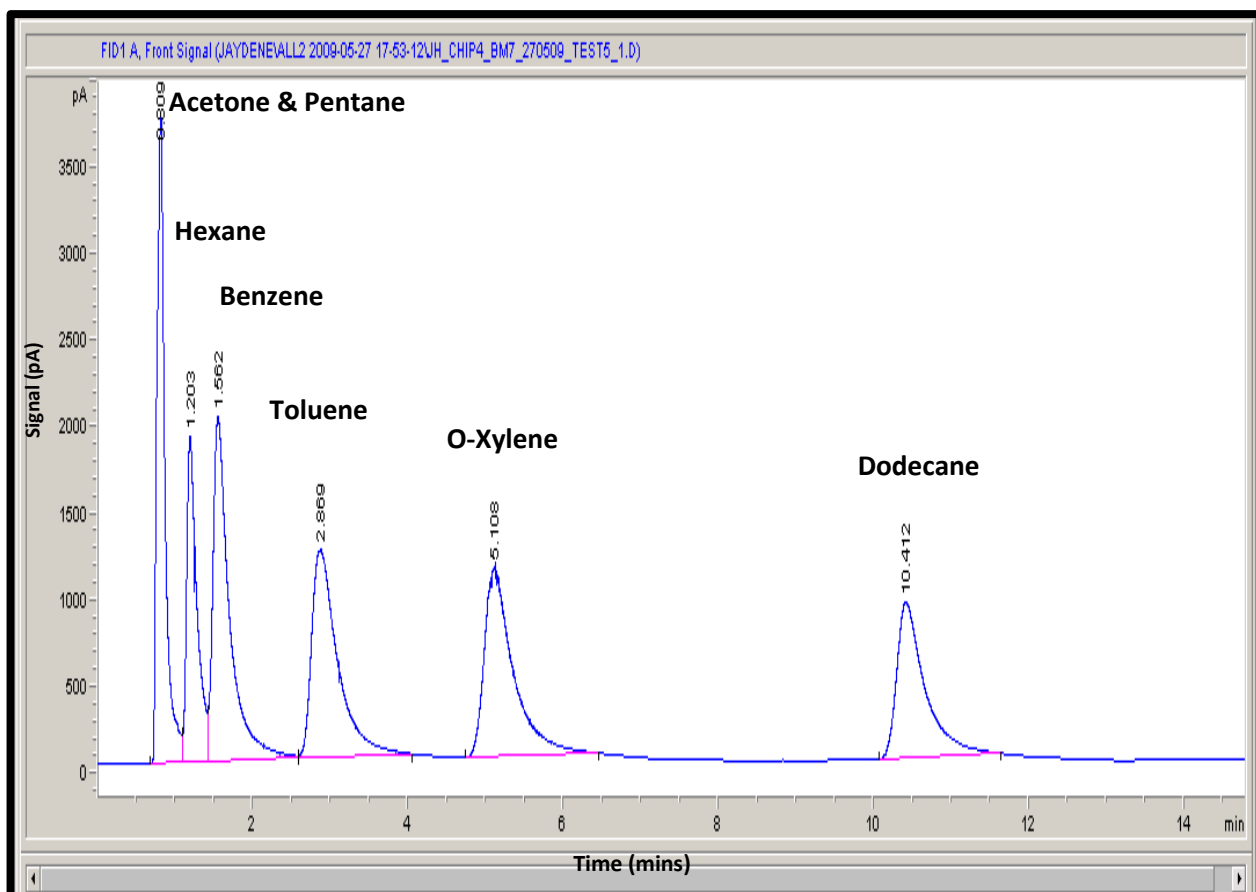


Figure 94: Acetone, pentane, hexane, benzene, toluene, o-xylene and dodecane using the 7.5 m x 0.25 mm on-chip glass column dynamically coated with a 20% v/v solution of OV-101 in pentane

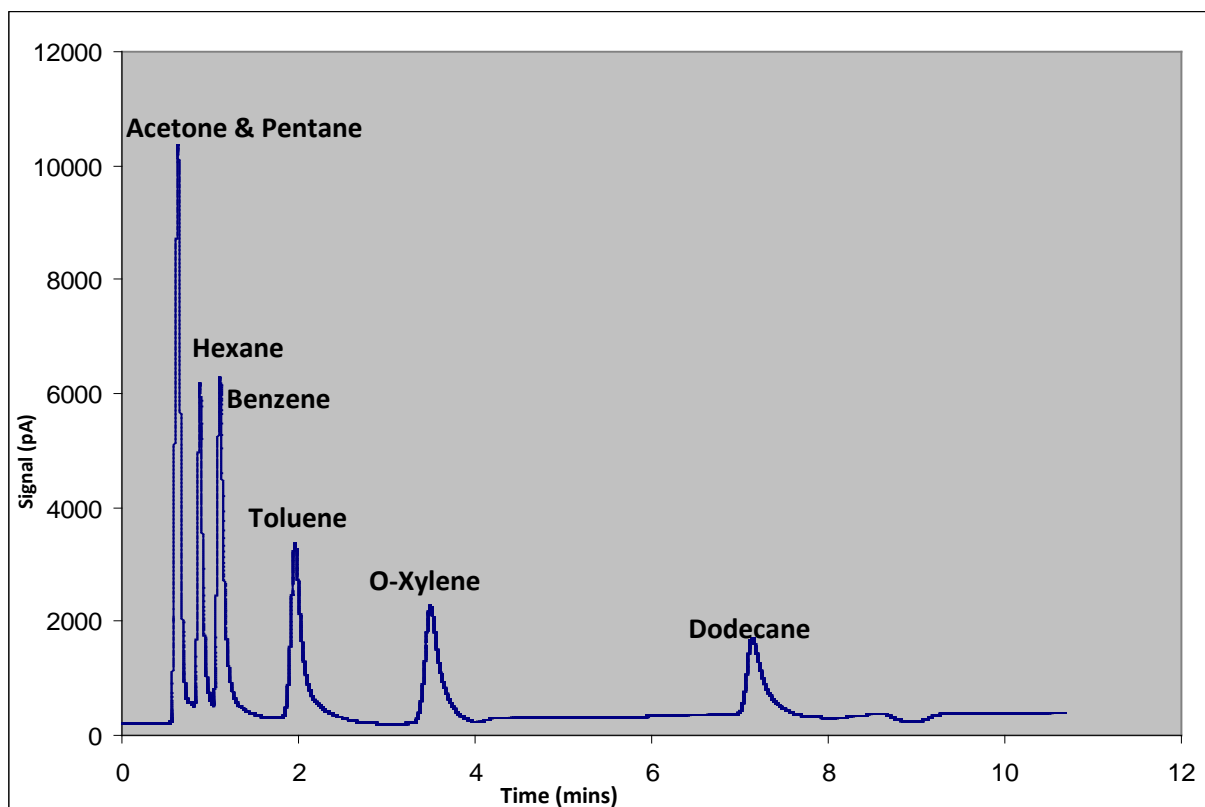


Figure 95: Separation of the same mixture using a column coated statically with a 2% v/v solution of OV-101 in pentane

6.4 References

1. Evander, M., et al., *Acoustophoresis in wet-etched glass chips*. Analytical Chemistry, 2008. **80**(13): p. 5178-5185.
2. *Fabricating MEMS and Nanotechnology*. 2011 01/06/2011 [cited 2011 15/12/2011]; Available from: <https://www.mems-exchange.org/MEMS/fabrication.html>.
3. Reidy, S., et al., *High-performance, static-coated silicon microfabricated columns for gas chromatography*. Analytical Chemistry, 2006. **78**(8): p. 2623-2630.

7.0 Fabrication of the Lab-on-a-Chip GC Manifold

As the overall purpose of creating the glass microfluidic devices was to assemble a fully portable, field operable gas chromatography system, a housing manifold for the chip containing all necessary components for GC operation was fabricated. The individual components making up this manifold are described in this chapter.

7.1 The Preconcentrator

For the lab-on-a-chip device described in this body of work, the complex process of sample preconcentration and thermal desorption previously described would not be appropriate. As such, LOC 2 was designed with a preconcentrator channel acid-etched in-line with the sample introduction port. A small hole allowed for adsorbent packing. Literature searches have unearthed entire theses dedicated to the development of micro-preconcentrator units for similar μ GC devices^[1]. The amount of work required to fully develop a μ -preconcentrator capable of replacing the TDU without a loss of functionality was, unfortunately, beyond the scope of this project. However, the preliminary work conducted with this project's on-chip μ -preconcentrator will be detailed next.

Thermoelectric devices or Peltiers were used to cool the preconcentrator to allow sample trapping, and a halogen bulb was used to rapidly heat the

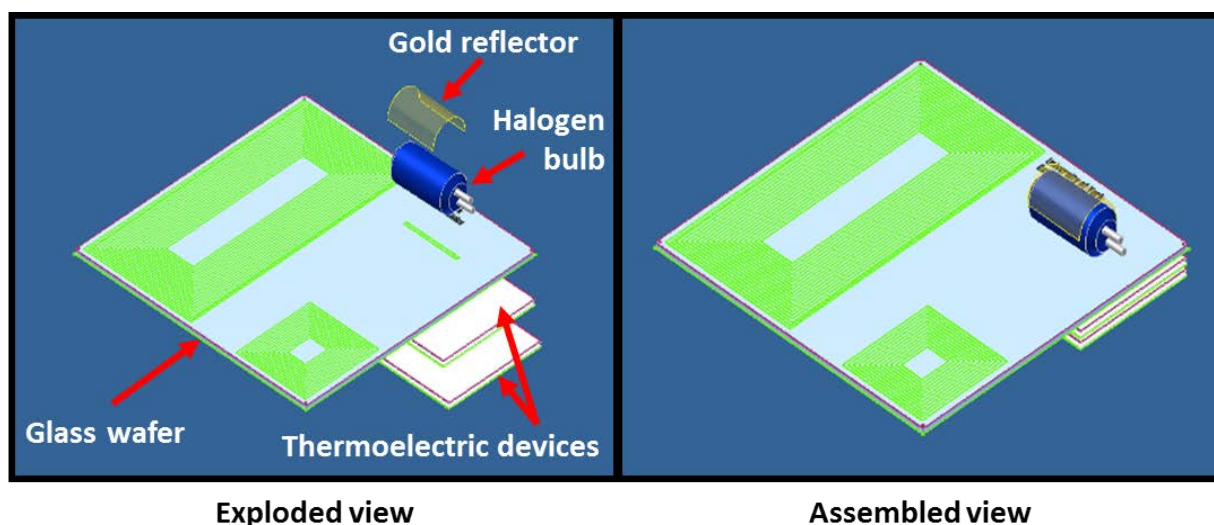


Figure 96: CAD model of the preconcentrator stage (provided by Dr Christopher Rhodes)

packing material to allow thermal desorption of the trapped analytes of interest. Ideally, a gold reflector, as shown in Figure 96, would have been used to minimise heat loss as it is a better reflector of IR light. However, due to difficulty in sourcing gold paint, the 12 V/10 W halogen bulb was instead painted 180° with silver dag.

To avoid the risk of blocking the channels of the actual glass chip, a small section of the glass device, with only the preconcentrator etched onto it, was obtained from the Dolomite Centre for performance testing.

Carbopak B 60/80 mesh was used to hand-pack the trap with the aid of a microscope (Figure 97). Carbopack B is known to provide a convenient balance of adsorption capacity and desorption efficiency over a wide range of volatilities and chemical functionality, however, it has a limited range of volatile analytes that are adequately trapped on each graphitized carbon. It was later decided that packing micro-glass beads either side of the Carbopak B would allow the halogen bulb to be concentrated on an area away from the weak packing hole (Figure 98).

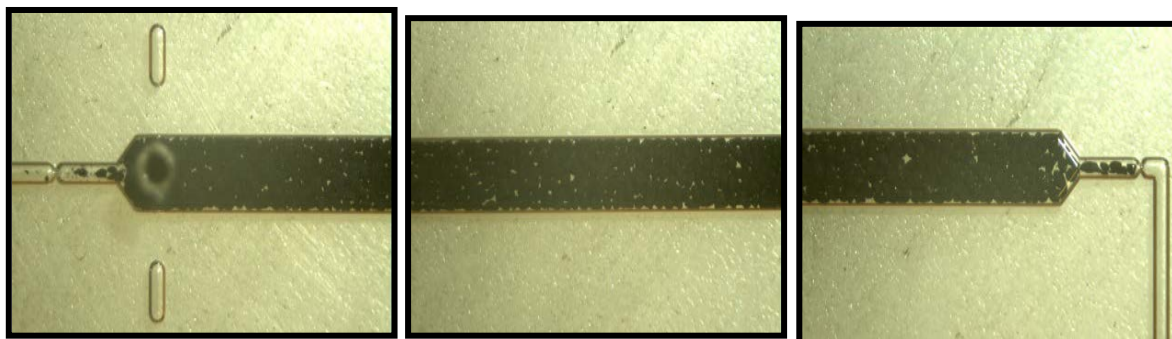


Figure 97: Microscopic image of preconcentrator packed with Carbopak B 60/80 mesh

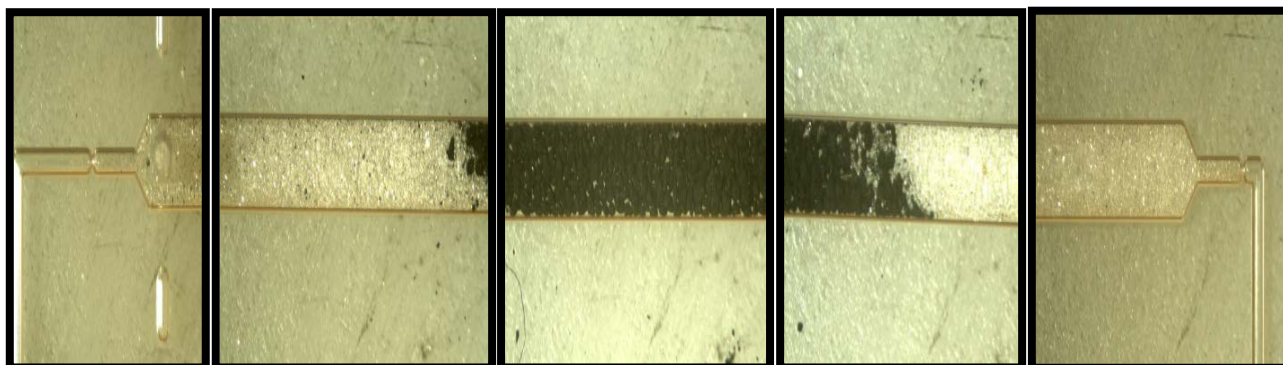


Figure 98: Microscopic image of preconcentrator packed with micro-glass beads on either end and Carbopak B 60/80 mesh inbetween

7.1.1 Preconcentrator Performance Testing

Performance testing of the packed preconcentrator was conducted as illustrated in Figure 99. A manual gas sampling valve with a 5 μl loop injected sample into the packed preconcentrator, which was then heated. The desorbed analyte was subsequently detected by the PID. It should be noted that the temperature of the trap during halogen heating was unknown, with only the resulting desorption effect being monitored.

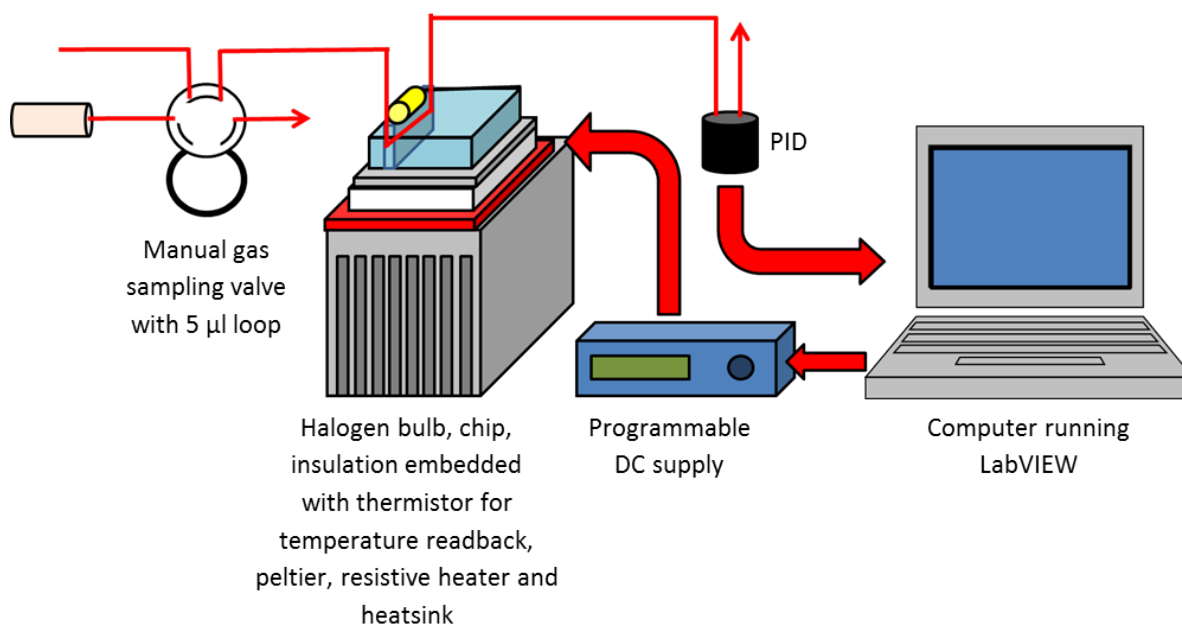


Figure 99: Set-up for trap section testing

Initial experimentation saw pentane being drawn through the preconcentrator and PID from the sample loop using a miniature diaphragm pump. No heating was applied to the glass section. This resulted in a significant restriction to the flow in the downstream-pumped system. A broad peak was subsequently recorded for pentane, as shown in Figure 100 a) as it had trouble desorbing from the trap.

Next, pentane vapour was propelled through the trap using nitrogen gas, rather than being drawn through with the use of a pump. Adsorption was achieved at 10 $^{\circ}\text{C}$, followed by desorption by halogen heating for a period of 30 seconds at 770 seconds. Using a positive flow of carrier gas rather than a pump to introduce the sample onto the adsorbent bed proved to be the better method, as illustrated by peak 1 of Figure 100 b), although, as can be seen,

5 μl of pentane gas was enough to saturate the detector. Peak 2 shows the desorbed pentane peak when heating was applied. The immediate presence of the large peak 1 indicates that the preconcentrator was not efficiently trapping the sample, with most of it flowing straight through the adsorbent packing. However, the appearance of peak 2 on heating indicates that some trapping of pentane by the Carbpak B was achieved.

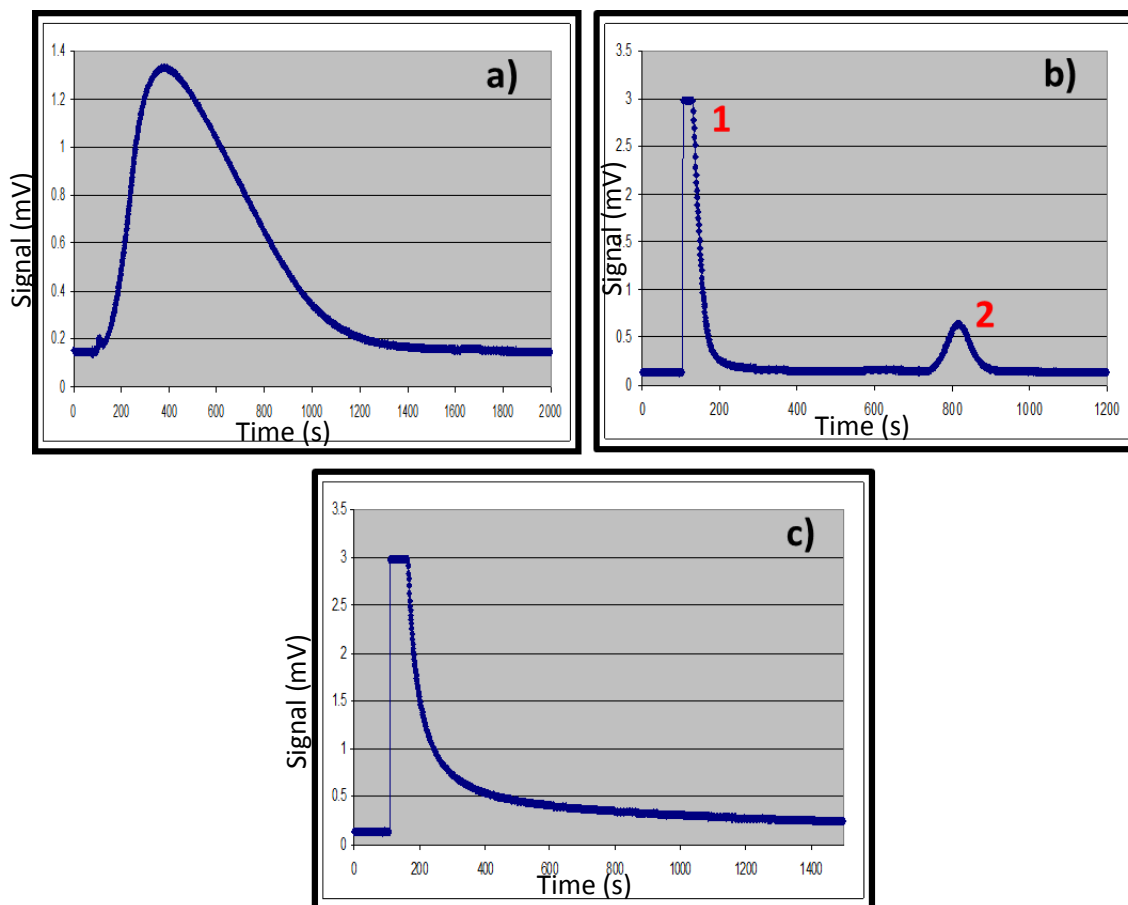


Figure 100: Desorption of a) pentane drawn through the preconcentrator by a pump at ambient temperature; b) pentane propelled through the preconcentrator with N_2 carrier at 10°C before thermal desorption for 30 s; c) isoprene propelled through the preconcentrator with N_2 carrier at 10°C before thermal desorption for 30 s

The above was also conducted with isoprene. Here, the compound was adsorbed onto the trap at 0°C followed by desorption by halogen heating at 770 seconds. As seen in Figure 100 c), no desorption effect was observed. It is possible, however, that desorption did take place but was masked by the chromatogram's unresolved baseline. Further experimentation in this area is required in order to determine the most appropriate packing material, or whether a mixture of packings would be better suited.

A factor that severely limited development was condensation of water and formation of ice on the exposed glass preconcentrator surface. This was found to occur at temperatures below 10 °C, with evaporation of the water film affecting the radiant heating effect from the halogen lamp. The trap, or the entire chip itself, would need to be placed inside a sealed chamber with a dry air purge to compensate for this.

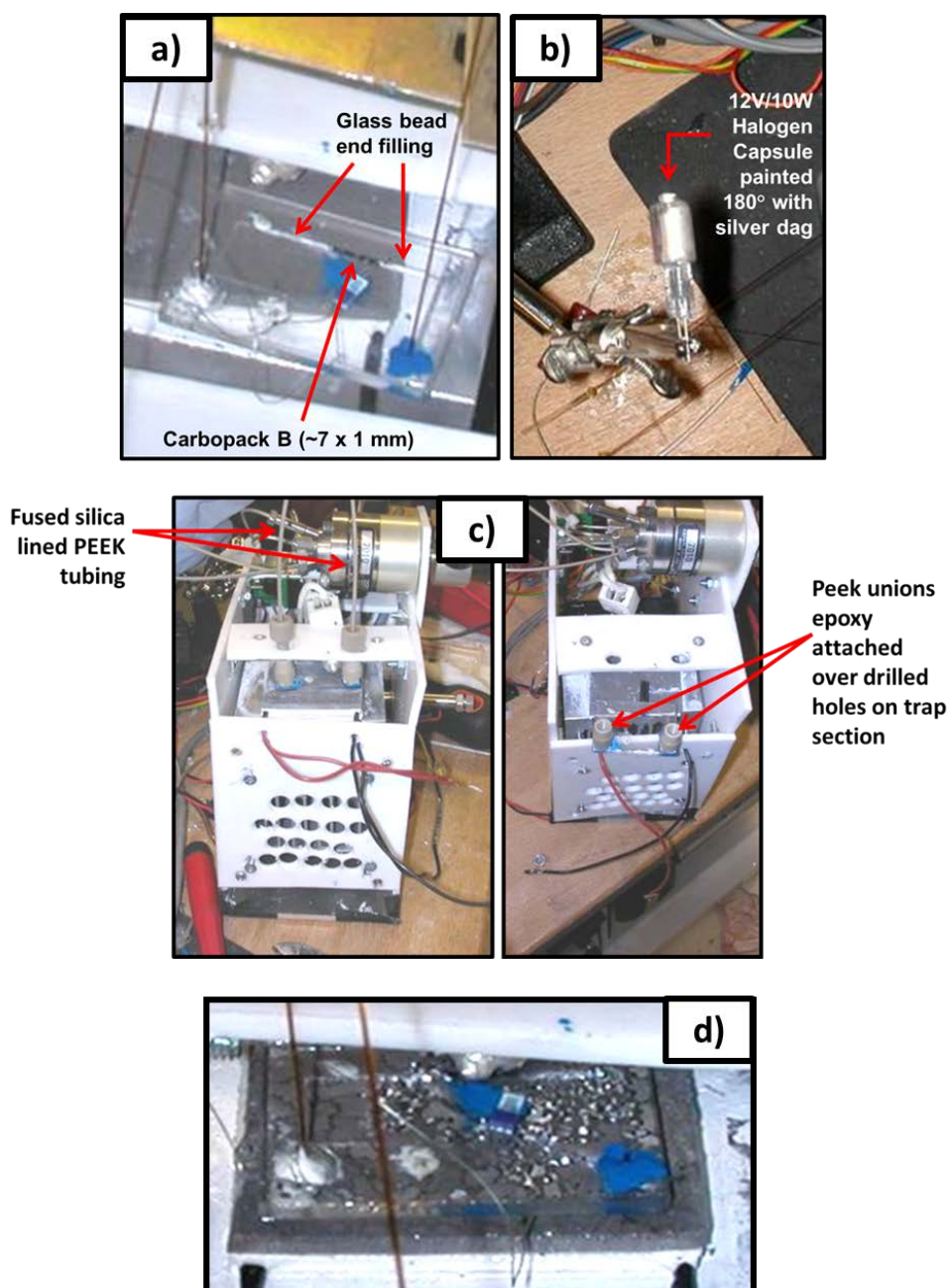


Figure 101: Views of a) the packing in the trap section; b) the lamp; c) the trap installed for testing; d) condensation of water on the exposed surface of the trap

7.2 Temperature Control

Uniform heating of a GC column is central to its performance, requiring accurate and reproducible column temperatures with minimal spatial temperature gradients.

For the device reported here, a combination of direct heating approaches was investigated. These included the direct heating of the glass wafer with metal heating elements placed above and below the device, and a more complex arrangement as shown in Figure 102. An aluminium heat sink was used for forced air cooling, equipped with a centrifugal blower for rapid cooling of the metal fins. The heater consisted of thin film resistive heating elements (etched foil embedded in a self-adhesive glass fibre matrix) positioned above Peltiers. Thermal interface material was used to fill any air gaps between the heating and cooling stages and the glass chip.

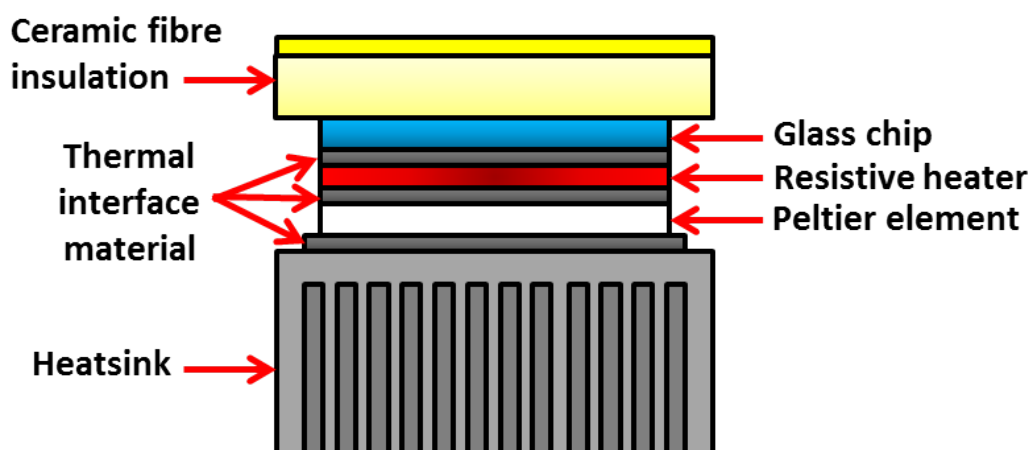


Figure 102: Side view showing the layout of components in the temperature controlled stack used for heating and cooling the glass GC

Since glass is a relatively poor heat conductor, the separation of the zones of the device allows the differential heating of the injector from the columns and other regions. This was tested using three different control thermal stacks and temperature zones as shown in Figure 103. Temperature monitoring of the stack was achieved using a PT100 polyimide encapsulated sensor placed between the heater and the glass chip. A configurable CompactRIO module supplied by National Instruments running LabVIEW Real-Time operating system was used to control the temperature of the stack. The temperature profile across the chip was determined using a matrix of sixteen thick film

platinum resistance temperature sensors (Labfacility DM503), which were attached across the chip surface in an X pattern using thermally conductive epoxy adhesive.

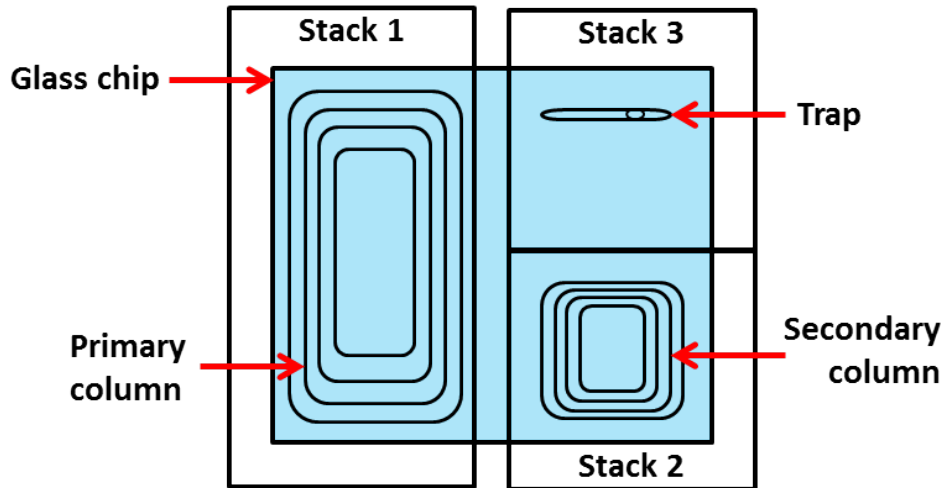


Figure 103: Plan view layout of the temperature controlled stacks. Stack 1 is under the primary 7.5 m long column. Stacks 2 and 3 are positioned under the secondary 1.4 m column and the injection region, respectively

The temperature data collected was displayed in the form of a colour map overlaid on a two dimensional image of the glass chip using LabVIEW software. Figure 104 a) shows the reproducible temperature profile across the

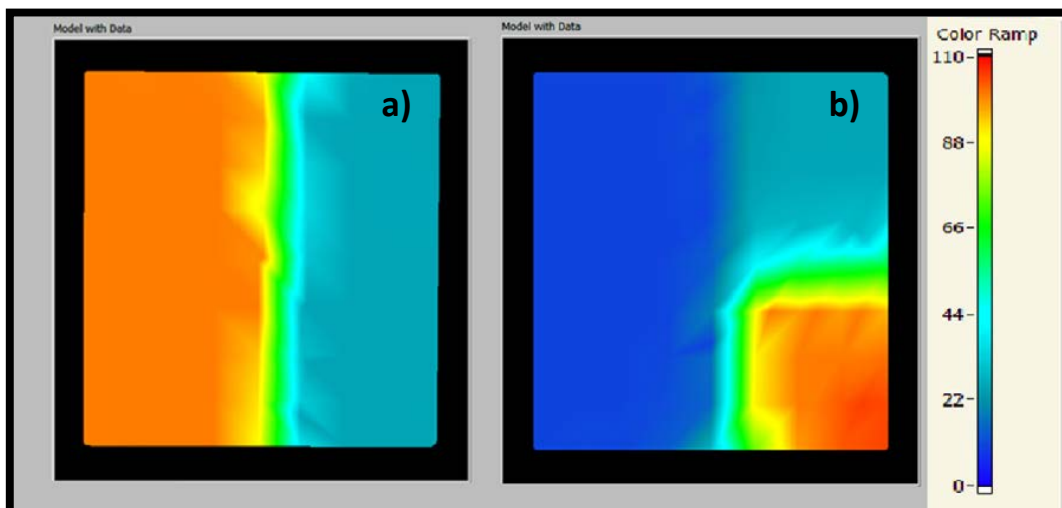


Figure 104: Measured temperature profile with a) stack 1 (under the 7.5 m column) heated to 100 °C, all other stacks left at ambient; b) stack 1 cooled to 10 °C whilst holding the temperature of stack 2 (the 1.4 m column) at 100 °C. The temperature remained uniform (± 2 °C) over stack 1 and the unheated stack 3 remained at ambient temperature

surface of the chip when stack 1 (7.5 m column) is heated to 100 °C and all other stacks are left at ambient, while Figure 104 b) shows the measured temperature profile when stack 1 is cooled to 10 °C, with stack 2 (1.4 m column) held at 100 °C and the unheated stack 3 (preconcentrator) remaining at ambient temperature. The 2D images reveal that the divided thermal stack arrangement is capable of independently controlling the temperature of at least three discrete regions of the glass GC device.

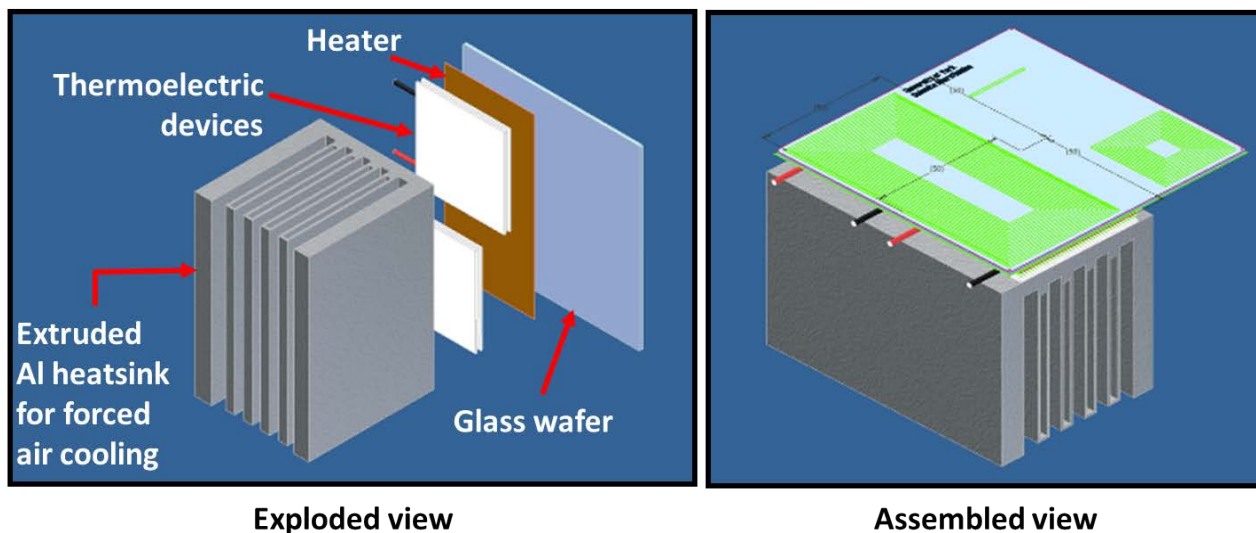


Figure 105: CAD model of the thermal control unit (provided by Dr Christopher Rhodes)

The column temperature range achieved was between 0-200 °C, with linear ramp rates of between 5 and 20 °C·min⁻¹. Typical power consumption was 25 W mean or 30 kJ per analysis, which is two orders of magnitude less than conventional turbulent fan ovens.

7.3 The Modulator

In order to achieve a 2-dimensional separation, LOC 2, LOC 3 and LOC 4 were designed so that the primary column was coupled to the secondary via a differential flow modulator in a manner illustrated in the diagram below. The acid-etched, on-chip, in-line fluidic modulator was based on work developed and reported by Seeley *et al.* in 2006^[2], as detailed in Chapter 4.

Helium carrier and modulator gases initially follow the paths indicated in Figure 106 a). The three-way modulator solenoid valve then changes its direction for a few seconds. The flow in the first gas transfer line stops while

the flow in the second line commences at a lower flow rate. The lower flow is the result of the second transfer line having a higher flow impedance than the first. This enables the elution and analysis of sample compounds in the second column, while the sample which elutes from the first analytical column is stored in the storage transfer line or collector channel. The short, high flow rate pulse not only flushes the sample from the collector into the second column, but also creates a higher pressure at the first T connector which simultaneously stops the elution of sample compounds from the first column.

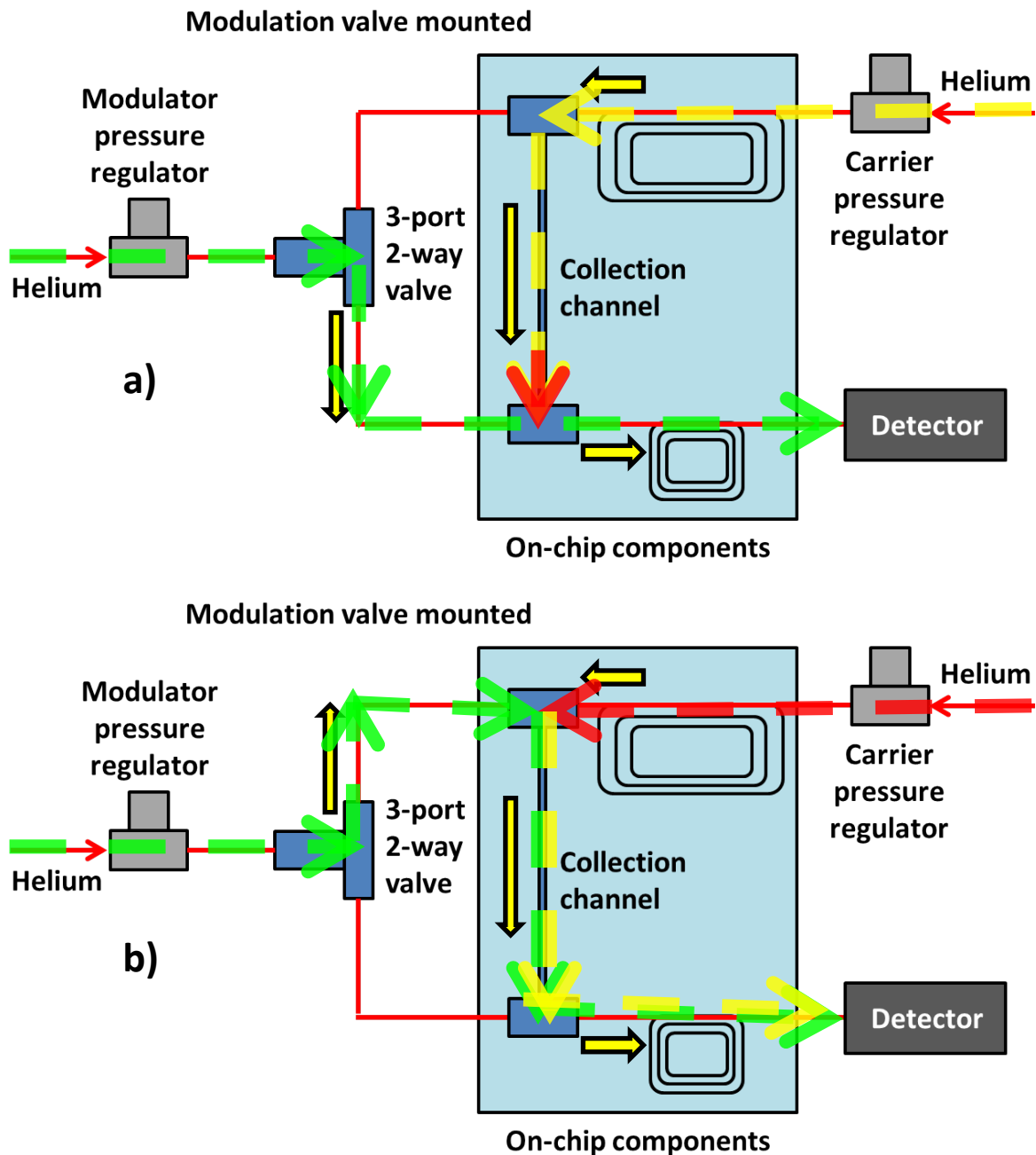


Figure 106: A schematic illustrating the layout of the on-chip modulator, as well as showing gas flow direction when in a) load; b) inject position

The on-chip modulation valve was tested with gas phase samples and narrow peaks were obtained by fine tuning the carrier and modulator gas pressures.

7.4 The Detector

As previously discussed, PIDs are similar to FIDs in many ways. The biggest difference between the two forms of detection is that FIDs are bulky in comparison, more expensive and require a hydrogen source. This greatly limits FIDs as a viable alternative in portable VOC monitoring.

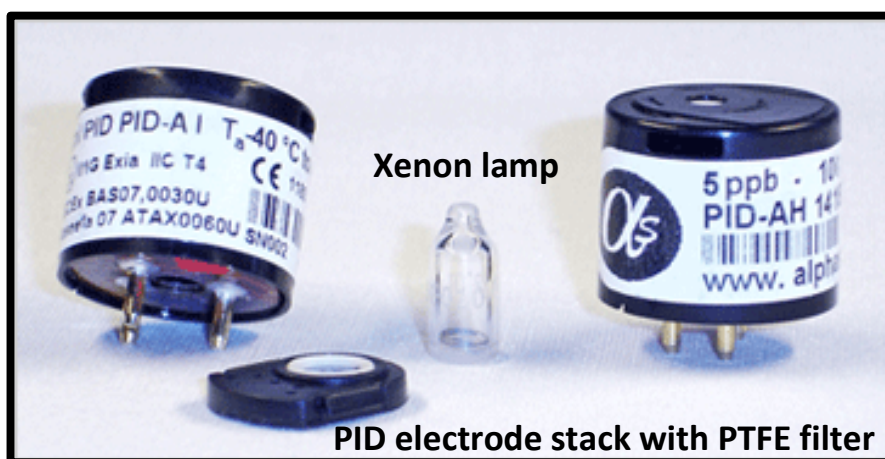


Figure 107: The photoionization detector sourced from Alphasense

A commercially available, low cost, and low power photoionization detector, sourced from Alphasense, was used for on-chip detection. This PID, which was designed for VOC monitoring in ambient air, weighed just 8.0 g, had a lamp with an ionization potential of 10.6 eV, and had a 100 mW nominal power consumption at 3.0 V. Further PID specifications are detailed in Table 26. For most portable instruments, the 10.6 eV lamp is most widely used because it detects most volatile organic compounds, and the lamp is easy to clean.

7.4.1 Detector Performance Testing

The PTFE particulate filter present on the detector was removed to allow gas to flow across the electrode stack. A holder was designed to fit around the PID to provide a gas tight seal and to allow connection to a capillary. A miniature diaphragm pump was used on the outlet capillary to draw sample into the detector. Very low noise power to the detector was provided by a hybrid

supply, and output was monitored via a differential input to prevent interference from ground connection.

Table 25: PID specifications^[3]

Target Gases	VOCs with ionisation potentials < 10.6 eV
Linear Dynamic range	5 ppb to 50 ppm (Isobutylene)
Power Consumption	110 mW typical (at 3.3 V)
Supply voltage	3.0 to 3.6 VDC (ideally regulated to 0.01 V)
On-board filter	To remove liquids and particulates
Working temperature range	-40 °C to +40 °C
Signal temperature dependence	0 °C to 40 °C: 99% of signal at 25 °C-20 °C 97% of signal at 25 °C
Response time	< 3 seconds, diffusion mode
Relative Humidity range	0 to 95% RH, non-condensing

Figure 108 illustrates the detector's signal response in both ambient air and when exposed to pentane vapour. Varying concentrations of pentane vapour were pumped into the detector in order to determine its speed of response. As

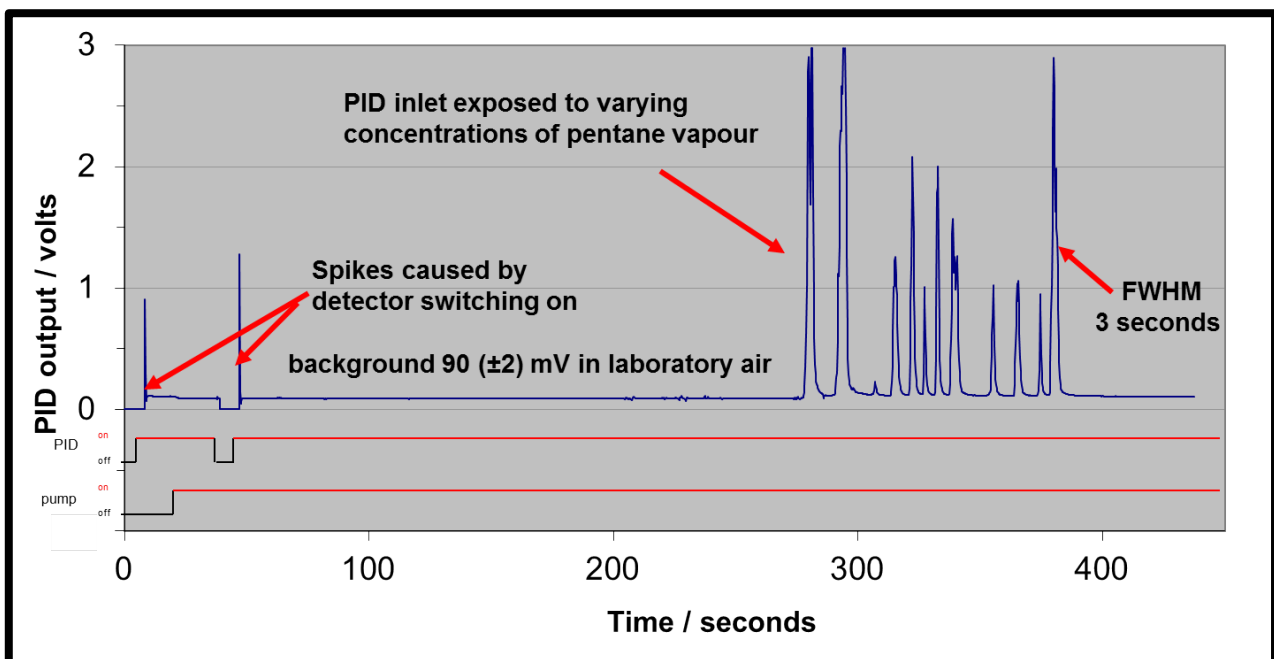


Figure 108: PID response to ambient air and varying concentrations of pentane vapour. FWHM = Full Width at Half Maximum

previously discussed, it was also determined that 5 μl of pentane gas is enough to saturate the detector.

7.5 Real-Time Control and Data Acquisition

A Windows operating system was not particularly suited for the real-time control and data acquisition applications of this project, as, for example, temperature control required a fast system response to prevent overshoot and offsets. As well as this, detector signal must be acquired at > 50 data points $\cdot\text{s}^{-1}$ to allow for a 2D GC analysis. As such, a real-time processor and interface was acquired from National Instruments. This was built into the overall manifold frame to provide control and acquisition for the LOC GCxGC in a relatively portable unit, and with the capability of being battery power operated. A USB data acquisition (DAQ) device with Digital I/O was used for interfacing the overall device to the LabVIEW software. This allowed digital multichannel temperature control and monitoring of the installed chip, and, obviously, digital data collection.

The system used IP addressing to allow data to be downloaded to a PC, but was also able to run in stand-alone mode with built in solid state memory for data storage. It could also be connected to a Wi-Fi or a land connection network. The implication here is that a separate computer (a lab-based one, perhaps) could be used to access data generated by the LOC GCxGC, which could be located anywhere in the world, on the site of sampling.

An important development in terms of software was the ability to generate two-dimensional GC plots in real-time using LabVIEW. Typically, visualisation of 2D data is performed post-process by matrix conversion of the 1D signal data before being displayed using software packages, such as Transform (Research Systems) or Zoex GC image (Zoex). Using the in-house developed software meant that, as a run progressed, the success of 2-dimensional separation or lack thereof could be monitored concurrently. This proved to be a significant time-saver.

7.6 References

1. Veeneman, R.A., *Design and Characterization of a Multi-Vapor Preconcentrator for a Micro-Scale Gas Chromatograph*, in *Chemistry*, . 2009, University of Michigan: USA. p. 186.
2. Seeley, J.V., et al., *Comprehensive two-dimensional gas chromatography with a simple fluidic modulator*. *American Laboratory*, 2006. **38**(9): p. 24-26.
3. *Specifications - Photo Ionisation Detectors (PID)*. 2010 01/06/2011 [cited 2012 10/01/2012]; Available from: http://www.alphasense.com/alphasense_sensors/pid_specs.html.

8.0 Experimental –Stand Alone One-Dimensional GC

Following the characterisation of the separation power of the glass first dimensional columns in a commercial GC instrument, their separation capabilities were next established in the in-house manufactured GC manifolds.

8.1 LOC 1

LOC 1 was tested in a simpler temperature control enclosure than the one previously described, using manual injections and the miniaturised photoionization detector.

Figures 109 and 110 show the set-up of the testing conducted. The chip was fixed between two metal heating plates and the temperature of the unit was electronically controlled. Cooling to ambient temperature was achieved with two fans fixed to the back of the unit. A two-stage regulator was used to provide constant head pressure and was connected to a 6-port valve which was operated manually. A 0.2 ml sample loop, made from treated stainless steel, was fitted to the valve in a configuration to allow sample filling in one position and sample injection in the other. During sample filling, the standard gas mixture flowed through the valve and the sample loop for a minimum of five minutes. During injection, the carrier gas flowed through the sample loop

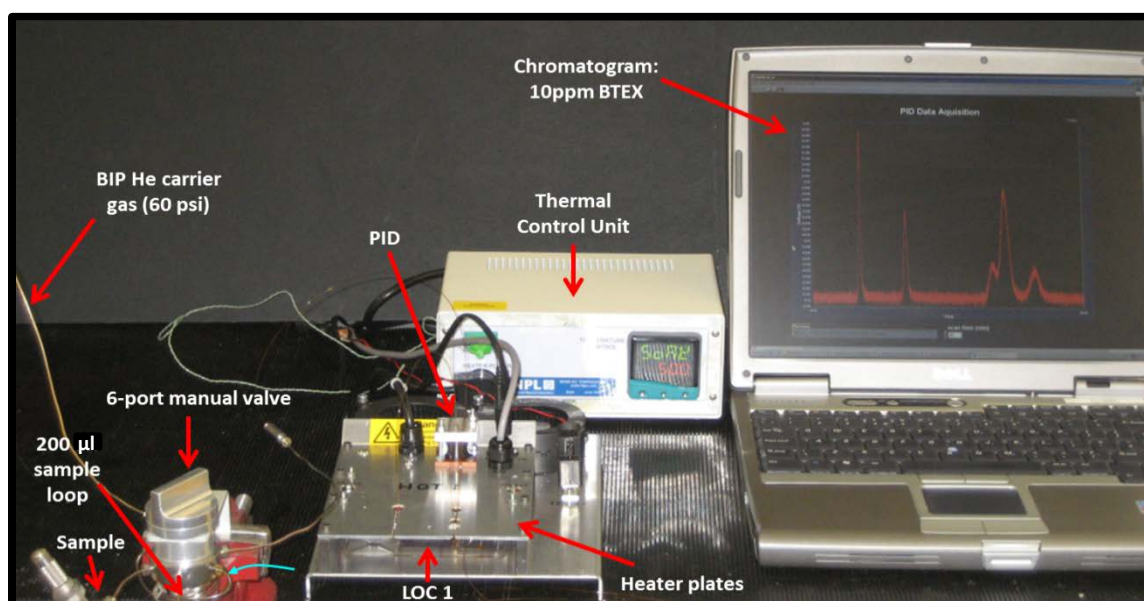


Figure 109: Photo (provided by NPL) of the heating and data acquisition set-up applied for performance testing of the primary column of LOC 1 with the miniaturised PID

for a short time to direct the sample onto the chromatographic column. The duration of the injection was selected to ensure all gas in the loop was flushed onto the column, but was limited to prevent peak tailing from compound desorption from metal surfaces. The 6-port valve was connected to the inlet of the chip by an approximate 10 cm length of 1/16" Silcosteel tube and an approximate 20 cm length of 0.32 mm inner diameter fused silica capillary connected by a reducing union.

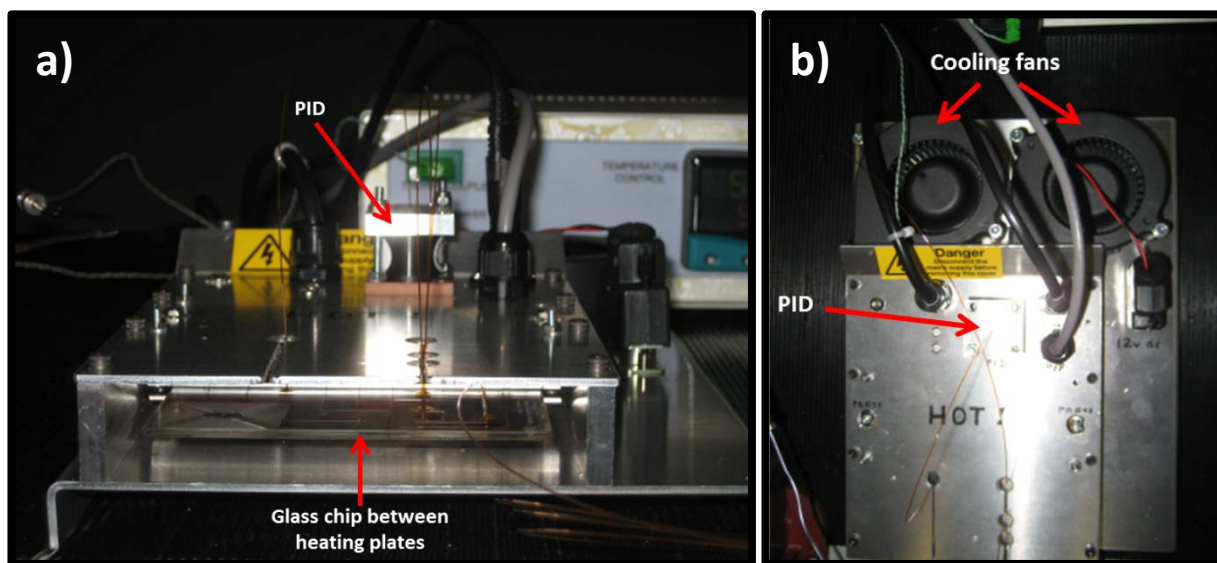


Figure 110: a) The side view and b) the over-head view of the testing set-up for LOC 1

The eluent from the 7.5 m long primary column was connected to the PID by 0.32 mm I.D. uncoated fused silica capillary. The detector was integrated into the unit and to a data acquisition system. The carrier gas head pressure was set to 3 bar providing a column flow of 12 ml·min⁻¹. The value deviates from theoretical calculations due to the presence of the 50 µm pinch point regions before and after the etched injector. A 1:5 split was introduced at the column outlet in order to prevent detector saturation. As a consequence, the flow rate arriving at the PID was measured to be 1.8 ml·min⁻¹.

The 10 ppm BTEX standard gas mixture previously run on the chip in the Agilent GC was injected onto the column at a starting temperature of 10 °C using the manual gas sampling valve. A temperature ramp of 20 °C·min⁻¹ up to 100 °C was applied. Chromatographic separation was sufficient to resolve o-xylene in approximately 225 s. The high PID response of aromatic compounds

ensured a good signal to noise ratio. The chromatogram generated (Figure 111) shows good peak shapes and height from the injection of approximately 1.5 ng of each compound. The detection limit with the PID was estimated to be ~ 100 pg for benzene.

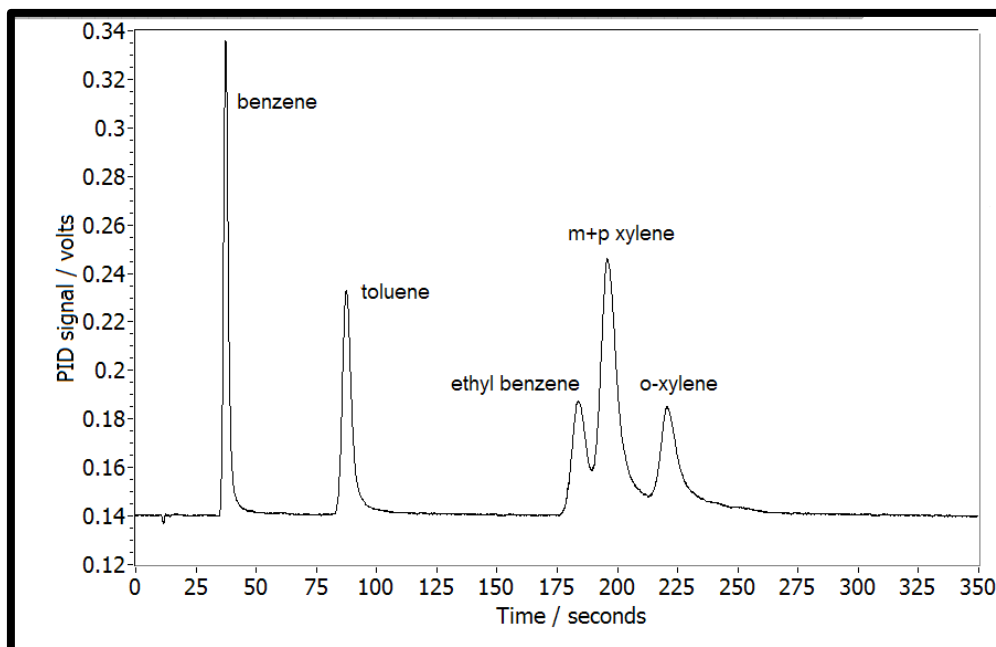


Figure 111: Response of PID to injection of the BTEX standard mixture with a 0.2 ml sample loop, run on LOC 1

8.2 LOC 2

The method detailed for LOC 1 was the initial one applied to LOC 2 to see if a similar separation of BTEX could be achieved with the more complicated chip containing interconnected channels. This was done using the heating set-up described above. The resulting Figure 112 is shown below. This was the first and only time LOC 2 was used on this set-up, and all other experimentation was conducted using the in-house built GC manifold described in the previous chapter. Figure 113 is an example of the result achieved after some method optimisation.

Method development determined that increasing the flow rate resulted in enhanced chromatograms, as seen in Figure 114 a) - c), which show results achieved with a 0.25 ml sample loop, a temperature program of 30-100 °C ramping at 20 °C·min⁻¹ and a) a flow rate of 1.5 ml·min⁻¹, b) a flow rate of 10

ml·min⁻¹ and c) a flow rate of 15 ml·min⁻¹. Figure 114 c) shows a very fast separation, with all compounds eluting in about 120 seconds.

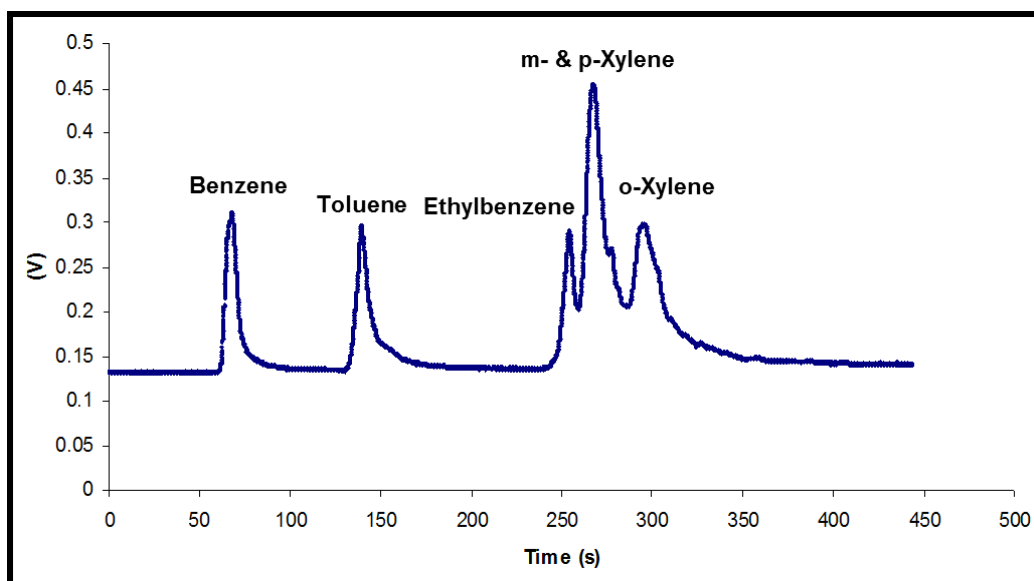


Figure 112: The separation of BTEX on LOC 2 achieved using the method detailed for LOC 1 but in the in-house built GC manifold with photoionization detection

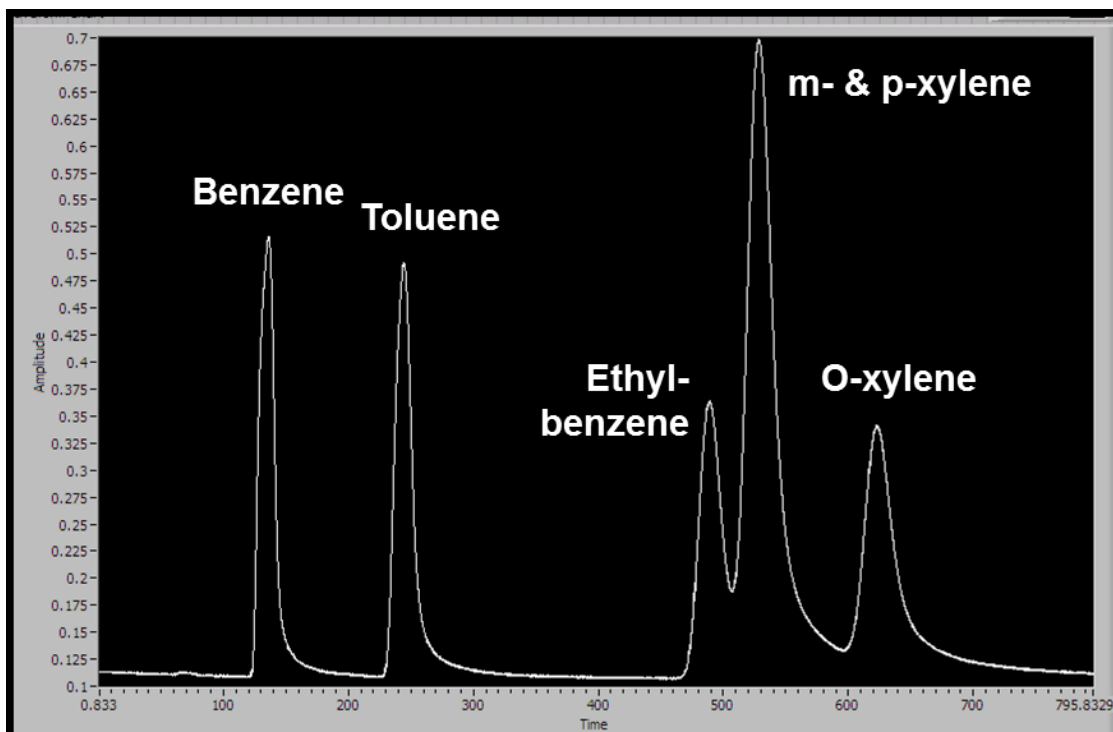


Figure 113: The separation of BTEX, achieved using LOC 2 in the in-house built GC manifold with photoionization detection. A 0.25 ml sample loop was used, helium carrier gas, a flow rate of 1.5 ml·min⁻¹, and a temperature program of 20-100 °C at 20 °C·min⁻¹

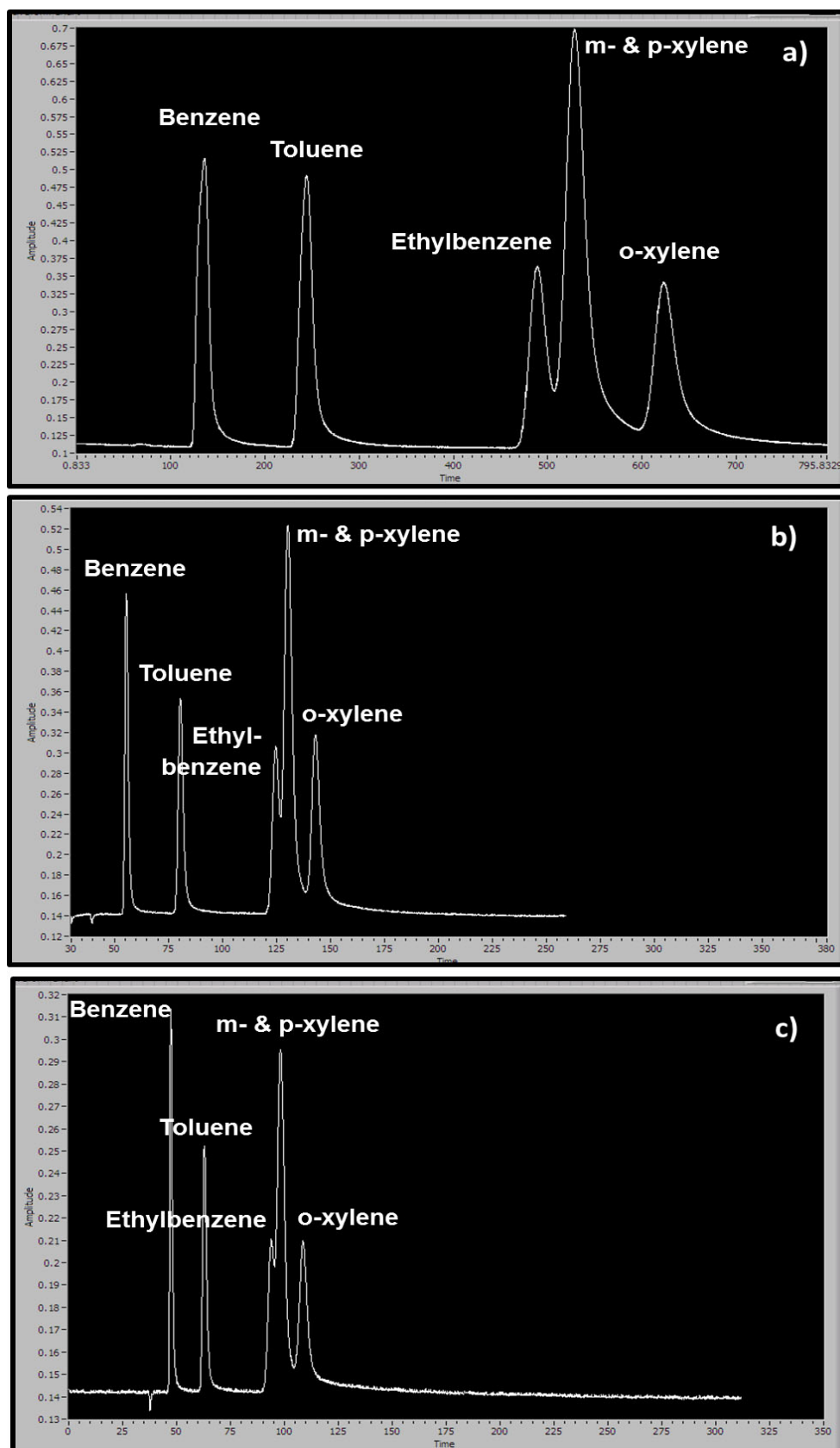


Figure 114: The separation of a 10 ppm BTEX gas mixture on the in-house built GC manifold, achieved using a 0.25 ml sample loop and a temperature program of 30-100 °C ramping at 20 °C·min⁻¹, with a flow rate of a) 1.5 ml·min⁻¹, b) 10 ml·min⁻¹, and c) 15 ml·min⁻¹

Improvement in resolution and analysis time were also seen when the starting temperature was lowered, as illustrated in Figure 115 a), b) and c) which shows the separation of petrol in helium carrier gas, with a ramp of $10\text{ }^{\circ}\text{C}\cdot\text{min}^{-1}$ and a starting temperature of a) $30\text{ }^{\circ}\text{C}$, b) $10\text{ }^{\circ}\text{C}$, and c) $3\text{ }^{\circ}\text{C}$. The lower temperatures resulted in enhanced separation of the highly volatile $\text{C}_5 - \text{C}_8$ fraction of the complex hydrocarbon sample.

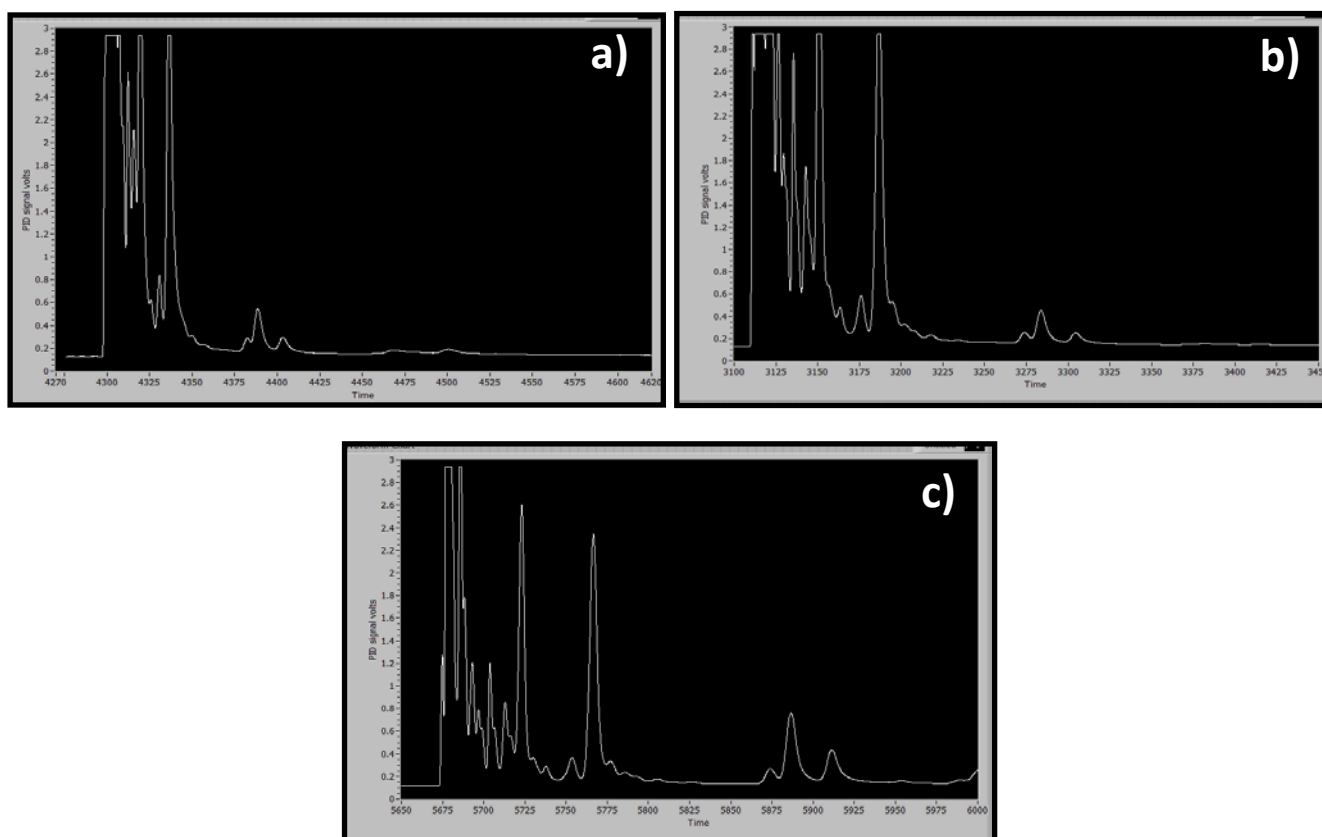


Figure 115: The separation of petrol on the stand-alone LOC system with a temperature ramp of $10\text{ }^{\circ}\text{C}\cdot\text{min}^{-1}$ and a starting temperature of a) $30\text{ }^{\circ}\text{C}$, b) $10\text{ }^{\circ}\text{C}$, and c) $3\text{ }^{\circ}\text{C}$

Experimentation using hydrogen and air as carrier gas were also conducted, and the results are shown in Figure 116. The first two chromatograms are of petrol in 116 a) hydrogen carrier gas at 12 psi, with a temperature program starting at $3\text{ }^{\circ}\text{C}$, ramping at $10\text{ }^{\circ}\text{C}\cdot\text{min}^{-1}$, and 116 b) air carrier at a pressure of 22 psi, with a starting temperature of $30\text{ }^{\circ}\text{C}$, ramping at $10\text{ }^{\circ}\text{C}\cdot\text{min}^{-1}$. Figure 117 is of a BTEX gas sample in air carrier gas at 22 psi, starting at $10\text{ }^{\circ}\text{C}$ and ramping at $10\text{ }^{\circ}\text{C}\cdot\text{min}^{-1}$.

While hydrogen carrier gas produced improved chromatograms as expected, chromatograms produced using air as carrier gas were nowhere near as resolved or separated as those achieved using either helium or hydrogen, but basic separation was still accomplished. Air was evaluated as carrier gas for the reasons outlined previously, with the major benefit being the elimination of the need for tanks of compressed gas, thus reducing the size and weight of the final portable instrument.

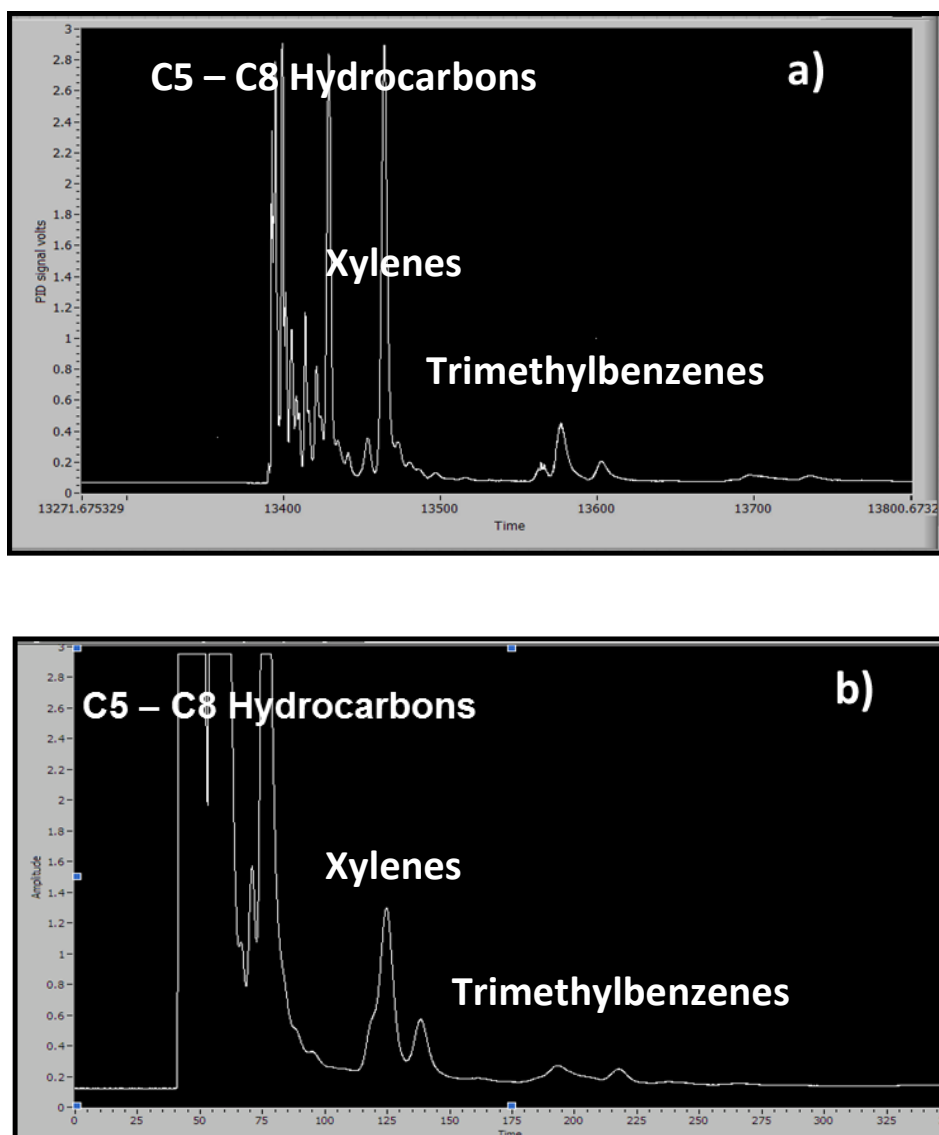


Figure 116: The separation of petrol in a) hydrogen carrier gas at 12 psi, with a temperature program starting at 3 °C, ramping at 10 °C·min⁻¹ and b) air carrier at a pressure of 22 psi, with a starting temperature of 30 °C, ramping at 10 °C·min⁻¹

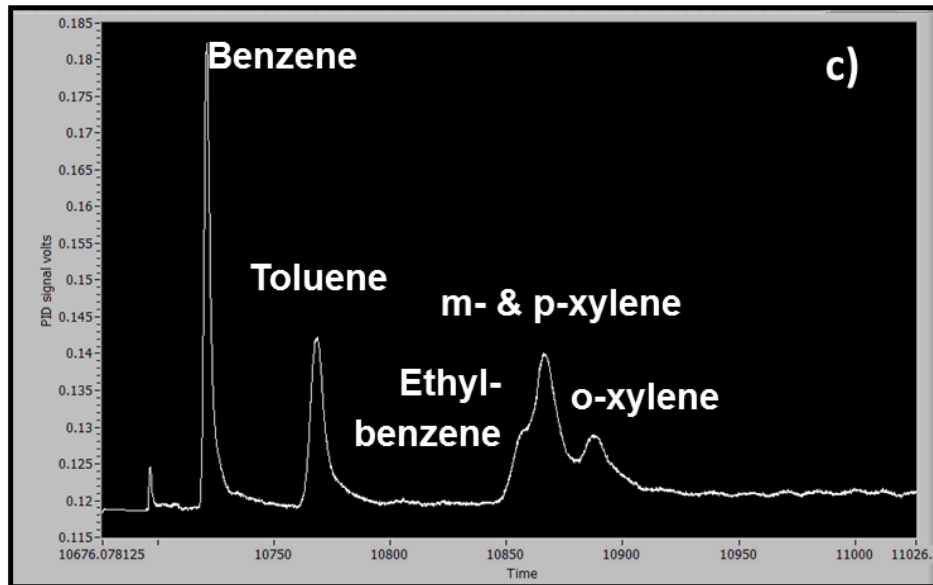


Figure 117: The separation of a BTEX gas sample in air carrier gas at 22 psi, starting at 10 °C and ramping at 10 °C·min⁻¹

9.0 Experimental –Two-Dimensional GCxGC

Based on the success of the one-dimensional experimentation, it was decided to coat the secondary column of the glass chips and work towards the optimisation of lab-on-a-chip two-dimensional GCxGC.

9.1 Initial Attempts at Stand-Alone GCxGC-PID

Previously LOC 2 had only the primary 7.5 m long column coated with a 1.25 μm thick film of non-polar 100%-dimethylpolysiloxane stationary phase (OV-101). The secondary 1.4 m long column had no coating applied. In order to achieve 2-dimensional separation the secondary column was coated as described below.

9.1.1 Dynamic Coating of Secondary Column

Initial coating of the secondary column was via the faster, easier dynamic method with a 20% v/v solution of OV-17 (50%-phenyl-50%-methylpolysiloxane). Subsequently, the chip was installed in the GC manifold and was used to achieve a 2-dimensional separation via the on-chip fluidic

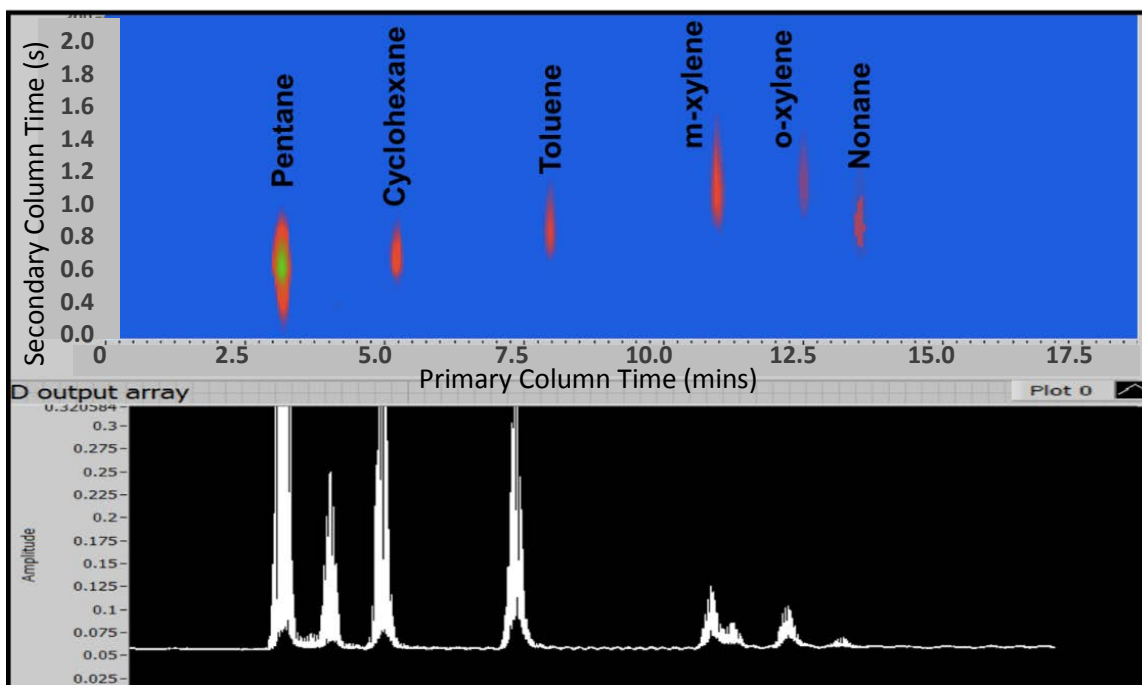


Figure 118: An example of the initial “2D” separation achieved with the fully coated LOC chip in the in-house-built manifold and the PID. Individual peaks have been rescaled to give common peak maxima intensity

differential flow modulator. A 6-port automatic injection valve was used fitted, with a 0.25 ml sample loop made from treated stainless steel. The valve was connected to the chip's edge connector by a short length of peek tubing. The eluent emerging from the 1.4 m secondary column was connected to the PID by a 0.25 mm inner diameter uncoated fused silica capillary. The carrier and modulator gas pressures were set to 15 psi and 14.5 psi respectively. The modulation period was set to 2 seconds, with filling set to 1.5 and flushing set to 0.5 seconds.

9.1.2 Two-Dimensional Performance Testing of LOC 2

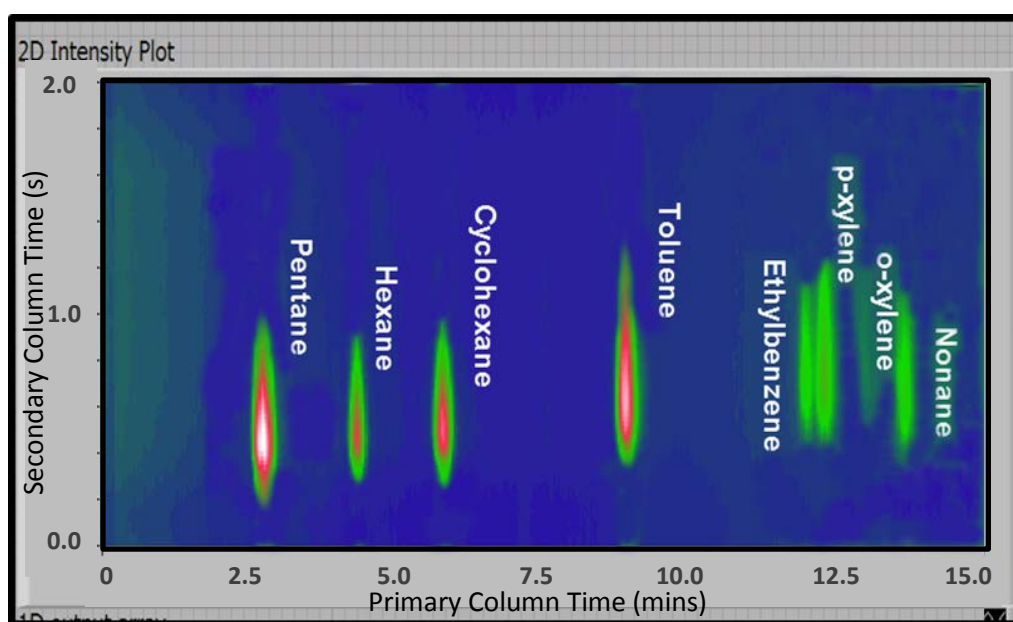


Figure 119: An 8 component 2D separation achieved with the stand-alone LOC GCxGC system

A gas mixture, comprising pentane, cyclohexane, toluene, p- and o-xylene, and nonane, was injected onto the column at a starting temperature of 30 °C. A temperature ramp of 20 °C·min⁻¹ up to 100 °C was applied. Figure 118 shows the result of the early experiment attempting 2D separation on the glass chip. Figure 119 shows the result of a slightly more complicated mixture.

9.1.3 Static Coating of Both Columns

Due to the lack of separation in the second dimension, it was decided to statically coat both the primary and secondary columns of a blank LOC 2 chip with a 2% v/v solution of OV-101 in pentane and OV-17, respectively.

The secondary column was coated by blocking the preconcentrator packing hole, as well as the first, second and third inlet holes. The detector port hole was left open and the stationary phase solution was introduced through the fourth inlet hole. Once filled, the detector port was blocked, as was the preconcentrator hole and the first and fourth inlet holes. A 2 %v/v solution of OV-101 in pentane was then injected onto the primary column through the second inlet, with the third inlet being left open. This method resulted in there being no overlap or mixing of stationary phases on either of the columns.

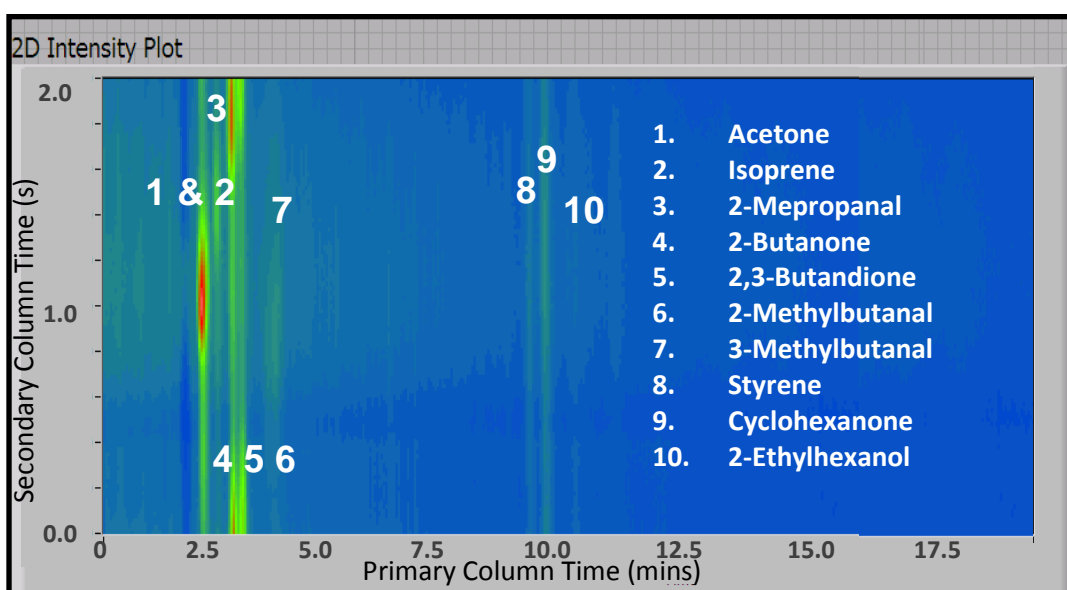


Figure 120: The separation of a 10 component oxygenated VOC mix on the stand-alone system using the LOC 2 chip with both columns statically coated

Once the stationary phase solutions had been introduced into the columns, the preconcentrator, modulator legs and collector were all washed out a number of times to ensure that no stationary phase remained in these sections. The chip was then placed inside the heated vacuum desiccator for solvent evaporation, before testing with gas mixes.

The temperature program was set to 20-120 °C at 10 °C·min⁻¹, with the secondary column temperature being set to 20 °C more than the primary. The carrier gas was set to 14.0 psi, and the modulator gas was set to 13.5 psi, with 5 second modulation. Unfortunately, while the PID was capable of giving good results, it was found to be prone to problems and detector response varied between the different PIDs used, making it difficult to replicate results. The

chromatograms shown below, for example, both of pentane, were achieved under the same conditions but with different PIDs.

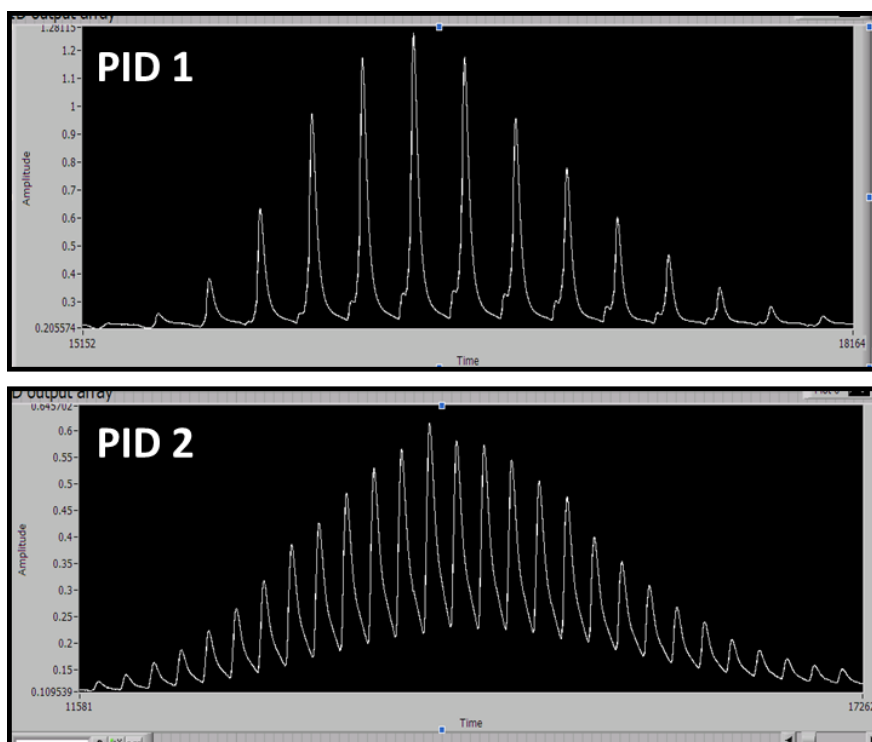


Figure 121: The modulated response of pentane using two different PIDs, but otherwise identical conditions

9.1.4 Introduction of Make-Up Gas

In order to determine if the presence of a make-up gas would improve or degrade chromatography, a 5 m x 0.25 mm deactivated fused silica capillary was superglued to the bottom of the PID, as shown in Figure 122. This was then connected to the make-up gas line. The length of the capillary was

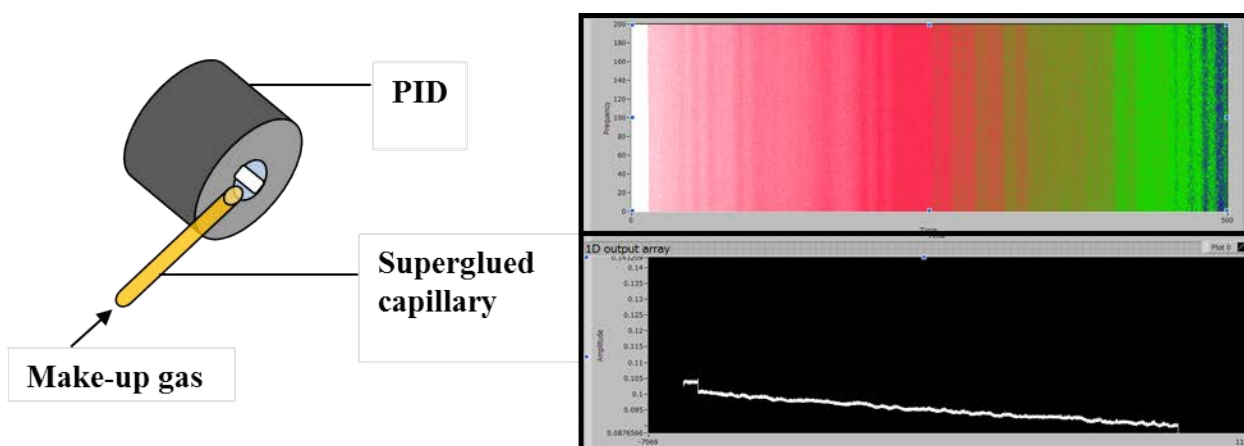


Figure 122: A schematic showing the set-up for PID make-up gas testing, and one of the resulting blank chromatograms

progressively shortened to adjust flow; however, it was found that with make-up gas flowing over the grid of the PID a blank chromatogram was achieved.

9.1.5 Improving PID Performance

Initially, the PID was positioned hovering just above the detector hole. A number of capillary-PID insertion methods were evaluated in an attempt to find the best set-up for PID detection, including an entirely sealed PID unit. This had the chip outlet capillary entering the PID through a small drilled hole behind the now sealed grid rather than through it, as illustrated in Figure 123. However, it was determined that simply having a short length of capillary sealed into the detector hole and inserted into the PID grid focused the eluting sample into the PID for detection.

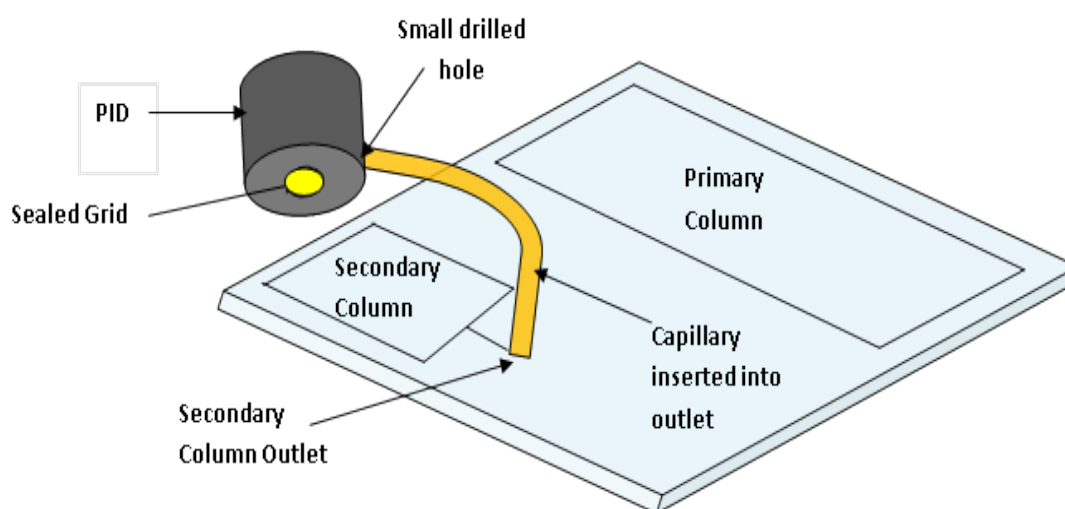


Figure 123: One of the many methods evaluated of transferring the eluate emerging from the secondary column into the PID

9.2 Stand-Alone GCxGC-Commercial FID

To determine how much of a limiting role the PID played, the glass lab-on-a-chip GC in its manifold was connected to the commercial FID of the Agilent 7890A GC system by means of an approximately 50 cm long unheated transfer line. A heated transfer line was first attempted by feeding the capillary through a length of stainless steel tubing and coiling heating tape around it, however, this resulted in the line being too heavy causing the capillary to break. A deactivated fused silica column was also connected from the Agilent GC's injector to the automatic injection valve of the lab-on-a-chip GC system allowing the Agilent GC to control the helium carrier gas. A number of gas

mixtures were run. The results of two are shown below. The FID chromatograms indicate improved detector response and peak widths. This suggest that the PID was a significant problem, and one that was limiting further progress in achieving 2D separation on the glass chip.

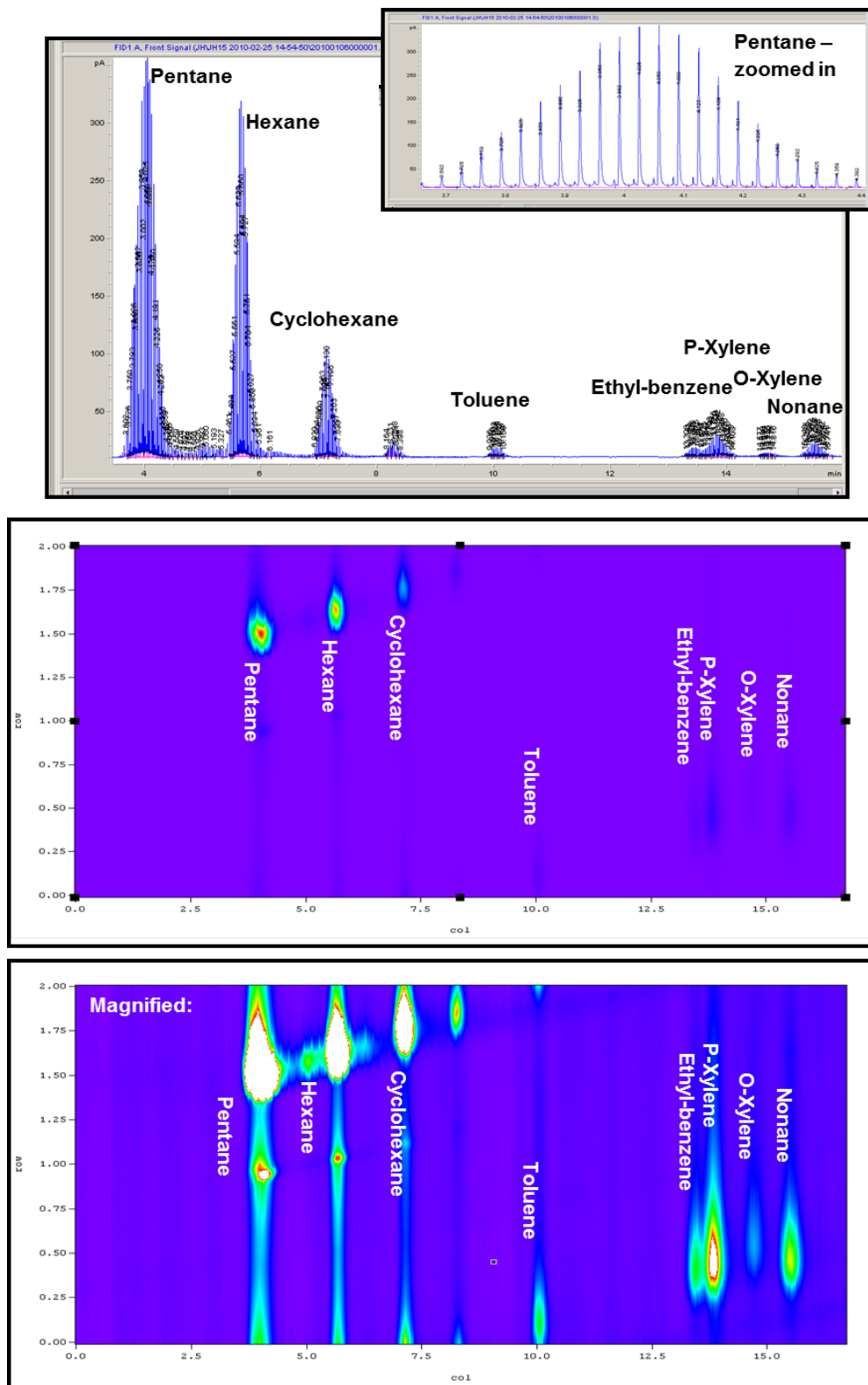


Figure 124: Separation of an 8 component mixture via the glass chip in the GC manifold with the FID of a commercial Agilent FID

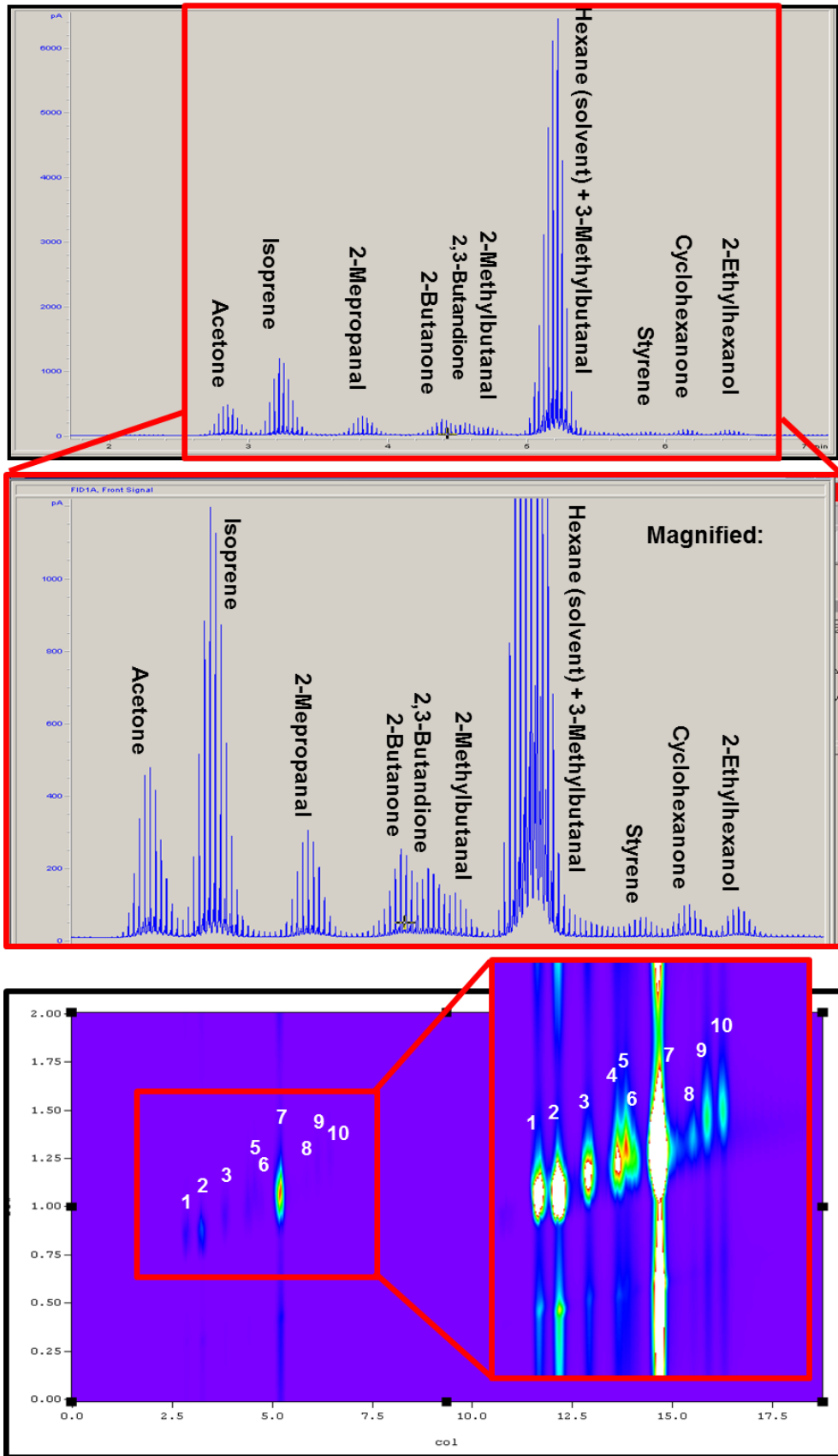


Figure 125: The results of the separation of a 10 component mixture via the glass chip in the GC manifold with the FID of a commercial Agilent FID

9.3 Benchtop GCxGC-FID

The final chip designed used for this project was LOC 4. The variable I.D. column dimensions of this chip were chosen based on the reasons outlined in Chapter 3. To summarise: flow modulated GCxGC conducted with a primary column I.D. that is larger than or equal to the secondary column I.D. can result in overloading of the second column. The result of this is reduced peak capacity in the second dimension. Since the amount of second dimension separation space is highly limited, any losses here (including those due to overloading) can seriously impair the performance of the system.

9.3.1 Static Coating of Both Columns

Static column coating was carried out as described for LOC 2, however, this time the shorter column with narrower I.D. (4 m x 0.18 mm) was coated with OV-101, while the longer, wider bore column (7.5 m x 0.25 mm) was coated with the more polar OV-17 phase. As before, the modulator, inlet and outlet channels were washed thoroughly before the chip was installed in the GC.

9.3.2 Two-Dimensional Performance Testing of LOC 4

To establish this chip's capabilities, it was first tested within the commercial Agilent 7890A GC instrument, and results were, again, obtained using Chemstation and 2D imaging software. Modulation was achieved using a diaphragm valve, which operates in a similar manner to the differential flow channels built into the chip, i.e. flow from the primary column is diverted to the secondary at regular intervals using the fast switching valve, with no sample being vented to waste.

The pressure parameters chosen for initial experimentation were those suggested by the concurrent work on LOC 2 in the stand-alone manifold at the time. Thus, high pressures of 75 psi and 70 psi for the primary and secondary columns, respectively, were used as a starting point for 2D optimisation. On running the following 12 component mixture, the result shown in Figure 126 was achieved:

1. Pentane
2. 2-Methylpentane
3. Isobutyraldehyde
4. Hexane
5. Propan-2-ol
6. 2-Methylbutyraldehyde
7. 2-Pentanone
8. Toluene

- | | |
|--------------------|------------------|
| 9. Ethylbenzene | 11. Ethyltoluene |
| 10. 3-Methyloctane | 12. Nonane. |

Operating conditions were as follows:

- **Injection volume:** 2 μ l
- **Inlet mode:** Split (50:1)
- **Inlet temperature:** 250°C
- **FID temperature:** 300°C

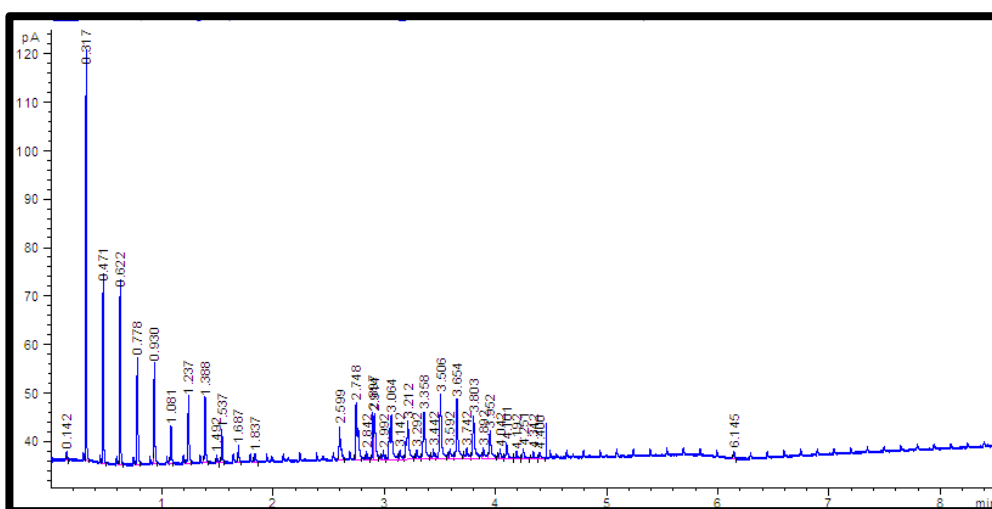
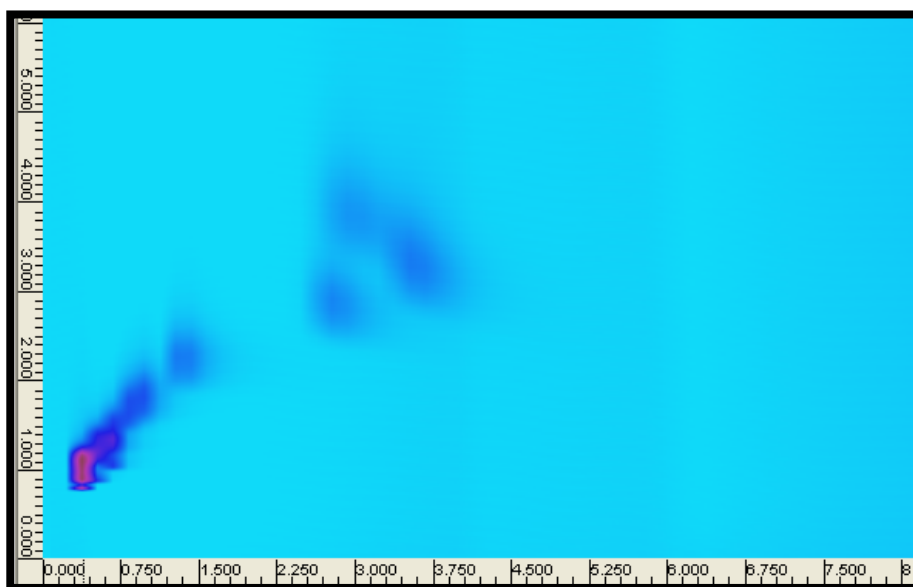
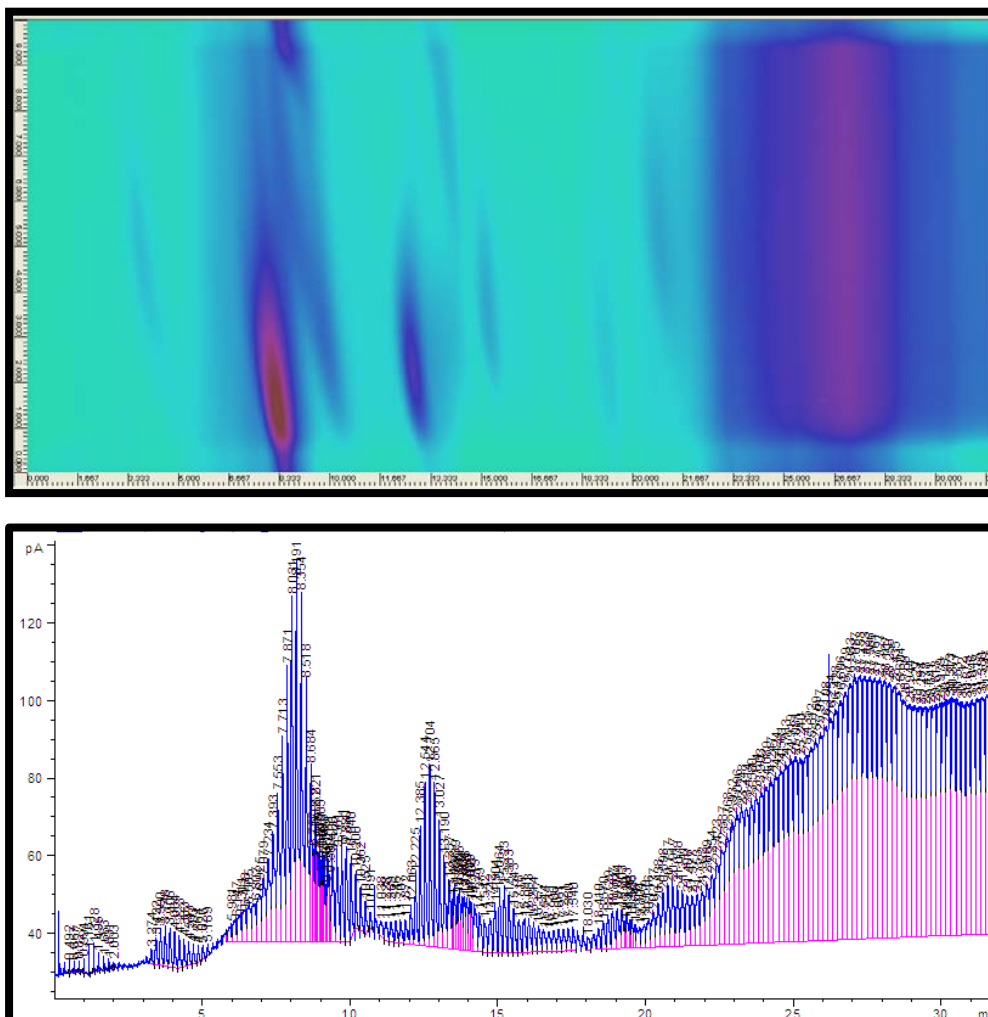


Figure 126: The separation of a 12 component mixture run on LOC 4 within a commercial GC with FID detection

Lavender oil was also run with approximately 10 peaks out of the 27 components that make the mixture up being visible.



9.3.2.1 Pressure Determinations

The aim was to lower the operating pressures of the column to minimise leaks, and it was experimentally found that a pressure difference of -15 and +10 psi gave the best results, with a primary column pressure of 75 psi and a secondary column pressure of 60 psi (Figure 128) and a primary column pressure of 25 psi and a secondary column pressure of 35 psi (Figure 129) performing best. As achieving lower pressures was the aim, it was decided to continue method development with the latter set of pressures.

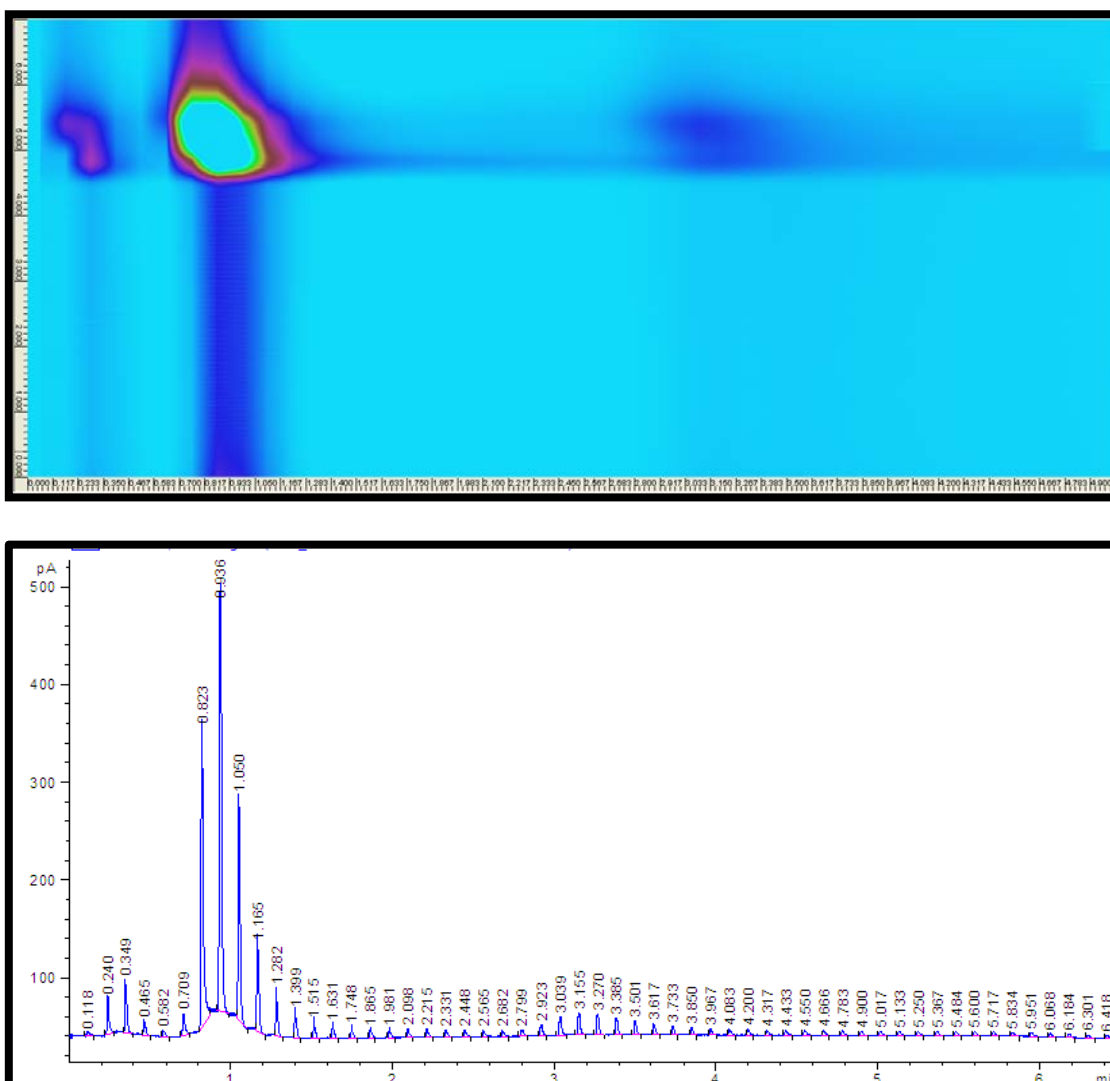


Figure 128: The separation of isobutyraldehyde, hexane, 2-pentanone, and nonane with a primary column pressure of 75 psi and a secondary column pressure of 60 psi

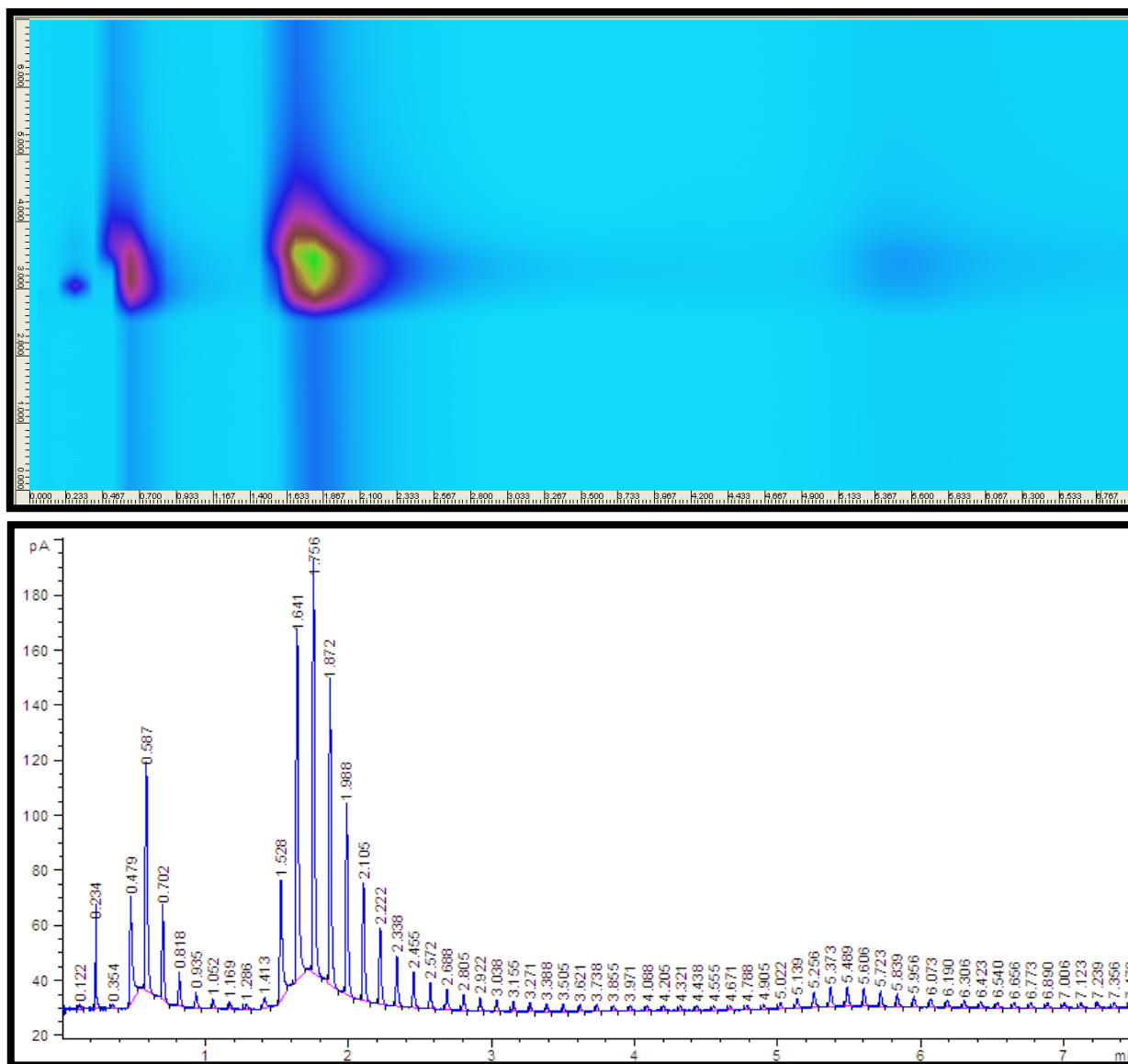


Figure 129: The separation of isobutyraldehyde, hexane, 2-pentanone, and nonane with a primary column pressure of 25 psi and a secondary column pressure of 35 psi

9.3.2.2 Temperature Determinations

Starting temperature was next evaluated, with a starting temperature of 30 °C found to be ideal. Whilst, a start at 25 °C did produce slightly better looking chromatograms, the length of time it took for the GC oven to cool to that temperature did not make the improvement achieved worthwhile.

Subsequently, the temperature ramp was examined, running with ramps of 1, 2, 5, 10, 15, 20, 25 and 30 °C·min⁻¹, all with an initial hold time of 1 minute. Experimentally, it was concluded that a ramp of 5 °C gave the better result.

9.3.2.3 Starting Hold Time Determinations

Starting hold times were next looked into, with runs starting at 30 °C with initial hold times of 0.2 min, 0.5 min, 1.0 min, and 2.0 min. An isothermal run at 30 °C was also performed, as was a gradient run with no initial hold time. Overall, it was decided that a hold of 1.0 min was preferential.

9.3.2.4 Split Ratio Determinations

The split ratio was the next parameter to be adjusted. The above chromatograms were achieved with a 50:1 split. It was not possible to increase the split above a ratio of 240:1 as the GC would report that the front inlet flow was limited. As such, it was experimentally found that the best result that could be attained within the limited available split range was 220:1.

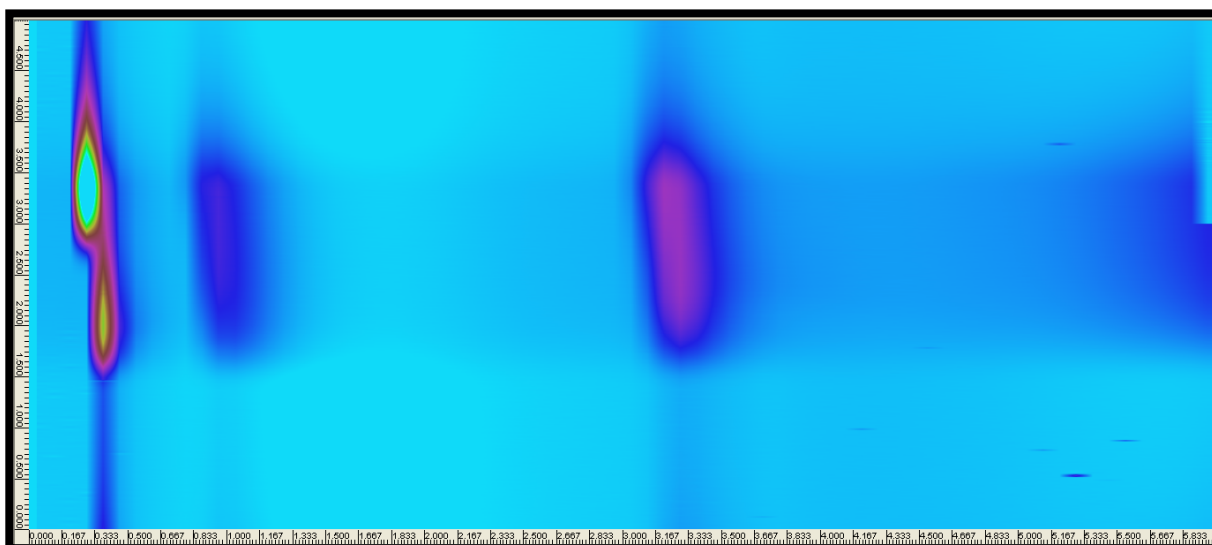


Figure 130: The separation achieved with a 220:1 split ratio

Thus, at this point, the overall method had a starting temperature of 30 °C, holding for 1 minute before ramping at a rate of 5 °C·min⁻¹ to 160 °C. The primary column pressure was 25 psi, whilst the secondary column pressure was set at 35 psi. A split of 220:1 was used.

9.3.2.5 Modulation Time Determinations

Modulation was the final parameter to be developed, with runs taking place with overall modulation times ranging from 1 to 11 seconds, and differing modulation ratios between filling and flushing. The above chromatograms were achieved with a modulation ratio of 3:2 seconds filling:flushing time. It

was found experimentally that a number of different ratios resulted in what can be considered good separation, with ratios of 2.5:2.5, 3.0:2.0, and 4.0:5.0 being selected as best. Overall, the modulation ratio of 4.0:5.0 provided the most separation/selectivity between isobutyraldehyde and hexane and so was selected for the final method.

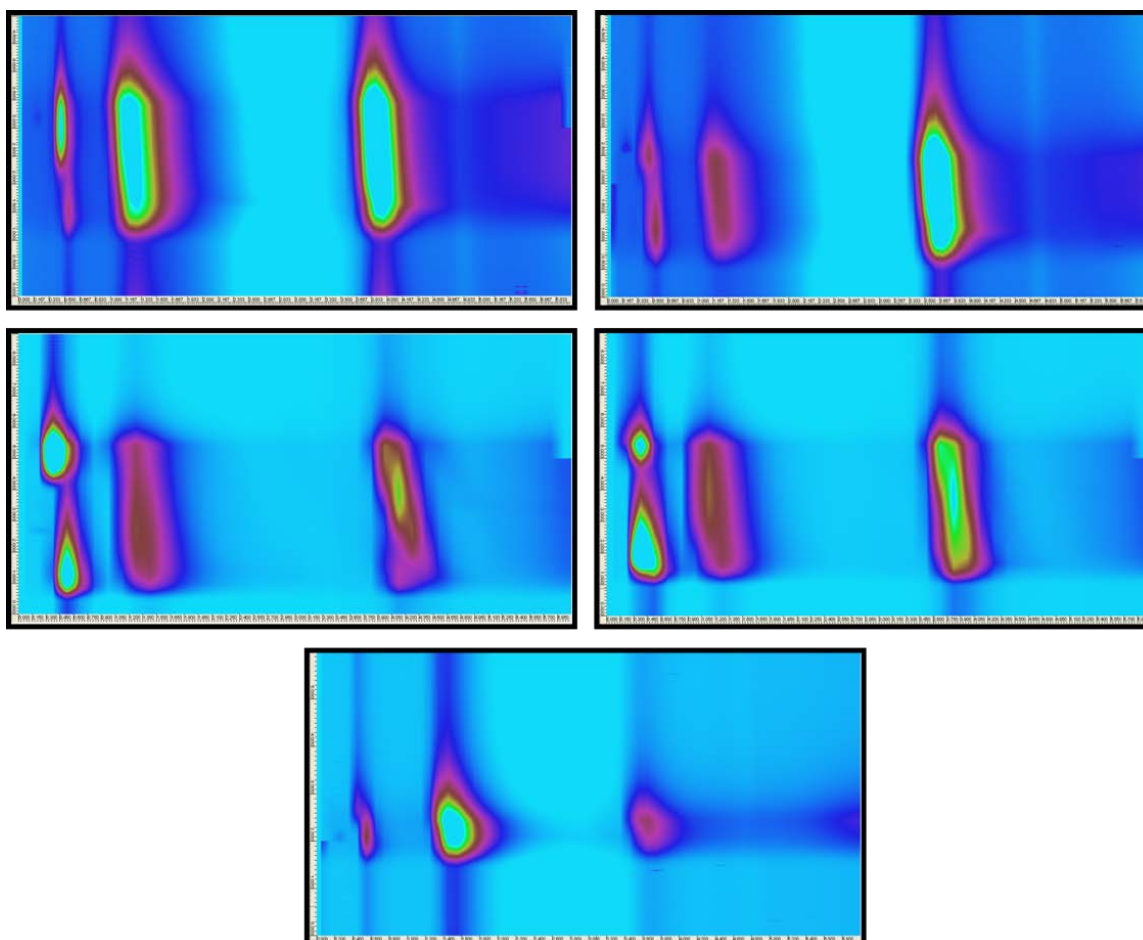


Figure 131: Separation achieved with a modulation ratio of a) 2.5:2.5; b) 3.0:2.0; c) 4.0:5.0; d) 4.5:4.5; and e) 5.0:1.0

9.3.2.6 Complex Mixtures

The following 7 component mixture was then prepared and run on the system, with the result being shown in Figure 132:

- | | |
|--------------------------|--------------------------|
| 1. Pentane | 5. 2-Methylbutyraldehyde |
| 2. 2-Butanone | 6. Ethylbenzene |
| 3. Hexane | 7. Nonane. |
| 4. 3-Methylbutyraldehyde | |

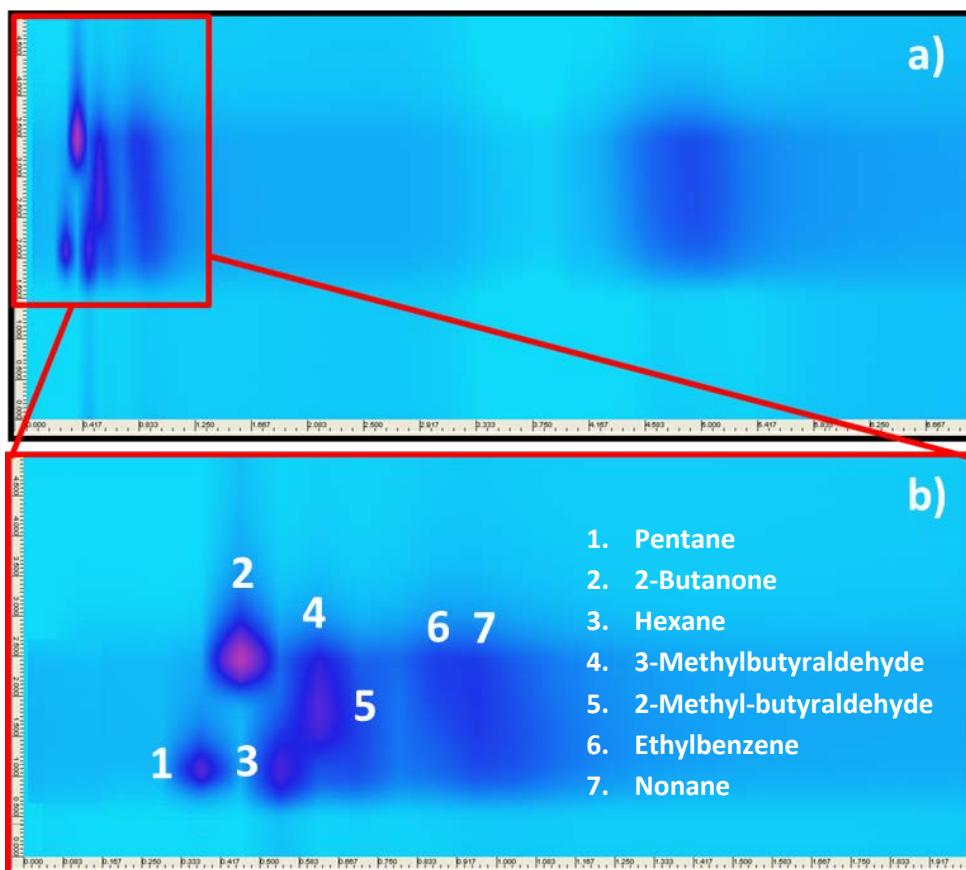


Figure 132: a) The separation of a 7 component mixture using the final method developed as described above; and b) Magnification to better show the two-dimensional separation achieved

This was followed by separation of a 9 component mixture of:

- | | |
|--------------------------|--------------------|
| 1. 2-Methylpentane | 6. Ethylbenzene |
| 2. Hexane | 7. 3-Methyloctane |
| 3. Propan-2-ol | 8. Nonane |
| 4. 2-Methylbutyraldehyde | 9. 3-Ethyltoluene. |
| 5. 2-Pentanone | |

Each component was added one at a time starting with 3-ethyltoluene, which has the highest boiling point. This technique initially worked well to allow for peak identification, with the peaks from 3-ethyltoluene to 2-methylbutyraldehyde being seen in Figure 133 a). However, with the addition of propan-2-ol, two peaks instead of one were seen, and no further peaks were visible despite the addition of hexane and 2-methylpentane.

Numerous repeat runs at the same and varying parameters did not alter this. Soon afterwards, an FID interconnect failure was experienced. This led to the replacement of the part. The same 14 component mixture was rerun under the

same conditions as before. The results suggested that the deteriorating interconnect had been affecting the chromatography for some time.

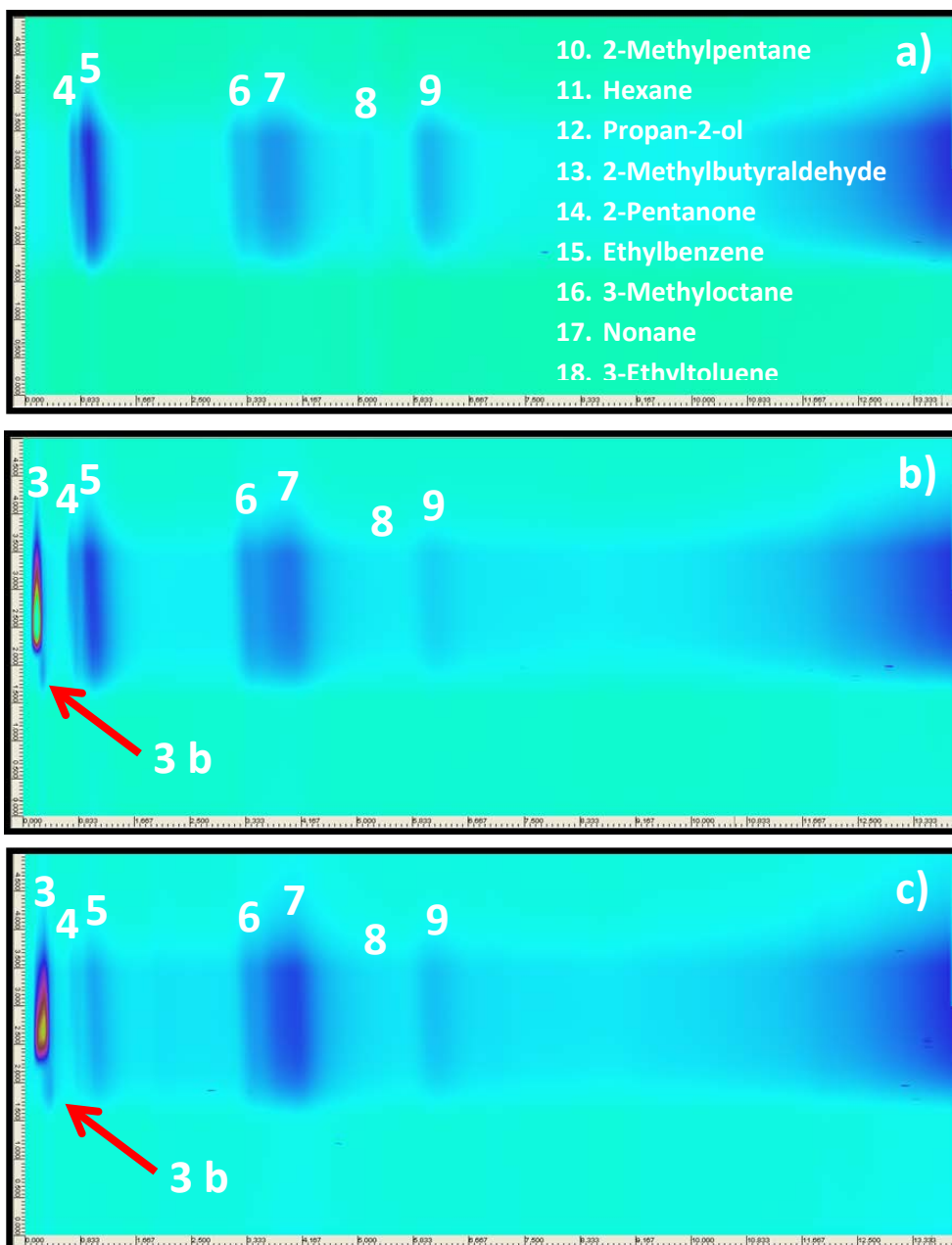


Figure 133: a) The separation of 3-ethyltoluene to 2-methylbutyraldehyde ; b) the addition of propan-2-ol resulting in two peaks; c) No further peaks seen despite the addition of hexane and 2-methylpentane

9.3.3 New FID Interconnect

The installation of the new interconnect brought with it a significant improvement in chromatographic performance – or rather an improvement in the reporting of the chromatographic performance of the coated glass chip.

This time, to prevent any over complication of experimentation, it was decided to start GCxGC method development using just one early eluting compound. Pentane was chosen. The following work was performed with a split ratio of 220:1 (1,151.7 ml·min⁻¹) and a modulation ratio of 3:2 s, with the GC oven operating isothermally at 30 °C.

9.3.3.1 Pressure and Modulation Ratio Method Development

Pressure was the first parameter to be tackled during this 2D GC method development process. As previously it had been noted that reasonable separation could be achieved with a “low” pressure ratio of 25:35 psi, development took place to see if these pressures could be reduced even further. A very comprehensive look at pressure and primary:secondary column pressure ratio was conducted, with small changes of both plus and

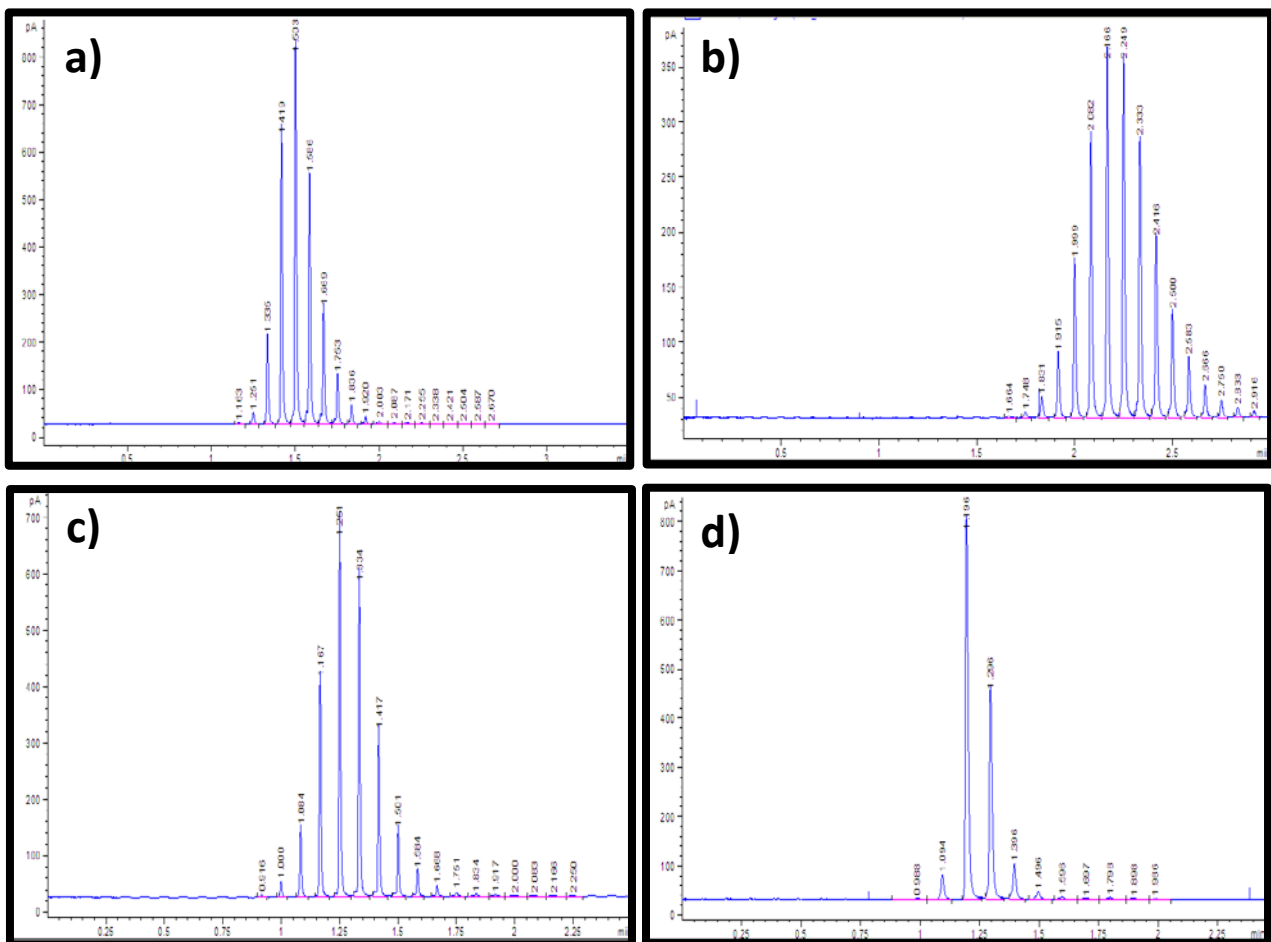


Figure 134: A modulated pentane peak. a) Pressure ratio = 11.0:19.6, Modulation ratio = 3.0:2.0; b) Pressure ratio = 10.5:20.0, Modulation ratio = 3.0:2.0; c) Pressure ratio = 16.4:30.0, Modulation ratio = 3.0:2.0; d) Pressure ratio = 10.5:20.0, Modulation ratio = 4.0:2.0

minus 0.5 psi being made. It was noted that a pressure build up within the chip would occur if the primary column ratio was above a pressure of 35 psi, and no peaks would be seen at all. The three best pressure ratios discovered were then further broken down into 0.1 psi increments to get the best possible results.

The primary:secondary column pressure combinations that resulted in the most improvement were determined to be 11.0:19.6 psi, 10.5:20.0 psi, and 16.4:30.0 psi.

Next, modulation ratio was examined in closer detail, looking at ratios where the flush time was either plus or minus 1 second that of the fill time over a range of 1-10 seconds total modulation time. This was done at each of the above three best pressures. The 3.0:2.0 s fill:flush ratio was found to give the best modulation.

9.3.3.2 Complex Mixtures

Next diesel, kerosene and lavender oil were injected onto the system. Primary column pressure was set at 16.4 psi, secondary column pressure was at 30 psi, the modulation ratio was 3:2, and the split ratio was 220:1. A starting temperature of 30 °C was used, with a 1 min hold time before ramping at a rate of 5 °C per minute to 160 °C. The results of each analysis are shown in Figure 135.

A 1 µl injection of the 12 component mixture previously used to generate Figure 128 was then run on the system, to evaluate the effect of the different primary and secondary column pressures deemed best during the pentane tests.

Again the split ratio was set to 220:1, and a temperature program of 30-160 °C was used, with 1 min hold time and a 5 °C·min⁻¹ ramp rate. Figure 136 a), b), and c) show the best results achieved. In comparison to Figure 128, all 3 chromatograms boast improved separation in the second dimension.

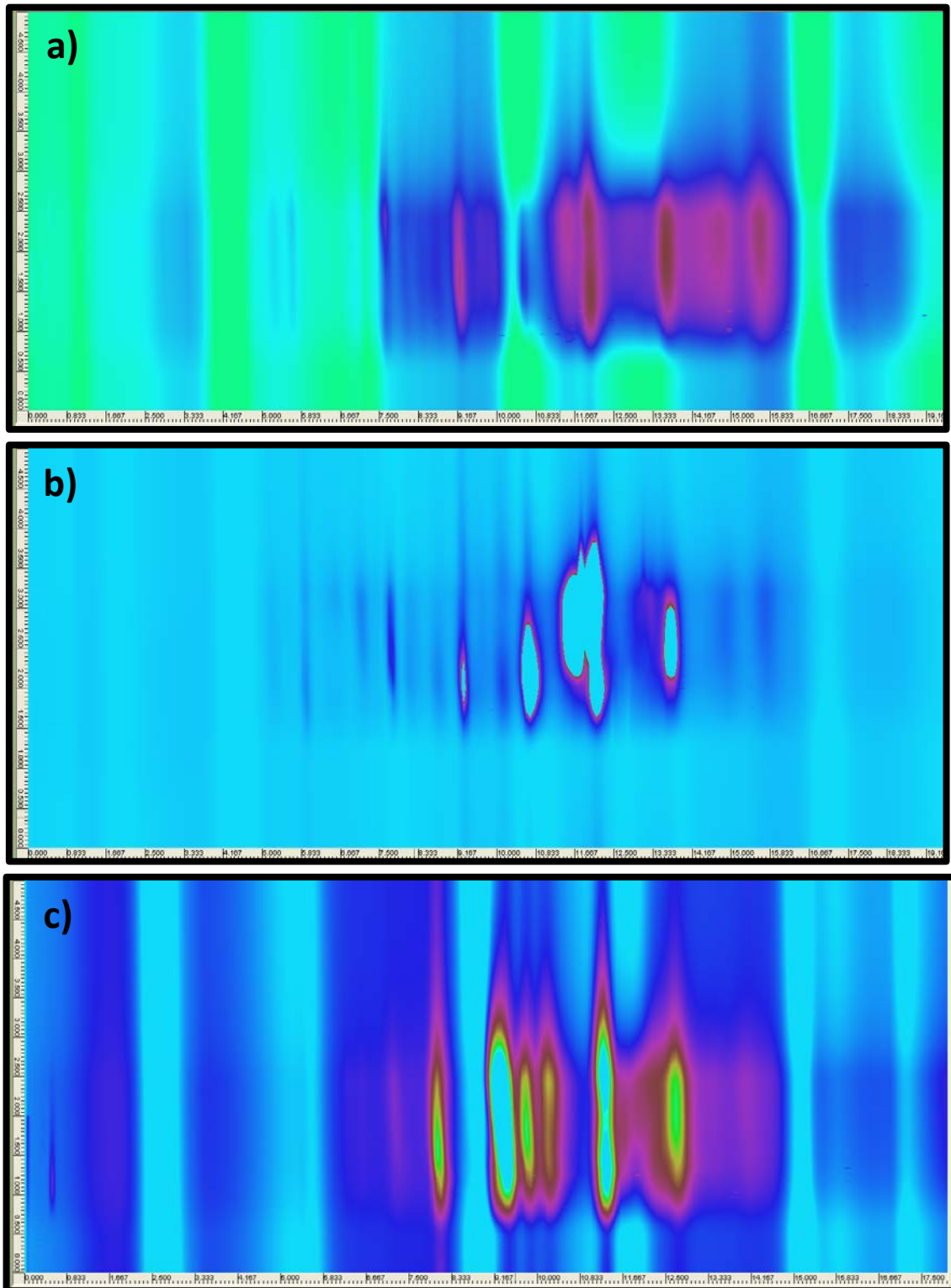


Figure 135: The separation of a) diesel; b) kerosene; c) lavender oil

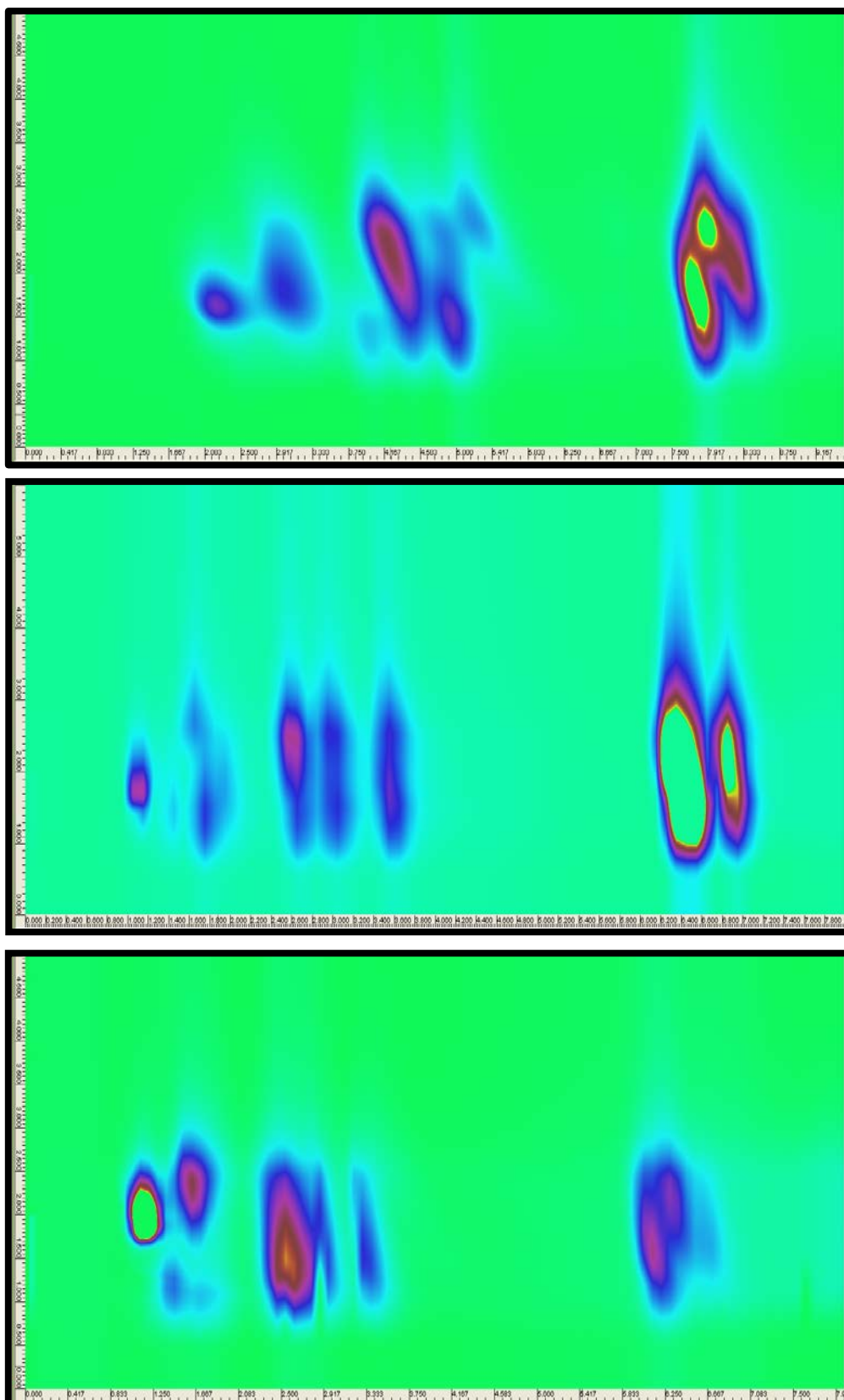


Figure 136: 1. pentane, 2. 2-methylpentane, 3. isobutyraldehyde, 4. hexane, 5. propan-2-ol, 6. 2-methylbutyraldehyde, 7. 2-pentanone, 8. toluene, 9. ethylbenzene, 10. 3-methyloctane, 11. ethyltoluene, 12. nonane. a) Pressure ratio = 10.5:20 psi, Modulation ratio = 3:2 s; b) Pressure ratio = 10.5:20 psi, Modulation ratio = 4:2 s; c) Pressure ratio = 16.4:30, Modulation ratio = 3:2

The coated chip was then tested with the following 16 component mixture, again at varying pressure ratios:

- | | |
|---------------------|----------------------------|
| 1. Pentane | 9. 2-methylbutyraldehyde |
| 2. 2-butanone | 10. Propyl acetate |
| 3. Isobutyraldehyde | 11. 3-Methyl-3-buten-2-one |
| 4. Hexane | 12. 2-Butenal |
| 5. Butanal | 13. 2-pentanone |
| 6. Ethyl acetate | 14. Ethylbenzene |
| 7. Cyclohexane | 15. 3-methyloctane |
| 8. Propan-2-ol | 16. Nonane. |

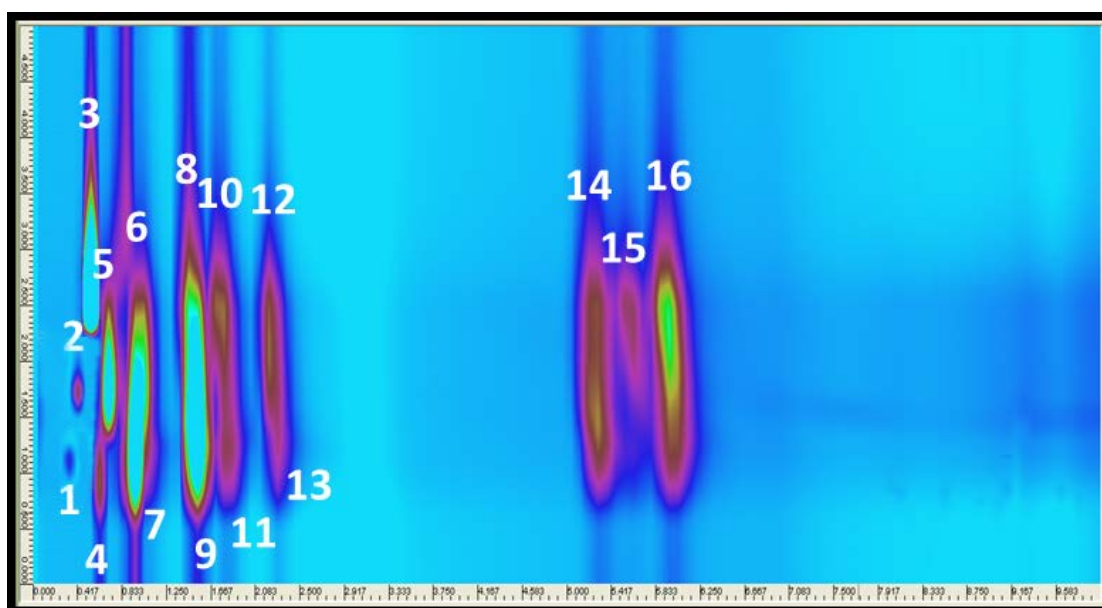


Figure 137: The separation of a 16 component mixture, with a pressure ratio of 16.4:30 psi and a modulation ratio of 3:2 s

Figure 137 shows the best separation achieved for this mixture, which was, again, run with a 220:1 split ratio and a 5 °C·min⁻¹ ramp from 30 °C to 160 °C.

9.4 Benchtop GC-FID

As the primary column of this chip was both shorter and had a narrower bore in comparison to the other chip designs investigated, the GC set-up was altered to allow for one-dimensional separation. The purpose of this experiment was to get an idea if the one-dimensional capabilities of LOC 4 in comparison to the previously evaluated chip designs. The following results were obtained:

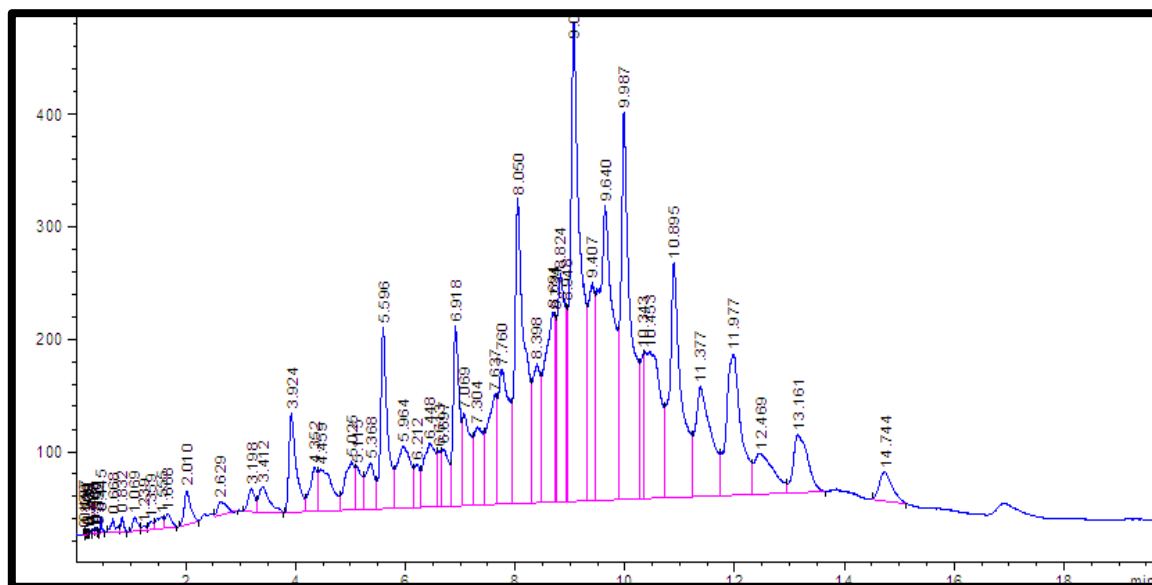


Figure 139: The one dimensional separation of diesel, achieved using only the 4 m x 1.8 mm primary column of the glass chip, with a split ratio of 220:1 and a temperature program of 30 °C to 160 °C at 5 °C·min⁻¹

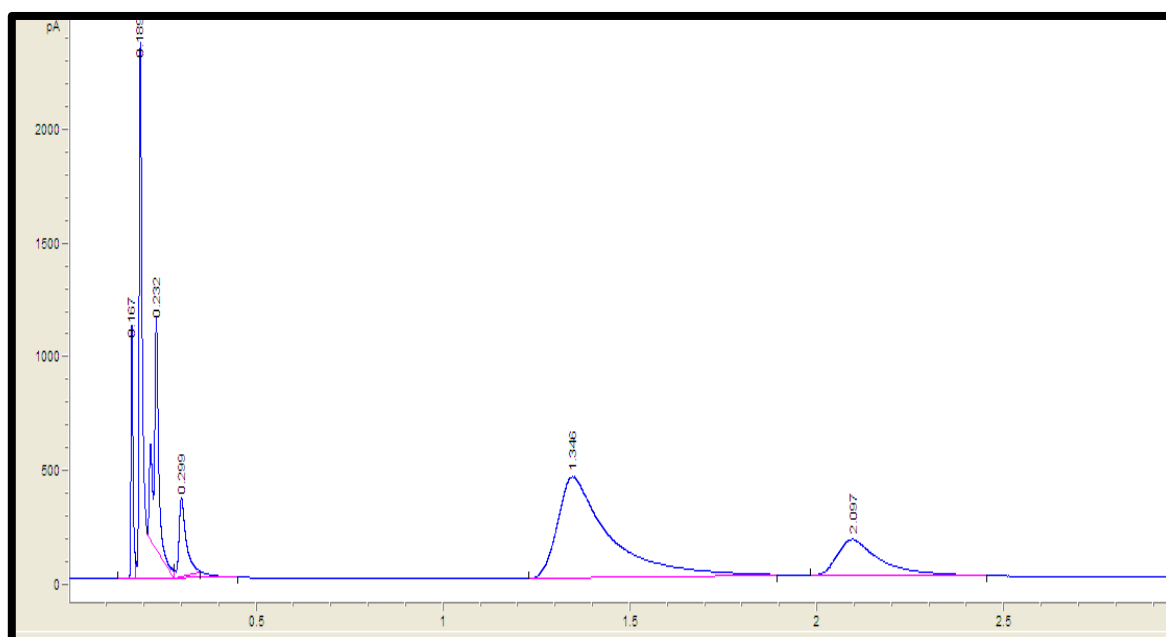


Figure 138: The separation of pentane, 2-methylpentane, isobutyraldehyde, hexane, propan-2-ol, 2-methylbutyraldehyde, 2-pentanone, toluene, ethylbenzene, 3-methyloctane, ethyltoluene, and nonane

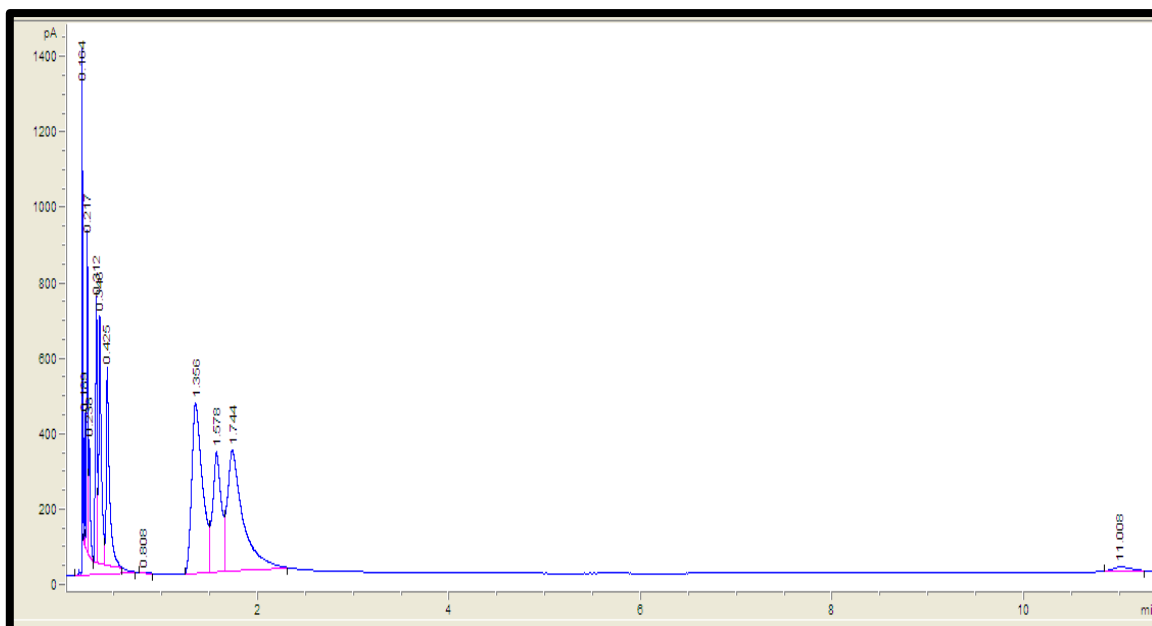


Figure 141: The separation of pentane, 2-butanone, isobutyraldehyde, hexane, butanal, ethyl acetate, cyclohexane, propan-2-ol, 2-methylbutyraldehyde, propyl acetate, 3-methyl-3-buten-2-one, 2-butenal, 2-pentanone, ethylbenzene, 3-methyloctane, nonane

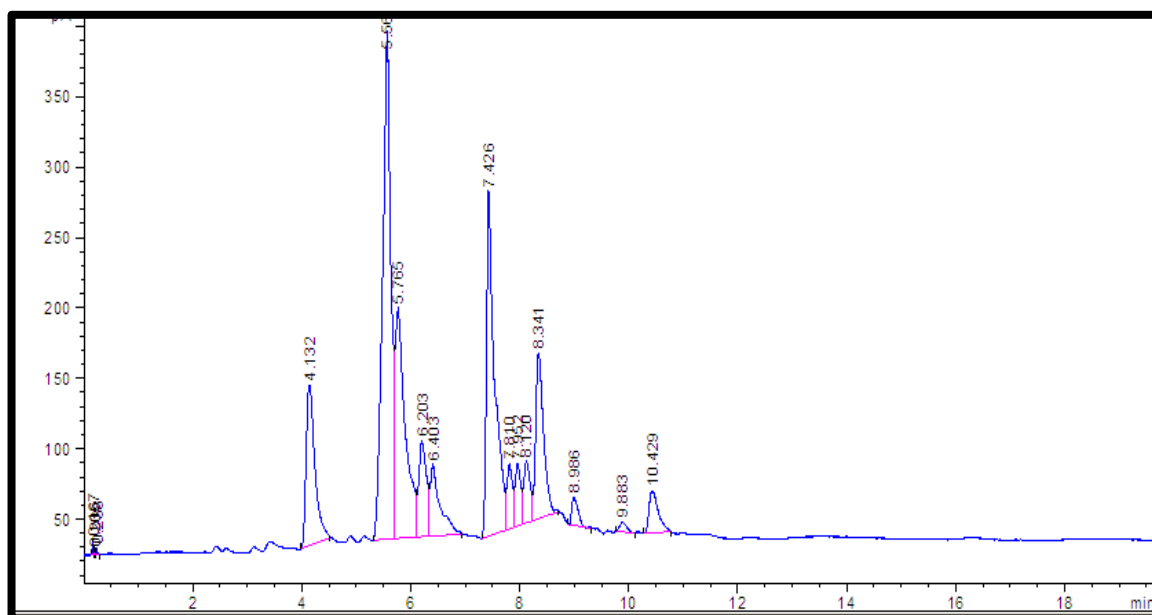


Figure 140: The one-dimensional separation of lavender oil using the before mentioned conditions on the primary column of LOC 4

It's clear to see that the separation achieved lacks efficiency, selectivity and resolution in comparison to that attained using the longer, wider bore primary columns. As well as that, the one dimensional peaks obtained on LOC 4 showed evidence of overloading in the form of fronting peaks.

This indicates that, while relatively good 2-dimensional separation was achieved using LOC 4 in comparison to the previous chip designs; overall separation could potentially be even better by increasing the length of the primary column to one that exceeds the secondary.

9.4.1 Validation and Calibration: LOC 4 GCxGC-FID

The proposed analytes of interest for the lab-on-a-chip GCxGC were VOCs in air. While, the use of standard cylinders containing known concentrations of NMHCs is a regular feature in atmospheric chemistry, such a standard was not available for use in this project. An alternative method of calibration was reported by J. Hopkins, *et al*^[1]. Here, a permeation tube method was used as the calibration system. Liquid samples were contained in small sections of thin wall 1/8" Teflon tubing which was then capped at each end using standard Swagelok fittings. The devices were then placed in a glass impinger within an aluminium block. This solid metal block was held at a constant known temperature and the impinger was flushed continuously with nitrogen at a reported flow rate of 100 ml·min⁻¹. The mass loss of the device over a known period of time was used to calculate the concentration of each VOC within the nitrogen gas. It was found that to produce a range of concentrations, the flow rate of nitrogen over the permeation devices could be altered, with a nitrogen flow of 100 ml·min⁻¹ producing concentrations in the order of 100 ppb.

While the recreation of the above method was considered for use in this work, it ultimately was decided that the determination of specificity should be suspended until a reliable gas standard could be obtained.

9.4.1.1 Quantitative Analysis – The Calibration Curve

Quantitative chromatographic analysis generally consists of the preparation of a series of standard solutions containing a known amount of the analyte of interest. The instrument response for each is measured, with a five-point calibration being typical. Measurement of the peak areas or peak heights of the resulting chromatograms are then taken and plotted as a function of concentration. This then allows for an estimate of the amount of actual analyte present in a sample based on comparison of either the sample peak's height or area with that of one of the standards.

A calibration curve can verify the proper functioning of an analytical instrument, and gives an indication of the following^[2]:

- Linearity
- Regression equation
- Calibration/Working range
- Limit of Detection
- Limit of Quantification
- Correlation efficient R^2

Three VOCs commonly emitted and found in the atmosphere, namely 2-butanone, pentane and ethyl acetate, were chosen as standards for calibration. As discussed, the chosen standards were not available in the preferred matrix. Instead each was injected onto the LOC GCxGC system in an appropriate non-interfering solvent, i.e. 2-butanone in ethylbenzene, pentane in cyclohexanone, and ethyl acetate in ethylbenzene. Thus, the method detection limits (MDLs) achieved with these standards can be described as "best case limits". It is important to note that MDLs found achievable in these clean samples are generally not analytically achievable in other matrices. Nonetheless, such a method is still often used for comparison of detection limits among different laboratories^[3]. All chromatographic separations up to this point had been of similar clean laboratory-prepared standards, thus, attainment of these best case limits was appropriate.

A 2,000 ppm ($2 \text{ g}\cdot\text{L}^{-1}$) stock solution of each standard compound was prepared, and four dilutions were made, resulting in five standard concentrations of 500 ppm, 800 ppm, 1,200 ppm, 1,600 ppm and 2,000 ppm. Each of these standard concentrations was then run on the GCxGC-FID system using LOC 4. Five repeats of each were performed.

The sum of total peak areas of all the pulsed or modulated peaks of the individual compounds were measured to give an overall peak area value. An average peak area value for each concentration of a particular standard was then calculated. The tables below show the peak area values attained for each of the three standards.

Table 26: Average peak area and height per concentration of 2-butanone in ethylbenzene

2-Butanone in Ethylbenzene		
Concentration (ppm)	Average Peak Area (mV·s)	Average Peak Height (mV)
500	413.44	189.39
800	518.74	272.51
1200	634.45	331.28
1600	733.43	420.43
2000	839.72	548.32

Table 27: Average peak area and height per concentration of pentane in cyclohexanone

Pentane in Cyclohexanone		
Concentration (ppm)	Average Peak Area (mV·s)	Average Peak Height (mV)
500	263.4	366.92
800	288.47	528.07
1200	497.31	906.69
1600	590.96	1108.81
2000	768.69	1469.25

Table 28: Average peak area and height per concentration of ethyl acetate in ethylbenzene

Ethyl Acetate in Ethylbenzene		
Concentration (ppm)	Average Peak Area (mV s)	Average Peak Height (mV)
500	360.67	156.57
800	406.73	231.09
1200	479.88	297.24
1600	575.43	370.61
2000	637.61	418.84

Peak height measurements were also taken; however, chromatographic quantitation is generally carried out on the basis of the more reliable peak area. Peak area is preferred as it is less sensitive to the influence of peak broadening or dispersion mechanisms. Thus, while peaks may become shorter, broader, and less symmetrical due to these effects, the total area under the peak remains proportional to the total quantity of substance passing into the detector^[4].

The averaged peak areas determined were then plotted against their respective concentrations. Figures 142, 143, and 144 show the calibration curves formed for each.

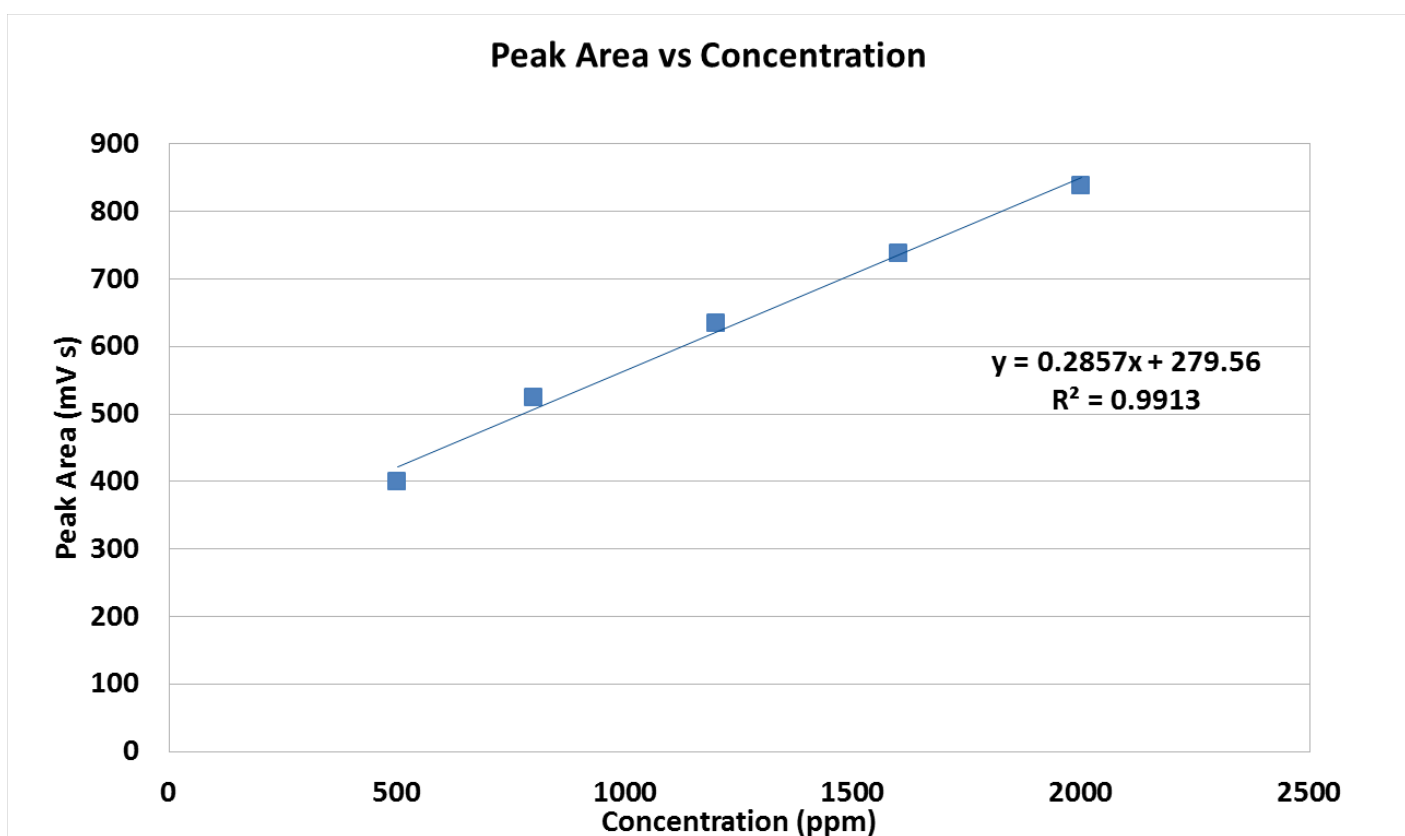


Figure 142: Calibration curve generated for 2- butanone in ethylbenzene

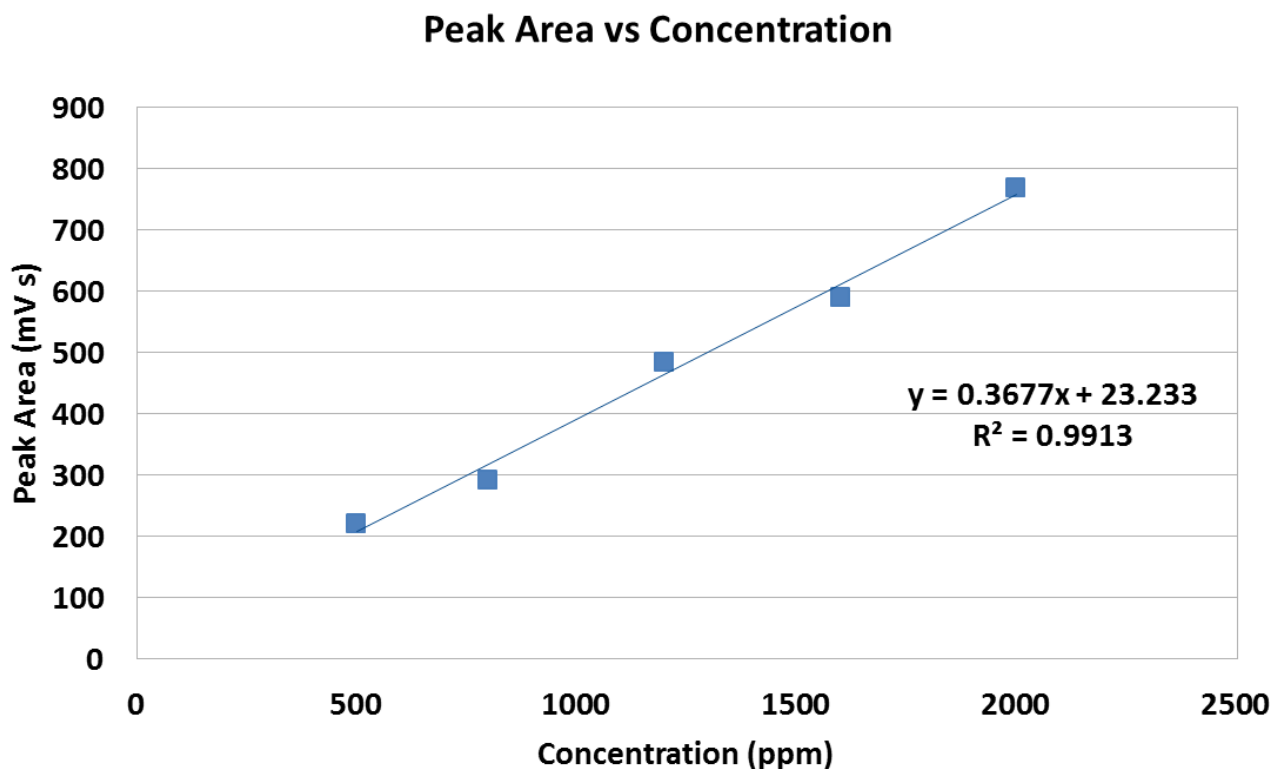


Figure 143: Calibration curve generated for pentane in cyclohexanone

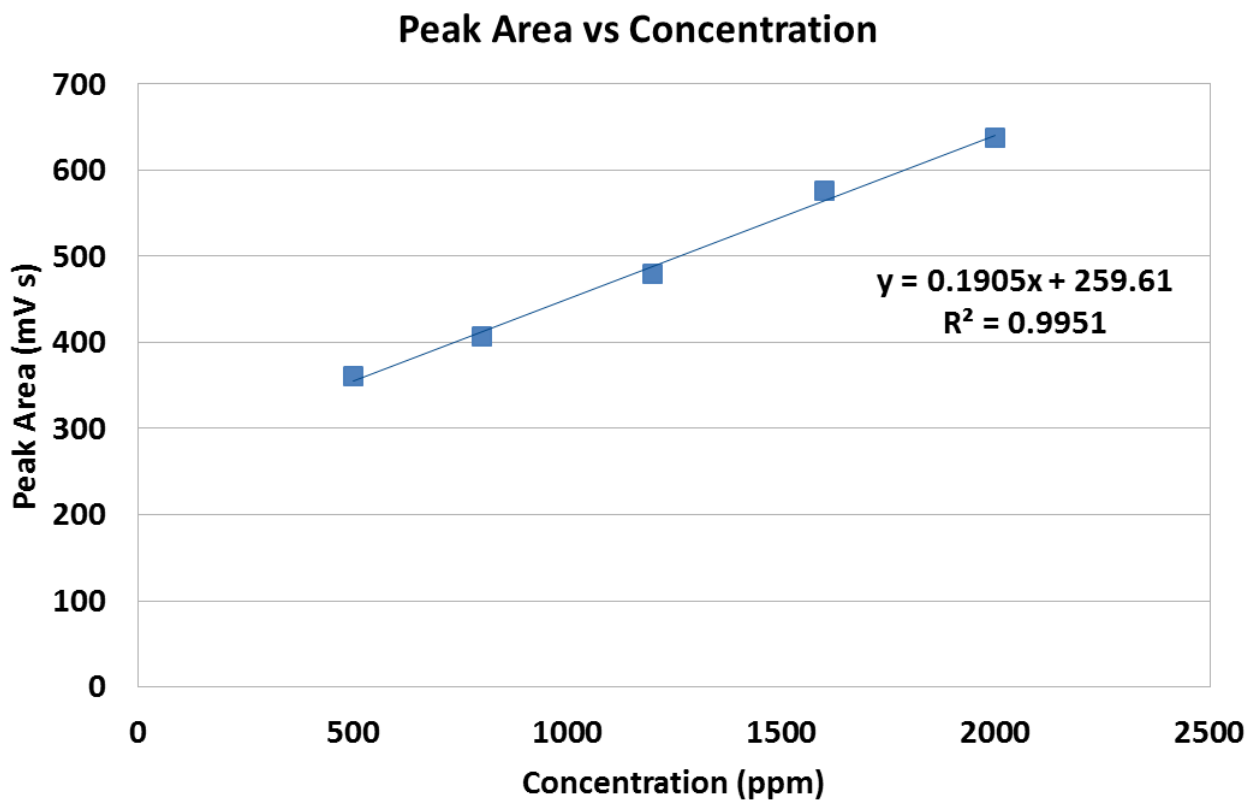


Figure 144: Calibration curve generated for ethyl acetate in ethylbenzene

9.4.1.2 Precision

The % RSD for each concentration of each standard is detailed in the Table 29 below.

Table 29: Calculated % RSD for the varying concentrations of each standard

Standard	2-Butanone	Pentane	Ethyl Acetate
Concentration (ppm)	% RSD		
500	4.90	7.59	4.01
800	5.53	2.39	11.98
1200	4.08	6.80	10.61
1600	14.11	1.43	7.11
2000	19.32	4.07	9.28

9.4.1.3 Limit of Detection (LOD)

Blank values were obtained by examination of the baseline of a blank. It was found that the mean noise or baseline height was 42.12 mV for 2-butanone, 42.00 mV for pentane, and 40.32 mV for ethyl acetate. A detector output of

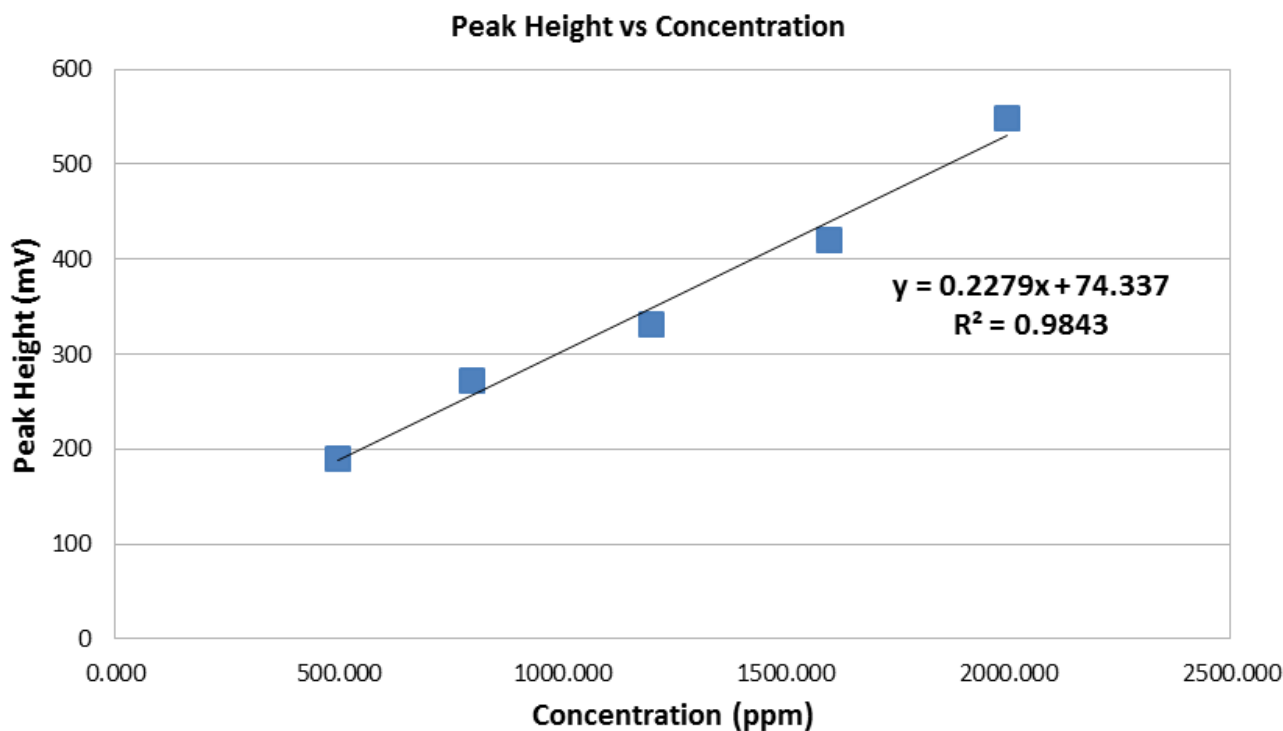


Figure 145: Calibration curve generated for 2-butanone by plotting measured peak height against concentration

± 10.00 mV is typically seen for baselines of commercially available columns in benchtop instruments. The high output seen with LOC 4 is more than likely due to column bleed issues.

The average peak height of each of the three standards was plotted against their respective concentrations. The resulting graphs are shown in Figures 145, 146 and 147. Despite the expected peak broadening and dispersion effects, the linearity for all three peak height generated calibration curves proved to be good.

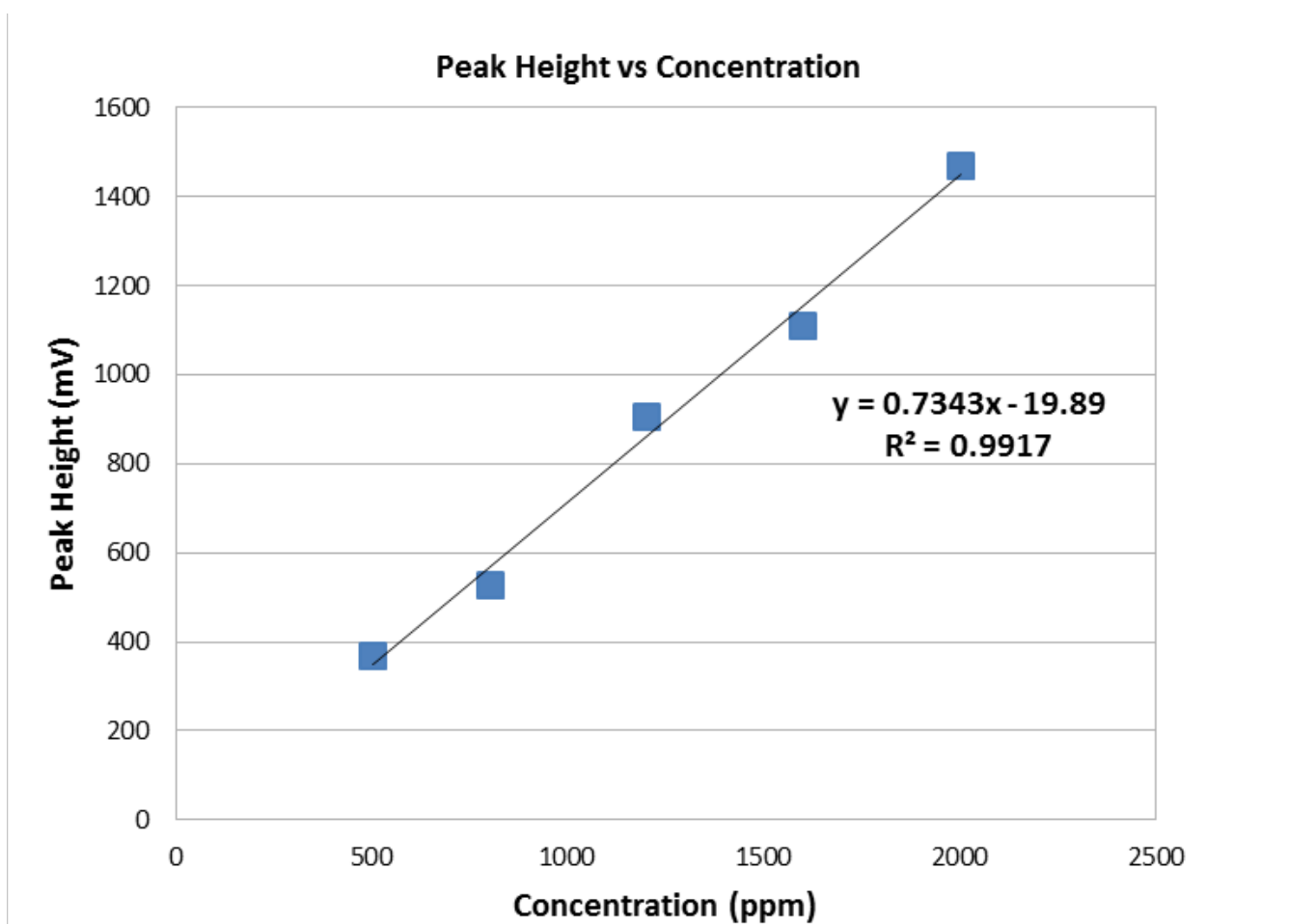


Figure 146: Calibration curve generated for pentane by plotting measured peak height against concentration

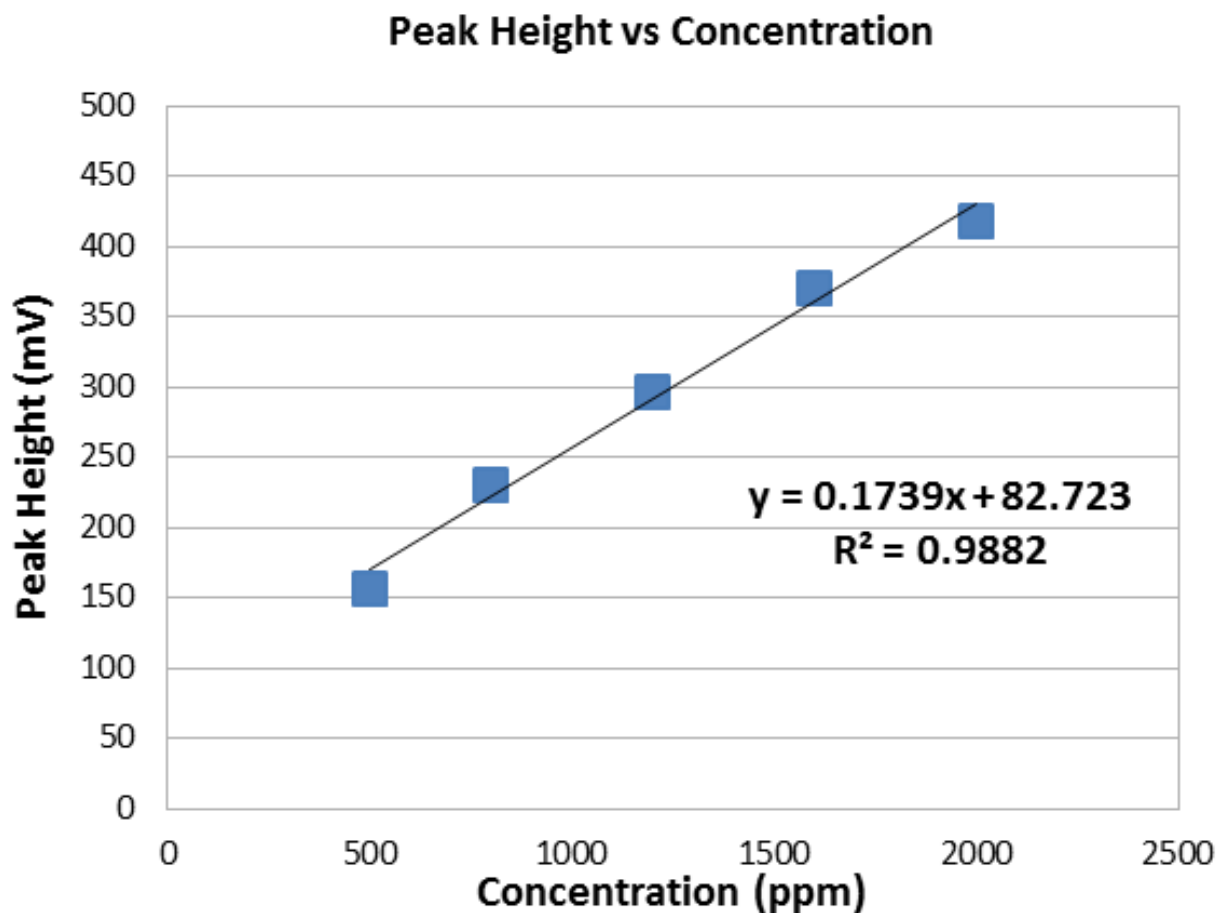


Figure 147: Calibration curve generated for ethyl acetate by plotting measured peak height against concentration

Table 30: Estimated limits of detection for each standard calibration curve

Standard	LOD (ppm)
2-Butanone	237.7
Pentane	172.1
Ethyl Acetate	202.5

Limits of detection were determined by multiplying the signal or peak height measured for the blank by 3 to get the value y of the equation of the line. This was then used to calculate the concentration x . Table 30 details the LODs

estimated via this method for the analysis of 2-butanone, pentane and ethyl acetate.

9.4.1.4 Limit of Quantitation (LOQ)

An analytical procedure's LOQ is the lowest amount of analyte in a sample which can be quantitatively determined with suitable precision and accuracy. Typically a signal-to-noise ratio of 10:1 can be used to estimate this value in much the same way as LOD is estimated^[3].

Thus, using the calibration curves above and their generated linear equations, the method's LOQs for each of the three standards were calculated. The results are detailed in Table 31.

Table 31: Estimated limits of quantitation for each standard calibration curve

Standard	LOQ (ppm)
2-Butanone	1,518.6
Pentane	570.8
Ethyl Acetate	1,954.3

The high values calculated gave an indication of the system and method limitations. High baseline noise made peak integration difficult. This provides evidence towards the importance of a stable coating of stationary phase to the overall chromatography achieved. It would be interesting to see the above experiments repeated with a chip whose coating had been cross-linked or otherwise bonded to the glass channel walls.

9.4.1.5 Qualitative Analysis – Retention Time

As temperature, flow rate, column length, and all other variables, besides concentration, were kept constant, the retention time of each compound should also have remained consistent. To determine whether this was the case, the average retention time observed at each concentration of standard

was calculated and used to determine the % RSD, as previously described. The results per concentration are detailed in Tables 32, 33, and 34.

Table 32: Retention time repeatability at different concentrations of 2-butanone

Concentration (ppm)	% RSD
500	0.99
800	1.91
1200	2.27
1600	2.32
2000	0.12

Table 33: Retention time repeatability at different concentrations of pentane

Concentration (ppm)	% RSD
500	4.09
800	5.33
1200	4.48
1600	7.54
2000	4.45

Table 34: Retention time repeatability at different concentrations of ethyl acetate

Concentration (ppm)	% RSD
500	2.91
800	0.52
1200	1.88
1600	3.14
2000	2.64

Overall, the retention time repeatability over the range of concentrations for each compound was calculated to be as follows:

- 2-Butanone = 2.05%
- Pentane = 0.83%
- Ethyl acetate = 0.73%.

9.5 References

1. Hopkins, J.R., A.C. Lewis, and K.A. Read, *A two-column method for long-term monitoring of non-methane hydrocarbons (NMHCs) and oxygenated volatile organic compounds (o-VOCs)*. *Journal of Environmental Monitoring*, 2003. **5**(1): p. 8-13.
2. EPA, *Calibration Curves: Program Use/Needs*. 2010 01/10/2010 [cited 2012 03/01/2012]; Available from: <http://www.epa.gov/fem/pdfs/calibration-guide-ref-final-oct2010.pdf>.
3. *Analytical Detection Limit Guidance & Laboratory Guide for Determining Method Detection Limits*. 1996 01/04/1996 [cited 2012 03/01/2012]; Available from: <http://www.iatl.com/content/file/LOD%20Guidance%20Document.pdf>.
4. O'Haver, T. *Integration and Peak Area Measurement*. 2008 17/05/2008 [cited 2012 03/01/2012]; Available from: <http://terpconnect.umd.edu/~toh/spectrum/Integration.html>.

10.0 Experimental – Stand-Alone LOC GCxGC-PID

As with the commercial GC instrument, when LOC 4 was installed into the stand-alone in-house built system, initial experimentation involved optimisation of headspace injections of pentane. Next method development and optimisation was carried out in order to successfully separate out a simple mixture of pentane, hexane and heptane. The set-up of the chip within the manifold was as previously described. The following parameters were changed systematically in an effort to determine the optimum separation method using the miniaturised PID for detection:

- Carrier gas and modulator gas pressure ratio (psi)
- Modulation and modulation period ratio (s)
- Starting temperature (°C)
- Hold time/ramp delay (s)
- Temperature ramp rate (°C)
- Temperature offset between columns (°C)

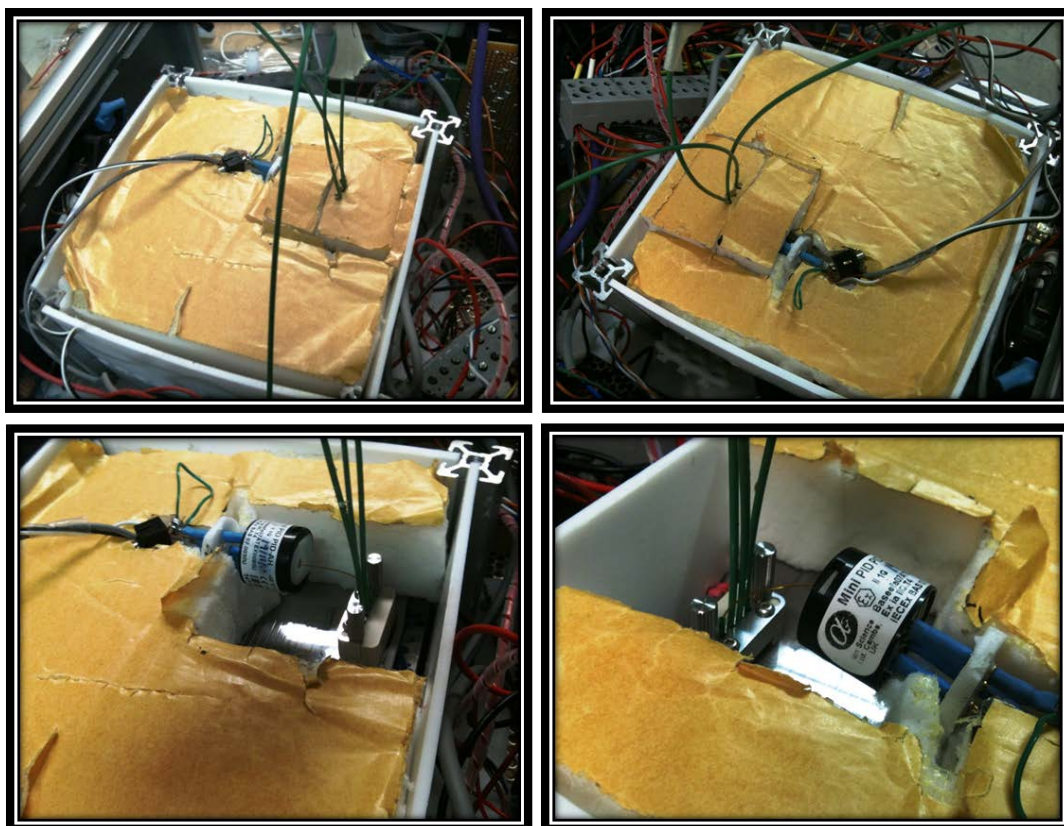


Figure 148: Images illustrating the chip within its housing. Input and output transfer lines are clearly visible. Connection to the PID was by a small 5 cm length of capillary

10.1 Pressure Determinations

Variation of the carrier and modulator gas pressures gave initial indications that the optimum pressure for both was 62 psi. Next, the modulation period and modulation ratio were adjusted. Examples of the effect of changing the modulation period are shown below, with Figure 149 a) having a modulation period of 3 s, b) 5 s, c) 7 s, and d) 9 s, all with a 1 s collector flushing time. Figure 149 e) also has a 9 s modulation period, but a 0.5 s flushing time, and illustrates, when compared to d), the effect of changing the modulation flushing and filling time ratio.

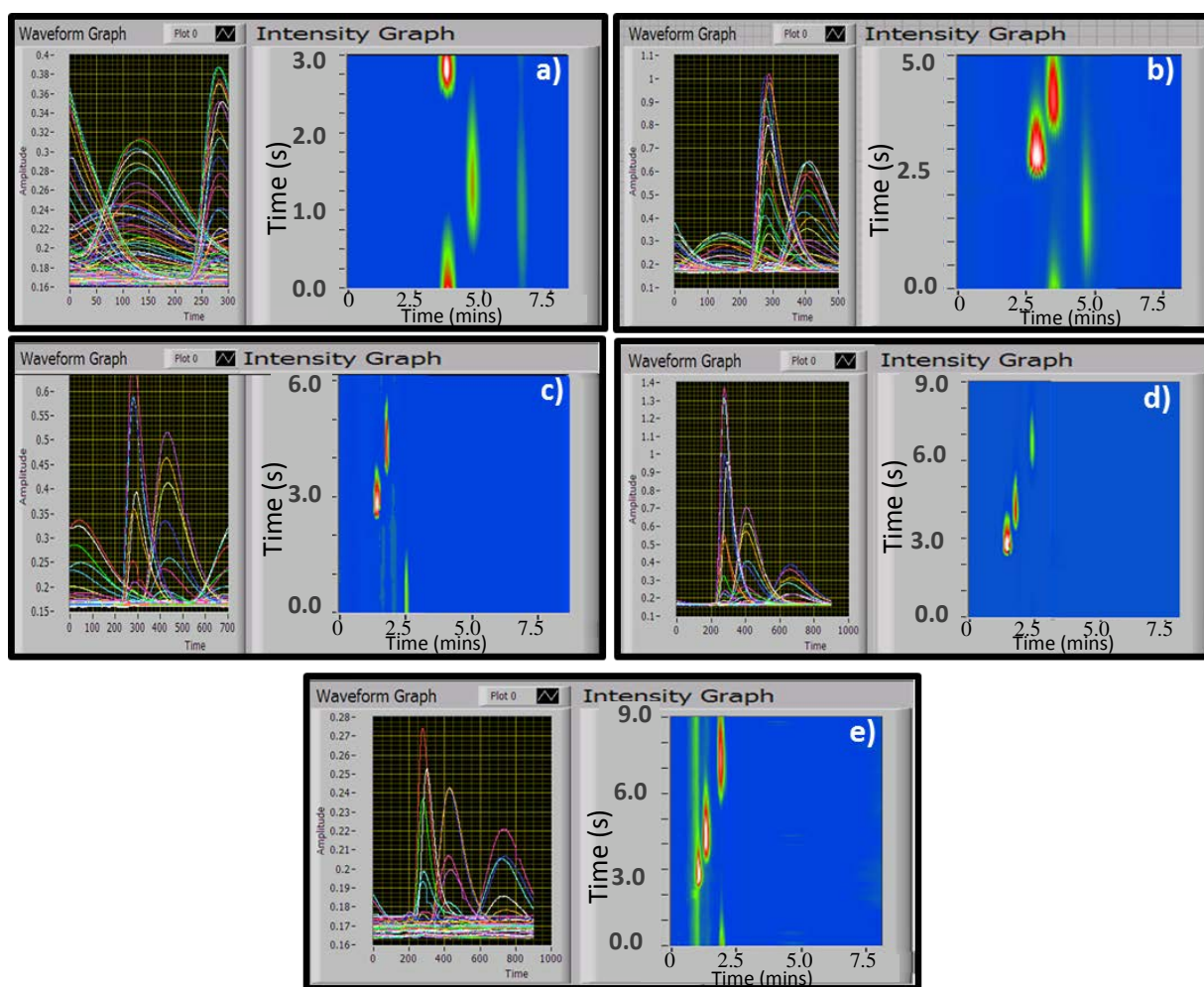


Figure 149: The 2D separation of pentane, hexane and heptane. Carrier gas and modulator gas pressure = 62 psi, temperature difference between primary and secondary column = 10 °C, temperature ramp = 25-60 °C at 10 °C·min⁻¹, ramp delay = 20 s. a) Modulation ratio = 3:1 s; b) Modulation ratio = 5:1 s; c) Modulation ratio = 7:1 s; d) Modulation ratio = 9:1 s; e) Modulation ratio = 9:0.5 s. Due to operation parameters injections were not 100% reproducible.

Based on the results of the above adjustments, it was decided that a modulation period of 9 s with a 1 s flushing time provided the best chromatogram.

10.2 Temperature Program Determinations

Next, the ramp rate was adjusted. It was determined that a ramp of $10\text{ }^{\circ}\text{C}\cdot\text{min}^{-1}$, as was initially being used, gave the optimal result. The ramp delay was subsequently examined and a delay of 60 s produced the improved chromatogram shown in Figure 150.

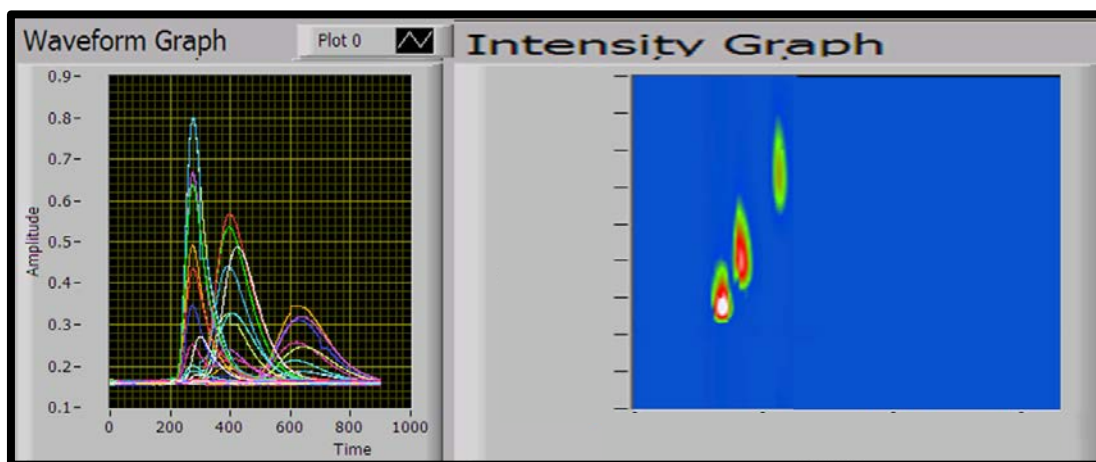


Figure 150: Pentane, hexane and heptane. Modulation ratio = 9:1 s, carrier and modulator gas pressures = 62 psi, temperature difference between columns = $10\text{ }^{\circ}\text{C}$, temperature program = $25\text{-}60\text{ }^{\circ}\text{C}$ at $10\text{ }^{\circ}\text{C}\cdot\text{min}^{-1}$, ramp delay = 60 s

Finally, the temperature offset between the primary and secondary column was varied. It was found that a difference of $80\text{ }^{\circ}\text{C}$ gave narrower, sharper peaks.

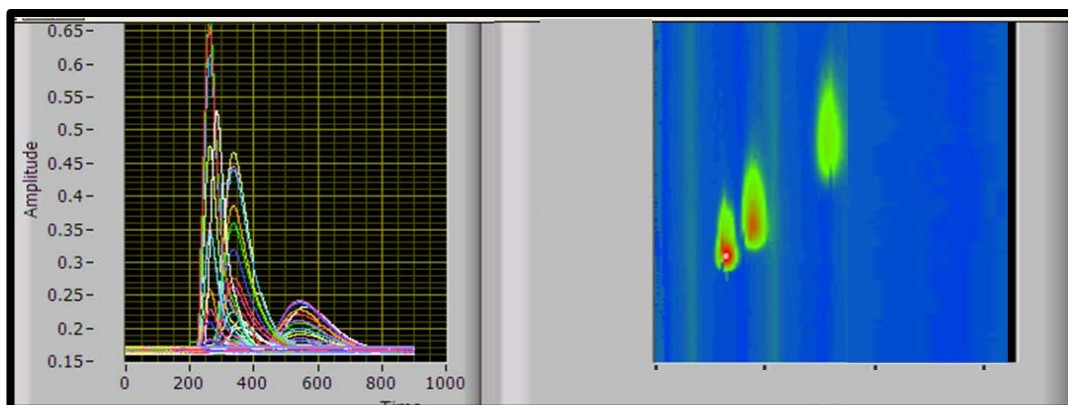


Figure 151: Pentane, hexane and heptane. Modulation ratio = 9:1 s, carrier and modulator gas pressures = 62 psi, temperature program = $25\text{-}60\text{ }^{\circ}\text{C}$ at $10\text{ }^{\circ}\text{C}\cdot\text{min}^{-1}$, ramp delay = 60 s, and temperature difference between columns = $50\text{ }^{\circ}\text{C}$

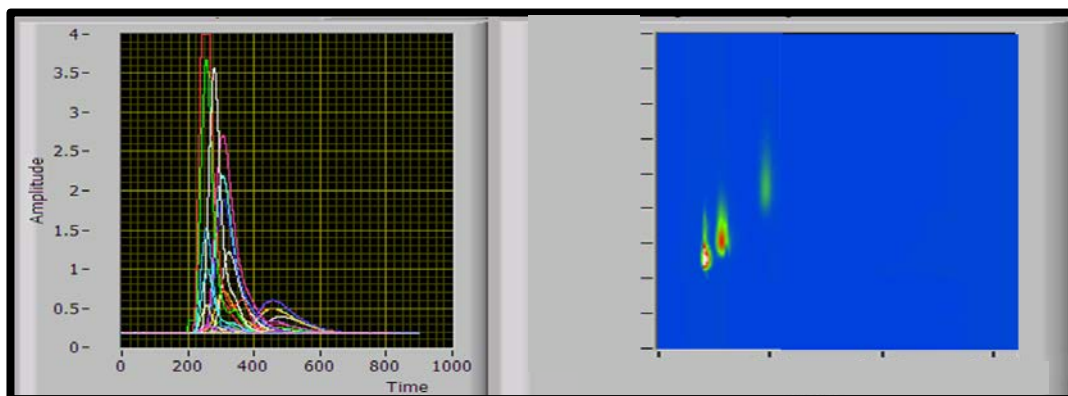


Figure 152: Pentane, hexane and heptane. Modulation ratio = 9:1 s, carrier and modulator gas pressures = 62 psi, temperature program = 25-60 °C at 10 °C·min⁻¹, ramp delay = 60 s, and temperature difference between columns = 80 °C

10.3 Commercial FID and Heated Transfer Line

As it was known that the PID had a derogatory effect on the separation results, it was decided to connect just the detector port of the chip in its LOC stand-alone manifold to the FID of the commercial Agilent GC. Chromatography initially proved to be worse, with very broad 2D peaks being produced. The set up was then altered so as to allow for a heated transfer line from the chip outlet to the Agilent's FID. This greatly improved the shape of the peaks, as illustrated in Figure 153.

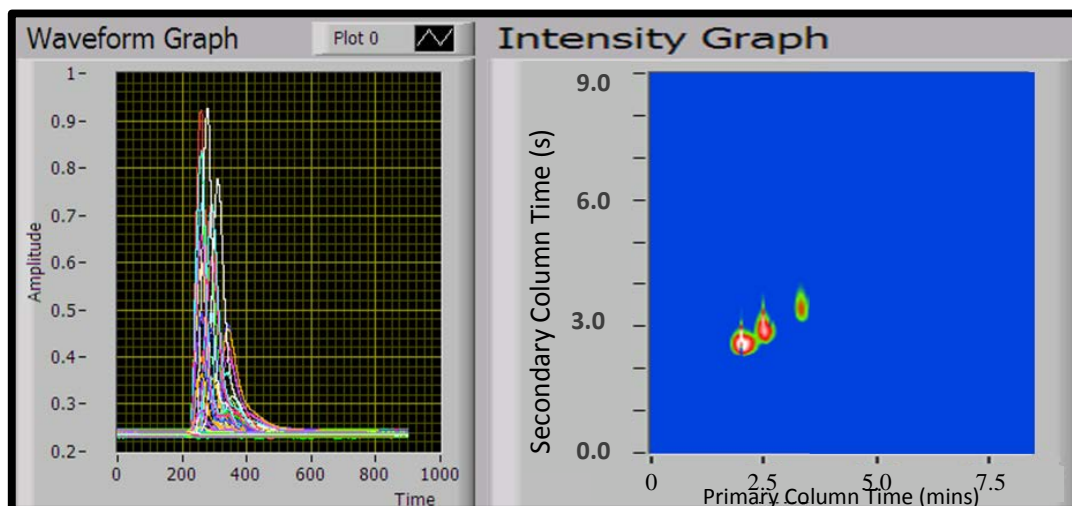


Figure 153: Pentane, hexane and heptane using a commercial FID for detection. Modulation ratio = 9:1 s, carrier and modulator gas pressures = 62 psi, temperature difference between columns = 20 °C, temperature program = 25-60 °C at 10 °C·min⁻¹, ramp delay = 60 s

The following 6 component mixture, containing aliphatic, carbonyl and aromatic compounds, was prepared:

- | | |
|---------------|--------------------|
| 1. Pentane | 4. 2-Methylbutanal |
| 2. Hexane | 5. Toluene |
| 3. 2-Butanone | 6. Ethylbenzene. |

A schematic of the two-dimensional chromatogram that would be expected for such a separation is illustrated by Figure 154.

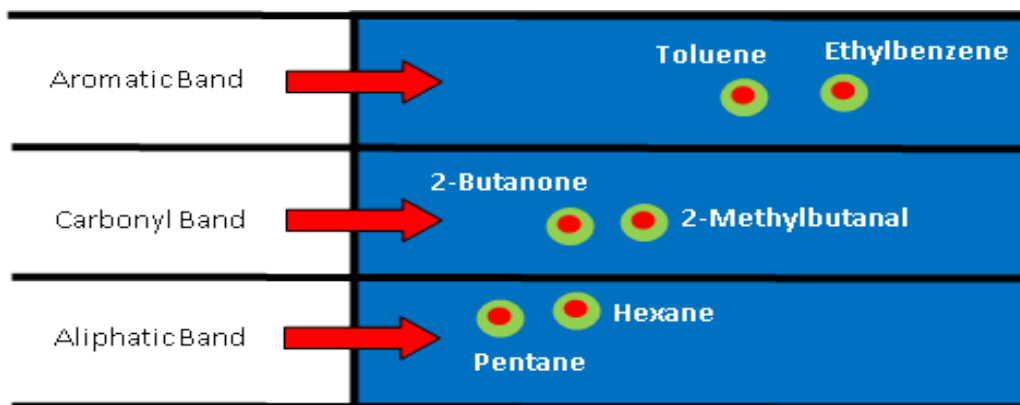


Figure 154: A schematic of the expected 2-dimensional plot that would result from the GCxGC separation of pentane, hexane, 2-butanone, 2-methylbutanal, toluene and ethylbenzene

The actual chromatogram is shown in Figure 155. As can be seen, the peak positions were as expected, indicating successful two-dimensional separation of the mixture.

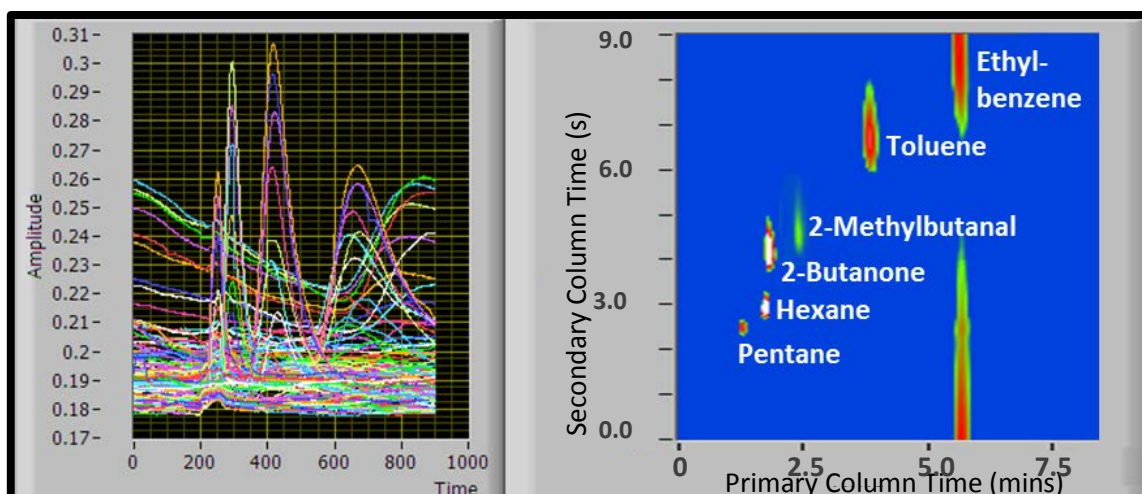


Figure 155: Separation of a 6 component mixture using a commercial FID for detection. Modulation ratio = 9:1 s, carrier and modulator gas pressures = 62 psi, temperature difference between columns = 20 °C, temperature program = 25-120 °C at 5 °C·min⁻¹, ramp delay = 120 s

Subsequently, heptane and nonane, two more aliphatics, were added to the mix. While separation was not fully optimised, the compounds did generally keep to the expected aliphatic, carbonyl and aromatic banding.

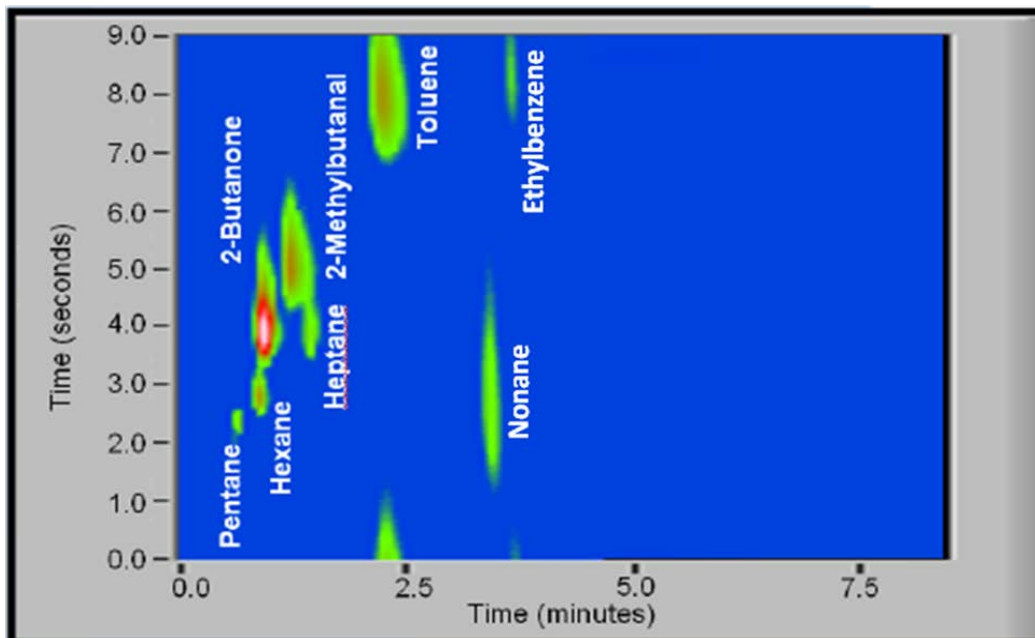


Figure 156: Separation of an 8 component mixture using a commercial FID for detection. Modulation ratio = 9:1 s, carrier and modulator gas pressure = 62 psi, temperature difference between columns = 20 °C, temperature program = 25-120 °C at 5 °C·min⁻¹, ramp delay = 120 s

10.4 Optimisation of PID

A miniaturised FID would be ideal for the purposes of the project reported here; however, it was not possible for one to be sourced. Thus, in order to achieve a field portable, miniaturised GCxGC instrument, all further development was conducted using the PID. As illustrated by Chromatogram 53, resolution, efficiency and retention are not as good as that seen with the FID.

As separation of relatively low molecular weight compounds was achievable using the coated LOC 4 in the GC manifold, it was decided to determine the chip's separation capabilities with regard to a higher molecular weight mixture. Initially, headspace injections of lavender oil and tea tree oil were attempted with the sample loop in place.

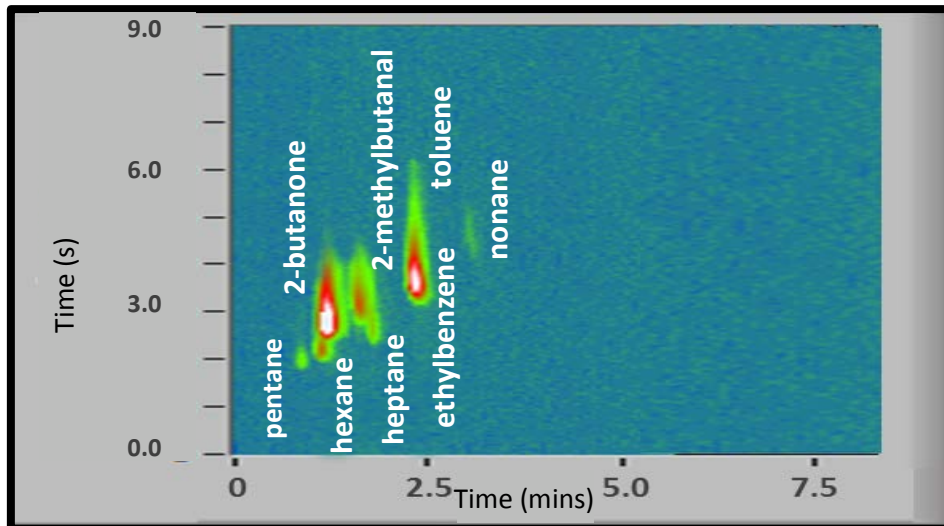


Figure 157: Separation of an 8 component mixture using the PID for detection. Modulation ratio = 9:1 s, carrier and modulator gas pressure = 62 psi, temperature difference between columns = 20 °C, temperature program = 25-120 °C at 5 °C·min⁻¹, ramp delay = 120 s

The boiling points of lavender oil components range from 100 °C to approximately 280 °C, as evidenced in Table 35, and tea tree oil components from 155 °C to 219 °C (Table 36). With the manifold providing no means of heating the inlet, it was only possible to see a limited number of peaks due to discrimination taking place within the cold injector. The chromatogram below is the result of the separation of lavender oil via this set-up.

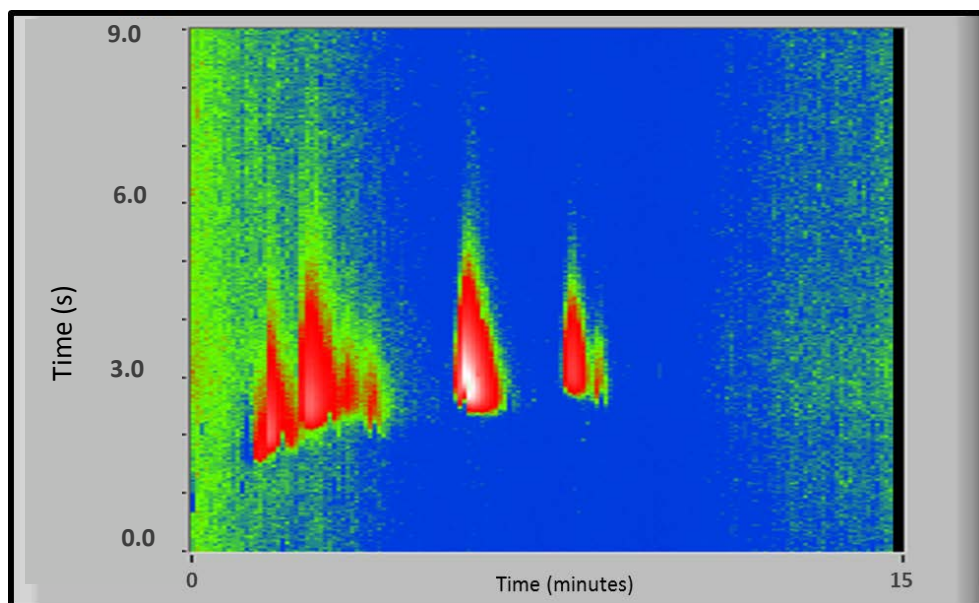


Figure 158: The separation of lavender oil. Modulation ratio = 9:1 s, carrier gas pressure = 65 psi, modulator gas pressure = 64 psi, temperature difference between columns = 10 °C, temperature program = 20-120 °C at 5 °C·min⁻¹, ramp delay = 120 s

Table 35: The composition of lavender oil

Composition	Boiling Point (°C)	Molecular Weight (g·mol ⁻¹)
E-β-ocimene	100	136.23
Z-β-ocimene	100	136.23
α-humulene	106	204.36
α-pinene	155	136.23
Camphene	159	136.23
β-pinene	164	136.23
Myrcene	167	136.23
Octanone-3	168	128.21
β-phellandrene	171	136.23
Eucalyptol (1,8-cineol)	176	154.25
Octene-3-yl acetate	189	196.29
Linalool	198	154.25
Camphor	204	152.23
Cryptone	108	138.21
Terpin-4-ol	212	154.25
Borneol	213	154.25
α-terpineol	219	154.25
γ-terpineol	219	154.25
Linalyl acetate	220	196.29
Nerol	224	154.25
Lavandulyl acetate	228	196.29
Lavandulol	229	154.29
Geranyl acetate	245	196.29
Neryl acetate	247	196.29
β-farnesene	261	204.36
β-caryophyllene	263	204.36
Germacrene	279	204.36

Table 36: The composition of tea tree oil

Composition	Boiling Point (°C)	Molecular Weight (g·mol ⁻¹)
α-pinene	155	136.23
α-terpinene	174	136.24
1,8-cineole	176	154.25
p-cymene	177	134.21
γ-terpinene	183	136.24
α-terpinolene	185	136.24
Terpinen-4-ol	212	154.25
α-terpineol	219	154.25

10.5 Heating the Inlet

It was clear that the inlet required heating. As a preliminary test, a Swagelok union tee was connected in line with the carrier gas just before its introduction to the first glass column. This metal fitting was then heated with a heat gun set at 300 °C, before liquid lavender oil was injected through the tee's plug (fitted with a septum) and into the heated path of the carrier gas for volatilisation. Unfortunately, this did not produce the desired effect, with the resulting chromatogram being shown below.

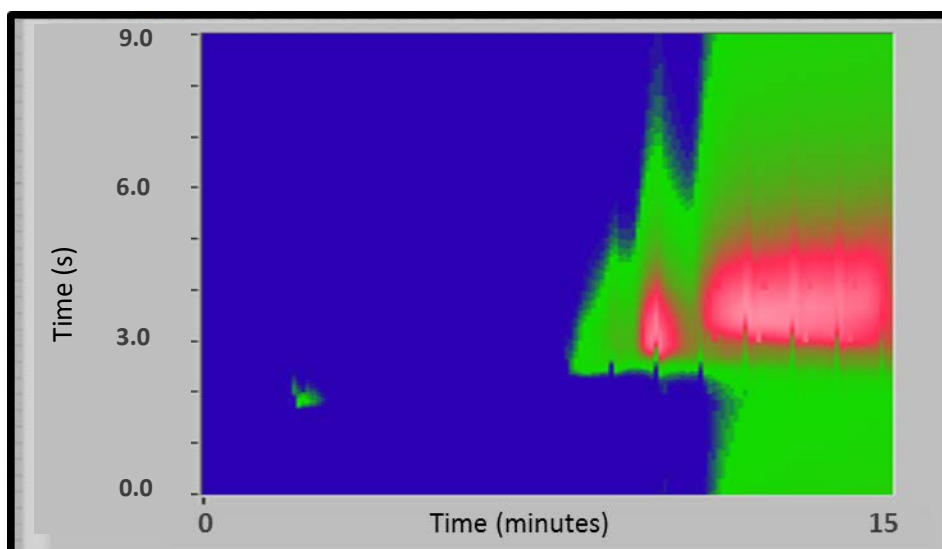


Figure 159: The separation of lavender oil as previously described. However, this time a heated metal fitting was used as inlet

A commercially manufactured split/splitless inlet, capable of heating, was sourced and adapted to fit the manifold (Figure 161). The inlet was fitted with a valve to allow switching between split and splitless mode, and was operated in split mode for the analyses to be described. Before testing, an appropriate liner was fitted, as was a new O-ring and gold-plated base seal.

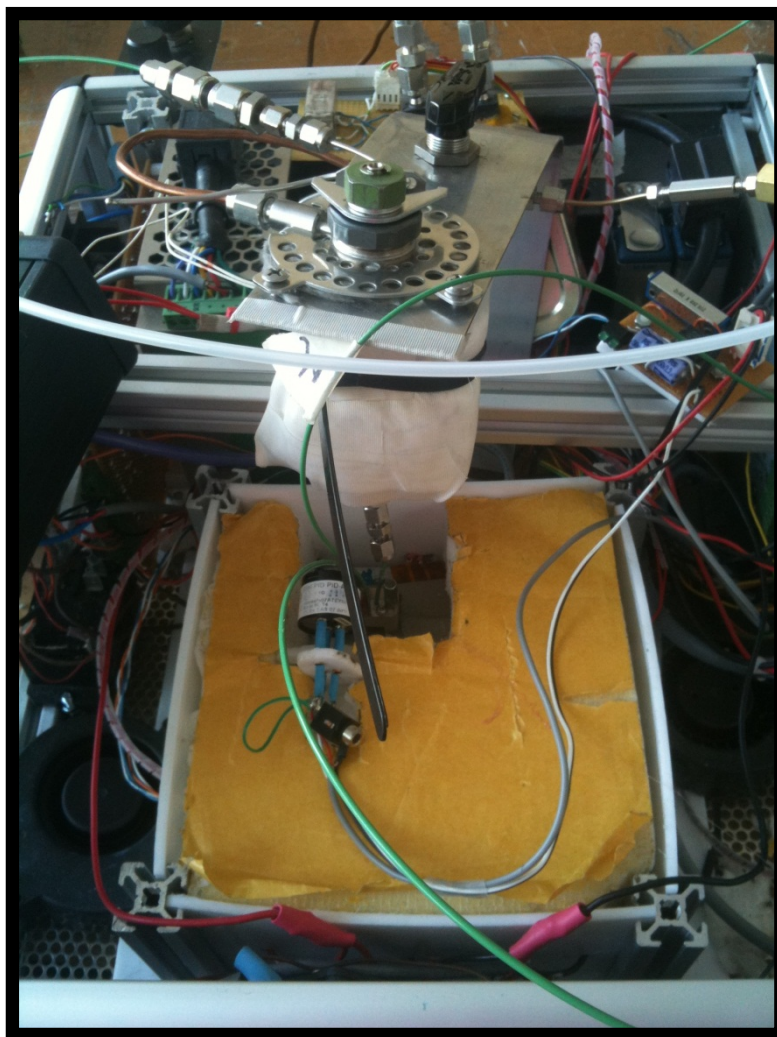


Figure 160: The commercial inlet coupled to LOC 4 within the in-house built GC manifold

The split ratio could not be accurately controlled, although it could be measured, and back calculated by using the following equation:

Equation 61

$$\text{Split ratio} = \frac{F_c}{(F_s + F_c)}$$

Where F_c is the column flow and F_s is the split exit flow.

Instead, the ideal split flow was determined on a trial and error basis. It's important to note here, that as the manifold lacked an electronics pneumatics control, which would generally be found on a commercial GC, parameters, such as the inlet flush time and flush flow were not automatically calculated and applied. With regard to split injection, it is important to ensure good mixing of the vapourised sample with the carrier gas. Fast mixing is required for consistent results.

The flow through the liner (F_l) is calculated as follows:

Equation 62

$$F_l = F_c + F_s$$

Thus, if the column flow is $1 \text{ ml}\cdot\text{min}^{-1}$ and the split flow is $9 \text{ ml}\cdot\text{min}^{-1}$, the flow through the liner is $10 \text{ ml}\cdot\text{min}^{-1}$. If the liner volume is 1 ml, it will take 1/10 minutes (6 seconds) for the liner to flush once. If the split ratio is 100:1 it will take 1/100 minutes (0.6 seconds) to flush. Generally, two flushes are recommended for complete transfer.

A simple mix of pentane, hexane, and heptane was run to optimise usage of the inlet, before moving on to more complex solutions. However, with the set up

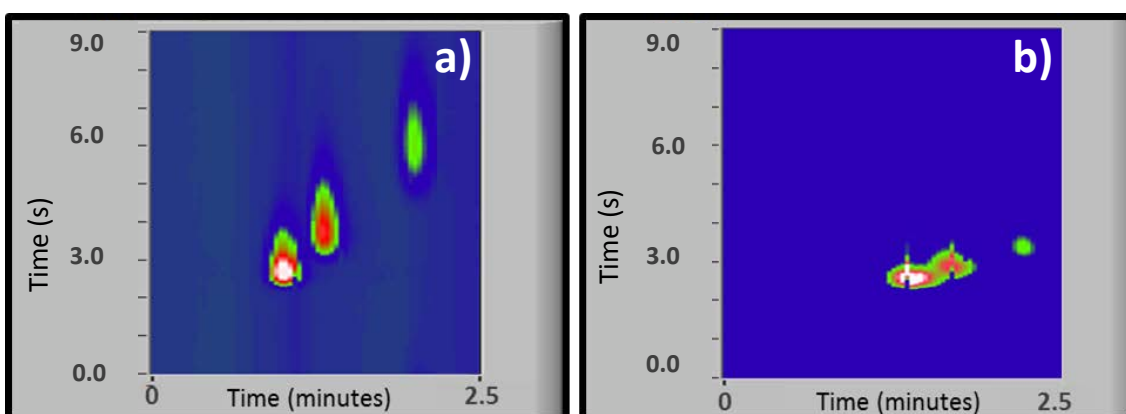


Figure 161: Pentane, hexane and heptane. Modulation ratio = 9:1 s, carrier and modulator gas pressure = 62 psi, temperature difference between columns = 20 °C, temperature program = 25-100 °C at 10 °C·min⁻¹, ramp delay = 60 s, a) without the extra heating applied to the inlet; b) with the extra heating applied

as it was, the maximum temperature that the inlet was capable of reaching was 135 °C. This value was much lower than the typical operating temperature of 250 °C of a commercial GC inlet. In an attempt to increase the temperature, heating tape was wrapped around the unit, bringing the resultant temperature up by approximately 15-20 °C. The chromatograms achieved with the additional heating to the inlet displayed improved peak shape, as illustrated by Figure 162, which shows the three separated compounds a) before the extra heating and b) after.

The 8 component mixture previously used, consisting of pentane, hexane, heptane, 2-butanone, 2-methylbutanal, toluene, ethylbenzene, and nonane was run using this new configuration, with the result shown in Figure 163.

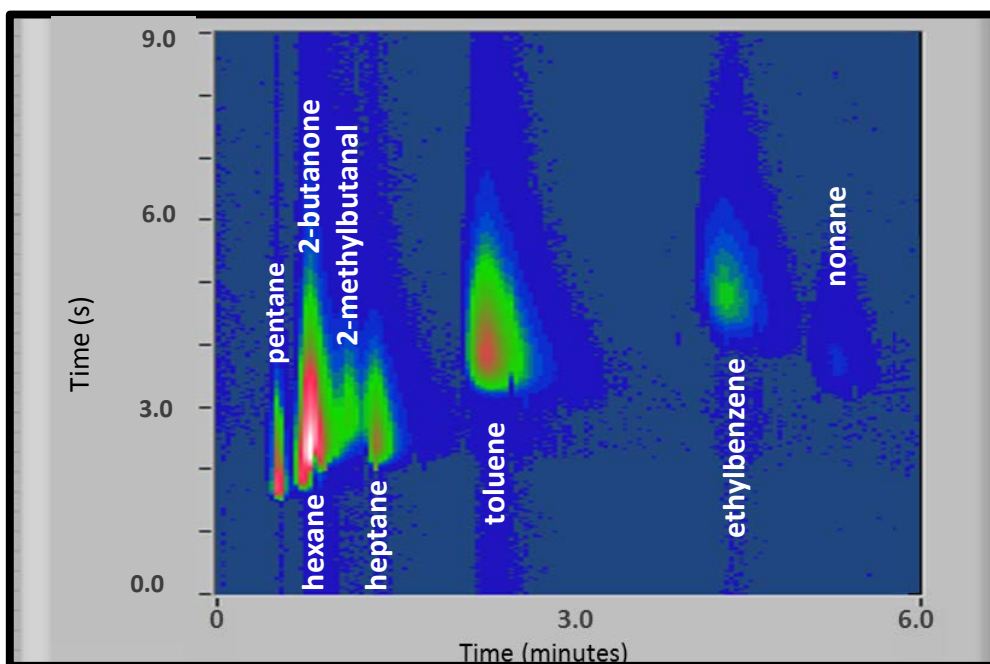


Figure 162: The separation of an 8 component mixture. Modulation ratio = 9:1 s, carrier and modulator gas pressure = 62 psi, temperature difference between columns = 20 °C, temperature program = 25-100 °C at 10 °C·min⁻¹, ramp delay = 60 s, with the extra heating applied to the inlet

On comparison of this chromatogram to previous ones, there does not seem to be evidence of significant improvement with the introduction of the commercial inlet. If anything, chromatography has degraded somewhat. This could be due to stationary phase leaching from the chip over time with use; however, a major factor will also be the addition of the inlet to the manifold. The inlet brought an unknown number of variables into the overall equation.

Thus, to achieve a fully functional and sufficiently heated inlet further work was required outside the scope of this project.

Lavender oil was also run on the system using the heated inlet, and the chromatogram is shown in Figure 163. This result initially seemed quite poor. However, on adjusting the intensity settings of the 2D plot and recording the visible peaks at each intensity level before compiling them in Figure 164, it's possible to see that, despite the inefficient heating provided by the inlet, a substantial number of lavender oil components were actually resolved.

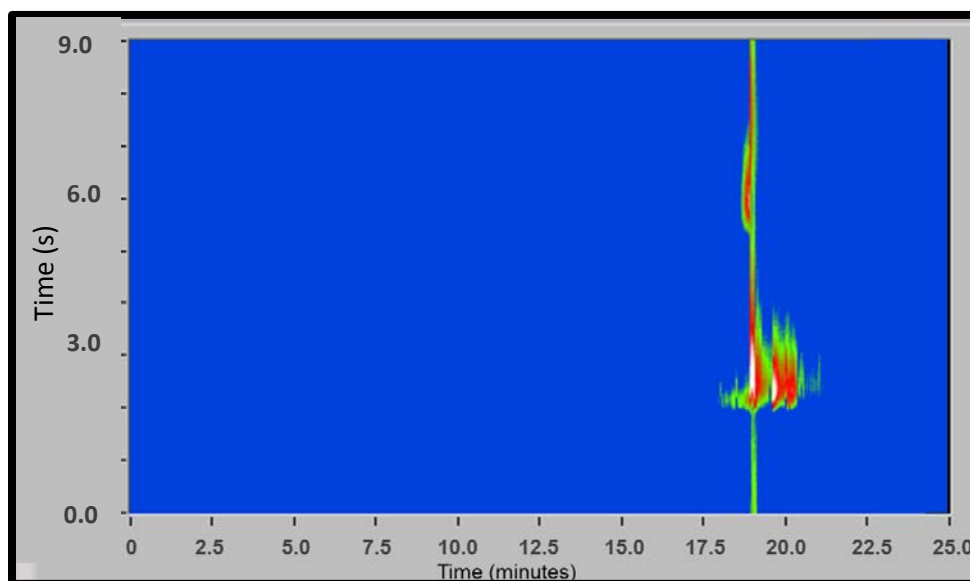


Figure 163: Lavender oil separated on LOC 4. Modulation ratio = 9:1 s, carrier gas pressure = 65 psi, modulator gas pressure = 64 psi, temperature difference between columns = 10 °C, temperature program = 20-120 °C at 2 °C·min⁻¹, ramp delay = 20 s

Numerous problems were experienced with regard to the inlet, with leaks being a key issue. Leak areas included the capped purge vent, the plugged column connection, the septum and/or septum nut, the zone where the gas lines were plumbed to the inlet, the O-ring and/or O-ring nut, and the inlet base seal. All required checking and, when necessary, tightening at various intervals throughout testing. As the inlet was one that had been found in the lab with no indication as to why it had been removed from its original instrument, it is possible that it may have been experiencing problems when originally in use and, hence, been replaced and discarded. Inlet discrimination was also still being experienced due to insufficient heating.

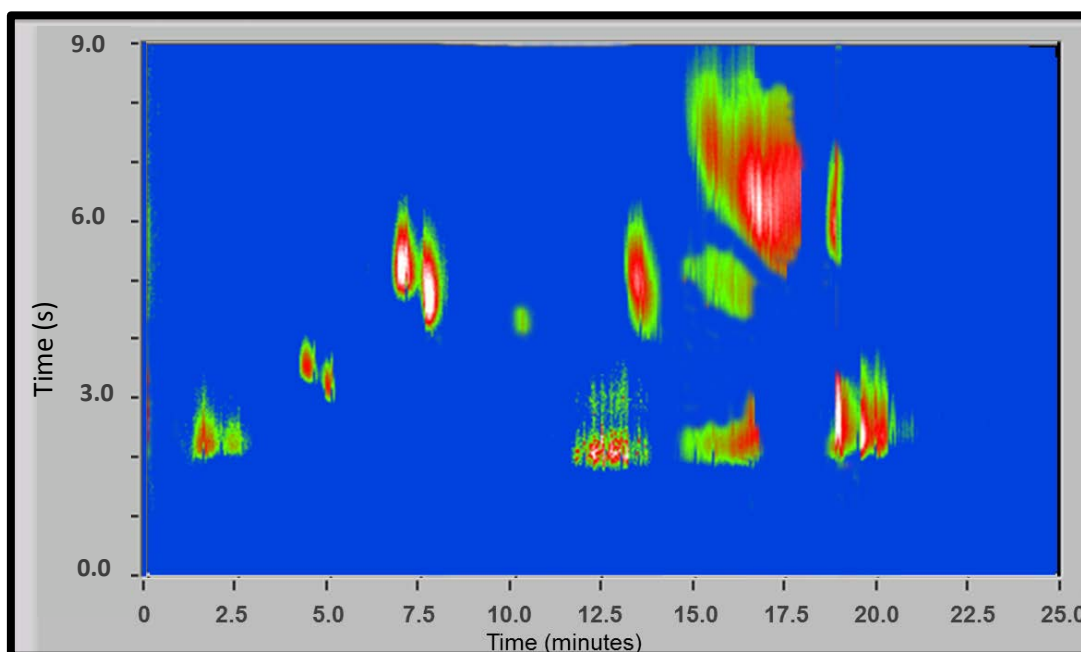


Figure 164: A compilation of lavender oil component peaks seen at varying intensities

10.6 Manifold Deterioration

In addition to the above, progress was also hindered further by component failure within the briefcase-sized manifold. Temperature control was one of the first areas where mechanical problems were encountered. The primary column heating was found to slow down and lag considerably when ramped. Thus, when, for example, a 10 °C temperature difference between primary and secondary columns was set, this difference would increase by as much as 40-50 °C over the course of a run. The Thermofoil heating pads were replaced, and while this did result in more efficient heating, it did not solve the temperature drift issue.

Weight was also applied to the insulation above the chip, forcing it to achieve better contact with the heating pad below. However, this was to no effect, and contact, or lack thereof, was obviously not an influence.

The cooling fans, Peltiers, and sensors, amongst other components, would also fail at varying points throughout runs. In an attempt to offset these issues, many of the manifold connections were rewired, whilst the remaining connections were checked and tightened. This would indicate that the

components in the final product would need to be secured tightly in place to prevent loosening over time and with transport and use.

Unfortunately, there was no real way to determine how and to what extent the faulty workings of the above mentioned components may have affected the chromatography of previous runs. It does, however, suggest an explanation as to why so much variation of results existed from run to run, even when the exact same parameters were used, and why such a notable degradation of chromatography occurred whenever the manifold was transported.

11.0 Conclusion

11.1 A Summary

The aim of this PhD project was to develop a novel microfabricated lab-on-a-chip two-dimensional gas chromatograph capable of achieving on-site VOC analysis. This thesis presented the steps taken over a period of nearly four years to reach the successful accomplishment of this goal.

Essentially, the prototype lab-on-a-chip 2D GC reported here gives an indication of what the future of GC could be, and provides an illustration of what is currently achievable within the world of micro-GC. Miniaturisation of analytical instruments is the next logical step in the progress and evolution of the separation sciences. There was a time when bigger was deemed to be better, but society has moved away from this idea, and the term “modern” is nowadays more often associated with phrases such as “compact” and “portable”. GC miniaturisation offers many benefits, not least those associated with savings in space, solvent consumption, waste disposal, time and, as a consequence of the former, costs.

Confucius said that one should *“study the past if you would define the future”*. As such, the preliminary Chapters 1 – 4 of this body of work provide an in depth introduction and history to the various disciplines that formed the basis of and drove forward the innovation of the developed miniaturised instrument.

Chapter 1 outlined the challenges faced by the atmospheric chemist and emphasised the vital need for analytical instruments capable of qualification and quantitation of the hundreds and even thousands of components present in complex atmospheric air samples. Without a comprehensive understanding of the Earth’s atmosphere and the reactions, transformations and transportations occurring within it our crops, ecosystems, and even our health is at risk. However, by studying the photochemistry of the molecular constituents of air, scientists are able to devise and test possible solutions to problems such as ozone depletion, acid rain, photochemical smog formation, toxic air pollution, increases in greenhouse gases and global warming.

In order to achieve this, field measurements are of crucial importance. The major challenge here is the incompatibility of commercial GC instruments for this purpose. The longer sample holding time and transportation handling associated with off-site laboratory analysis can produce a lower detected VOC concentration when compared to duplicate samples analysed on-site.

Chapter 2 reiterated that, despite its portability and power consumption limitations with regards to on-site usage, GC is the most suited and well used analytical tool within atmospheric chemistry. The fundamental principles of chromatography were described in detail as they are the “rules” to which the developed lab-on-a-chip GC must adhere. Resolution is the ultimate aim of chromatography, and the theoretical and practical considerations relevant to this objective were thoroughly deliberated.

While conventional GC has widespread applications, it often fails to provide the necessary resolution for particularly complex samples, such as air. In recent years, GCxGC, the principles of which were detailed in Chapter 3, has emerged as the solution to this restricting problem. This technique is still relatively new and is constantly evolving, with the planar two-dimensional GC chip fabricated here being a representative example of this.

Chapter 4 highlighted the reported attempts at miniaturising both one-dimensional and, on a lesser scale, two-dimensional gas chromatographs. It was shown that the vast majority of portably sized GCs comprise commercially available capillary columns, which generally have been wound tighter than what would be considered the norm, and housed within small units that contain all the usual components but on a smaller scale. In terms of microfabrication, the majority of reported GC attempts have been using silicon as substrate. Etching of silicon results in rectangular or square channels. These allow pooling of stationary phase in the column corners on coating, and chromatograms generated via these chips suffer from peak broadening and general degradation of separation performance. Circular channels, such as those achieved for the glass chips reported here, are the ideal as they function in much the same way as traditional capillary columns. While micro-GCxGCs have been reported, separations to the scale of that demonstrated in this thesis have not yet been achieved.

Ultimately, the result of this work has been the microfabrication, stationary phase coating, system development, and chromatographic optimisation of a planar two-dimensional glass GC chip. Relatively long column lengths and standard internal diameters have been achieved. Low-power direct resistive heating and cooling of the glass chip produced a uniform heating profile across the columns when held at both above and below ambient temperatures, and multiple temperature zones have been achieved within the same chip. The ability to directly cool this device using the Peltier effect may offer substantial advantages for the analysis of very volatile species over typical cryogenic cooling of drawn capillaries in standard GC ovens.

A successful coating method was experimentally determined by initially coating a number of deactivated fused silica capillary columns with OV-101, before progressing to coating the primary and secondary columns of the glass device. Static coating was determined to be the best coating method for the purpose of this project.

The one-dimensional performance of the device was proven using a standard GC oven for injection, heating and FID detection. Coupling of the directly heated column to a low-cost, low-power PID showed reasonable separation of a simple BTEX mixture in 230s with sub ng sensitivity.

Two-dimensional separation has shown promising results from the separation of ppm gas mixtures of up to 16 VOCs. The miniaturised GC system as a whole, with built-for-purpose heating, cooling and control, was found capable of comprehensive separation with photoionization detection. When equipped with appropriately sized gas cylinders and battery power, this instrument offers substantial potential as a field portable GC, overcoming some of the portability limitations associated with drawn capillary columns and turbulent fan GC ovens.

A limited validation study was conducted that showed the LOC system to be both precise and linear, with good repeatability. Estimated limits of detection and quantitation were high, however, as the system itself has not yet been validated, this is not entirely unexpected or unexplained.

The results of this study are significant and provide original contributions to the fields of chromatography, instrument miniaturisation and atmospheric chemistry. If produced on a commercial scale this instrument would find application for a wide range of other subject areas.

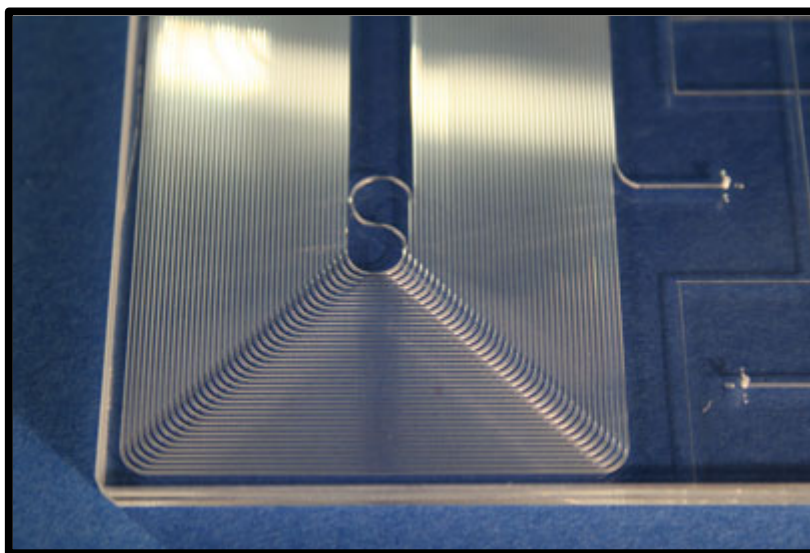


Figure 165: A close-up of the spiral primary column of LOC 1

11.2 Limitations and Problems Experienced

As discussed, the durability of the housing unit was a problem. If issues were encountered within the controlled environment of the development laboratory, the system would not be capable of handling adverse conditions, such as the high humidity of the Bornean jungles, or the low ambient temperature of the Antarctic.

The miniaturised PID from Alphasense was another limitation, with variable, unreliable response. A more appropriate and capable detector would need to be sourced.

Column, or stationary phase, bleed was a major issue experienced throughout experimentation. Bleed is a result of the elution of stationary phase degradation products. On leaving the column, bleed not only causes high background signal, but ultimately fouls the detector as well. While all columns produce bleed products, column exposure to oxygen in air can accelerate this process. As there was no real way to cap the glass chip channels, they were open to air on a constant basis.

The second significant limitation of the chips was that no cross-linking or bonding of the stationary phase to the channel walls took place. Bonding occurs through covalent linking of the stationary phase to the solid support of the channel wall. Cross-linking involves covalently linking the individual polymer chains of the stationary phase. These techniques provide enhanced thermal and solvent stability.

Generally, columns should also be deactivated before coating. A deactivation program for silica and soft glass columns that is suitable for most applications would first entail an acid wash by filling with 10% w/w hydrochloric acid, sealing the ends and heating the column to 100 °C for 1 hour. This procedure is believed to remove traces of heavy metal ions that can cause adsorption effects. The column is then filled with a solution of hexamethyldisilazane contained in a suitable solvent, sealed, and again heated to the boiling point of the solvent for 1 hour^[1]. This blocks any hydroxyl groups that were formed on the surface during the acid wash.

As with bonding or cross-linking, a deactivation step was not included in the coating process for the glass chip columns. This was purposefully omitted so as to allow for chip recycling. However, had there been more time, these steps would definitely have been a part of the continued development of the LOC GCxGC system.

The project, as a whole, was challenged by the constraints of time, finance, suitable testing facilities and equipment, as well as the lack of an appropriate team of engineers and chemists with pertinent expertise in the relevant areas. If time was not a factor, one person alone potentially could see the development through from start to finish. Unfortunately, within the restraints of a PhD timeframe it was not possible to produce and present a fully designed, developed, and validated gas chromatographic system with fully developed, optimised and validated methods. However, enough data and chromatographic evidence has been collected within this time to realise the very real potential of this lab-on-a-chip GCxGC-PID, and, considering the limitations detailed, the results achieved are excellent.

11.3 Future Work

While a significant body of work has been presented here, additional research is both foreseen and required in order to bring the prototype developed to market.

Ultimately, a light, portable, battery-powered device capable of performing automatic injections is desired. Future work would include the evaluation of gas cylinder size requirements. As well as this, an important consideration would be the minimisation of power requirements for battery powered operation. In order for the instrument to be truly portable it would need to be self-contained with no exterior power source.

Very little work was done on sample injection and preconcentration. Trapping material evaluation is required in order to determine the best suited packing, or mixture of packings, for VOC analysis. Investigations into sample delivery options would be another interesting step to determine the feasibility of supporting a variety of sampling techniques, such as loop and syringe injection, sampling by probe, or even SPME.

Ideally, the final miniaturised instrument will have been pre-loaded with analysis methods and documentation specific to the methods required. Thus, studies into ensuring the ease of operation for unskilled operators would be a priority.

Determining the instruments detection limits and dynamic range, and testing with real samples would be a significant step in the instrument's development, as would actual field testing.

Limitations were identified with regard to detection, thus, finding a suitable replacement detector would be important. The portability of an instrument depends on the volume and weight of each component. While micro-FIDs have been reported, this detector would not be suitable for portable GC as it requires at least two gas sources. TCD and ECD need one gas source and so could hold potential if a PID with a better and more reliable response could not be sourced.

Only very preliminary evaluation of LOC 3 took place – such a small amount that it was not deemed worthwhile to even mention in this thesis. This smaller chip, however, offers potential, as does the possibility of other chip designs. If further funding and time were available, extensive evaluation of LOC 3 would take place, followed by comparison of the achieved results with those of LOC 4.

Finally, working with a selected subcontractor on the design of the casing for the final product would be required, before formulating a plan of marketing.

11.4 Final Words

Gas chromatography as a technique is well established. It is one of the most demanded and informative analytical methods available. However, the evolution of this technique has not yet reached completion, as evidenced by the work reported in this thesis, as well as that seen in the current literature.

While a substantial and significant amount of work was accomplished over the duration of this project, there is much scope for future studies. As Albert Einstein once said, *“Science is not, and will never be a completed book. Any new success brings up new questions. Any evolution uncovers new difficulties”*.

11.5 References

1. Scott, R.P.W., *Principles and Practice of Chromatography*, 2003, Library4Science, LLC. p. 106.